The Role of Vitamin D Autocrine Activity and Signalling in Osteoclast Formation and Activity

Daniel Christopher Reinke, B.Sc.(Hons)

Thesis by combined publication and conventional formats in fulfilment of the requirements for the degree of Doctor of Philosophy

July/2020

The Discipline of Orthopaedics and Trauma

Adelaide Medical School

Faculty of Health and Medical Sciences

The University of Adelaide

Table of Contents

Thesis Abstract

The role of Vitamin D receptor (VDR) signalling within the osteoclast is not fully elucidated, with even the presence of VDR in the osteoclast debated. However, the presence of the enzyme, 25-hydroxyvitamin D 1α hydroxylase (CYP27B1) responsible for the final conversion step of the Vitamin D pro-hormone into active Vitamin D, within the osteoclasts, osteoblast and osteocytes, and the potential for modified activity and maturation within the bone cells under the effects of Vitamin D has been established.

The aim of the studies within this thesis were to examine through the use of genetic knock out models (KO) the role(s) vitamin D plays in osteoclast proliferation, maturation, activity and the underlying potential genetic mechanisms. Experimental work first optimised osteoclast maturation from wild type (WT) littermate matched splenocytes and then focused on osteoclastogenesis from genetic KO models, *Cyp27b1*KO and *Vdr*KO with the aim of identifying the role of autocrine vitamin D. This was expanded into the role of the V-ATPase pump as a compensatory mechanism for loss of autocrine function and the effect of vitamin D on mature osteoclasts through the *Ctsk*-Cre.Vdr$^{fl/fl}$ mouse model in co-culture.

The deletion of the *Cyp27b1* and *Vdr* genes and the subsequent impairment of the vitamin D metabolic pathway resulted in changes in TRAP-positive multinucleated cells (MNC) as well as per cell increase in osteoclast resorptive activity. Osteoclast related gene expression was significantly reduced in both gene KO models and deranged in the V-ATPase subunits. It is worth mentioning that several genes from both *Cyp27b1* and *Vdr*KO cultures had almost identical patterns of gene expression, reinforcing the notion that the effects seen were mediated through the loss of the vitamin D metabolic pathway. *Ctsk*-Cre.Vdr$^{fl/fl}$ osteoclast cultures indicated that mature WT osteoclasts resorptive activity is suppressed

by the presence of the vitamin D receptor. The loss of VDR in mature osteoclasts in co-cultures resulted in a deregulated increase in resorptive activity and aberrant maturation. Overall, the findings of this thesis establish that there is a role for autocrine vitamin D activity within the osteoclast lineage. The loss of the vitamin D metabolic pathway in the case of *Cyp27b1*KO and *Vdr*KO, result in significant changes to osteoclast maturation, proliferation, activity and gene expression and it is evident that there are compensatory mechanisms present that help minimise the impact. Further experimentation is warranted to further elucidate the effects of vitamin D activity in the osteoclast lineage and to overall fully understand how vitamin D works in human bone and aging.

List of Abbreviations

Abbreviation	Abbreviations and gene names expanded
1,25D, calcitriol	1α25-dihydroxyvitamin D_3
25D	25-hydroxyvitamin D
αMEM	Alpha Minimal Essential Media
ADP	Adenosine Diphosphate
ADTP	Australian Digital Thesis Program
Ap-1	Activator Protein 1
ATP	Adenosine Triphosphate
B220	Cluster of Differentiation 45R
B2m	Beta Two Microglobulin
Bax	B-Cell Lymphoma Two Associated X protein
Bcl-2	B-Cell Lymphoma Two
Bcl-xl	B-Cell Lymphoma-extra Large
Bim	B-Cell Lymphoma Two Like protein Eleven
Cd11b	Cluster of Differentiation Eleven b
Cd3	Cluster of Differentiation Three
Cd4	Cluster of Differentiation Four
Cd8	Cluster of Differentiation Eight

Ca2	Carbonic Anhydrase Two
Csf-1	Colony Stimulating Factor-1
C-fos	Transcription Factor Proto Oncogene
Clcn-7	Chloride Channel Seven
Ctr	Calcitonin Receptor
Ctsk	Cathepsin K
CYP	Cytochrome P450 Enzyme
Cyp27b1	25-Hydroxyvitamin D One Alpha Hydroxylase
*Cy27b1*KO	25-Hydroxyvitamin D One Alpha Hydroxylase Global Knockout Mice
DBP	Vitamin D Binding Protein
Dc-Stamp	Dendrocyte Expressed Seven Transmembrane Protein
DEPC	Diethylpyrocarbonate
DNA	Deoxyribonucleic Acid
F-actin	Filamentous- actin
FBS/FCS	Foetal Bovine Serum/ Foetal Calf Serum
GCTB	Giant Cell Tumours of Bone
HPRT1	Hypoxanthine Phosphoribosyltransferase One
ITAM	Immunoreceptor Tyrosine – Base Activation Motif

KO	Knock Out
M-CSF	Macrophage Colony Stimulating Factor
M-CL1	Induced Myeloid Leukemia Cell Differentiation protein
MEM	Minimal Essential Media
MNC	Multinucleated Cell Number
mRNA	Messenger Ribonucleic Acid
NFATC1	Nuclear Factor of Activated T-cells, Cytoplasmic One
nM	Nanomolar
OCN	Osteocalcin
OPG	Osteoprotegerin
OPN	Osteopontin
OSCAR	Osteoclast-Associated Immunoglobulin-Like Receptor
PBMCS	Peripheral Blood Mononuclear Cells
PTH	Parathyroid Hormone
RANK	Receptor Activator of Nuclear Factor kappa B
RANKL	Receptor Activator of Nuclear Factor kappa B ligand
RNA	Ribonucleic Acid
RT-PCR	Real Time Polymerase Chain Reaction

RXR	Retinoid X Receptor
SEM	Scanning Electron Microscope
siRNA	Small Interfering Ribonucleic Acid
TBAC	TRIS Buffered Ammonia Chloride
TE	Tris EDTA
TNAP	Tissue Non-specific Alkaline Phosphatase
TNFR	Tumour Necrosis Factor Receptor Family
TNSFII	Tumour Necrosis Factor Superfamily Member 2 (RANKL)
TNSF2A	Tumour Necrosis Factor Superfamily Member IIA (RANK)
TRAFs	TNF Receptor Associated Factors
TRAF5	TNF Receptor Associated Factor Five
TRAF6	TNF Receptor Associated Factor Six
TRAP	Tartrate-Resistant Acid Phosphatase 5
TREM-2	Triggering Receptor Expressed on Myeloid Leukaemia Cell Differentiation Protein
TYRO	Tyrosine Kinase Binding Protein (Dap12)
UV-B	Ultra-Violet B
V-ATPase	Vacuolar-type H+- Adenosine Triphosphate
VDR	Vitamin D Receptor

VDRE	Vitamin D Response Element
*Vdr*KO	Vitamin D Receptor Knock Out

Declaration

This thesis contains no material which has been accepted for the award of any other degree or diploma in any university or other tertiary institution to Daniel Christopher Reinke and, to the best of my knowledge and belief, contains no material previously published or written by another person, except were due reference has been made in text.

I give consent to this copy of my thesis when deposited in the University of Adelaide library, being made available for loan and photocopying, subject to the provisions of the Copyright Act 1968.

The author acknowledges that the copyright of published works contained within this thesis as listed below resides with the copyright holder of those works.

I also give permission for the digital version of my thesis to be made available on the internet, via the University Digital Research Repository, the library catalogue, the Australasian Digital Thesis Program (ADTP) and also through web search engines, unless permission has been granted by the University to restrict access for a period of time.

Statement of Authorship

Reinke DC, Kogawa M, Barratt KR, Morris HA, Anderson PH, Atkins GJ. (2016) Evidence for Altered Osteoclastogenesis in Splenocyte Cultures from Cyp27b1 Knockout Mice. *Journal of Steroid Biochemistry and Molecular Biology* 164:353-360. doi: 10.1016/j.jsbmb.2015.11.015

REINKE, D.C. (Candidate)

Performed data analysis on all samples, interpreted data, drafted manuscript.

I hereby certify that the statement of contribution is accurate:

Signed ..... Date 30/06/2020

KOGAWA, M.

Assisted with data interpretation and evaluation.

I hereby certify that the statement of contribution is accurate:

Signed ..... Date 6/5/2020

BARRATT, K.R.

Performed mouse breeding, genotyping, animal care and provided of tissues for experimentation.

I hereby certifv that the statement of contribution is accurate:

Signed ..... Date 8/5/2020

MORRIS, H.A.

Deceased.

ANDERSON, P.H.

Provided genetically modified animals, supervised the development of work and evaluated the manuscript.

I hereby certify that the statement of contribution is accurate:

Signed ..... Date 8/5/2020

ATKINS, G.J.

Supervised development of work, helped in data analysis, manuscript editing and acted as corresponding author.

I hereby certify that the statement of contribution is accurate:

Signed .... Date 5/5/2020

Statement of Authorship

Reinke DC, Starczak Y, Kogawa M, Barratt KR, Morris HA, Anderson PH, Atkins GJ. (2018) Evidence for altered osteoclastogenesis in splenocyte cultures from VDR knockout mice. *Journal of Steroid Biochemistry and Molecular Biology* 177:96-102. doi: 10.1016/j.jsbmb.2017.07.033.

REINKE, D.C. (Candidate)

Performed data analysis on all samples, interpreted data, drafted manuscript.

I hereby certify that the statement of contribution is accurate:

Signed ..... Date 30/06/2020

YOLANDI STARCZAK

Assisted with data analysis and manuscript evaluation.

I hereby certify that the statement of contribution is accurate:

Signed ..... Date 5-5-2020

KOGAWA, M.

Assisted with data interpretation and evaluation.

I hereby certify that the statement of contribution is accurate:

Signed ..... Date 6/5/2020

BARRATT, K.R.

Performed mouse breeding, genotyping, animal care and provided of tissues for experimentation.

I hereby certify that the statement of contribution is accurate:

Signed ..... Date 8/5/2020

MORRIS, H.A.

Deceased.

ANDERSON, P.H.

Provided genetically modified animals, supervised the development of work and evaluated the manuscript.

I hereby certify that the statement of contribution is accurate:

Signed ..... Date 8/5/2020

ATKINS, G.J.

Supervised development of work, helped in data analysis, manuscript evaluation and acted as corresponding author.

I hereby certify that the statement of contribution is accurate:

Signed ....Date 5/5/2020

Statement of Authorship

Starczak Y, Reinke DC, Barratt KR, Ryan JW, Russell PK, Clarke MV, St-Arnaud R, Morris HA, Davey RA, Atkins GJ, Anderson PH. (2018) Absence of vitamin D receptor in mature osteoclasts results in altered osteoclastic activity and bone loss. *Journal of Steroid Biochemistry and Molecular Biology* 177:77-82. doi: 10.1016/j.jsbmb.2017.10.022.

YOLANDI STARCZAK

Performed data analysis on all samples, interpreted data, wrote manuscript.

I hereby certify that the statement of contribution is accurate:

Signed ..... Date 5-5-2020

DANIEL REINKE (Candidate)

Contributed to data generation and interpretation, and manuscript writing.

I hereby certify that the statement of contribution is accurate:

Signed ..... Date 30/06/2020

KATHERINE R. BARRATT

Performed mouse breeding, genotyping, animal care and provided of tissues for experimentation.

I hereby certify that the statement of contribution is accurate:

Signed ..... Date 8/5/2020

JACKSON W. RYAN

Assisted with provision of experimental material.

I hereby certify that the statement of contribution is accurate:

Signed ..... Date 8/5/2020

PATRICIA K. RUSSELL

Assisted in the creation of the mice and collection of tissue samples.

I hereby certify that the statement of contribution is accurate:

Signed Date7/4/2020

MICHELLE V. CLARKE

Assisted in the creation of the mice and collection of tissue samples.

I hereby certify that the statement of contribution is accurate:

Signed Date12/05/2020

HOWARD A. MORRIS

Deceased.

RENÈ ST-ARNAUD

Provided expertise in vitamin D biology. I hereby certify that the statement of contribution is accurate:

Signed ..... Date 2020-05-13

RACHEL A. DAVEY

Supervised the creation of the mice and collection of tissue samples. Participated in manuscript revision.

I hereby certify that the statement of contribution is accurate:

Signed ..... Date 6/5/2020

GERALD J. ATKINS

Supervised development of work and manuscript evaluation; co-senior author.

I hereby certify that the statement of contribution is accurate:

Signed ..... Date 5/5/2020

PAUL H. ANDERSON

Supervised development of work, helped in data analysis, manuscript evaluation and acted as co-senior and corresponding author.

I hereby certify that the statement of contribution is accurate:

Signed ..... Date 8/5/2020

Acknowledgements

Firstly, I would like to thank my Supervisors Professor Gerald Atkins and Associate Professor Paul Anderson for their support and knowledge throughout the completion of this Degree. Their continued support and supervision has ensured the success of my candidature.

Funding for this work came from an internal Post Graduate Award by the Faculty of Health Science (Discipline of Orthopaedics and Trauma). I would like to thank members of the Bone Biology Lab and Musculoskeletal Biology Research lab; Dr Masakazu Kogawa, Dr Matthew Prideaux, Dr Andrew Turner, Dr Asiri Wijenayaka, Ms Shelly Hay, Dr Yolandi Starczak and Kate Barratt for their generous support, help and guidance.

I would also like to thank my family for their generous support and guidance.

Publications Directly Arising from Thesis

Reinke DC, Kogawa M, Barratt KR, Morris HA, Anderson PH & Atkins GJ (2016) *Evidence for altered osteoclastogenesis in splenocyte cultures from Cyp27b1 knockout mice.* Journal of Steroid Biochemistry & Molecular Biology 164:353-360. doi: 10.1016/j.jsbmb.2015.11.015 PMID: 26639637

Reinke DC, Starczak Y, Kogawa M, Barratt KR, Morris HA, Anderson PH & Atkins GJ (2018) *Evidence for altered osteoclastogenesis in splenocyte cultures from VDR knockout mice.* Journal of Steroid Biochemistry & Molecular Biology 177:96-102. doi: 10.1016/j.jsbmb.2017.07.033.

Starczak Y, Reinke DC, Kogawa M, Barratt KR, Ryan JW, Russell PK, Clarke MV, St-Arnaud R, Morris HA, Davey RA, Atkins GJ & Anderson PH (2018) *Absence of Vitamin D receptor in mature osteoclasts results in altered osteoclastic activity and bone loss.* Journal of Steroid Biochemistry & Molecular Biology 177:77-82. doi: 10.1016/j.jsbmb.2017.10.022.

Other Publications arising from thesis

Ryan JW, Reinke DC, Kogawa M, Turner AG, Atkins GJ, Anderson PH & Morris HA, 2013*, Novel Targets of Vitamin D Activity in Bone: Action of the Vitamin D Receptor in Osteoblasts, Osteocytes and Osteoclast.* Current Drug Targets (1683-8)

DOI: 10.2174/138945011131400212

Scientific Presentations arising from thesis

Daniel C. Reinke, Masakazu Kogawa, Paul H. Anderson, Howard A. Morris, and Gerald J. Atkins (2013) Evidence for Altered Splenocyte Derived Osteoclast Activity in Cultures Generated *Ex Vivo* from Mice with a Global Deletion of *Cyp27b1* Gene. 16th Workshop on Vitamin D, San-Francisco, CA, USA (Poster presentation)

Daniel C. Reinke, Masakazu Kogawa, Paul H. Anderson, Howard A. Morris, and Gerald J. Atkins (2013) Evidence for Altered Splenocyte Derived Osteoclast Activity in Cultures Generated *Ex Vivo* from Mice with a Global Deletion of *Cyp27b1* Gene. 23rd Australian New Zealand Bone and Mineral Society (ANZBMS) Annual Scientific Meeting, Melbourne, VIC, Australia (Poster presentation)

Daniel C. Reinke, Masakazu Kogawa, Paul H. Anderson, Howard A. Morris, and Gerald J. Atkins (2013) Evidence for Altered Splenocyte Derived Osteoclast Activity in Cultures Generated *Ex Vivo* from Mice with a Global Deletion of *Cyp27b1* Gene. (2014) 8th Clare Valley Bone Meeting, Clare, SA, Australia (Poster presentation)

Daniel Reinke, Masakazu Kogawa, Kate Barratt, Paul H. Anderson, Howard A. Morris, Gerald J. Atkins (2014) Evidence for Altered Osteoclastogenesis in Splenocyte Cultures

from *Cyp27b1* Knockout Mice. 20th Australian New Zealand Orthopaedic Research Society (ANZORS) Annual Conference. Adelaide, SA, Australia (Podium presentation)

Daniel Reinke, Masakazu Kogawa, Kate Barratt, Paul H. Anderson, Howard A. Morris, Gerald J. Atkins (2015) Evidence for Altered Osteoclastogenesis in Splenocyte Cultures from *Cyp27b1* and *Vdr* Knockout Mice. Australian Society for Medical Research (ASMR) Annual Scientific Meeting. Adelaide, SA, Australia (Podium presentation)

Chapter 1: Review of the Literature

Chapter 1 is a review of the current literature pertaining to vitamin D metabolism and activity in bone, including the role of autocrine and endocrine vitamin D activities and the role of vitamin D in calcium and phosphate homeostasis. To understand the role of vitamin D specifically within the osteoclast lineage at the autocrine level, an understanding of the current state of knowledge, not just in the field of vitamin D but of bone cell biology, is required. This review is therefore divided into four sub-sections; the first sub-section focuses on vitamin D and its role in the endocrine system. The second sub-section reviews the current general knowledge in bone cell biology. The third sub-section examines the role of vitamin D at a cellular level in the three major bone cell types, osteoclasts, osteoblasts and osteocytes, and finally, the fourth sub-section covers the aims and hypotheses for this thesis.

1.0 Introduction: Scope and Structure of the Literature Review

The active form of vitamin D, 1α25-dihydroxyvitamin D_3 (1,25D; calcitriol), is recognised as being essential in maintaining calcium homeostasis, principally by stimulating intestinal calcium absorption. By doing so, vitamin D indirectly contributes to maintaining mineralised bone. However, vitamin D also is known to directly regulate bone formation and resorption, in processes which appear to enhance bone formation under certain circumstances and promote bone resorption under other circumstances. In this review, we will briefly cover the known pathways related to the synthesis and actions of 1,25D with respect to the endocrine system. We will also cover the known actions of 1,25D on the autocrine activities of vitamin D in the various bone cell types. Finally, we will focus on the main topic of this thesis, the autocrine and paracrine actions of vitamin D metabolites on the major bone resorbing cell type, the osteoclast.

Cellular effects of 1,25D are mediated following the ligation of the hormone to the vitamin D receptor, which is a member of the nuclear receptor family. Vitamin D has a diverse range of activities in bone and other tissues, which is attributed to the fact that the VDR is almost ubiquitously expressed, including in the three major bone cell types, osteoblasts, osteocytes and osteoclasts (1). This diverse expression pattern of the VDR is reinforced by the presence of putative vitamin D responsive elements (VDREs), occurring in the proximal and distal promoter regions of a large percentage of mammalian genes (1) . Recent studies have demonstrated that osteoblast-lineage cells contain the enzyme CYP27B1 which is required to convert 25D to active 1,25D (2). In addition, our group has been principal in demonstrating that cells of the osteoclast lineage also have the ability to convert 25D to 1,25D through the expression of *CYP27B1* (3, 4), and are thus capable of

autocrine 1,25D signalling, as well as responding to paracrine or endocrine 1,25D-mediated signals.

The osteoclast is a unique cell type, highly adapted for resorbing bone. As well as being multi-nucleated, it also has specialised internal structures that promote efficiency in bone resorption and ATP generation. These include an unusually dense electron transport chain within the mitochondria, high levels of expression of the multi-subunit V-ATPase pump and the ability to form an (Filamentous) F-actin ring, a specialised structure enabling a tight seal to form between the basolateral cell membrane of the osteoclast and the mineralised bone matrix (5). The various functional proteins of the osteoclast are potentially sensitive to regulation by 1,25D. Strong evidence for a paracrine role of vitamin D in the osteoclast is provided by the recognised regulation of expression of key cytokines, such as receptor activator of nuclear factor kappa-B ligand (RANKL) and colony stimulating factor (CSF-1), also known as macrophage colony stimulating factor (M-CSF), which together are essential for the differentiation of osteoclast precursors into mature osteoclasts (5, 6). Recent studies from our group demonstrate that osteoclasts metabolise 25D to form active 1,25D resulting in the modulation of osteoclastogenesis, the bone-resorbing activity and migration of osteoclasts (7). The proposed stages of osteoclast differentiation and function influenced by paracrine and autocrine signalling of vitamin D are depicted in Figure 1.1. However, little is known about the underlying molecular mechanisms responsible for these effects.

Bone is an essential part of the human ambulatory system providing structure, support and tension, protecting critical organs and enabling movement from respiration to locomotion. Bones are fibrous mineralised tissues and structures consisting primarily of collagen type

I (90%) structured into an organic matrix. The organic matrix is mineralised with a calcium phosphate mineral, a biological analogue of hydroxyapatite. The matrix and mineral phases act in conjunction with each other, providing strength and flexibility, respectively. Bone is not a static tissue but is continually remodelled by coordinated cycles of resorption and formation in a process commonly referred to as bone remodelling. Resorption is undertaken by haematopoietic-derived osteoclasts and their precursors, and formation is carried out by mesenchymal-derived osteoblast-lineage cells.

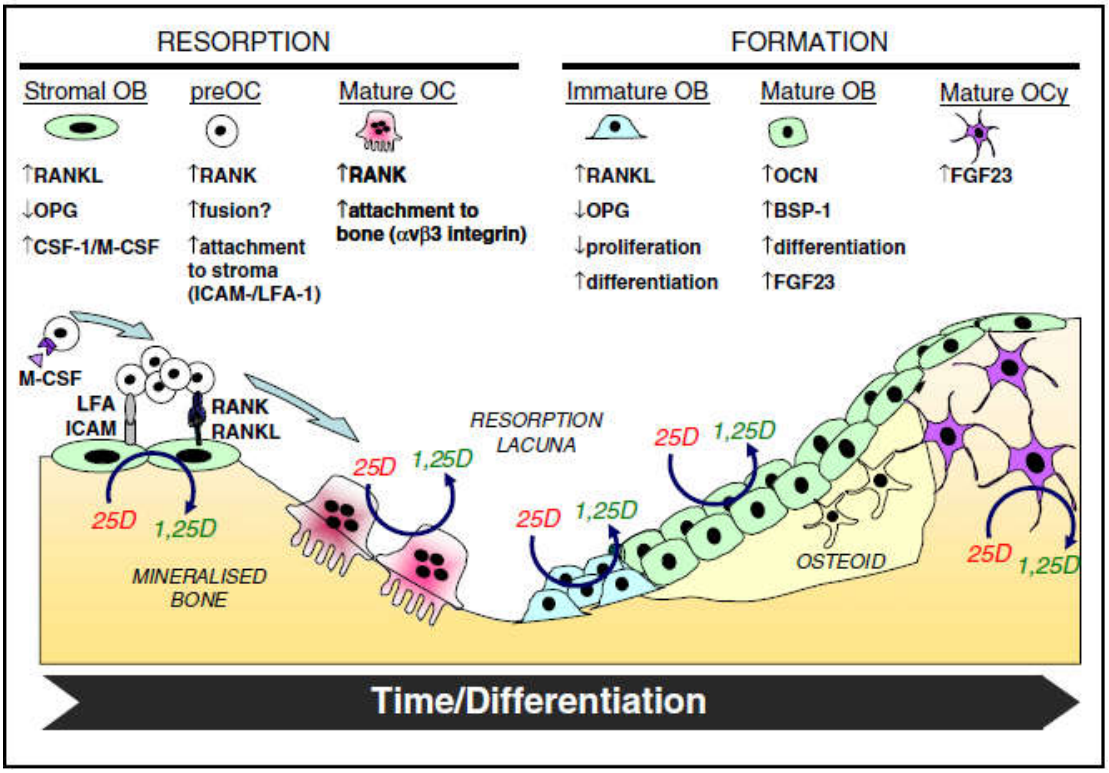

Fig. 1.1: Vitamin D activity in bone cells. The role of vitamin D metabolism and activity in the various bone cell types. (Taken from (8) with permission)

This review of the literature examines the current understanding of vitamin D activity in calcium homeostasis, as well as the endocrine and autocrine effects of vitamin D on bone biology, with a major focus on the osteoclast lineage.

1.1Vitamin D and the Endocrine System

Vitamin D, bone and vascular pH are directly linked in a complex regulatory system (9). The bone acts as mineral storage for calcium and phosphate and in times of need calcium is liberated from the bone (10). When vitamin D and calcium levels are insufficient over extended periods of time skeletal structural stability becomes affected. Since the primary role of vitamin D is regulation of calcium homeostasis, the maintenance of bone strength can be considered a secondary contrivance. Thus, calcium is preferentially removed from the bone in favour of calcium homeostasis over bone structural integrity. Extended calcium deficiency over a lengthy period of time causes the bone strength to become compromised, resulting in increased fracture rates due to reduced stress absorbing potential (11). Identifying the genetic mechanisms and biochemical pathways in bone cells regulated by vitamin D metabolism, potentially enables more accurate vitamin D dosage for osteoporosis patients. If these biochemical pathways and genetic mechanisms stimulated by vitamin D can be demonstrably related to the changes in fracture rates, this may allow modification of biochemical or genetic pathways to maintain or improve bone strength. This could also provide insight into stabilising bone remodelling in older age (12, 13).

1.1.1 Synthesis of Vitamin D_3 in the Skin

Vitamin D can be ingested through dietary intake in the calciferol D_2 form and the cholecalciferol D_3 form, the primary mechanism of vitamin D synthesis is through photolytic conversion in the skin. The vitamin D metabolite 7-dehydrocholesterol undergoes photolytic conversion with exposure to UV-B radiation within epidermal cells, in particular within the stratum basale and stratum spinosum, to become vitamin D_3 (11, 14, 15). 7-dehydrocholesterol absorbs UV-B radiation at the wavelengths of 290-320nm and converts to the pre-vitamin D_3 ($C_{27}H_{44}O$) form, which under reversible thermal isomerisation rearranges its double bond structure over three days to the more thermodynamically stable form, cholecalciferol or vitamin D_3 (16). Human body temperature naturally pushes this equilibrium towards the vitamin D_3 form (8). vitamin D_3 requires two further hydroxylation steps before it becomes an active metabolite, each catalysed by a cytochrome P450 (CYP) enzyme CYP2R1, and CYP27B1 (8). Vitamin D_3 is hydroxylated at position C25 to 25D via CYP2R1 in the liver. 25D is the major circulating form of vitamin D. 25D is further hydroxylated at position C1 via CYP27B1 activity to 1,25D in the kidney. 1,25D is the recognised active hormone form of vitamin D.

Excess 25D and 1,25D are broken down by the cytochrome P450 enzyme, CYP24A1. CYP24A1 further hydroxylates 25D or 1,25D adding a hydroxyl group at C24, generating 24,25-dihydroxyvitamin D and 1,24,25-trihydroxyvitamin D, respectively (17). These short-lived metabolites are then rapidly catabolised by CYP24A1 into calcitroic acid, which is then excreted through the urine.

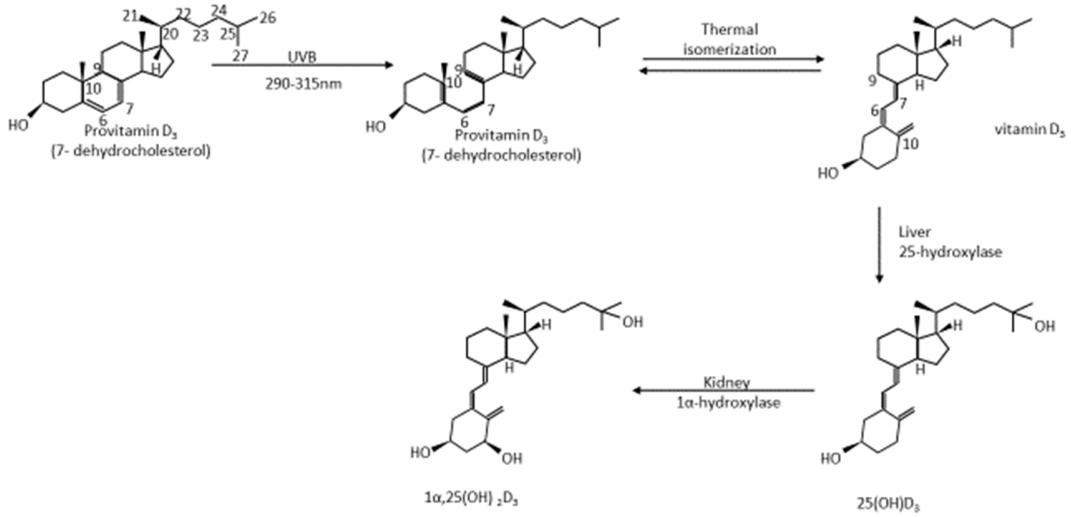

Fig. 1.2. Vitamin D metabolites. Identifies the chemical changes that occur in vitamin D metabolites from the skin to the active form of vitamin D. Recreated from (18)

1.1.2 Synthesis of 25-hydroxy Vitamin D in the Liver

Vitamin D_3 produced in the skin is released into the blood bound to vitamin D binding protein (DBP), which both stabilises the metabolite and mediates delivery to the liver for further processing. The conversion of vitamin D_3 to the metabolite 25D (calcidiol) is catalysed by the cytochrome P450 enzyme, CYP2R1 (19-21). Currently, the majority of conversion of vitamin D to 25D occurs within the liver, which under constitutive conditions releases 25D into the circulation. Circulating 25D levels are currently considered the most reliable indicator of an individual's vitamin D status, as 25D has a long half-life of 15-35 days (22).

1.1.3 Synthesis of 1α,25-dihydroxy Vitamin D3 in the Kidney

The final step in the synthesis of active vitamin D hormone is the conversion of 25D to 1,25D, by the P450 enzyme CYP27B1, a critical regulatory step of the vitamin D endocrine system. The conversion of 25D to 1,25D has been demonstrated to take place almost ubiquitously throughout the human body (19). The kidney is the primary producer of circulating 1,25D levels in the blood (23). 1,25D has a short half-life and also acts as a negative regulator of itself (24). 1,25D is a highly active metabolite and as such needs to be tightly regulated.

1.1.4 Role of DBP in the Vitamin D Pathway

The majority of 25D released from the liver is bound to the chaperon protein DBP. DBP also binds to 1,25D but has a higher affinity for 25D ($7x10^8\ M^{-1}$) than that of 1,25D ($4x10^7\ M^{-1}$) (25). The mechanism behind 25D entry into cells has not yet been fully elucidated. Free ligand diffusion and DBP mediated endocytosis are the current proposed mechanisms for the entry of bound 25D into cells (26). Free ligand diffusion proposes that the smaller percentage of unbound 25D in the blood limits the conversion of 25D to 1,25D (26). DBP mediated endocytosis hypothesises that DBP is taken up, following DBP binding to cellular receptors. The mechanism behind the uptake of DBP bound 25D has not yet been fully elucidated, however, cubilin and megalin have been shown to play a role in 25D uptake (25).

1.1.5: 1,25D as a Transcriptional Activator

1,25D mediates its biological activity via high affinity binding to the VDR, which is expressed in most cells of the human body (14). Liganded VDR binds to retinoid X receptor (RXR) forming a heterodimer. This becomes conformationally changed allowing it to bind to specific Deoxyribonucleic Acid (DNA) sequences, usually in the promoter regions of responsive genes termed VDRE, allowing enhanced recruitment of co-factors for transcriptional activation (8). Renal-derived 1,25D acts upon key genes in intestinal enterocytes and renal proximal tubule cells, to mediate calcium absorption and re-absorption respectively (27-29). However, there is to date little evidence that the relatively low affinity of 25D for VDR is sufficient at physiological levels to contribute to VDR mediated signalling.

1.1.6: Endocrine actions of Vitamin D

Vitamin D is a primary regulator of endocrine calcium and phosphate homeostasis (30). The effects of vitamin D on the endocrine system are well established (3, 4, 7, 30, 31). Levels of 25D at 20 nmol/l or less, result in secondary hyperparathyroidism due to improper 1,25D production and calcium absorption. Vitamin D endocrine activity is substrate limited. Chronically low vitamin D levels, below 20 nmol/l combined with low dietary calcium result in diseases, such as rickets and osteomalacia (9, 32). It has been demonstrated in multiple studies that decreased levels of 25D below 50 nmol/l result in

increased fracture risk (12, 33) (34). The Institute of Medicine report for nutritional guidelines state that 50 nmol/l is now considered the minimal healthy vitamin D level required under minimal sun exposure. This indicates the potential for vitamin D to have additional mechanisms that take affect when 25D is above 20 nmol/l but below 50 nmol/l. One of the currently proposed mechanisms for this is, the autocrine conversion of 25D to 1,25D requires a higher circulating 25D level in order to become active.

1.1.7 Endocrine Actions of Vitamin D on Bone

Bone cells are targets of the vitamin D endocrine system and are also purported to be regulated by an internal autocrine/paracrine system within the cells themselves. In the case of the endocrine system, bone cells are directly affected by 1,25D produced from renal synthesis. Renal-derived 1,25D regulates osteoblast gene transcription, differentiation and mineralisation (35). It has been observed that 1,25D results in the induction of RANKL Messenger Ribonucleic Acid (mRNA) and the down regulation of Osteoprotegerin (OPG) mRNA expression. This decrease of OPG to RANKL ratio is known to promote osteoclastogenesis (36) and increase bone mineral resorption in humans. It was also reported that 1,25D may act to increase the progenitor pool of osteoblasts (37). 1,25D enhances the availability of osteoclast precursors for osteoclastogenesis (38). The next section will introduce the three major bone cell types in detail.

1.2.0 Bone Cell Biology

1.2.1 Osteoblasts

Osteoblasts in the axial skeleton are derived from mesenchymal stem cells. Interestingly, osteoblasts in the skull are likely derived from neural crest ectoderm (9). Osteoblasts are the bone matrix builders of the body and have prominent endoplasmic reticulum and Golgi organelles, indicative of a large protein manufacturing and transport capacity. This enables the osteoblast to rapidly produce and transport collagen and other protein components for the organic matrix of the bone. Osteoblasts lay down the organic matrix of the bone that primarily consists of collagen type 1 fibrils (9).

Newly formed, un-mineralised bone matrix is termed osteoid and is the section of the bone that gives flexibility. The mineralisation of the bone is undertaken by pre- or osteoid-osteocytes and the mineral composite of the bone provides the strength and load bearing capacity to the bone. Osteoblasts complete the organic matrix production and deposit bone mineral in a tightly regulated manner to form a strong elastic matrix (39). This matrix is capable of functioning as a load-bearing mechanical structure (39). Along with collagen type 1, osteoblasts secrete non-collagenous proteins that are essential for optimal bone formation including, tissue non-specific alkaline phosphatase (TNAP), bone sialoprotein, osteopontin and osteocalcin (40). TNAP is amongst one of the most important of these non-collagenous proteins, as it converts the ubiquitous inhibitor of mineralisation, pyrophosphate to inorganic phosphate. This conversion enables the mineralisation of osteoid matrix to proceed.

Osteoblasts, while playing a critical role in the formation of bone, are also directly involved in the regulation of bone resorption. Osteoblasts are known to secrete OPG, a member of the tumour necrosis factor receptor (TNFR) family. OPG, unlike the other members of the TNFR family, is not bound to cellular membranes and acts as a decoy receptor for RANKL. As such, it is a competitive inhibitor of osteoclastogenesis (41). OPG's structure has the standard amino terminal half ligand binding domain associated with the TNFR family members (42). Its carboxy terminal domain resembles that of a decoy receptor encoded in virulence as is often found in proxy viruses (42).

The deletion of the *Opg* gene in mice results in severe osteopenia associated with excessive osteoclastic resorption (43-45). In mouse over-expression models of OPG, the bone becomes a near solid mass and presents with limited bone marrow space, a state termed osteopetrosis. OPG blocks the RANKL- Receptor Activator of Nuclear Kappa B (RANK) interaction and therefore the differentiation of osteoclasts resulting in a negative effect on osteoclastic bone resorption (42). OPG production is not solely the providence of osteoblasts and is produced by other cells. Along with the production of collagen and OPG, osteoblasts also produce numerous cytokines essential in efficient osteoclast differentiation and osteoclastogenesis (46). Current research suggests that these cytokines, such as M-CSF, are also provided by the osteocytes (2).

Previous scientific research has indicated that osteoblasts present osteoclasts with the majority of RANKL involved in their RANK/RANKL interactions (47). However, recent *in vivo* models have indicated the increased possibility that it is in fact the osteocytes that are the major source of RANKL for osteoclastogenesis in the adult skeleton, rather than the more immature osteoblasts. One of the most compelling pieces of evidence for this is

work done by Xiong *et al.* (48) that showed that mice whose osteocytes were unable to produce RANKL had a significant inhibitory effect on osteoclastogenesis. Supporting this is other studies showing that osteocytes are essential for the remodelling of bone through osteoclastic activation in mature animals (49). It is theorised that the hypertrophic chondrocytes and immature osteoblasts are also important sources of RANKL in growing animals (48, 49).

In humans, osteoblasts have an average life span of three months. However, research has indicated that high levels, 120 nmol/l or greater, of 25D can potentially increase the life span of osteoblasts. As osteoblasts remain active for longer, more osteoid is laid down. In the case of increased life span an overall increase of bone osteoid is observed (9). This has been shown to produce lower quality osteoid. During the process of laying down bone, around 5% of osteoblasts differentiate into osteocytes and become enveloped within the bone matrix (9). The remaining osteoblasts become bone lining cells or undergo cell mediated apoptosis (50). The bone lining cells remain on the bone surface and are interconnected with osteocytes (50). Currently knowledge about the role of the bone lining cell function is limited.

1.2.2 Osteocytes

Osteocytes are long-lived cells that make up 90-95% of all bone cells, sometimes living in excess of 25 years (9). Osteocytes are considered one of the final stages of differentiation of the osteoblast. Late stage osteoblasts either undergo apoptosis, differentiate into bone

lining cells, or become embedded in the bone matrix as osteocytes. The embedding process occurs concomitantly with the differentiation of the osteocytes. Osteocytes are thought to transition from osteoblast to osteocyte through several interim stages, with each differentiation state being associated with altered functional modalities (51).

Initially, a small percentage of osteoblasts become embedded in the bone matrix they secreted and will differentiate into pre-osteocytes or osteoid osteocytes. Pre-osteocytes are purported to regulate and lay down mineral in the formation of new bone. As the osteocyte matures, it extends dendrite-like processes throughout the organic matrix (51). Osteocytes have been observed to extend up to 50 of these processes, which are ostensibly used as an interlaced communication structure known as the osteocytic syncytium. The syncytium senses fluid dynamics in the bone, enabling responses to external mechanical stimuli. The processes in the syncytium facilitate intracellular communication via gap junctions similar to synapses, such as found in the nervous system and cardiac muscle (52). Gap junctions facilitate the transport of small signalling molecules (53). Examples of these molecules are; nitric oxide and prostaglandins which can interact with the opposing dendrite, resulting in alterations in cellular function and gene expression. It is theorised that osteocytes interact with other bone cell types including, bone lining cells, osteoclasts, other cells in the bone marrow (50) and possibly, bone neurons and vascular endothelial cells.

Currently, there is debate on how osteocytes sense mechanical stress. Despite this it is accepted that, the ability to detect load on bone plays a critical role in bone remodelling. It is known that new bone matrix is added when load or stress is increased and that when load is reduced, bone matrix is reduced, such as, in microgravity or prolonged bed rest (52). It is currently thought that high frequency of use of the skeletal structure is necessary in order

to achieve peak bone mass. Several studies have shown that the use of imperceivable vibration on bovine bone increases the bone matrix density in comparison to a negative control (54). In effect, bone mass is regulated by peak tension and bone formation rate is regulated by frequency of use.

Under conditions of everyday use, such as locomotion, bone is placed under mechanical stress. This stress results in micro-fractures in the bone matrix. These can over time result in a significant undermining of bone structure, unless the bone matrix is replenished. If bone is not repaired then micro-fracture propagation may occur potentially resulting in structural failure. Osteocytes are considered to be sensitive to micro-fractures and damage to the osteocytic syncytium (50). This results in the osteocytes undergoing apoptosis. When an osteocyte undergoes apoptosis, it results in the promotion of bone resorption around the site of damage. The mechanism for this up regulation is still unknown and several possibilities have been theorised. One, is that dead osteocytes may release or breakdown into vacuoles that contain promoters for osteoclasts, such as RANKL. Another possibility is that the process of apoptosis in the osteocytes results in osteoclast stimulating cytokines, principally RANKL, being produced by viable osteocytes neighbouring apoptotic cells (52). Osteocyte apoptosis also results in the up-regulation of the survival factor B-cell lymphoma 2 (BCL-2) in neighbouring osteocytes. The survival of the osteocytes restricts osteoclast activity to the damaged regions of bone thus preserving healthy bone (50).

1.2.3 Osteoclasts

Osteoclasts, like macrophages, are derived from cells of the haematopoietic lineage due to identical progenitors. These cells have many similarities to one another. The addition of M-CSF to haematopoietic stem cells promotes the differentiation and survival of osteoclast precursors and macrophages *in vivo* (5). M-CSF regulates the motility and cytoskeletal organisation of both osteoclasts and macrophages. However, unlike macrophages, osteoclast precursors require RANKL, Tumour Necrosis Factor Super Family Member 11 (TNSF11), in order for differentiation into osteoclasts to occur (49). RANKL binds to the cell surface receptor Tumour Necrosis Factor Superfamily Member 11A (RANK/TNFRSF11A), a marker of committed pre-osteoclasts (55).

Osteoclasts are the cells responsible for the majority of bone resorption. Osteoclasts liberate phosphate and calcium from the bone in times of calcium deficiency and resorb damaged or fractured bone. The resorption and proliferation of the osteoclasts are highly regulated. This regulation appears to primarily occur through the RANK/RANKL interaction (5). RANK transduces its signal through the TNF receptor associated factors (TRAFs), primarily TRAF6 (56), (6). It was originally proposed that the predominant mode of repetitive presentation of RANKL to osteoclasts was via the osteoblast, however evidence has emerged that mature osteocytes play a key role in regulating osteoclastic function (48). Other cell types express RANKL, including immature osteoblasts, bone marrow stromal cells, hypertrophic chondrocytes, certain subsets of T-lymphocytes and the osteoclasts themselves (48). It is also possible that osteoclastogenesis can be driven or partially regulated by other conditions, such as growth, fracture repair, inflammation and bone cancer, independently of, or in addition to, osteocytes and osteoblasts (48, 49).

Osteoclasts are one of the few multi-nucleated cell types and each typically contain 15-25 nuclei. Very large osteoclasts, such as those present in Giant Cell Tumours of Bone (GCTB) or those derived under *in vitro* differentiation conditions, may contain a hundred or more nuclei (55). Osteoclasts have a large number of unique features in addition to their multinucleated nature (4). They have large cytoplasmic regions, increased vesicle transport capacity and a modular filamentous actin ring that enables the formation of a sealed isolated zone, under which is the ruffled border (57). The ruffled membrane is a specialised structure through which the osteoclast secretes; concentrated hydrogen and chloride ions forming hydrochloric acid and proteases to resorb the bone forming characteristic resorption 'pits', known as Howship's Lacunae (9). This enables precise resorption of bone that has been fractured or weakened to be targeted (35). It is believed that the nuclei in the osteoclasts function together at the same transcriptional rate, enabling a massive output of mRNA, functional enzymes and proteins for the resorption of bone. In order to examine the effects of vitamin D on the osteoclast, it first must be understood how the osteoclast resorbs bone and how vitamin D may interact and affect this process, be it via the CYP27B1 pathway or other alternatives.

Osteoclasts are regulated by multiple complex mechanisms, of which the most prominent is the aforementioned RANKL/RANK pathway. Despite the essential nature of this pathway and the self-inducing properties of the major transcription factor, Nuclear Factor of Activated T-cells, Cytoplasmic One (NFATC1) once it has been acted upon via the RANK pathway other factors play critical roles in the regulation of osteoclasts. CSF-1/M-CSF is essential for the regulation differentiation, proliferation and survival of osteoclast precursors and plays a role in the phosphorylation of pathways outside of the primary

RANK/RANKL pathway. Of these pathways several are immunoreceptor tyrosine-based activation motif (ITAM) regulated. The factors, osteoclast-associated immunoglobulin-like receptor (OSCAR) and triggering receptor expressed on myeloid cells 2 (TREM2) bind to the ITAM family member, TYRO protein tyrosine kinase binding protein also known as dap12 (58, 59). These together influence osteoclastogenesis and in double mutant (TREM2 and OSCAR) mice the ability of osteoclasts to form are lost. In mice carrying a single mutation in either OSCAR or TREM2, osteoclast size and ability to resorb is reduced or lost. Further examination of the role of TREM2 in raw cells using TREM2 antibody to inhibit expression resulted in failure of mature osteoclasts to resorb. Interestingly, there are reports that the loss of TREM2 resulted in an increased rate of osteoclastogenesis (60). This implies that the presence of TREM2 played a critical role in not just osteoclastogenesis and resorption but also the rate of osteoclastogenesis. While the loss of TREM2 in murine KO models did not result in complete osteoclast failure, it did result in osteopetrotic cysts forming in the bone. TREM2 is of great interest in the osteoclast lineage as it has been reported to be inhibited by vitamin D activity (1,25D) in the lungs.

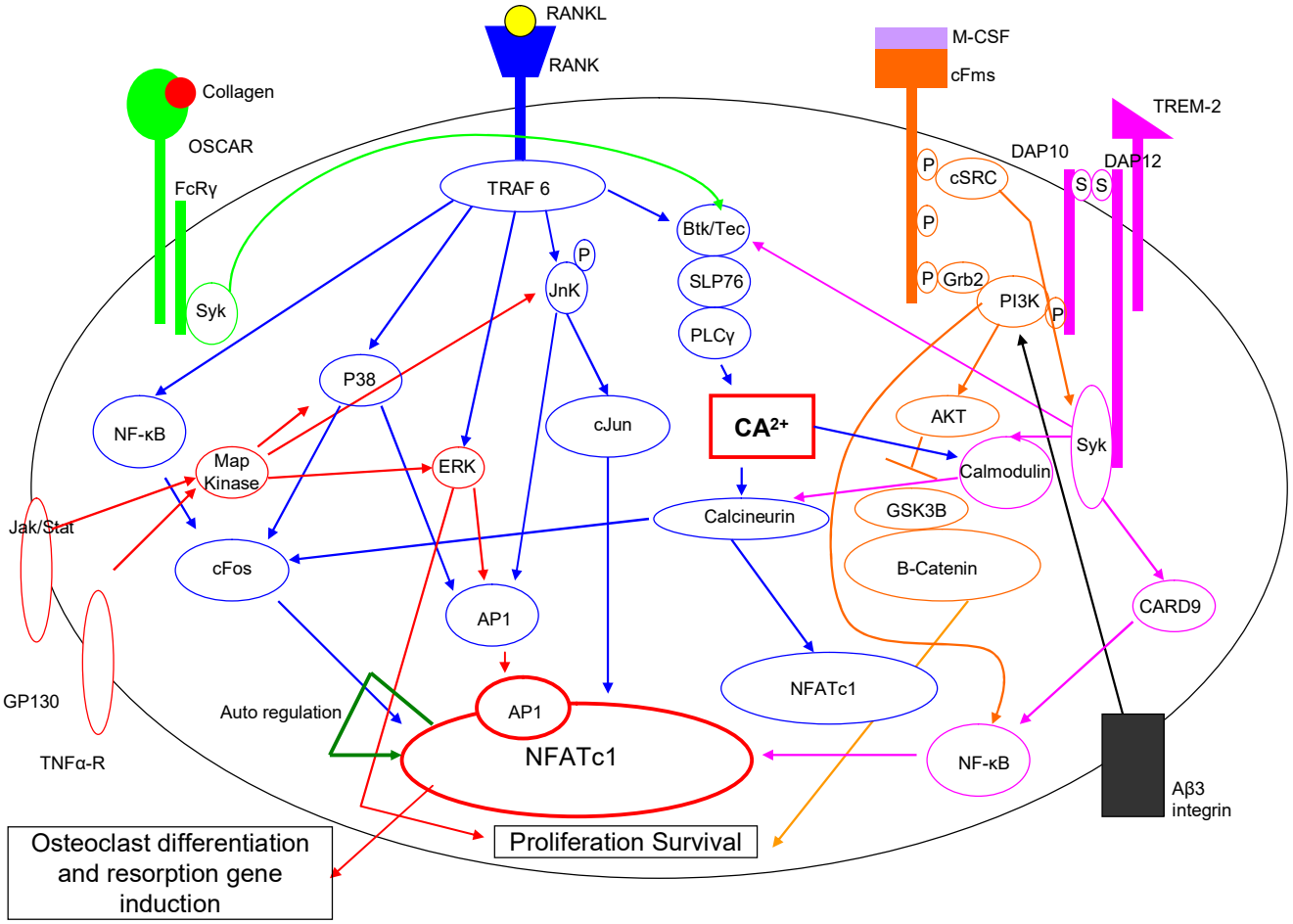

Fig. 1.3: Signalling in the osteoclasts. Overview of the mechanistic pathways involved in RANKL and M-CSF signalling within the osteoclast. This was compiled from multiple studies referenced in the text.

1.2.3.1 V-ATPase subunits

The V-ATPase pump is essential to the functioning of the osteoclast as it enables the acidification of the resorption zones without which the osteoclast would be unable to remove bone. The V-ATPase in mammals has at least 26 individually transcribed and translated subunits organised into two major functional domains, peripheral and internal. V-ATPase is a membrane bound hydrogen ion pump that uses the hydrolysis of ATP to adenosine diphosphate (ADP) to actively transport H^+ from the cytoplasm of osteoclasts through the ruffled membrane and into the isolated acidified sealed zones (57). While the underlying concept of the V-ATPase pump in the active transport of H^+ is well accepted, the activities and responses of the subunits within the pump are less well known. Hydrogen ion transportation is undertaken using rotational translocation. The central rotor of the hydrogen ion pump is bound to the peripheral rotors. Peripheral rotors are in turn attached to stator subunits that are bound into heterodimers of subunit, a and b bound to the central rotor d in the V_1 domain and is located within the cytoplasm as seen in Fig 1.4. The V_1 rotary section converts ATP to ADP causing rotary motion. The central rotor of the V_1 section is directly bound to the corresponding central rotor in V_0 domain of the pump located intracellularly. The V_1 and V_0 regions are bound via a heterodimer of v_1e and v_1g subunits. The V_0 domain is bound within the plasma membrane and can spontaneously form within this membrane upon the adhesion of the v_0c subunit. The rotation initiated by ATP to ADP conversion continues on to the v_0d subunit which also is bound to the rotary subunit v_1d. This binding causes the rotation of the subunit Ac45, which acts as the central rotor for V_0 and is bound to the c subunits responsible for transporting the hydrogen ions with the rotational movement of the pump. Like passing through a revolving door, the

hydrogen ion is moved around and then exported through the v_0a subunits. This entire system is regulated by v_1h and v_1f regulatory subunits (61). Literature has as yet only examined a few of the 26 subunits of the V-ATPase pump, others such as M8-9 and v_0e have no reported role in hydrogen ion transport. However, this does not mean they lack importance. The gene knockout models of both M8-9 and v_0e indicate severe failure of osteoclastogenesis when there is an inhibition in their overall function (61). In osteoclasts, expression of the subunit known as v_1c is highly regulated by RANKL and M-CSF (57). The loss of v_1c impairs acidification and causes the actin ring not to form. This inhibits osteoclast formation and prevents bone resorption. It was demonstrated that the V-ATPase pump as a whole has enhanced protein expression under 1,25D treatment (62). The individual subunits that respond to 1,25D however have as yet not been isolated (57). It is known that expression of the v_0a_3 subunit is up regulated 100-fold in osteoclasts. Impairment of subunit function can affect not only osteoclast resorption but also the ability for the fusion (57, 63-68) of the osteoclast precursors, indicating the essential role that the V-ATPase pump and its 26 subunits play in the osteoclast.

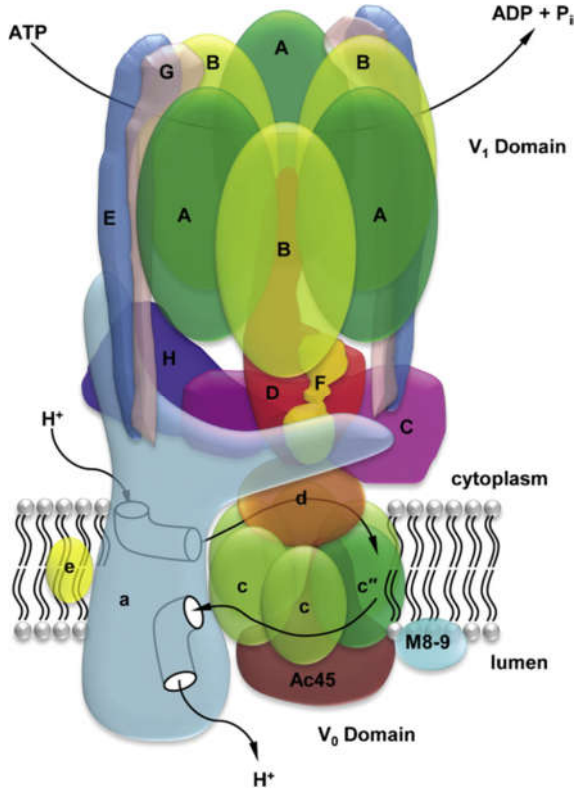

Fig.1.4: V-ATPase Structure. Structural composition of the V-ATPase subunit with all of the primary subunits displayed (57).

1.2.3.2 Integrin αvβ3 and Formation of the Sealed Zone

The recruitment of osteoclasts to the bone occurs through the interaction of the αvβ3 integrin. The gene deletion of both subunits of the αvβ3 integrin results in the functional impairment of the osteoclast's resorptive activity (69). Mice with non-functional αvβ3 integrin present with an increasingly osteopetrotic phenotype that increases with age, consistent with bone resorption being impaired (46, 70, 71). The deletion of the αvβ3 integrin results in a reduction of osteoclastogenesis, however it has been observed that M-CSF is over-stimulated in these conditions in an apparent attempt to compensate for the impairment of osteoclastogenesis (5). As knockout mice $\beta3^{-/-}$ (72, 73) still display a mild osteopetrotic phenotype, it is clear that M-CSF does not fully compensate for the loss of the αvβ3 integrin. The αvβ3 integrin is known to be sensitive to vitamin D (5). This sensitivity entails that 1,25D may act upon the cytoskeletal arrangement of the osteoclast, possibly providing a mechanism for decreased resorption despite the increase in osteoclast number observed in RAW cells (3, 4). The loss of αvβ3 integrin results in impaired attachment. When attachment occurs incorrectly or the integrin is not present, then the osteoclast's podosomes and actin ring complexes will not form correctly, resulting in the failure to resorb bone (5).

Attachment of the osteoclast occurs through the αvβ3 integrin binding to osteopontin (OPN), which is found throughout murine and human bone, as well as dentine, enabling cross reactive osteoclast activity between mammalian species. The αvβ3 integrin is essential in the cytoskeletal rearrangement of F-actin to form a complex, known as a podosome. The podosomes form a ring like structure that is intertwined together with additional cross-linking actin filaments. This combined structure forms the sealing zone

and osteoclasts are able to form 2-3 sealing zones simultaneously. It has been shown that TRAP acts to dephosphorlyate OPN and causes the αvβ3 integrin binding to break down. It has been postulated that this enables the osteoclast to move to another location to start resorption anew (74).While the αvβ3 integrin is essential for the ring formation to take place, Geblinger *et al.* (75) have provided evidence that indicates that bone roughness/smoothness is directly responsible for the frequency of the rings that form, as well as, their overall duration. Irregular and coarse regions result in increased resorption corresponding to old bone sections or simulated breaks representing damaged bone (75). The regulation of ring shape and structure by bone surface is subsumed by the deletion of the αvβ3 integrin due to the inability to rearrange the F-actin preventing the formation of podosomes and the F-actin ring. The resulting osteoclasts also present with abnormal ruffled membranes (5). This is due to the function of αvβ3 integrin in activating small Guanosine Triphosphateases, Rho and Rac, essential in the formation of the F-actin ring (76). The characteristic ruffled border of the osteoclast forms within the sealed zone, under a resorbing osteoclast and constitutes the basolateral membrane.

1.2.3.3 Acidification of the Bone Matrix

After the osteoclast has attached to the bone matrix, the osteoclast forms its characteristic ruffled membrane beneath the bone cell. The basolateral plasma membrane consists of finger like projections which secrete protons and proteases (5). The formation of the sealing zone enables the osteoclast to acidify the bone matrix releasing charged hydrogen and chloride ions in a highly localised and controlled manner (Fig 1.5). Demineralisation of the

bone is undertaken using hydrogen ions produced by the cytoplasmic enzyme, carbonic anhydrase 2 (CA2) which functions by converting water and carbon dioxide into bicarbonate and hydrogen ions (77, 78). Osteoclastic resorption of bone requires the formation and activation of the V-ATPase which transports hydrogen ions through the ruffled membrane of the osteoclasts, causing the dissociation of calcium and phosphate from the bone matrix (79). In addition, this creates a suitable pH for the activity of the protease cathepsin K.

In order to compensate for the change in membrane potential caused by the secretion of a large number of hydrogen ions, the ions are released in concert with a chloride channel (CLCN-7) (80). This channel promotes the movement of chloride ions into the sealed zone in exchange for sodium or potassium ions, depending on the surrounding extracellular matrix. This maintains the membrane potential of the osteoclast. The alteration of the membrane potential can alter the gradient of the cell causing an influx or loss of water resulting in apoptosis of the cell (4, 5, 57, 81).

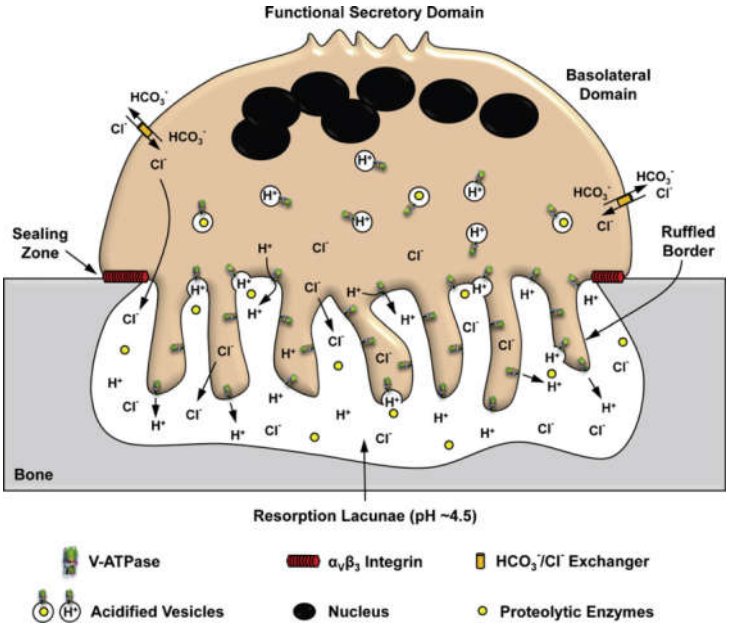

Fig. 1.5: Actively resorbing osteoclast. Osteoclast resorption through the use of an integrin mediated sealing zone. (Image taken from A. Quin *et al.* 2006)

1.2.3.4 Degradation of the Bone Matrix

The removal of the hydroxyapatite-like mineral component of the bone by hydrogen ions exposes the previously mineralised collagen fibrils (collagen type I) and non-collagenous bone matrix proteins to the activity of proteases. The micro-environment of the resorption zone is highly acidic requiring an enzyme optimised for low pH. Cathepsin K is an osteoclast-derived cystine protease that degrades type I collagen and can function in a low pH environment with an optimal pH being 5.5 with a functional range up to 7.5. Cathepsin K is produced as a zymogen and is converted to an active form as it is transported via vesicles from the Golgi (82). Vesicles containing cathepsin K fuse with the basolateral membrane releasing their contents through exocytic processes into the micro-environment between the osteoclast and the bone surface (83). Cathepsin K is a unique protease as it is able to target sites both inside and outside of the tri-helical fibrils that make up the structural components of collagen (84). Cathepsin K is a marker of mature osteoclasts as it is only produced by osteoclasts that are undergoing active bone resorption. Impairment or genetic deletion/inactivation of any one of the many components involved in the osteoclastic resorption of bone can result in diseases presenting with an osteopetrotic phenotype. In particular, the loss of cathepsin K results in a sclerosing bone disease, known as pycnodysostosis, in which collagen is unable to be degraded, resulting in the phenotype of short stature and brittle bones (84).

Cathepsin K is secreted along with TRAP. TRAP is a glycosylated, iron-containing metalloenzyme that is highly expressed in osteoclasts and chondrocytes, and has optimal activity under low pH conditions (85). It has been proposed that TRAP regulates bone matrix phosphoproteins activity by dephosphorylation and plays a role in intracellular

collagen degradation through the formation of reactive oxygen species (86). Loss of TRAP expression in mice results in a mild osteopetrotic phenotype due to reduced function of the osteoclasts. The exact function of TRAP in osteoclasts is still surprisingly not fully known but is associated with osteoclast motility (85-87). Due to TRAP being highly expressed in osteoclasts it makes an ideal histological marker for these cells (85-87).

1.2.3.5 Apoptosis and Autophagy in Osteoclasts

Self-regulated apoptosis plays a significant role in osteoclasts function. As a destructive cell that actively removes the structural elements of the skeleton, the ability to regulate osteoclast activity is essential. Examples of unregulated osteoclast activity can be seen in GCTB that actively resorb the bone around them until the structure of the bone in question is compromised and fails. Osteoclasts, like many cells use, BCL-2 and BCL-2 associated X (BAX) proteins to regulate their survival (88). BCL-2 acts to prevent apoptosis and inhibits BAX and other pro-apoptotic proteins by binding to the B3 domain, altering their structure, preventing the activation of the apoptotic cascade. BAX serves the opposite function of BCL-2, in that, it activates apoptosis (89). BAX acts in the mitochondria and activates the cytochrome C pathway. BAX is bound by BCL-2 in the cytoplasm before it can pass into the mitochondria and initiate apoptosis. It is common practice to compare the ratio of BAX to BCL-2 protein or mRNA to indicate if a given cell culture is leaning towards apoptosis (90). As this ratio increases, the rate of apoptosis increases and, as the ratio decreases, then the rate of apoptosis also decreases. While BAX and BCL-2 are the major players in apoptosis, other proteins such as Induced Myeloid Leukemia Cell

Differentiation protein (MCL-1), BCL-2 Like protein Eleven (BIM) and B-cell Lymphoma-extra Large (BCL-XL) are also important in this regard. MCL-1 and BCL-XL bind to pro-apoptotic proteins inside the mitochondria and prevent their conformational change, preventing the activation of cytochrome C (91).

Autophagy plays critical roles in cell remodelling and the regulation of cell survival. In the osteoclast, autophagy is essential for protease release, osteoclast motility and self-mediated apoptosis. Of particular note, BAX plays an essential role in autophagy. BAX has been indicated as a major player in the release of vesicles containing bone degrading elements. This enhances the importance of the BAX/BCL-2 ratio, as elevated BAX levels may be essential for osteoclast activity. It has been hypothesised that an osteoclast will require high levels of BAX to function and will require higher BCL-2 levels to offset this. Literature has indicated that vitamin D may play a role in multiple cell types in regulating apoptosis by altering the levels of BAX and BCL-2 (92). Thus the regulation of the loss or impairment of the vitamin D metabolic pathway may result in changes to apoptosis and may provide insight into the role of autocrine vitamin D activity within the osteoclast.

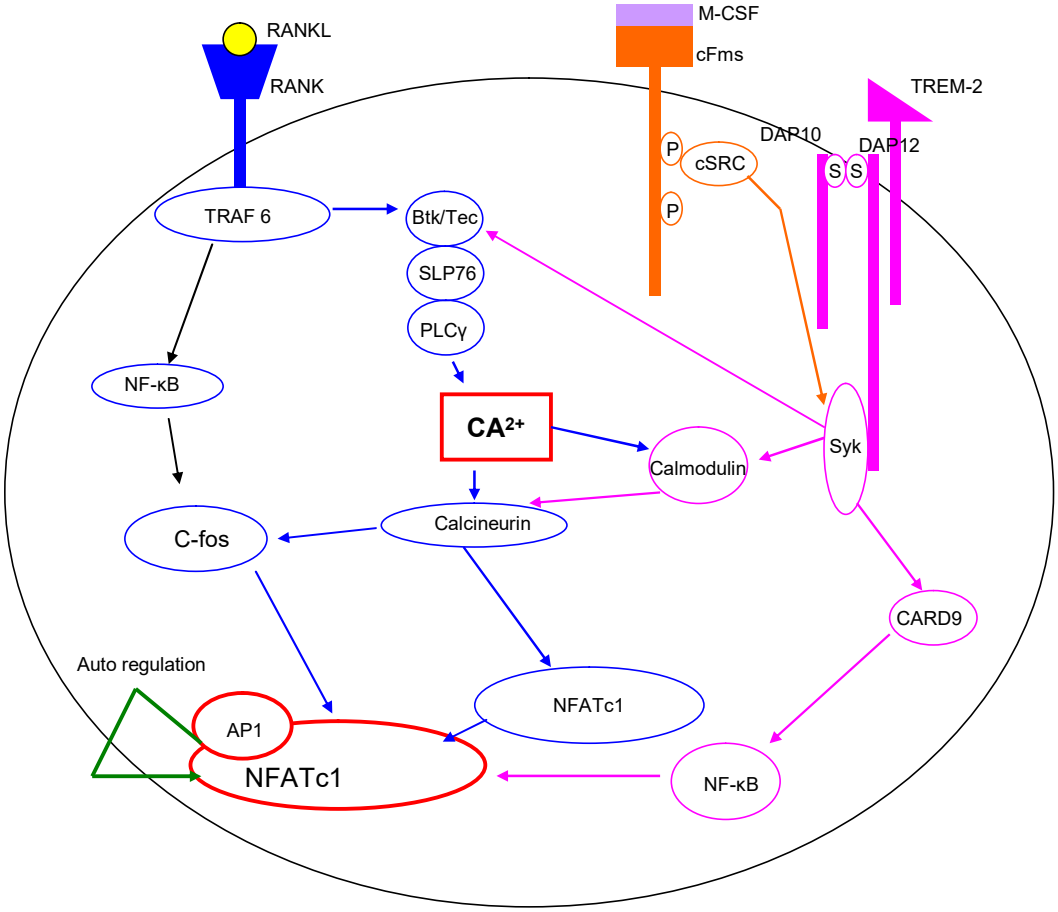

Fig. 1.6: Simplified signalling in the osteoclasts. Simplified overview of the mechanistic pathways involved in RANKL and M-CSF signalling within the osteoclast. This was compiled from multiple studies referenced in the text.

1.3 Autocrine Actions of Vitamin D in Bone

The presence of the VDR has been established in multiple tissues using numerous techniques (93). The role of vitamin D in the osteoclast has been debated for almost as long as the osteoclast has been established as an essential bone cell. While it has been well established that the osteoblast and osteocyte has the ability to respond to the exogenous and autocrine vitamin D, the ability for the osteoclast to respond to vitamin D is debated (94). Contradictory articles can be found towards the presence of VDR receptors in osteoclasts (95) and (94). This reinforces the need for the clear establishment of the presence of VDR in the osteoclast and a way of identifying the presence of VDR using multiple techniques.

1.3.1 Autocrine Actions of the Osteoblasts

Vitamin D through its active metabolite 1,25D has been demonstrated to regulate osteoblast functions. 1,25D upregulates RANKL expression in immature osteoblasts (36). Atkins *et al.* (2) demonstrated that the presence of both 25D and 1,25D resulted in the inhibition in osteoblast proliferation and increased mineralisation. HOS cells combined with Small Interfering Ribonucleic Acid (siRNA) knockdown specifically targeting CYP27B1 was used to demonstrate the reliance of 25D conversion to 1,25D on CYP27B1 within the osteoblasts. Atkins *et al.* also demonstrated that human osteoblastic cell lines and primary cells constitutively expressed CYP27B1. The presence of autocrine vitamin D activity within the osteoblast indicated the potential for autocrine regulation to present within the other bone cells.

The osteoblast was reported by Van Driel *et al.* (96) to exhibit autocrine-paracrine activities under the local conversion of 25D to 1,25D. This conversion inhibits osteoblast proliferation and increases the expression of RANKL mRNA. Osteocalcin (OCN) and OPN are vitamin D responsive genes transcribed by the osteoblast and associated with ontogenesis, both of which are regulated by 25D (2). Cubilin and megalin were examined by Atkins *et al.* (2) and it was observed that cubilin mRNA, which is found at high levels in the osteoblast, was down-regulated upon exposure to 25D. Megalin was shown to be present basally but at low levels and no regulation of expression was observed (2). This finding was surprising as megalin is believed to operate with cubilin as co-transporters in the kidney (97). The down-regulation of cubilin expression however, indicates possible autocrine activities of 25D.

CYP27B1 activity has been associated with key genes of osteoblast maturation and mineralisation. It has become apparent that autocrine activity of CYP27B1 plays an important role in the regulation of the osteoblasts at varying stages of development (96). CYP27B1 activity is higher in osteoblast derived cells that are mineralising than in osteoblasts that are proliferating. This is presumed to be due to the more immature proliferating osteoblasts mounting a RANKL response to 1,25D, unlike the mineralising osteoblasts that promote osteogeneic function (98). The significance of autocrine responses to vitamin D in osteoblasts is not yet fully elucidated (2, 96, 99).

1.3.2 Autocrine Actions of Vitamin D in Osteoclasts

Kogawa *et al.* (3) showed that CYP27B1 activity in the osteoclast results in the conversion of 25D to 1,25D and has an up-regulatory effect on many of the characteristic genes of the osteoclast. Overall, Kogawa *et al.* (3) suggested that increased CYP27B1 activity results in the increase of osteoclastogenesis while causing a reduction in resorption. In particular 25D conversion altered the expression of many well-established osteoclast related genes.

It was observed that 25D conversion resulted in the up-regulation of *Nfatc1*, Transcription Factor Proto Oncogene (*C-Fos)*, *Oscar*, (Calcitonin Receptor) *Ctr*, *Trap*, *Ctsk* and *Ca2* in the mouse macrophage cell line with osteoclastogenic potential, RAW 264.7 (4). In human cells, the expression of *Nfatc1*, *C-Fos, Oscar, Ctr, Trap, Ca2, V-ATPase, Clcn-7* and (Dendrocyte Expressed Seven Transmembrane Protein) *Dc-stamp* were all up-regulated (4) (100, 101). The effect of 25D on apoptosis was also examined.

Caspase 3 activity was measured in human peripheral blood mononuclear cells (PBMCs), a source of osteoclast precursors, to examine the effects of 25D on osteoclast apoptosis as a possible mechanism for 25D effects on osteoclastic resorption (102). While caspase activity was increased when 1,25D was present in early stage osteoclasts, 25D had no effect on caspase activity (102) and it was apparent that there was no increase in cell death above that of baseline cells treated with RANKL and M-CSF.

In a previous study by Kogawa *et al.* (4), it was shown that in the presence of RANKL, 25D time-dependently increased the levels of *C-Fos*, a critical component of the dimeric transcription factor Activator Protein 1 (*Ap-1)* and *Nfatc1*. *Ap-1* and *Nfatc1* are essential in osteoclastogenesis. The presence of 25D increases the levels of *Ap-1* and *Nfatc1*

transcription factors resulting in the promotion of osteoclastogenesis. It was noted that the expression of osteoclast marker genes, such as *Oscar* (103), a co-stimulatory regulator for osteoclast differentiation, *Ctr* and *Trap* was also increased. The change in gene expression under 25D was modified under the addition of exogenous 1,25D.

The paper presented by Kogawa *et al.* (4) observed that 1,25D resulted in the suppression of osteoclast differentiation. The varying effects of 25D and 1,25D were suggested by Kogawa *et al.* to be due to CYP24A1 activity. It was observed that 25D at 50 nmol/l stimulated *Cyp24a1* mRNA expression 100-fold less than 1,25D at 1 nmol/l. The use of siRNA knockdown approach resulted in the reduction of *Cyp27b1* and the subsequent impairment of the conversion of 25D to 1,25D causing the inhibition of osteoclastogenesis (4). As treatment with 25D resulted in an increase of gene function and did not instigate cellular apoptosis, decreases in resorptive activity of the osteoclast are hypothesised to be achieved via a modification of a post-translational mechanism.

One of these proposed post translational mechanisms is the subunits of the V-ATPase pump that have been demonstrated to be sensitive to 1,25D (7). This is just one possible post-translational mechanism, by which locally synthesised 1,25D might modulate osteoclast activity. Characterisation of such mechanisms will be critical in our understanding of the role of vitamin D metabolism in osteoclasts.

1.3.3 Mouse Models of Vitamin D Activity in the Skeleton: *Vdr*KO and *Cyp27b1*KO

Mouse lines carrying global deletions of the *Vdr* or *Cyp27b1* genes have been used to study the effects of vitamin D on the skeleton, and have also provided proof of autocrine synthesis within bone cells. The *Vdr*KO mouse was developed by Li YC *et al.* (104). These mice have difficulty maintaining calcium homeostasis and rapidly present with hypocalcaemia. By 35 days of age, the mice present with a significant amount of un-mineralised bone. The *Vdr*KO mice also present with alopecia, which is apparently unrelated to the inability of these mice to respond to 1,25D (104). The usefulness of this mouse model was enhanced by the finding by Amling *et al.* (105) that after weening the health of mice could be maintained through the use of a rescue diet.

The gross phenotype of *Vdr*KO mice can be normalised with a 2% calcium, 1.25% phosphate and 20% lactose 'rescue' diet. In $Vdr^{-/-}$ mice fed with a normal chow diet, 85% of their bone is composed of osteoid by day 70, the osteoid volume being 30-fold greater than that of their wild-type littermates. *Vdr*KO mice that are fed the rescue diet have normal calcium homeostasis. The implication being that vitamin D is restricted to the role of maintaining calcium homeostasis in the endocrine system. However, there were limitations of the work done by Amling *et al.* (105), who only reported the phenotype of mice to the age of ten weeks. Further studies looked at mice in older age.

Panda *et al.* (31), using the same strain as the Amling *et al.* (105), reported on *Vdr*KO mice to the age of 17 weeks. It was reported that mice fed the rescue diet until 17 weeks of age still had significantly decreased percentage of trabecular bone volume: tissue volume

(%BV/TV), in the range of 50%, compared to wild-type animals. From this it can be concluded that vitamin D is essential in maintaining bone health at older ages independently of endocrine actions on calcium homeostasis. This mouse model was useful in examining the effects of the loss of vitamin D.

*Vdr*KO mice lack the ability to respond to 1,25D (105) (Fig 1.8). *Cyp27b1*KO mice, on the other hand, lack the ability to synthesise the active form of vitamin D (Fig 1.7). Calcitriol however, can be introduced into experimental protocols and due to the functioning *Vdr* result in cells that respond to 1,25D. The inability of cells from these animals to convert 25D to 1,25D enables the examination of vitamin D metabolism at the autocrine level within the osteoclast.

The *Cyp27b1*KO model was first reported by Dardenne *et al.* (32), who stated that these mice had retarded growth, hypocalcaemia, secondary hyperparathyroidism and bone anomalies that included rickets and osteomalacia (32). The same group then published data showing that the *Cyp27b1*KO mice could also be rescued by the introduction of a high phosphate, calcium and lactose diet, as was seen in the *Vdr*KO mice (106, 107). This paper also provided evidence that the use of a rescue diet completely restored *Cyp27b1*KO mice and indicated that vitamin D was only involved in endocrine calcium homeostasis. Panda *et al.* (31), extended the experimental protocol past ten weeks and showed that *Cyp27b1*KO mice of 17 weeks of age had reduced trabecular bone volume, implying that the aforementioned rescue diet in fact does not fully compensate for vitamin D loss.

Panda *et al.* also used a CYP27B1, VDR, double KO mouse, which had a phenotype that was a combination of the deficiencies present in the other KO models (31). Panda *et al.*

hypothesised that vitamin D played a greater role than that of regulating calcium homeostasis (31). This conclusion was reached as the KO of CYP27B1 resulting in the inability to convert 25D to 1,25D did not have the same effect as that of the *Vdr*KO mouse model. Panda *et al.* observed that in both the double-knockout and the *Vdr*KO mouse models that Parathyroid Hormone (PTH) levels were elevated and that osteoclast size was reduced (31). It was proposed that the loss of 1,25D signalling resulted in the increase of PTH causing an increase in osteoclast formation (31). High concentrations of PTH in the *Cyp27b1* and *Vdr*KO mice were observed. This was hypothesised to result in increased osteoclast numbers, however no changes were observed. Similar levels of increased PTH expression in a wild-type murine model would be expected to result in increased osteoclast numbers. This was not observed in the KO models (31).

Spleen cells were selected preferentially over other potential sources of osteoclast precursors, such as RAW 264.7 cells and PBMCs. PBMCs were excluded as the ability to delete CYP27B1 in these cells is limited to siRNA knockdown methods. RAW 264.7 cells can be genetically modified to not express CYP27B1 but as it is an immortalised cell line, other significant changes to the underlying genetics are likely to be present. The animal models in mice for *Cyp27b1* global knockout were available and have a well-established phenotype.

Several types of cell culture from KO mice were considered. Co-culture of the spleen cells with other cells and bone marrow cultures were undertaken. The culture of splenocytes with bone marrow can provide insights into osteoclast behaviour. However, the global deletion of *Cyp27b1* and *Vdr* results in modification to all of the cells in the bone marrow making it a less specific culture model. By using a splenocyte monoculture we were able

to observe the effect of *Cyp27b1* deletion independent of the mesenchymal signalling. Co-culture models are the predominant use for splenocytes.

The addition of 1,25D to RANKL and M-CSF treated PBMCs has had contradictory reports of both inhibitory and stimulatory effects on osteoclast formation (3, 4). The addition of 1,25D to raw 264.7 cells enhanced osteoclast formation. The effect of 1,25D addition on osteoclast formation is highly dependent on the model of osteoclast used. In this experiment we used spleen cells, therefore the direct comparison of these results to other models, such as PBMCs and RAW cells, must be undertaken with caution.

The use of human derived PBMCs in particular are important, as they enable a direct comparison between autocrine effects in mouse osteoclasts and human osteoclasts. It is worth noting, that the cytokines used for this experiment were human derived but still work on murine cells, indicating the potential for similarity between the two models. However, the role of autocrine activity in osteoclasts is still being debated. The use of mouse models as a precursor step, especially as the modification of humans at the genetic level for the use of scientific experimentation is unethical, to establish autocrine activity in the osteoclast is essential before moving onto discussion of similarity between the two models.

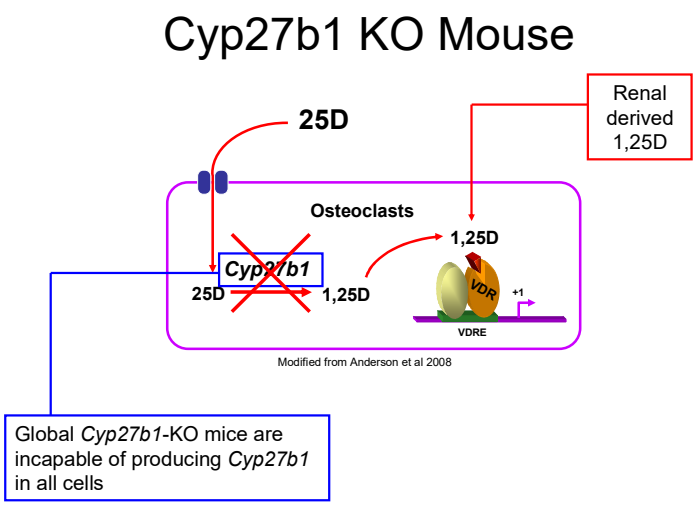

Fig.1.7. Effect of *Cyp27b1* deletion in osteoclast lineage cells. The effect of *Cyp27b1* deletion within the osteoclast while identifying the vitamin D pathways that are still functioning.

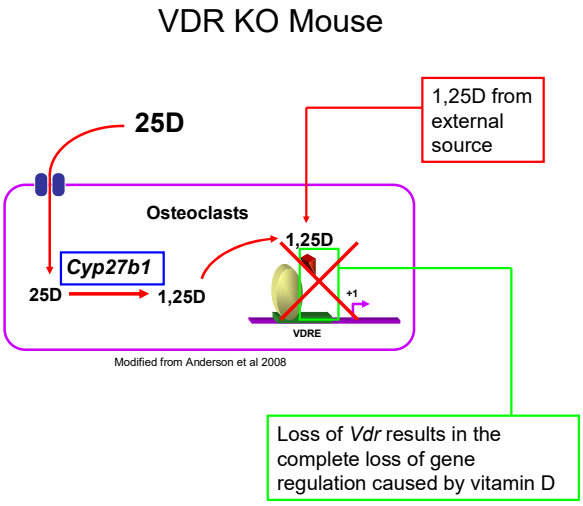

Fig. 1.8. Effect of *Vdr* deletion in osteoclast lineage cells. The effect of *Vdr* deletion within the osteoclast identifying the vitamin D pathways that are still functioning.

1.4 Aims and Hypotheses

The aim of this thesis is to extend previous findings indicating the presence of an autocrine vitamin D response in the osteoclast lineage, particularly in murine osteoclast cultures and seek to elucidate the cellular pathways involved. This will be undertaken through the use of *Vdr* and *Cyp27b1*KO mouse models in the absence of stromal signalling. This enables the examination of potential autocrine vitamin D response through multiple experimental pathways including osteoclast activity, maturation, proliferation and gene expression.

Overall, we hypothesise that the loss of vitamin D autocrine signalling will have a deleterious effect on osteoclast maturation and proliferation, and result in osteoclasts with greater bone resorptive activity. This overarching hypothesis is divided into multiple smaller hypotheses: Thus, we hypothesise:

1) That the deletion of CYP27B1 will result in the failure of the autocrine vitamin D pathway in osteoclast lineage cells resulting in altered gene expression and increased resorption activity although osteoclasts formed will still be able to respond to exogenous 1,25D;
2) That the deletion of VDR will result in the failure of both the autocrine vitamin D pathway and the ability to respond to exogenous 1,25D in osteoclast lineage cells, resulting in osteoclasts with altered gene expression and increased bone resorption activity;
3) That the addition of exogenous 1,25D will be unable to completely restore functionality in both *Cyp27b1*KO and *Vdr*KO-derived osteoclasts;

4) That the loss of vitamin D autocrine pathways in osteoclast lineage cells will result in significant modifications to the individual subunits of the V-ATPase.

Chapter 2

Materials and Methods

2.0 Materials and Methods

2.1 Animals

Mice with global gene deletions (knockout; KO) of either *Cyp27b1* (*Cyp27b1*KO) (32) or *Vdr* (*Vdr*KO) (104), or with conditional deletion of *Vdr* under control of the cathepsin K promoter (CTSK-Cre.Vdr$^{fl/fl}$) (32) were housed at ambient temperature with free access to water and food, with established 12 hour day-night cycles. All mice were fed the KO 'rescue diet', consisting of chow containing 2% calcium, 1.25% phosphate and 20% lactose, which prevents rickets and bone abnormalities associated with these models (107), until genotyped and removed for weaning. After weaning, confirmed KO mice were fed the rescue diet while heterozygous KO and wild-type (WT) mice were fed a standard chow diet. All animal procedures were approved and performed in accordance with the requirements of the animal research ethics committees of the University of Adelaide and the University of South Australia.

2.2 Mouse Tail Processing

The tip of all mouse tails were collected at 10 days of age using surgical clippers as there is no vascularisation at this age. Anaesthetic is not required and has no impact on the health of the animal. Tails were stored at -21°C. The removal of the tail tips has a minimal effect on animal health at this age. Tails were then processed in a digestion buffer consisting of 500µl tail buffer (10% SDS, 1M Tris HCL, 500mM EDTA, 4M NaCl and Milli Q water) and 10µg Proteinase K. Tails were digested overnight at 55°C in a dry block heater (Ratek Instruments) until completely dissolved. Samples were then centrifuged for 5 mins at

1500g (Centrifuge 5417r Eppendorf 22331 Hamburg, Germany). 90% supernatant was transferred to a new Eppendorf tube and diluted in 1ml of 100% isopropanol (Sigma Aldrich Steinem, Germany 89552). Samples were spun at 5009g, then the supernatant discarded and the pellet dissolved in 75µl of Tris EDTA (TE) buffer. DNA levels were quantified using a nano-spectrophotometer (General Electric, Nano View +). Samples were diluted to 20ng/µl and then used in RT-PCR.

2.3 RT-PCR of Genotype

Real Time Polymerase Chain Reaction (RT-PCR) of *Vdr* and *Cyp27b1*KO mice used primers designed to detect the unmodified *Cyp27b1* and *Vdr* gene and the genetically modified versions of these genes. The genetically modified form of this gene was manufactured through the use of restriction enzymes and the insertion of a neomycin cassette resulting in inactivity.

Primers (Gene Works Australia, SA, Adelaide) were then run consecutively in a RT-PCR using SYBR green master mix (Qiagen Sciences Maryland, USA) in a thermocycler (Bio Rad CFX-Connect USA). Genotype was established through the presence and absence of gene amplification. Amplification of WT or KO genes only identified homozygous WT or KO mice. Amplification of both sets of genes denoted heterozygous mice (Fig. 2.1-2.3.).

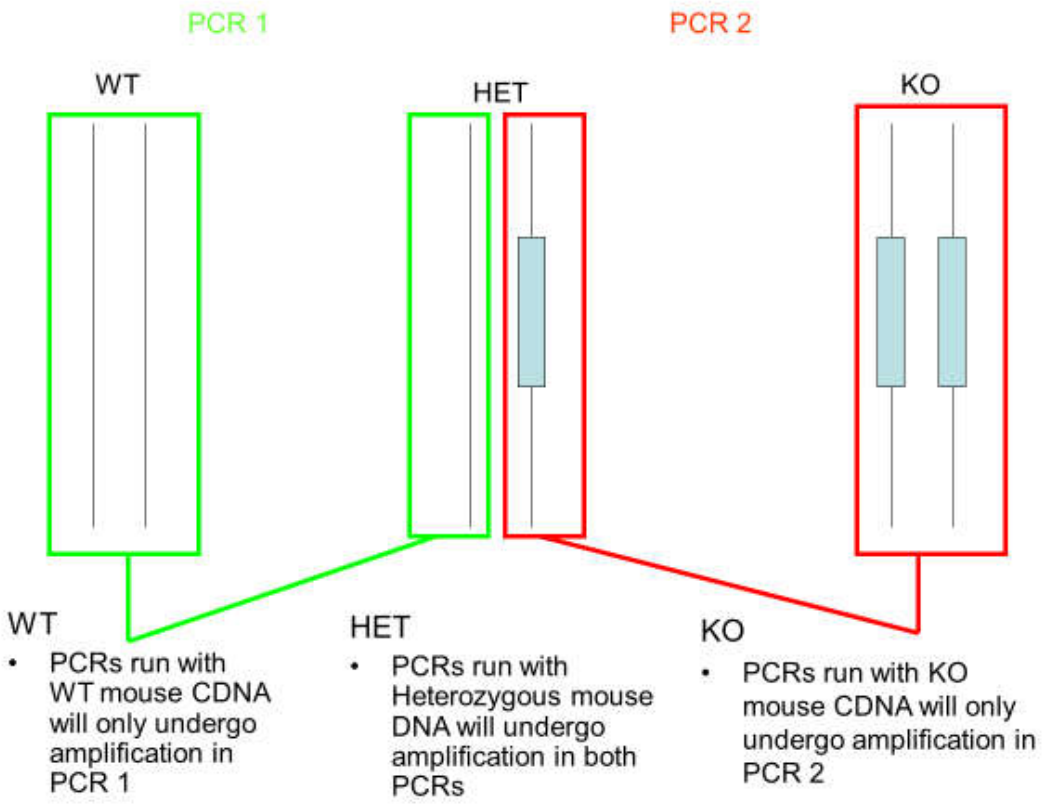

Fig. 2.1. Amplification of mouse DNA. The amplification of WT mouse genetic material is highlighted in green. Amplification of mouse DNA from the KO genetic material is highlighted in red. It can be observed how WT heterozygous and KO mice can be identified from genetic amplification.

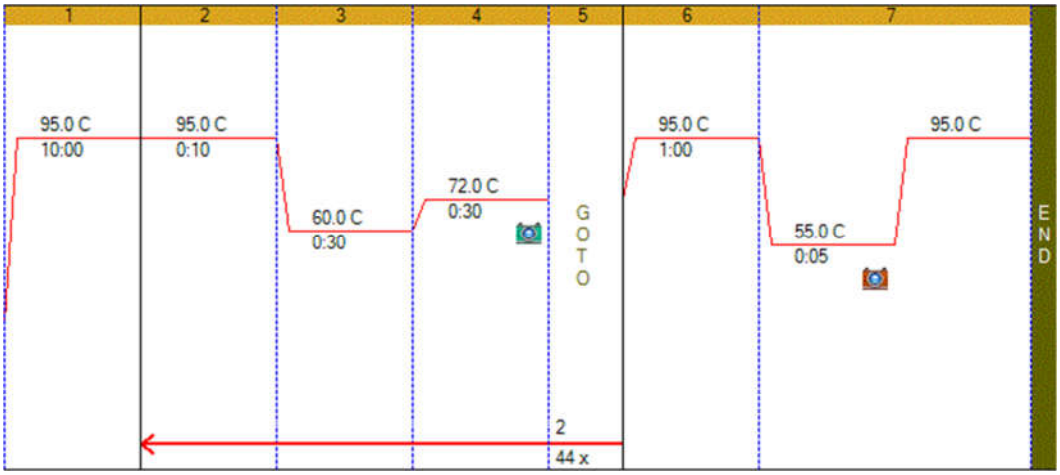

Fig. 2.2. Amplification protocol. Amplification protocol for real time RT-PCR. Initial heating was done for 10 minutes at 95°C. Samples were amplified over 46 cycles with each cycle consisting of 95°C for 10 seconds, then 60°C for 30 seconds, followed by 72°C for 30 seconds. Samples were heated to 95°C slowly by increments of 0.5°C to establish melting point.

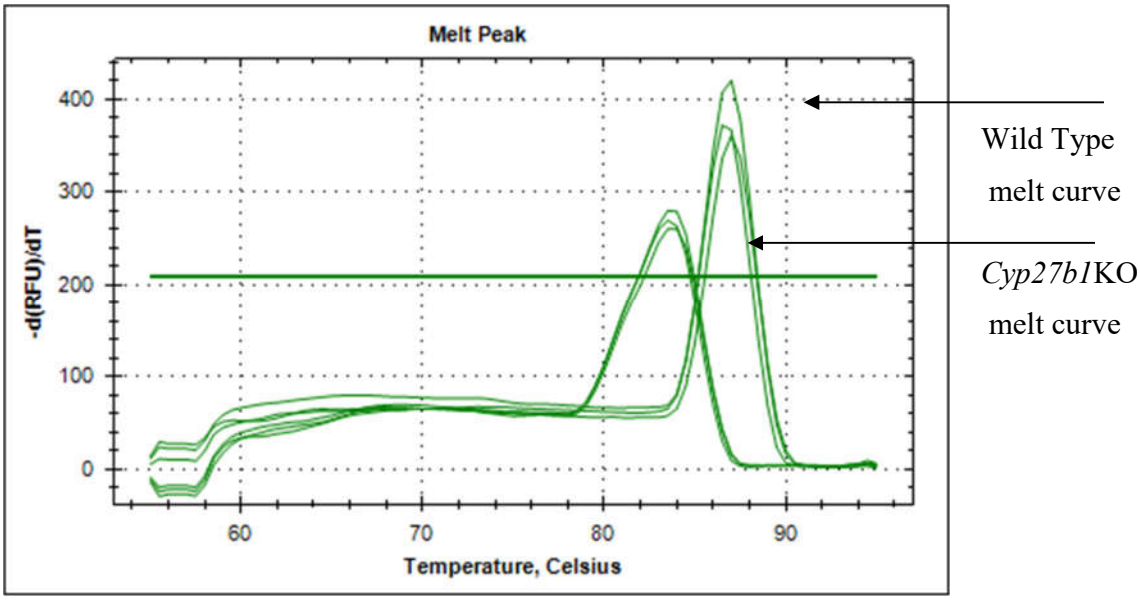

Fig. 2.3. Melt Curves. Melting points for WT and *Cyp27b1*KO mice gene amplification. All samples are run in triplicate. It was observed that the melting points between these amplified genes were easy to identify as the melting points were different. This allowed easy identification of WT, heterozygous and KO mice from genomic DNA. The lower peak represented *Cyp27b1*KO melt curve and the second peak represented WT melt curve.

2.4 RNA/DNA Gel

In order to confirm the quality of the DNA, genotyping samples were also run on agarose gels (1% w/v in TE buffer). For this, agarose was heated in a microwave until dissolved. Sodium hydrochloride (500µl) and 2-3µl of Gel Red TM (Sigma Aldrich Steinem, Germany 89552) was added to the agarose gel and the solution poured into a gel cassette. The DNA samples (6µl) were loaded individually and the gel run at 80-120 voltage on an electrophoresis unit. (Horizon 20.25, Life Technologies)

2.5 Preparation of Splenocytes for Osteoclastogenesis Assays

Mice were humanely euthanized through carbon dioxide euthanasia and dislocation of the vertebrae. The carcass was washed in 70% ethanol to minimise contamination and to prevent aerosolization of murine fur. The carcass was then placed in a Class II biohazard cabinet. Spleens were aseptically excised and placed in Minimal Essential Media-alpha (αMEM; Sigma Chemical Co., St Louis, MO, USA). Spleens were dissected with surgical scissors and the pieces gently ground between two sterile glass microscope slides in order to release the cells from the surrounding tissue. Alternatively, mouse spleens were dissected with surgical scissors and the pieces gently ground through a 20µm cell strainer using a 1ml syringe plunger. Red cell lysis buffer, consisting of Tris Buffered Ammonium Cholride (TBAC) was then added and cells washed three times in αMEM, containing 10% (v/v) charcoal stripped foetal bovine serum (S-FBS) (HyClone, Logan, UT, USA), 1% penicillin, 2mM L-glutamine and HEPES. Where indicated, cells from four spleens/genotype were pooled, counted using Trypan blue (0.4%) exclusion, and plated

into 96-well tissue culture plates for TRAP staining (section 1.8) and onto sperm whale dentine or onto Osteologic^{TM} slides (BD Biosciences, Bedford, USA) for measuring osteoclastic resorption activity, at 2 x 10^5 cells/well. Alternatively, cells were added at $1x10^6$ cells/well into 24 well plates for TRIzol based RNA extraction (108). Cells were treated with differentiation media consisting of αMEM supplemented as above, with the addition of: recombinant M-CSF (Millipore, Temecula, CA, USA) (25 ng/ml = *untreated/UT*) or M-CSF + RANKL (Millipore) (100 ng/ml = *positive control*). In some experiments the effects of exogenous 1,25D and 25D (Wako Pure Chemicals, Japan) were assessed. The level of 1,25D used was 1 nM, which we have shown to be equivalent in efficacy to that of a physiological concentration of 25D (100 nM) in terms of inhibiting resorption in cultures of both RAW 264.7 cells and PBMC (4). All cell cultures and lines were maintained at 37°C with 95% humidity and 5% CO_2 to mimic physiological conditions.

2.6 Preparation of Bone Marrow for Osteoclastogenesis Assays

Mice were humanely euthanized and spleens excised and placed in αMEM (Sigma Chemical Co., St Louis, MO, USA), as described above. After the excision of the spleen, the tibia and femora were removed. Bones were removed carefully to ensure that they were structurally intact ensuring maximum yield of bone marrow. Additional care was taken with *Vdr*KO mice as their bones were brittle. The distal and proximal ends of each bone were removed and the marrow was flushed with media using a 0.6mm diameter needle (BD Precision Glide). The bone marrow was combined from multiple mice of each genotype

(n=3) and from both femora and tibias. Cells were then pelleted by centrifugation at 176g (Megafuge 1.0R, Heraeus) in a 50ml sterile tube (Falcon) and then treated with lysis buffer (TBAC) to remove red blood cells. The cells were then washed by centrifugation three times in media before being resuspended in 10 ml of media containing FBS (10% v/v). Cells were then counted using the Trypan blue dye exclusion method and resuspended to a concentration of 1 x 10^6 cells/ml. Cells were then plated into 96-well plates for TRAP staining or into 24 wells plates for mRNA.

2.7 Preparation of Osteoclast Cell Line RAW 264.7 for Culture

RAW 264.7 cells were kindly supplied by Dr. David Thomas (Peter McCallum Institute, Melbourne, Australia) and were originally from the American Type Culture Collection. RAW 264.7 cells were thawed, cultured and frozen down as described previously (109). Briefly RAW 264.7 cells were thawed from cryogenic storage using a slow drip method of media of 1 ml over 1 minute at 5 minute intervals in order to dilute the freezing mixture and ensure cell survival of the cryogenic storage. RAW 264.7 cells were cultured in t-75 (Interpath Sheehan Rd, Heidelberg West, VIC, Australia) flasks under media and FBS (10% v/v) until confluent. Cells were scraped using a cell scraper (7-9 Summit Road, Noble Park North, VIC, Australia 3174,). Cells were collected, then counted using the Trypan blue dye exclusion method and resuspended to a concentration of 1x10^6 cells/ml for further passage or resuspended to 1x10^3 cells/ml for 96 well plates for osteoclast assays. Excess raw cells were frozen down using DMSO freezing mix and an insulated container in a -80°C freezer (TSE Series, Thermo Scientific) before being transferred to a liquid nitrogen storage facility for long-term storage.

2.8 TRAP Staining of Osteoclast Cultures

TRAP staining was performed, as described previously (4). Briefly, quadruplicate cultures were stained for TRAP using a commercial kit (Sigma). Cell cultures were fixed with 10% formaldehyde for 10 minutes before being washed. TRAP stain was then added to cultures for 46 minutes after which cultures were washed three times and then counted (TRAP staining Kit Sigma-Aldrich, Steinem, Germany). Osteoclasts were defined as magenta stained cells containing three or more nuclei. Osteoclast nuclei numbers were assessed using light microscopy (Nikon Eclipse Te300). TRAP staining was examined at multiple time points during the experiment. Osteoclast nuclei were counted at the same time and divided into categories of size, this being 3-10, 11-25 and 25+ nuclei. Data was analysed using two way ANOVAs and Tukey post hoc tests. Images were taken using Olympus CKx-41 with DP20 camera and u-rflt50 lamp (Fig. 2.4-2.5.).

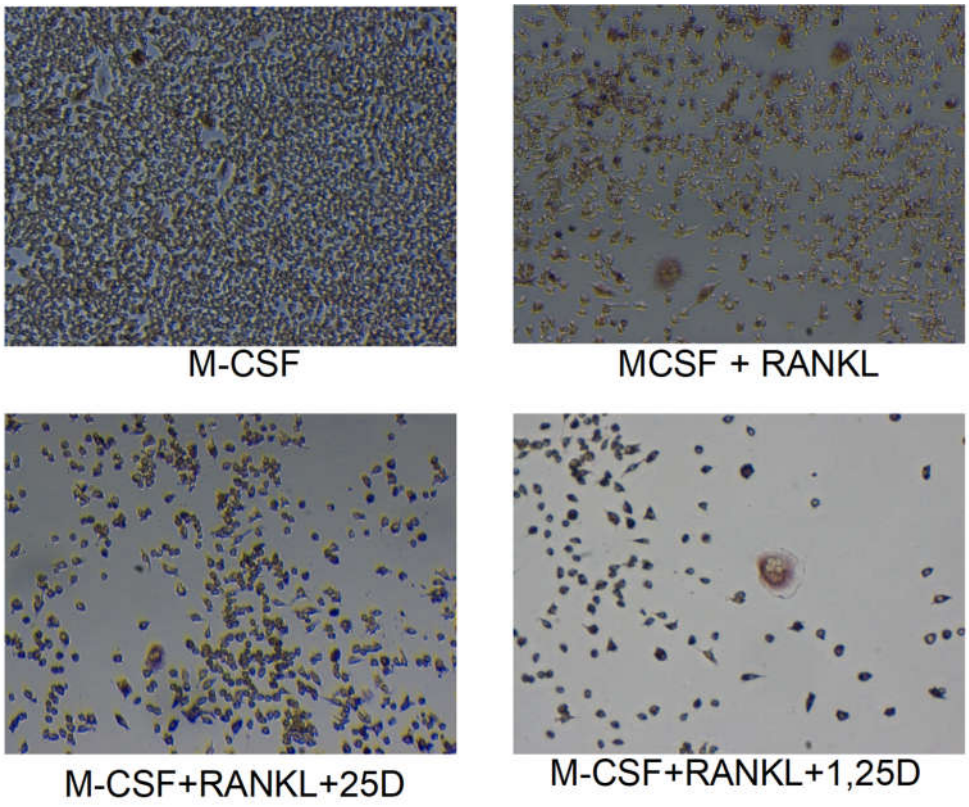

Fig. 2.4. RAW 264.7 cells. Confocal light microscopy images of RAW 264.7 cells under osteoclastogenic conditions and TRAP staining.

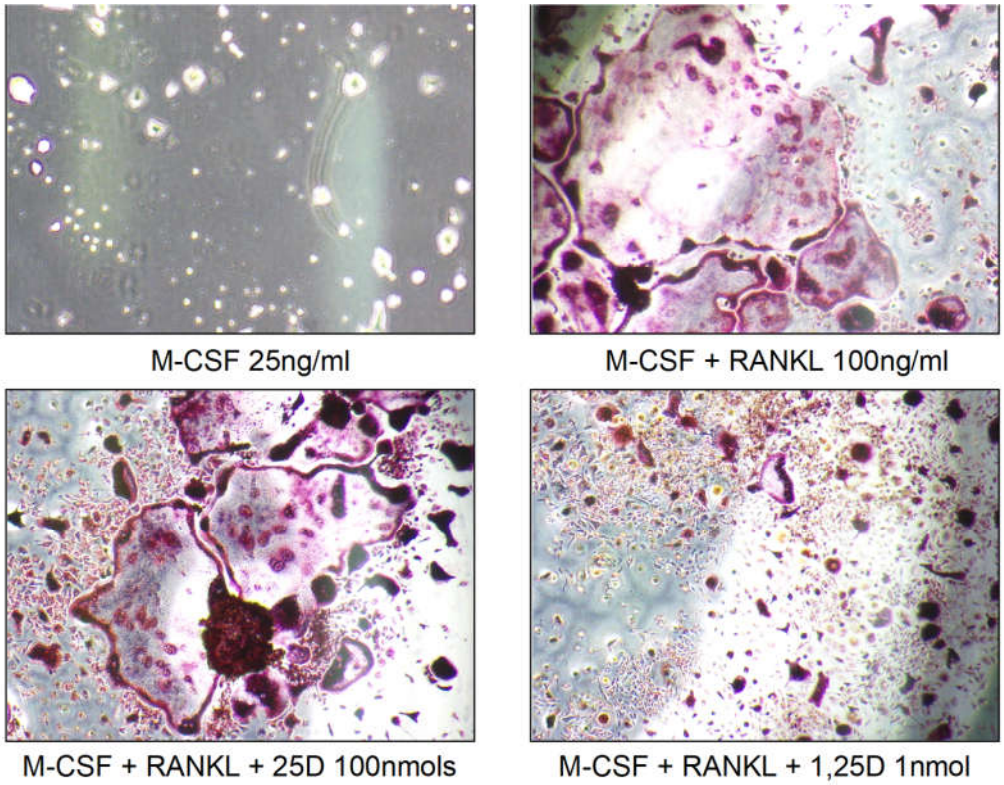

Fig. 2.5. Spleen cells. Confocal light microscopy images of spleen cells under osteoclastogenic conditions and TRAP staining.

2.9 Resorptive Activity

Resorptive activity was measured as described previously (4). Briefly, following the 10 day (d) culture period, Osteologic^{TM} slides resorption sites were visualised using Von Kossa staining which stains the non-resorbed mineral background, highlighting areas of osteoclastic activity. Resorption was quantified using light microscopy and Image J software (V 1.47, National Institute of Health) analysis.

2.10 Von Kossa Staining

Sodium hypochlorite (1 %) was added to the culture to remove cells without impacting on the hydroxyapatite layer on the bottom of the slides. Silver nitrate (5%) wash was added to the wells under a bright lamp for 30 min (110). The wells were then rinsed with reverse osmosis (RO) water and then the stain was developed by adding a drop of 5% sodium carbonate in 25% formalin. The stain was fixed through the addition of 5% sodium thiosulphate; culture plates were washed and left to dry. After drying, the culture plates were imaged using light microscopy.

Image analysis was performed using Image J software. Images were taken with Adobe Photoshop software in black and white. These were then imported back into Image J. The area of the image was selected, measured and then inverted to white on black, with black sections now being representative of resorption. Inbuilt tools within Image J allow the identification of the area and size of each section. This, together with the total area from the initial selection, enables the quantification of resorption.

Unstained Osteologic Slide

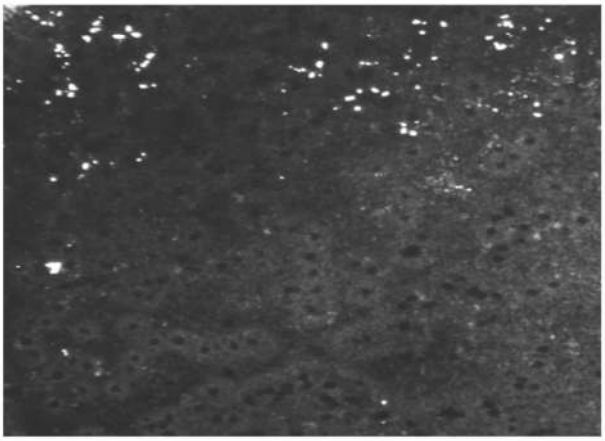

Von Kossa Stained
osteologic Slide

Fig.2.6. Osteologic ™ slides. Images of Osteologic ™ slides with and without the Von Kossa staining.

2.11 Osteoclastogenesis Cultures

25D and 1,25D was purchased from Wako (Osaka, Japan). All cultures were seeded at the equivalent of 2 x 10^5 cells per well. Cultures were checked daily and fed every three days. This was identical for bone marrow, spleen cells and PBMC cultures. RAW 264.7 cells were seeded at 1 x 10^3 cells/well. Cultures were divided into four treatment groups; M-CSF (25 ng/ml) ; M-CSF (25 ng/ml) + RANKL (100 ng/ml) ; M-CSF (25 ng/ml) + RANKL (100 ng/ml) + 25D (100 nM) ; and RANKL (100 ng/ml) + M-CSF (25 ng/ml) + 1,25D (1 nM). Cultures were run for 9-12 days and analysed by TRAP staining and processed for total RNA isolation and RT-PCR, dependent on peak observation of osteoclasts and dentine. Bone resorption cultures using either Osteologic ^{TM} cultures or dentine were run for 14 or 22 days as indicated.

2.12 Dentine Processing

Mouse spleen cells were also cultured on sperm whale dentine as a resorption substrate. Dentine after being cut using a diamond-edged saw with ethanol lubricant, using a Sloco speed saw, was cut into smaller pieces approximately 4 x 4 mm using a scalpel. Slices were marked in graphite pencil with an ‘F’ in order to identify the side of the dentine that osteoclast precursors were plated onto. Dentine was sterilized with 80% ethanol and sterile PBS washes to ensure no contamination was present. Dentine was then moved into 96-well culture plates and immersed in neat FBS for 24 hours to enhance cellular adhesion to the dentine. The FBS was removed and osteoclast cultures were added and fed every three days. Dentine resorption assays were run for 22 days. At this time point, dentine slices were removed from the plate, and the surrounding cells were TRAP-stained, as described

previously (2.8). The dentine was washed with Extran (Decon Laboratories Limited Sussex) to lyse all remaining cells and remove cell debris. Dentine was subjected to multiple washes of PBS mixed with ethanol, starting at 50% ethanol and increasing by 10% until reaching 100%. Following air drying, dentine was mounted on stubs, and coated with carbon/pallidum depending on availability. Dentine was imaged using scanning electron microscopy (Adelaide Microscopy X-L30 SEM) (Fig. 2.7). Images were analysed using Image J which was then used to analyse the resorbed bone regions (109).

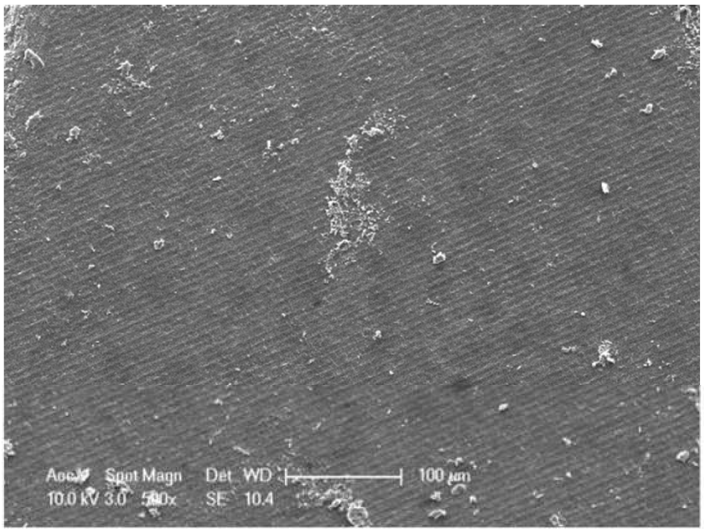

Dentine

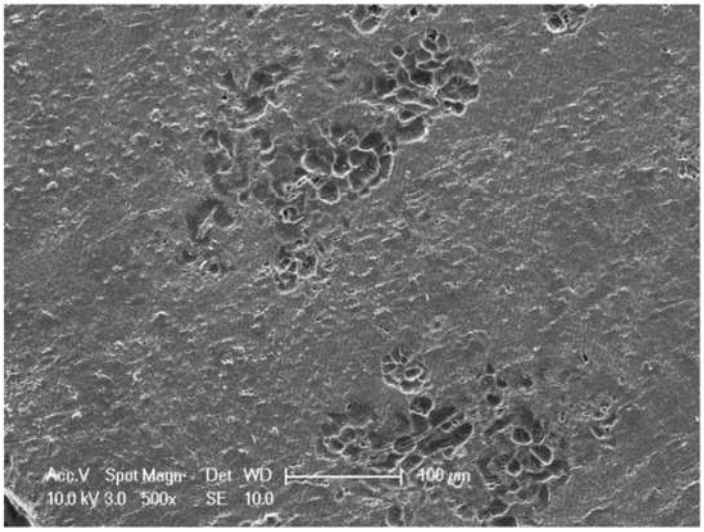

Dentine With Resorption Pits

Fig. 2.7. **Dentine under scanning electron microscopy.** Images of dentine under 500x magnification using scanning electron microscopy with a voltage of 10kv. Top image represents dentine without resorption and bottom image dentine with typical clusters of resorption pits or lacunae. The scale bar in each image indicates 100 µm.

2.13 Peripheral Blood Mononuclear Cells (PBMCS)

Human PBMC were obtained from healthy volunteers and isolated using Lymphoprep Gradient Media (Nycomed Pharma, Oslo, Norway), as previously described (4) and with Human Research Ethics approval (RAH Protocol No: 140216a). Briefly, 15 ml of heparinised peripheral blood was diluted in 25 ml pre-warmed HANKS solution. Lymphoprep (15 ml) was under layered into a 50ml tube using a cannula (Uno Medical). Tubes were centrifuged at 277xg for 30 minutes (Megafuge 1.0R Heraeus) and stopped without using a brake. The aqueous interface layer was collected and transferred to another 50ml sterile tube using a cannula. This was topped up to 50ml with HANKS solution and then centrifuged again at 277xg for 5 minutes with the centrifuge brake on. Cells were then washed twice with HANKS by centrifugation and the third and final wash was with α-MEM (Sigma). Cells were counted and plated at 1 x 10^6 cells/ml in either 96-well (0.2 ml/well; TRAP assays) or 24-well (1.0 ml/well; RNA isolation) tissue culture plates. PBMCs were cultured and treated under the same conditions as spleen cells, with the exception of the addition of Dexamethasone (Aspen Pharmacare, St Leonards, NSW Australia) at 10^{-8} M.

2.14 RNA Extraction

Osteoclastogenesis was performed, as described above, and cells were cultured for the times indicated. Media was removed and TRizol (Life Technologies, Carlsbad, CA, USA) was added for 5 minutes before being transferred to 1.5 ml tubes. Chloroform (100 µl) (Analytic R) was added and tubes centrifuged at 11269 g for 15 minutes (Centrifuge

5417R, Eppendorf) at 4°C. The aqueous layer was then removed and transferred to another 1.5 ml tube. Glycogen (2 µl) (Roche Diagnostics, Manheim, Germany) and isopropanol (250 µl) (Merik Millipore) were added to the tube and left for 30 minutes at 4°C and the tubes centrifuged at 11269g for 30 minutes. Pelleted RNA samples were then washed with 75% ethanol (500 µl) (Merik Millipore) with centrifuging at 11269 g. RNA was then redissolved in diethylpyrocarbonate (DEPC) treated water (15µls at 63°C) (dry block heater, Ratek Instruments). This process was unchanged for all cell types used in this thesis.

2.15 Reverse transcription

In order to generate cDNA, RNA concentrations from the TRizol extractions were measured using a Nano-spectrometer (NanoVue Plus, General Electric, Boston, MA, USA). Total RNA (1.0 µl) was diluted in DEPC-water and made up to a volume of 16 µl. Reverse transcription mastermix Iscript (4 µl) (Bio Rad, CA, USA) was then added and cDNA generated, as per the manufacturer's instructions.

2.16 RT-PCR

RT-PCR was performed using the SYBR Green (Qiagen Maryland USA) incorporation technique, as described previously (4). RT-PCR was performed for *Nfatc1, Trap, Ctr, Ca2, Cathepsin K* and *C-fos* mRNA expression using previously published oligonucleotide primer sequences (4) in a real-time thermocycler (CFX-Connect, Bio-Rad, NSW, Australia).The *Bcl-2* and *Bax* mRNA ratio was also measured using RT-PCR. mRNA expression was compared against the housekeeping genes Beta 2 Microglobulin (*B2m)* and Hypoxanthine Phosphoribosyltransferase One (*Hprt1)*. RT-PCR was used to compare mRNA expression of mouse spleen cells from day 1 before any pro-osteoclastic factors

had been added to the media using primers for Cluster of Differentiation (CD) markers *CD4, CD8, B220*, *CD3* and *CD11b* (Table 2.1).

Name	Forward Primer	Reverse Primer	Annealing	Size
Mouse *Bcl-2*	5’ GACTGAGTACCTGAACCGGC 3’	5’ ATAGTTCCACAAAGGCATCCCAG 3’	60	74bps
Mouse *Bax*	5’ TGCTACAGGGTTTCATCCAGG 3’	5’ TTGGATCCAGACAAGCAGCC 3’	60	383bps
Mouse *Hprt1*	5’ GGTTAAGCAGTACAGCCCCA 3’	5’ TGCAGATTCAACTTGCGCTC 3’	60	234bps
Mouse *Trem-2*	5’ CACAGCACCTCCAGGAATCAA 3’	5’ ACTTGCTCAGGAGAACGCAG 3’	60	82bps
Mouse *CD3* (antigen) Variant 1	5’ TTCAGAAATGAAGTAATGAGCTGGC 3’	5’ TCGTCACTGTCTAGAGGGCA 3’	60	206bps
Mouse *Atp6V$_1$h*	5’ CGAGGCTATCCAGGTCTGTG 3’	5’ TTTAGCACACTGGCTGCCTT 3’	60	134bp
Mouse *Atp6V$_0$D$_2$*	5’ ATTCTTGAGTTTGAGGCCGACA 3’	5’ CAGCTTGAGCTAACAACCGC 3’	60	
Mouse *Atp6V$_1$f*	5’ CGCCACCCTAATTTCCTGGT 3’	5’ AGAAATTGCCTGAAAGTGTCTTCG 3’	60	
Mouse *C-fos*	5’ GTGAAGACCGTGTCAGGAGG3’	5’ CTGTCTCCGCTTGGAGTGTA3’	60	175bps

Table 2.1. Previously unpublished mRNA-specific oligonucleotide primers, designed to flank at least one intron/exon boundary.

2.17 Designing mRNA-Specific Oligonucleotide Primers

Primer sequences were designed to set characteristics to ensure optimal amplification, including ensuring the amplified sequences spanned an intron/exon binding site with a maximum of three overlapping base pairs. This prevented genomic sequences from being amplified along with the mRNA. Primers were tested *in silico* with Primer Blast (National Library of Medicine, USA) to check for specificity to the desired target gene. They were then examined with Amplify software (Bill Engels, 2015, University of Wisconsin) to test for predicted secondary binding to the target gene and for the potential amplification of primer dimers that would have caused amplification of alternate products in the PCR. Finally, primer sequences were analysed with an electronic amplification program E-PCR (retired) (National Library of Medicine, USA) to confirm that there was no binding to unrelated genomic sequences. Primers that failed were redesigned until they met the required specifications. Primers were ordered from and produced by Geneworks (Thebarton, SA, Australia, 5031). All primers were tested empirically by RT-PCR for optimal performance, including by melt-curve analysis on both reverse transcribed and non-template controls.

2.18 V-ATPase Methods

For RT-PCR amplification of the multiple subunits of the mouse V-ATPase, primers were kindly donated by Professor Minghao Zheng (University of Western Australia). These primers consisted of a forward and reverse set for all 26 known subunits of the V-ATPase pump. Messenger RNA from day 8 *Cyp27b1*KO and WT osteoclast monocultures were then subjected to RT-PCR for the entire primer set. Identification of changes in mRNA observed from this analysis was used as a basis for more in-depth analysis of defined subunits of the V-ATPase hydrogen ion pump. Sub-units that showed changes in their mRNA expression due to the deletion of *Cyp27b1* or changes under 25D or 1,25D treatment were further analysed. This was done through the designing of alternative primers specific for these genes.

2.19 Dentine, Scanning Electron Microscope (SEM)

Dentine after being washed, as described previously (Section 2.2), was then transferred to a SEM aluminium stub with an adhesive patch applied. Dentine was attached to individual stubs according to treatment and genotype. Dentine was coated with carbon to provide the appropriate surface for SEM and imaged, using a 10kv voltage at a magnification of both 500x or 200x under an Olympus XL30 electron microscope. 200x images were used as a map for collating the 500x images together. This prevented double counting of osteoclast resorption pits. Images were analysed using Image J software.

2.20 MLO-Y4

MLO-Y4 cells are derived from murine long bone osteocytes. They are an osteocyte-like cell line known for producing pro-osteoclastogenic cytokines. MLO-Y4 cells were obtained and handled, as described previously (111). Briefly, cells were thawed from cryogenic storage using a slow drip method of media in order to dilute the freezing mixture and ensure cell survival of the cryogenic storage. MLO-Y4 cells were cultured in rat tail type 1 collagen-coated T-75 tissue culture flasks under media conditions of FBS 2.5% (v/v), New Born Calf serum 2.5% (v/v) and ascorbate, until confluent. Cells were removed from the flask using trypsin and then counted using a haemocytometer. Cells were transferred to collagen coated 96-well flat bottomed tissue culture plates for osteoclast assays or to another collagen coated T-75 for further passages. For experiments, MLO-Y4 cells were seeded at 1 x 10^3 cells/96-well plate.

2.21 SAOS2

SAOS2 are a human osteosarcoma derived osteoblast-like cell line. SAOS2 osteosarcoma were obtained as previously described (112). Cells were thawed from cryogenic storage using a slow drip method of media in order to dilute the freezing mixture and ensure cell survival of the cryogenic storage. SAOS2 cells were cultured in T-75 flasks under media of FBS 10% (v/v) and ascorbate. Cells were removed from the T-75 using trypsin. Cells were collected then counted. Cells were transferred to 96 well plates for osteoclast assays or to another T-75 for further passages. SAOS2 cells were seeded at 1 x 10^3 cells/96 well plate.

2.22 Co-Culture

Co-cultures were undertaken with splenocytes isolated from *Ctsk-Cre.Vdr*$^{fl/fl}$ mice and the cell lines MLO-Y4 or SAOS2. The cell lines were seeded at 1 x 10^3 cells/96 well plate. Cell lines were seeded onto 96-well plates with and without dentine slices. Cells were incubated overnight at 37°C, 5% CO_2 under media conditions appropriate for each cell type. Spleen cells were added in fresh cellular media at previously determined optimal density of 2 x 10^5 cells/96-well. Cells were incubated overnight then media was changed to remove non-adhered cells. Cells were fed every three days with α-MEM media with 1% (v/v) HEPES, 1% (v/v) L-glutamate, 1% (v/v) penicillin and streptomycin, FBS 10% (v/v) and ascorbic acid. Treatment groups included two monoculture controls, one of spleen cells and one of either MLO-Y4 or SAOS2 cell lines. Additional treatments included 25D (100 nM) and 125D (1 and 100 nM). The SAOS2 culture was identical except for the final treatment group. This group was treated with 1nM of 1,25D and potassium di-hydrogen orthophosphate (Ajax Chemicals, Sydney, Australia), which is known to stimulate mineral precipitation under defined media conditions.

2.23 Statistical Analysis

Statistical analysis was performed using Graph Pad Prism software (GraphPad Prism, La Jolla, CA, USA). Statistical significance was tested using Student's T-Test or 2-way ANOVA, as appropriate. Statistical significance was defined as p less than or equal to 0.05. All experiments were performed a minimum of four times. Each experiment utilised

between three and four individual spleens in each treatment group. All RT-PCR assays were performed in triplicate for each experimental set.

2.24 Addendum on *Cyp27b1* and *Vdr* KO Mouse Colonies.

The maintenance of *Vdr*KO and *Cyp27b1*KO mice require the administration of a special (rescue) diet. This diet ensures that the mice survive past the weening stage at four weeks. It does not however restore the mouse phenotype to wild-type. This means that homozygous *Cyp27b1*KO and *Vdr*KO mice have specific phenotypic traits that are still present on the rescue diet. *Cyp27b1*KO mice show minimal phenotype on the rescue diet, however the most noted of these is reduced fertility. This is also observed in *Vdr*KO mice. The other noted effect is that KO mouse pairs do not breed well and KO and heterozygous mouse pairs breed infrequently. This results in heterozygous breeding pairs being essential for mouse breeding. This breeding strategy ensures a supply of specific WT littermates to compare against homozygous *Vdr*KO and *Cyp27b1*KO mice.

It was noted that mice of the *Vdr* strain had a tendency to develop neurological defects in the offspring of the breeding pairs and had to be re-derived before more mice were available*Ctsk-Cre.Vdr*$^{fl/fl}$ and *Ctsk-Cre.Cyp27b1*$^{fl/fl}$ mice did not show the reduced fertility and phenotype of their global knockout counterparts.

Chapter 3

Optimisation of Osteoclastogenesis

Osteoclasts like most cells are influenced by a myriad number of variables which are specific to the type of culture and often to the laboratory in which experiments are performed.

This Chapter resulted from observations made in initial experiments using previously derived experimental protocols to artificially stimulate osteoclastogenesis. Experiments performed using identical experimental protocols often yielded quite different levels of success for unknown reasons. In order to maximise experimental outcomes and minimise wastage of resources, optimisation of multiple aspects of osteoclastogenesis was undertaken. This chapter examines the variables of sex, cytokine administration, foetal bovine serum, media, cell density and splenocyte source derivation on osteoclastogenesis. Surprisingly, the most effective modification was the pooling of the primary spleen cells from multiple genetically-identical mice, which significantly reduced experimental variation and enhanced experimental outcomes.

Chapter 3

Optimisation of Osteoclastogenesis

3.0 Introduction

The direct action of the cytokines M-CSF and RANKL when added to primary haematopoietic cell cultures in the formation of mature resorbing osteoclasts is well established and has revolutionised the ability to study osteoclasts (5). Until this discovery, experimental observations were restricted to bone marrow cultures and *in vivo* experimental observations. The addition of recombinant RANKL and M-CSF to precursors found in the blood, bone marrow, liver and spleen stimulates osteoclastogenesis (113) (114) (115). In addition to RANKL and M-CSF concentration, the time of cytokine administration, L-Glutamine availability, presence of vitamins, concentration of FBS, percentage of oxygen available, cell density, folate concentration and culture medium are some of the large effectors on osteoclastogenesis.

However, despite numerous articles investigating osteoclastogenesis, variation in optimal conditions between experimental protocols are observed in cultures and between cell types. Examples of these variations include: concentration of cytokines; length of culture; oxygen concentrations. Due to the lack of a defined optimal protocol for the formation of mature osteoclasts, optimisation for each individual experimental protocol is required when undertaking experimental work with hematopoietic stem cells. Even cell line models such as RAW 264.7 cells have been demonstrated to be highly dependent on the additives present in FBS (109). Further, more complex experimental procedures, such as co-cultures,

must take into account dual cell survival requirements and even the optimal number of cells for both cell types.

Experimental optimisation is essential, particularly when using cells derived from a primary source. Primary cells are often less robust than immortalised cell line counterparts and are more likely to respond negatively to minute changes in their surrounding environments. This often results in major physiological changes, such as, inhibited differentiation, altered cellular function or more commonly cell mediated apoptosis. The optimisation of experimental protocol minimises unwanted changes reducing cell death, while maximising potential experimental outcomes.

The osteoclasts' ability to respond to numerous signals likely prohibits true optimal conditions being achieved, due to the large number of potential variables, expense and the lack of full elucidation in the interactions the osteoclast undertakes with other bone cells. Osteoclast cultures can be obtained from multiple sources, such as, mouse spleen cells, mouse or human bone marrow cells, human PBMCs and RAW 264.7 cells. All have varying optimal conditions. Mouse spleen cells and PBMCs were undertaken as monocultures in this study. Spleen cells were also co-cultured with either MLO-Y4 or SAOS2 cells. The use of co-cultures in this *ex vivo* work enables the examination of the osteoclasts under functioning osteocytic signalling which is not possible in global KO models and monocultures. Additionally the use of SAOS2, a human derived cell line, to stimulate murine cells would allow the isolation of mRNA in a species independent manner while potentially isolating other factors that influence osteoclasts.

Optimisation here focused on varying cell density, sex variations, cytokine concentration, culture medium and the type of FBS used. It also briefly examines the effects of SAOS2 and MLO-Y4 as when co-cultured with mouse spleen cells.

It should be noted that there are limitations in the comparison of *ex vivo* artificially induced osteoclasts to that of *in vivo* models, and *vice versa*. This chapter sought to optimise osteoclastogenesis using isolated splenocytes form each genotype through the use of recombinant cytokines. The *in vitro* system has the advantage of being controllable and independent of the confounding effects of various other cell types and factors that influence the formation and activity of these cells. Indeed, the discovery of RANKL and the requirement of M-CSF, and determination of the basic culture conditions required (116, 117) revolutionised osteoclast research and was responsible for an explosion of research in this field. However, in some instances, the *in vitro* model can be considered oversimplified. Some features are non-physiological. For example, it has been noted that osteoclasts in the bone rarely exceed sizes of 20-25 nuclei in healthy animals. However, in this experimental protocol osteoclasts with more than 100 nuclei were often seen. This could potentially be due to alterations in the osteoclast adhesion to the plastic substrate of the culture plates or could be caused by unregulated access to the osteoclastogenesis cytokines RANKL and M-CSF. Additionally, osteoclasts of this size were not observed in the later co culture work performed. This however does raise the possibility that the artificial induction of osteoclasts may result in an exaggerated response from osteoclast precursors. Further investigation of this would be required to identify what alterations if any that a non-bone culture substrate and non-regulated access to cytokines have on osteoclast precursors.

3.1 Materials and Methods

3.1.1 Cell Number Optimisation

Initial experiments used Sigma α-MEM with normal FBS 10% (v/v) (HyClone, Logan, UT, USA) with the additives of L-glutamine, penicillin and streptomycin mix and Hepes, all at 1% (v/v) to establish the most effective cell concentration. Recombinant RANKL (Millipore, Temecula, CA, USA) was given at 100ng/ml. Cells were fed every three days. Cells scavenged from murine spleens as described in section 2.5 of Chapter 2 were administered at concentrations of $1x10^5$, $1.5x10^5$, $2x10^5$ and $2.5x10^5$ cells/ml. They were placed in a dark incubator at 37°C at 5% CO_2. M-CSF only negative controls were used alongside RANKL + M-CSF treatments. Cell cultures were checked daily by phase contrast light microscopy for the appearance of multinucleated cells. Experiments were performed in quadruplicate in 96 well plates.

3.1.2 RANKL Concentration Optimisation

In order to establish an optimal RANKL concentration, spleen cells were treated with 25, 50, 75 and 100 ng/ml RANKL. M-CSF was maintained at 25ng/ml. Of the two cytokines essential for osteoclastogenesis, it was considered that RANKL was more likely to show an apparent effect. Cells were fed every three days. Basal cell culture medium was Sigma α-MEM with normal FBS 10% (v/v). Cell concentration of 2×10^5 was utilised before optimisation of cell density assays had been undertaken and was used as was indicated in Kogawa *et al.* (3, 4). Cells were cultured as above 3.1.1

3.1.3 Media and FBS Optimisation

Cells were cultured under three variations of media. Two of the media batches were Sigma α-MEM with two different batch numbers, an externally sourced (ES-MEM), and an internal batch used for the majority of cell cultures within the lab (S-MEM). The third variation was a Gibco α-MEM batch (G-MEM). FBS at 10% (v/v) was used for both normal FBS (FBS) and charcoal stripped FBS (S-FBS), resulting in six treatment groups. Cells were treated with 100ng/ml RANKL and 25ng/ml M-CSF. M-CSF negative controls were used alongside RANKL + M-CSF treatment. Cells were cultured at 1.5×10^5 cell/ml. Cells were cultured as described in section 3.1.1

3.1.4 TRAP Staining

TRAP staining was performed on quadruplicate wells using a commercial kit (Sigma Chemical Co.), as described previously (4). Osteoclasts were defined as magenta stained $TRAP^+$ cells containing three or more nuclei. Osteoclast number and size were assessed using light microscopy (Nikon Eclipse TE300) at a minimum of three time points between days 6 and 9, encompassing early and peak formation periods.

3.2 Results and Discussion

The optimisation of osteoclastogenesis cultures was an essential step in ensuring that the experimental work undertaken used an effective, reproducible methodology. The effect of the cell density of the starting population of splenocytes on osteoclastogenesis was undertaken through TRAP staining and light microscopy. Cell density was observed to play a critical role in the formation of osteoclasts. Wells seeded with densities below 1.5 x 10^5 cells/well and above 2 x 10^5 cells/well resulted in a significant reduction in osteoclast formation at day 8 (Fig. 3.1 and 3.2) in pooled splenocytes.

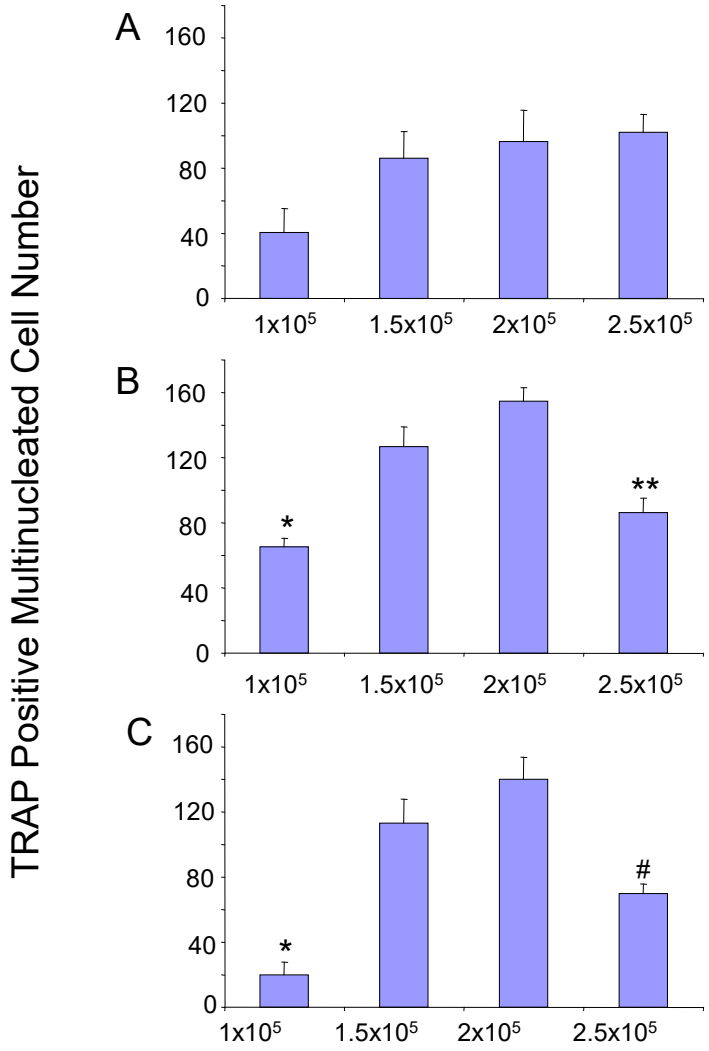

Fig. 3.1: Cell density cultures. The effect of varying mouse splenocyte concentration on resulting TRAP+ MNC. Splenocytes seeded at $1x10^5$, $1.5x10^5$, $2x10^5$ and $2.5x10^5$ cells/well of a 96-well tissue culture plate were treated with recombinant human RANKL (100 ng/ml) and M-CSF (25ng/ml) and cultured and assayed for TRAP+ MNC at a) 7 days, b) 8 days and c) 9 days. Data are means ± SEM of quadruplicate wells. Significant difference is indicated by *, **, # = $p<0.05$ indicating difference to the $2x10^5$ treatment group. Analysis by student T-test n=3. TRAP staining performed in quadruplicate.

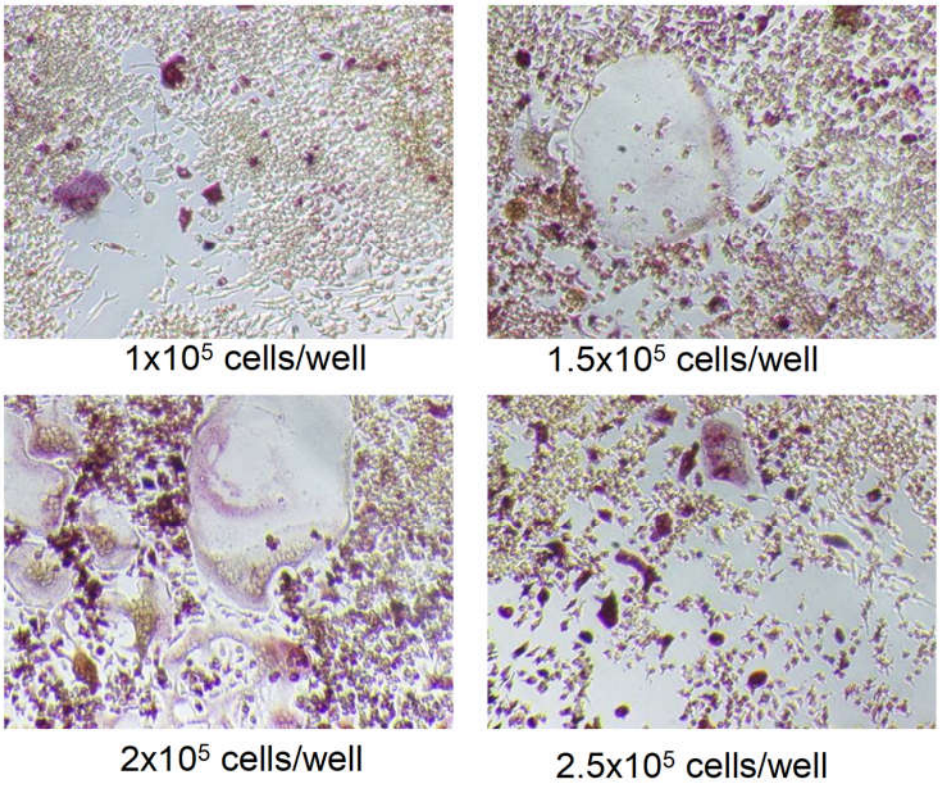

Fig. 3.2: Cell density images. Representative light microscopy images of TRAP stained MNC under varying spleen cell density. Splenocytes in a 96-well tissue culture plate were treated with recombinant human RANKL (100ng/ml) and M-CSF (25ng/ml) and cultured for ten days.

3.2.1 Cell Density

Cell density was found to be one of the most critical factors in osteoclast formation (Fig. 3.1). Despite consistent levels of M-CSF and high levels of RANKL the alteration of cell density had drastic effects on osteoclast formation. Optimal osteoclastogenesis was confined to a range of cell density that peaked at 1.5×10^5 (75000cell/cm^2). The reduction in osteoclast formation due to a lower number of cells was expected, as lower precursor density means fewer differentiating mononuclear cells are available for fusion.

The inhibition due to a higher cell density, however, was unexpected. It is possible that high cell density may simulate the conditions in the spleen resulting in cell to cell signalling that inhibits osteoclastogenic differentiation.

3.2.2 Effect of Recombinant RANKL Concentration

Osteoclastogenesis assays are highly dependent on the cytokines, RANKL and M-CSF. Having established optimal cell density under cytokine replete conditions, it was identified, as expected, that the TRAP-positive MNC number decreased as the RANKL concentration decreased (Fig. 3.3). A significant reduction was observed in a linear regression pattern such that the TRAP+ MNC number was directly proportional to the RANKL concentration administered. Indeed, an approximate 50% reduction in cell number was observed for every 25 ng/ml reduction in of RANKL concentration. Potential variation due to gender under both cytokine replete and reduced conditions in mouse spleen cells were examined simultaneously; no significant differences were observed between the sexes (Fig. 3.3).

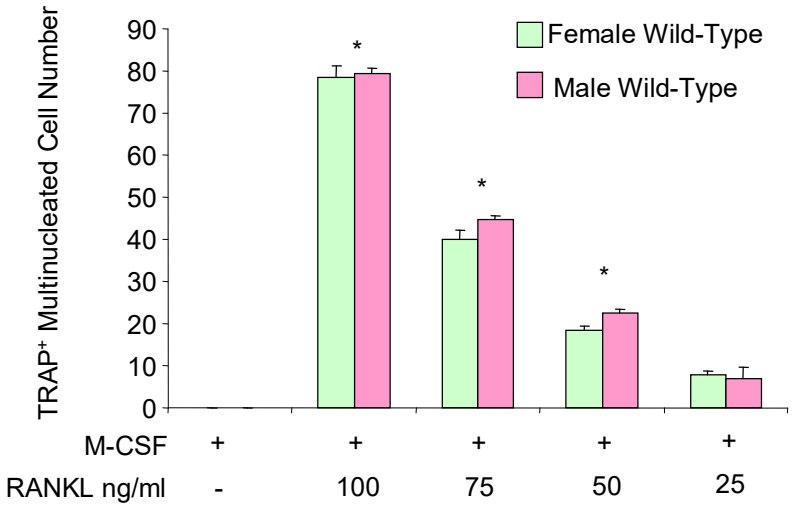

Fig. 3.3: **The effect of RANKL concentration and mouse sex on osteoclast survival and differentiation.** Mouse splenocytes were seeded at a density of 2 x 10^5 cells/well into 96 well culture plates with α-MEM and FBS 10% (v/v) with M-CSF (25ng/ml) and RANKL (25-100ng/ml). *, Significant difference between treatments, combined sex data ($p < 0.05$). Data are means ± SEM of quadruplicate wells. Students T-test was used with an n = 3.

Overall, the addition of 100 ng/ml of RANKL combined with 25 ng/ml of M-CSF was the most effective at producing osteoclasts from mouse splenocytes with the three day feeding cycle and culture conditions employed.

3.2.3 Precursor Cells

Another important contributor to experimental outcomes is variability due to the quality of the cell populations used. The time taken to remove spleens from euthanised mice and isolate splenocytes was subtlety but potentially importantly different between individual mice. This may have impacted on splenocyte viability of metabolic state due to effects such as hypoxia. Indeed, it was observed that within each genotype of wild-type, heterozygote and homozygous knockout in the *Cyp27b1*KO mice, there was variability in TRAP+ MNC formation (data not shown). It was also observed that the spleens of *Cyp27b1*KO mice were more likely to form dark clots on their surface than WT mice. In order to overcome this individual variability, pooling of spleens was tested.

Individual spleens were taken from either WT, KO or heterozygous genetic backgrounds of either sex. Each individual mouse spleen was plated in quadruplicate with a minimum of four individual spleens used per experiment. In the pooled experimental protocol up to three and at least two mouse spleens were used to create the pool of spleen cells depending on availability. Three sets of pooled spleen cells were used in each experimental replicate and these were plated in quadruplicate. Each experiment was replicated a minimum of three times for each genotype.

The use of two or more spleens resulted in increased osteoclast formation and reduced variability between experimental replicates (Fig. 3.4).

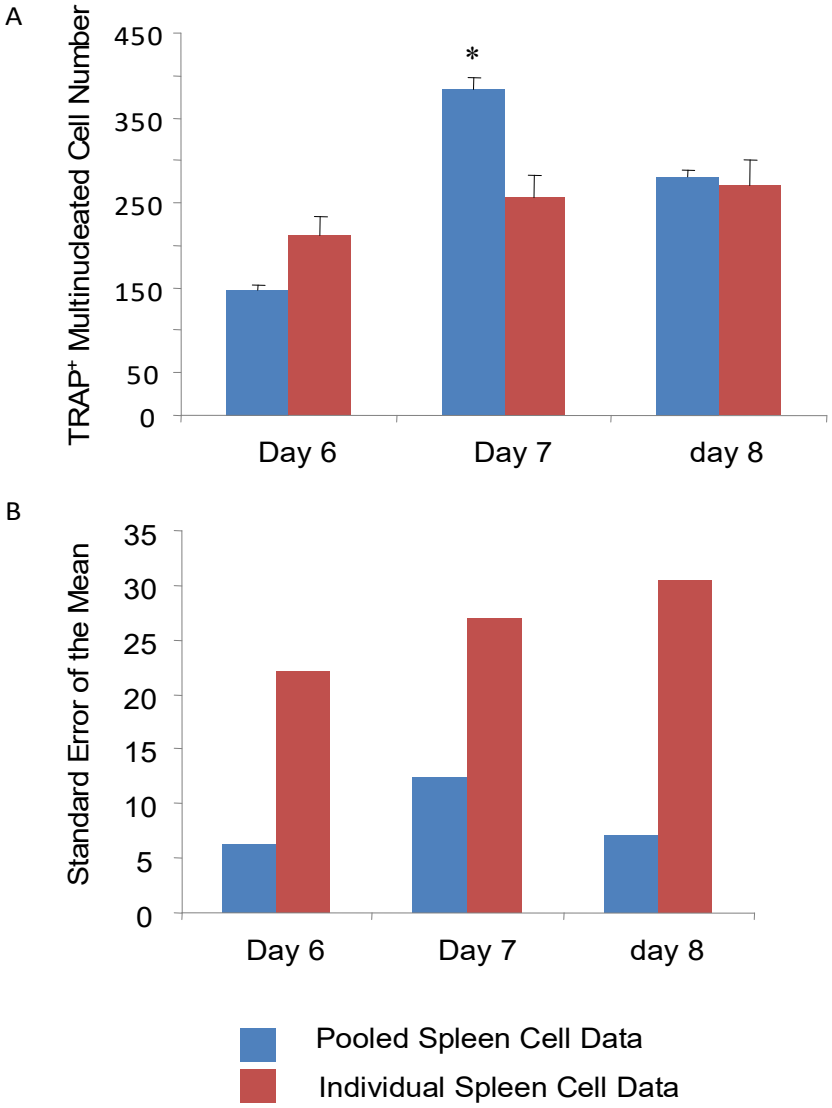

Fig. 3.4: The effect of pooled spleen precursors on osteoclast formation and inter-well variation. A) Spleen cells were seeded at a density of $2x10^5$ cells/well into 96 well culture plates with α-MEM and FBS 10% (v/v) with M-CSF (25ng/ml) and RANKL (100ng/ml). *, denotes significant difference between treatments ($p < 0.05$). B) The standard error of the mean from individual and pooled spleen precursors. n=4 for the pooled spleen cells and n=5 for the individual mice.

It was predicted that the use of multiple spleens would result in a more homogenised balance of osteoclast precursors, and that by combining these pools the ratio of motile to stationary osteoclast precursors was enhanced, resulting in increased and more stable osteoclastogenesis, as supported by the findings of Geblinger *et al.* (75).

3.2.4 Foetal Bovine Serum

The type of FBS used was also tested as a variable. FBS is a poorly defined source of nutrients, hormones and growth factors that promotes cell growth *in vitro* but may also contain inhibitors of certain processes, including osteoclastogenesis. Steroid hormones can be removed from FBS by charcoal stripping. Charcoal stripped FBS was compared against normal FBS combined with Sigma or Gibco α-MEM for the propensity to support osteoclastogenesis. There was a significant increase in osteoclast formation when stripped FBS was used (Fig. 3.5). Interestingly both Gibco and Sigma α-MEM promoted nearly identical osteoclast growth under osteoclastogenic conditions when used with normal FBS (Fig. 3.6). However, for unknown reasons Gibco α-MEM when combined with stripped FBS resulted in failure of osteoclasts to form (Fig. 3.6).

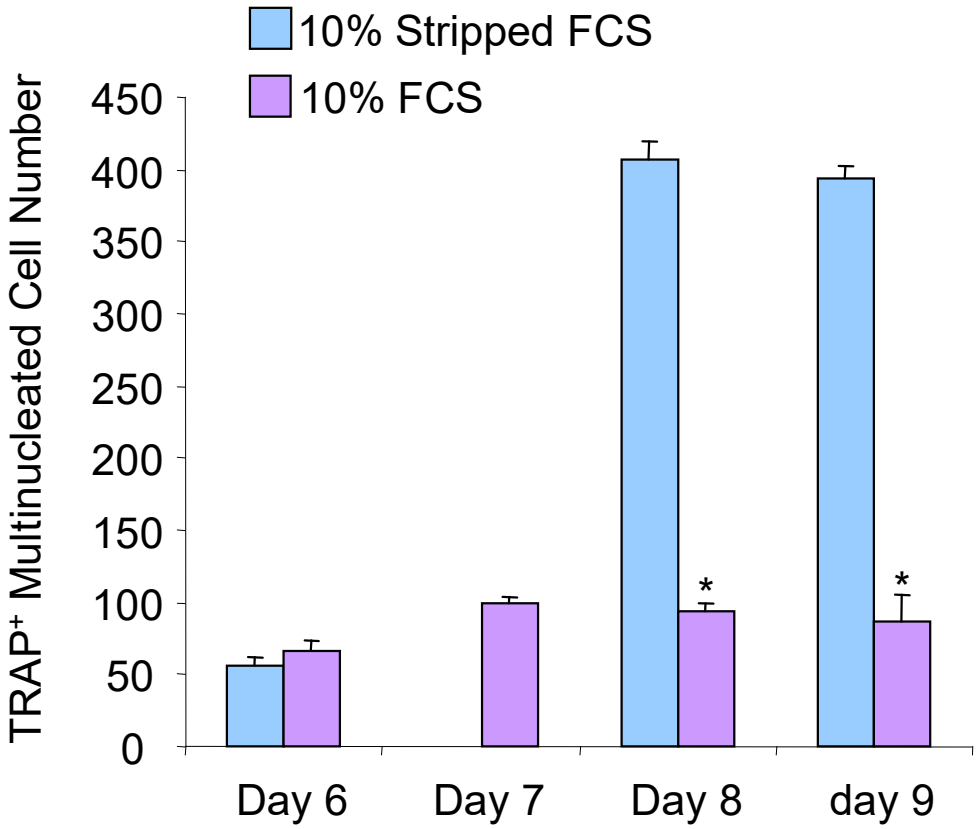

Fig. 3.5: The effect of charcoal stripped FBS on osteoclastogenic cultures. Mouse splenocytes were seeded at a density of $1.5x10^5$ into 96 well tissue culture plate with α-MEM with recombinant human RANKL (100 ng/ml) and M-CSF (25ng/ml) with either FBS 10% (v/v) or S-FBS 10% (v/v). Data are means ± SEM of quadruplicate wells. Significant difference is indicated by * = $p<0.05$.

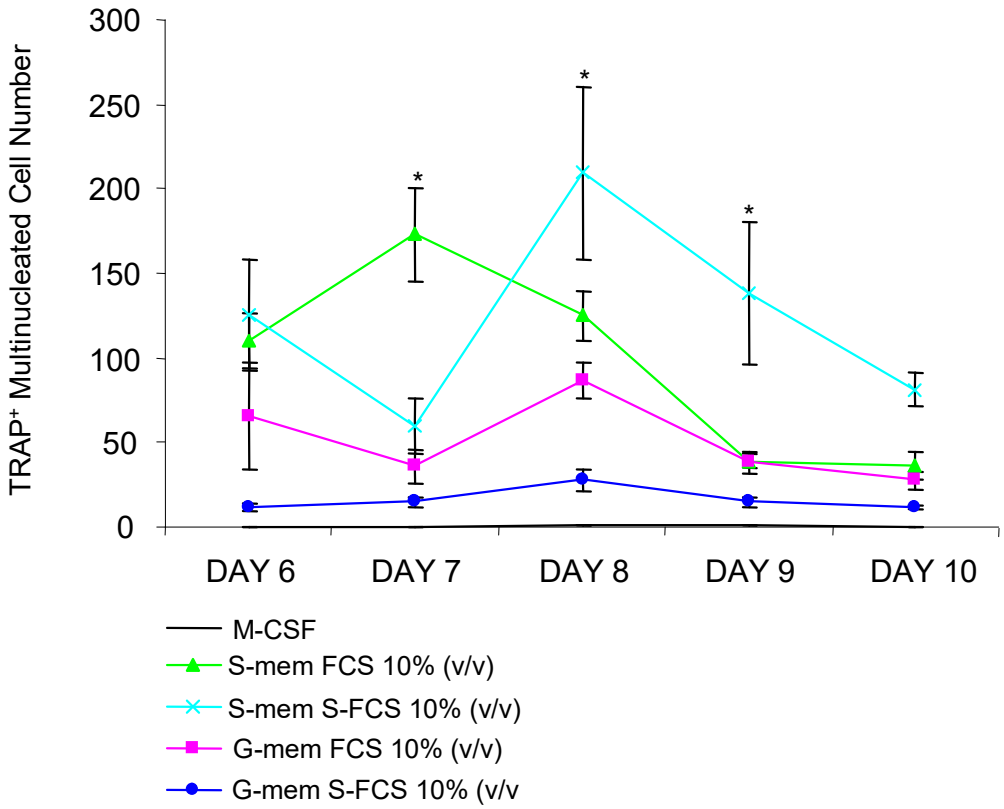

Fig. 3.6. The effect of S-MEM and G-MEM under FBS or S-FBS. Mouse splenocytes were seeded at a density of $1.5x10^5$ into 96 well tissue culture plates with either G-MEM or S-MEM, S-FBS 10% (v/v) or FBS 10% (v/v) with recombinant human RANKL (100 ng/ml) and M-CSF (25ng/ml). Plates were assayed for TRAP staining over multiple time points. Data are means ± SEM of quadruplicate wells. Significance is indicated by * = $P<0.05$ using Two Way ANOVA with n=3 in pooled splenocytes.

Table 3.1 identifies some of the more significant changes in chemical composition documented due to charcoal stripping. The largest change in stripped FBS is a reduction in folate (folic acid) concentration. It has been reported that folate inhibits osteoclastogenesis (118) which is a possible explanation for the effect seen. However, the observed increase in osteoclastogenesis could also be caused by the reduction or change in a combination of numerous chemicals due to charcoal stripping.

TEST	Pre-Treatment (untreated)	Post Treatment	
Testosterone	30	<3	Ng/dl
Oestrogen	26	2.5	Pg/ml
Vitamin D, 1,25D	90	41	Pg/ml
Pteroylglutamic Acid (folate)	545	2.3	nM/L

Table 3.1. FBS composition before and after charcoal stripping. Focusing on substances that have demonstrated the ability to influence osteoclastogenesis and activity. Data was provided by the manufacturer of the Stripped FBS.

The effects of varying the source of α-mem was unexpected. The formula of Gibco and Sigma α-MEMs are similar with only minor changes in salt concentrations. The reduction in TRAP positive osteoclast formation observed when 10% (v/v) stripped FBS and Gibco α-MEM were used in conjunction, cannot be readily explained but should be noted for future experimentation. Stripped FBS in Sigma α-MEM was used for all subsequent experimental work in mouse splenocyte cultures.

The optimisation of osteoclastogenesis assays enhanced the results and repeatability. However, there are many additional aspects that were not investigated due to time and financial constraints. One example of those is the influence of hypoxic conditions. Hypoxia has been demonstrated to enhance osteoclastogenesis (115). However, no hypoxia incubator was available at the time of experimentation.

3.2.5 Osteoclast-Forming Co-Cultures

Attempts were also made to develop osteoclast forming co-culture cross-species assays. Cross-species assays have proven useful for identifying cell specific effects during osteoclastogenesis (119, 120). In particular, the use of human derived cells enables the detection of mRNA from the stromal and osteoclast components through species-specific gene variations. Here, the human SAOS2 was investigated as a potential stromal layer for murine osteoclast formation because of its known expression of RANKL (112). Co-cultures demonstrated that the SAOS2 cells were not sufficiently adept at stimulating osteoclastogenesis through both TRAP staining and resorptive assays on dentine analysed using SEM. The addition of 25D, 1,25D and ascorbic acid all failed to osteoclastogenesis when SAOS2 cells were co-cultured with splenocytes. The mouse osteocyte-like cell line MLO-Y4 was also investigated, as this has been demonstrated previously to support

osteoclastogenesis form both splenocytes and human PBMC (111, 121). The use of MLO-Y4 enables the production of murine based cytokines as well as the potential for the signalling between osteoclasts and osteocytes to be present. MLO-Y4 cells were able to initiate the maturation of osteoclasts. MLO-Y4/splenocyte co-cultures showed resorptive events on dentine confirming the presence of mature osteoclasts in these cultures. The addition of 25D concentration increased the number of osteoclasts formed but to a much lower extent than that of 1,25D at both 1 and 10nM (See Chapter 7a Fig 7a.1). It was observed that the presence of 1nM 1,25D was optimal for osteoclast formation from splenocytes under MLO-Y4 co-culture.

3.2.6 PBMCs

In separate experiments designed to test the effects of vitamin D metabolism on osteoclastogenesis the use of PBMCs was investigated as an addition to the spleen cells. PBMCs successfully formed osteoclasts from the addition of RANKL and MCS-F as expected. Large scale experimentation was undertaken in order to observe the effect of vitamin D metabolites on PBMCs and to replicate previous work undertaken by our group (3, 4, 7) on a large scale. Our PBMCs were collected from male volunteers ranging from their late twenties to the late fifties. There was great disparity between PBMCs formed from different individuals. This was not surprising as variation between non-genetically related individuals is usually high. Unfortunately due to this high variation between individuals minimal significance was observed. We did not observe any significant changes in cell number under 25D treatment. We did confirm that there was a significant effect of 1,25D on osteoclast formation in PBMCs (Fig. 3.7) as reported previously (3, 4, 7). To overcome the variation observed, the use of a higher *n* value in future studies may be useful to explore this area further.

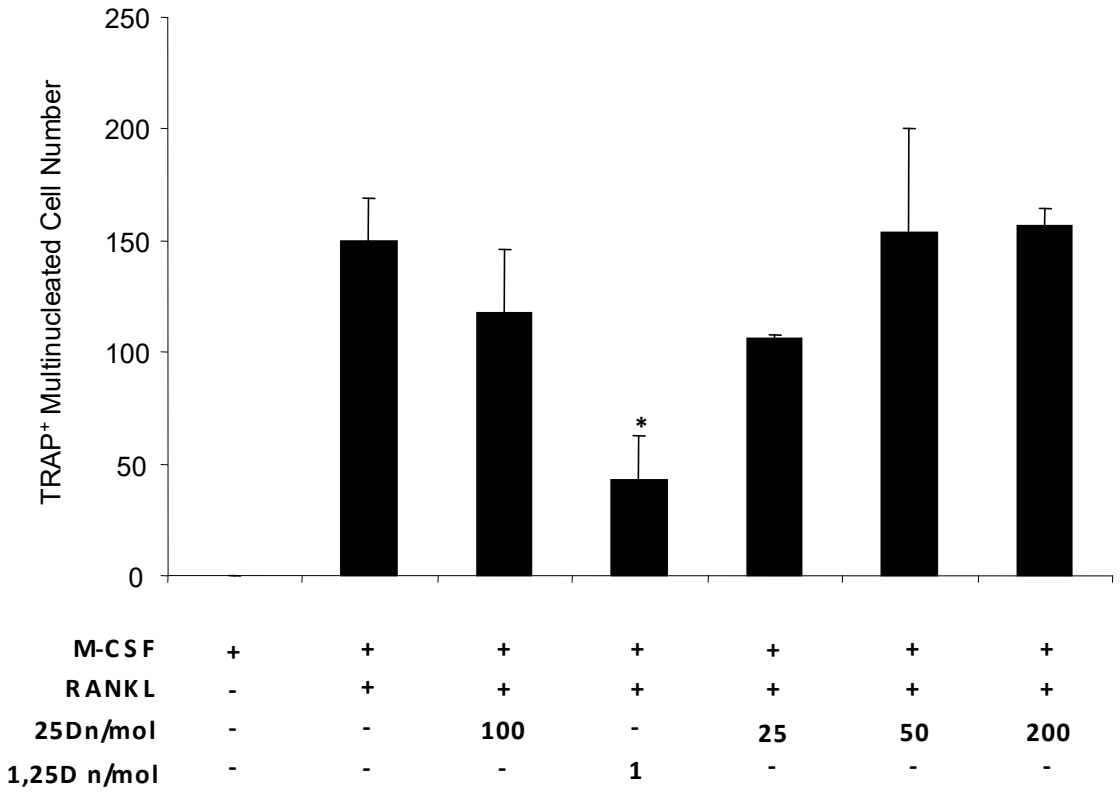

Fig. 3.7. The effect of Vitamin D metabolites on PBMCs. PBMCs were cultured under seven treatments; control, pro-osteoclastogenic conditions, pro-osteoclastogenic conditions + 100nM 25D, pro-osteoclastogenic conditions + 1nM 1,25D, pro-osteoclastogenic conditions + 25nM 25D, pro-osteoclastogenic conditions + 50nM 25D, pro-osteoclastogenic conditions + 200nM 25D as described in Materials and Methods for the times indicated and assayed for $TRAP^+$ multinucleated cell formation. Total $TRAP^+$ cell numbers were combined from two independent experiments, each using PBMCs from the same donor, and shown as means ± SEM. Significant differences from RANKL/M-CSF treatment are indicated by asterisks ($p< 0.05$) with n=3 under student T-Test.

Chapter 4

Evidence for altered osteoclastogenesis in splenocyte cultures from *Cyp27b1* knockout mice

Based on previous studies by our group, it was considered ideal to examine the effect of vitamin D at an autocrine level. *Cyp27b1*KO mice are unable to undertake autocrine vitamin D conversion but are still able to respond to endocrine vitamin D. Because of the germline deletion of *Cyp27b1* in these mice, they were an ideal source of osteoclast progenitors to test for the effects of loss of CYP27B1 activity. This chapter is represented by a published manuscript and covers the effect of the deletion of *Cyp27b1* in a mouse model in *ex vivo* splenocyte cultures. This is examined through TRAP assays, analysis of mRNA expression and bone resorption assays on a mineralised substrate.

Journal of Steroid Biochemistry & Molecular Biology 164 (2016) 353–360

Contents lists available at ScienceDirect

Journal of Steroid Biochemistry & Molecular Biology

journal homepage: www.elsevier.com/locate/jsbmb

Review

Evidence for altered osteoclastogenesis in splenocyte cultures from *Cyp27b1* knockout mice

Daniel C. Reinke[a], Masakazu Kogawa[a], Kate R. Barratt[b], Howard A. Morris[b], Paul H. Anderson[b,1], Gerald J. Atkins[a,*,1]

[a] Bone Cell Biology Group, Centre for Orthopaedic & Trauma Research, University of Adelaide, Australia
[b] School of Pharmacy and Medical Sciences, University of South Australia, Adelaide, SA 5005, Australia

ARTICLE INFO

Article history:
Received 15 June 2015
Received in revised form 4 November 2015
Accepted 25 November 2015
Available online 27 November 2015

Keywords:
Osteoclast
Osteoclastogenesis
Vitamin D
Metabolism
CYP27B1
Apoptosis

ABSTRACT

The association between increased serum 25-hydroxyvitamin D (25D) and reduced osteoclastic bone resorption is well known. Previously, we have demonstrated that mechanism by which this occurs, may include the conversion of 25D to 1,25-dihydroxyvitamin D (1,25D) by osteoclasts, catalysed by the CYP27B1 enzyme. Local 1,25D synthesis in osteoclasts was shown to regulate osteoclastogenesis and moderating resorptive activity. Thus, we hypothesised that osteoclasts differentiated from mice with global deletion of the *Cyp27b1* gene (*Cyp27b1* KO) would display enhanced resorptive capacity due to the lack of an ameliorating effect of 1,25D. Splenocytes isolated from *Cyp27b1* KO mice or their wild-type (WT) littermates between 6 and 8 weeks of age were cultured under osteoclast-forming conditions for up to 14 days. Osteoclast formation was measured by staining for the osteoclast marker tartrate resistant acid phosphatase (TRAP). Bone resorption activity was measured by plating the cells on a bone-like substrate. In *Cyp27b1* KO cultures, osteoclastogenesis was reduced, as indicated by fewer TRAP-positive multinucleated cells at all time points measured ($p < 0.05$) when compared to wild-type (WT) levels. However, *Cyp27b1* KO osteoclasts demonstrated greater resorption on a per cell basis than their WT counterparts ($p < 0.03$). In addition, the ratio of expression of the pro-apoptotic gene *Bax* to the pro-survival gene *Bcl-2* was decreased in *Cyp27b1* KO cultures, implying that these smaller osteoclasts survive longer than WT osteoclasts. Our data indicate abnormal osteoclastogenesis due to the absence of CYP27B1 expression, consistent with the notion that endogenous metabolism of 25D optimises osteoclastogenesis and ameliorates the resulting activity of mature osteoclasts.

Contents

* Corresponding author at: Centre for Orthopaedic & Trauma Research, University of Adelaide, Adelaide 5005, Australia. Fax: +61 8 8232 3065.
E-mail address: gerald.atkins@adelaide.edu.au (G.J. Atkins).
[1] Equal author contribution.

http://dx.doi.org/10.1016/j.jsbmb.2015.11.015
0960-0760/

1. Introduction

Osteoclasts are the cell type responsible for the majority of targeted bone resorption. Their multinucleated nature combined with a large cytoplasm and endoplasmic reticulum enables the rapid production of enzymes, proteins and ions in order to resorb bone [1]. Vitamin D metabolism through the conversion of 25-hydroxyvitamin D (25D) to 1α,25-dihydroxyvitamin D (1,25D) via renal CYP27B1 activity is known to increase calcium uptake in the small intestine [2]. In addition to the endocrine effects of vitamin D, autocrine/paracrine pathways of vitamin D metabolism also exist in the skeleton [2]. Previous studies have demonstrated that bone cells including both osteoblasts [3,4], osteocytes [5] and osteoclasts [6] express the vitamin D receptor (VDR) and CYP27B1, and are capable of metabolising 25D into 1,25D.

A major effect of 1,25D activity in bone is thought to be the regulation of expression by osteoblast lineage cells of cytokines that regulate osteoclastogenesis, such as RANKL and osteoprotegerin (OPG) [7–9]. Furthermore, the net effects of 1,25D activity appear to depend on the differentiation stage of the osteoblast in question, with the pro-osteoclastic effects appearing to be mediated by relatively immature osteoblasts, perhaps as a function of the proximity of these cells to the bone surface [10–13]. However, we previously demonstrated that 25D metabolism by osteoclast-lineage cells also has direct consequences for osteoclast formation and activity, and while osteoclast differentiation was enhanced in the presence of 25D at concentrations above 60 nM, osteoclast resorptive activity was reduced [6,14]. These findings suggested that adequate 25D levels are necessary in order to ameliorate osteoclastic bone resorption. Consistent with these findings, previous studies have demonstrated that the deletion of the *Cyp27b1* gene in mice and the subsequent loss of the autocrine vitamin D pathway results in reduced osteoclast number and decreased osteoclast size [15].

In the current study, we examined the influence of autocrine vitamin D metabolism in the osteoclast lineage using the global gene knockout (KO) mouse model, *Cyp27b1* KO [16]. Mouse splenocytes were used to generate osteoclasts *ex vivo* by treating with recombinant RANKL and M-CSF, enabling the examination of the intrinsic ability of haemopoietic cells to form osteoclasts and the assessment of their resultant bone resorbing activity without the influence of osteoblastic stromal cells. Various markers of gene expression relating to osteoclast formation, activity and survival were analysed.

2. Materials and methods

2.1. Animals

Global *Cyp27b1* KO mice [16] were housed at ambient temperature with free access to water and food, with established 12 h day–night cycles. All mice were fed the KO 'rescue diet', consisting of chow containing 2% calcium, 1.25% phosphate and 20% lactose, which prevents rickets and bone abnormalities associated with this model [15], until genotyped and removed for weaning. After weaning, confirmed *Cyp27b1* KO mice were fed the rescue diet while wild-type (WT) mice were fed a standard chow diet. All animal procedures were approved and performed in accordance to requirements of the animal research ethics committees of the University of Adelaide and the University of South Australia.

2.2. Osteoclastogenesis

All experiments conducted were repeated at least 3 times. Mice were humanely euthanised and spleens excised and placed in Minimal Essential Media-alpha (αMEM; Sigma Chemical Co., St Louis, MO, USA). Spleens were dissected and the pieces gently ground between two glass slides in order to release the cells from the surrounding tissue. Red cell lysis buffer was then added and cells washed three times in αMEM, containing 10% charcoal stripped FCS (HyClone, Logan, UT, USA), 1% penicillin, 2 mM L-glutamine and HEPES. Cells from four spleens/genotype were then pooled, counted using trypan blue exclusion, and plated into standard 96 well tissue culture plates for TRAP staining and into Osteologic™ slides (BD Biosciences, Bedford, USA) at 2×10^5 cells/well, or at 1×10^6 cells/well into 24 well plates for TRIzol based RNA extraction [6]. Cells were treated with differentiation media consisting of αMEM supplemented as above, with the addition of: recombinant M-CSF (Millipore, Temecula, CA, USA) (25 ng/ml = *untreated/UT*) or M-CSF + RANKL (Millipore) (100 ng/ml = *positive control*). In some experiments the effects of exogenous 1,25D and 25D (Wako Pure Chemicals, Japan) were assessed. The level of 1,25D used was 1 nM, which we have shown to be equivalent in efficacy to that of a physiological concentration of 25D (100 nM) in terms of inhibiting resorption in cultures of both RAW 264.7 cells and peripheral blood mononuclear cells (PBMC) [14].

2.3. TRAP staining

TRAP staining of quadruplicate wells was performed using a commercial kit (Sigma Chemical Co.), as described previously [14]. Osteoclasts were defined as magenta stained $TRAP^+$ cells containing three or more nuclei. Osteoclast number and nuclearity were assessed using light microscopy. TRAP staining was examined at at least 3 time points between days 6 and 9, encompassing early and peak formation periods in both genotypes, as determined in preliminary optimisation experiments (data not shown). Stained cells were imaged using a 4× objective on an Olympus CKX41 light microscope attached to a camera (Olympus DP20).

2.4. Analysis of gene expression by real-time RT-PCR

RT-PCR was performed, as described previously [6] with some modifications. Briefly, RNA was extracted using 0.5 ml TRIzol (Invitrogen, Carlsbad, USA), as per the manufacturer's instructions. Real-time RT-PCR was performed using the SYBR Green incorporation technique for nuclear factor of activated T-cells, cytoplasmic, calcineurin-dependent 1 (*Nfatc1*), *Trap,* calcitonin receptor (*Ctr*), carbonic anhydrase 2 (*Car2*) and Cathepsin K (*Ctsk*) mRNA expression using previously published oligonucleotide primer sequences [6] in a real-time thermocycler (MyIQ, Bio-Rad, NSW, Australia). Custom primers for the amplification of monocyte chemotactic protein 1 (*Mcp1*), *Bax* and *Bcl2* mRNA were designed in-house and purchased from Geneworks (Thebarton, SA, Australia). Oligonucleotide sequences were: *Mcp1*: forward 5′-ggctggagagctacaagagg-3′, reverse 5′- ttgagcttggtgacaaaaactacag-3′; *Bax*: forward 5′-tgctacagggtttcatccagg-3′, reverse 5′-

ttggatccagacaagcagcc-3′; *Bcl2*: forward 5′-gactgagtacctgaaccggc-3′, reverse 5′-atagttccacaaaggcatcccag-3′, *Voa3*: forward 5′-gctgcagagcggctcaag-3′, reverse 5′-aaggggaatgtgatgatggtgtag-3′. For the purpose of normalisation of gene expression of the above genes, the house keeping genes *B2m* and *Hprt1* were chosen, as these have been shown to be stably expressed during osteoclast differentiation [17]. Oligonucleotide sequences were: *B2m* forward 5′-ctgctacgtaacacagttccaccc-3′ reverse 5′-catgatgcttgatcacatgtctcg-3′; *Hprt1* forward 5′-ggttaagcagtacagcccca-3′ reverse 5′-tgcagattcaacttgcgctc-3′.

2.5. Resorption activity

Resorptive activity was measured, as described previously [14]. Briefly, following the 14 day culture period on Osteologic™ slides, resorption was visualised using Von Kossa staining, which stains the non-resorbed mineralised collagen background, highlighting areas of osteoclastic activity. Light microscopic images were converted to black and white then resorption was quantified using Image J (V 1.47, National Institutes of Health) software. Resorption assays were also undertaken under the above conditions, using whale dentine slices tailored to fit 96 well plates, which were subsequently examined by scanning electron microscopy, as previously described [18].

2.6. Statistical analysis

Statistical analysis was performed using GraphPad Prism software (v6.05 GraphPad Software, San Diego, CA, USA). Analysis was performed using two-way ANOVA followed by Holm–Šídák multi-comparison post-hoc tests or multiple or standard Student's *T*-tests.

3. Results

3.1. Relative osteoclastogenic potential of Cyp27b1 KO splenocytes

n this study, we analysed the ability of splenocytes isolated from mice deficient in CYP27B1 activity or from their WT counterparts to differentiate into osteoclasts. Following stimulation with recombinant RANKL/M-CSF, conditions well known to stimulate osteoclastogenesis, TRAP staining at four time points, chosen to capture the early, mid- and late stages of multinucleated cell formation (Fig. 1), indicated that *Cyp27b1* KO osteoclast differentiation was consistently reduced compared to WT by approximately 50%.

The addition of exogenous 1,25D (1 nM) to WT cultures inhibited the number of TRAP$^+$ multinucleated osteoclasts formed, to approximately the same number as seen in untreated *Cyp27b1* KO cultures (Fig. 1). The addition of 1,25D to *Cyp27b1* KO cultures resulted in a trend for decreased osteoclast formation on day 8, consistent with these cells retaining responsiveness to exogenous 1,25D. The addition of 25D to WT cultures caused a decrease in osteoclast formation at day 8 and a significant increase at day 9. As expected, 25D had no effect on *Cyp27b1* KO cultures (Fig. 1).

As depicted in Fig. 2, osteoclast size was decreased in the *Cyp27b1* KO cultures compared with WT. 1,25D treated WT cultures appeared similar to the untreated and 1,25D treated *Cyp27b1* KO cultures (Fig. 2). 25D had little noticeable effect on osteoclast size in cultures of either genotype. The difference due to genotype alone translated into fewer average nuclei per cell in *Cyp27b1* KO TRAP$^+$ cells than in WT cultures (Fig. 3A). Analysis of osteoclast size distribution based on the number of nuclei/cell showed significantly more small osteoclasts (3–10 nuclei/cell) present in *Cyp27b1* KO cultures than in WT cultures at day 9 of culture (Fig. 3C). The most prominent difference seen was a marked decrease in larger osteoclasts (containing >25 nuclei) seen in *Cyp27b1* KO cultures (Fig. 3D).

3.2. Effect of genotype on resorptive activity

The ability of osteoclasts formed in these experiments to resorb a bone-like matrix was confirmed on whale dentine and quantified on a mineralised collagen substrate (Osteologic™) (Fig. 4A). Despite fewer osteoclasts formed from *Cyp27b1* KO splenocyte cultures, the total area resorbed per well was not significantly different compared to WT, although there was a trend for less resorption in the case of *Cyp27b1* KO cultures ($p = 0.07$; Fig. 4B). However, by correcting for the peak numbers of TRAP$^+$ osteoclasts formed in replicate wells, observed at day 8, *Cyp27b1* KO osteoclasts resorbed 1.55 ± 0.12-fold more per osteoclast when compared to WT (Fig. 4C).

3.3. Effect of genotype on osteoclast gene expression

The analysis of the mRNA expression of the osteoclast-associated genes *Trap*, *Nfatc1*, *Car2* and *Ctsk* revealed that gene expression within the *Cyp27b1* KO osteoclast cultures was

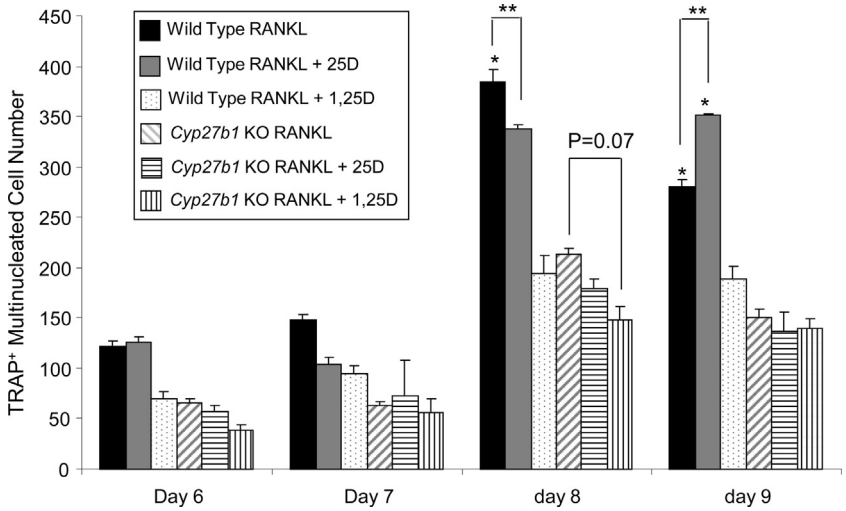

Fig. 1. The effects of *Cyp27b1* deletion on TRAP-positive osteoclast formation. Splenocytes were cultured under control or pro-osteoclastogenic conditions, as described in Section 2 for the times indicated and assayed for TRAP$^+$ multinucleated cell formation. Total TRAP positive cell numbers were combined from three independent experiments, each using splenocytes pooled from at least 4 animals/group and shown as means ± SEM. Significant differences from WT are indicated by asterisks ($p < 0.05$).

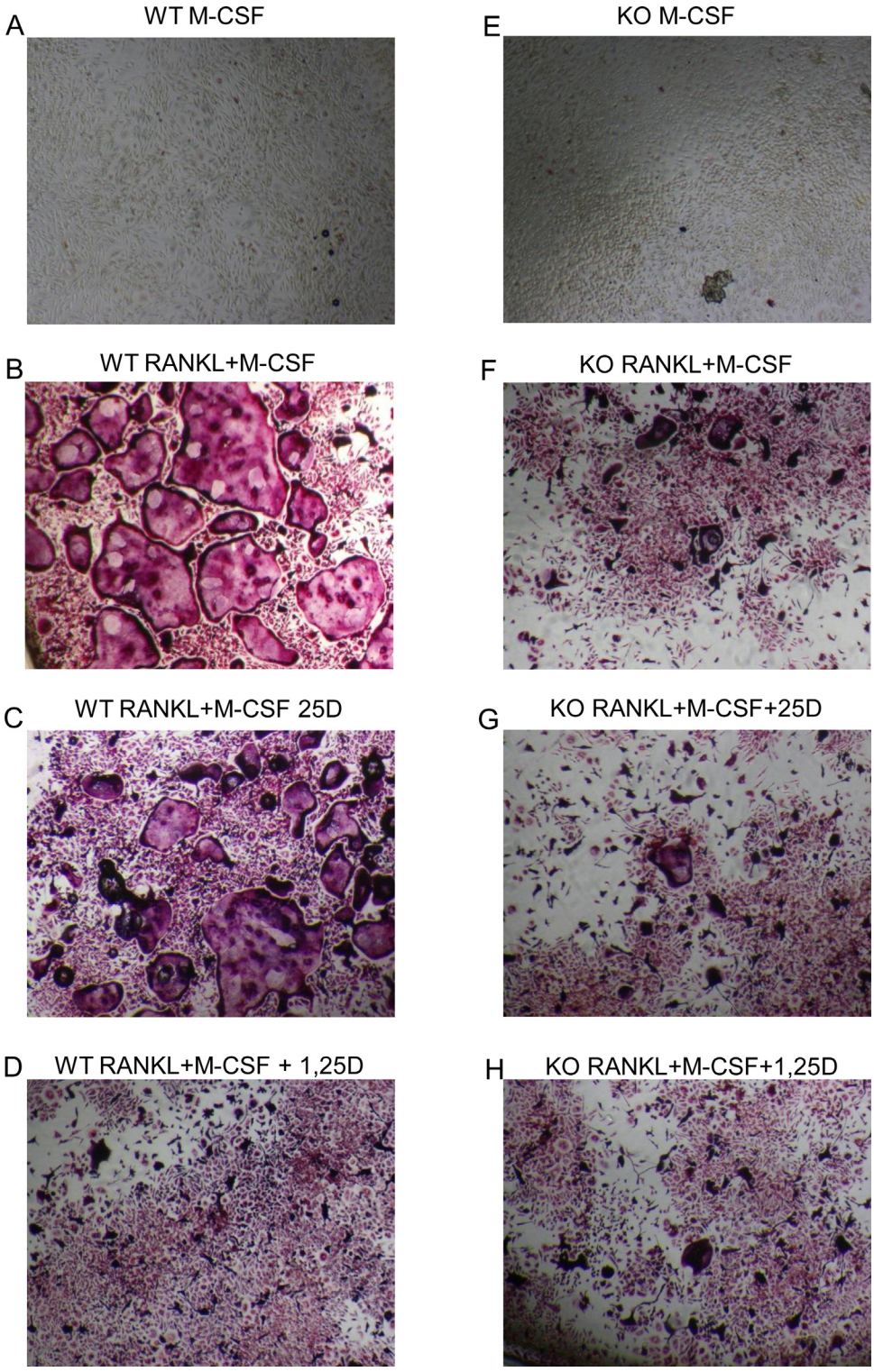

Fig. 2. Representative micrographs of TRAP-positive multinucleated cells from both WT and *Cyp27b1* KO cultures under multiple treatments. Splenocytes were cultured under control or pro-osteoclastogenic conditions, as described in Section 2 for the times indicated and assayed for $TRAP^+$ MNC formation. WT splenocytes treated with (a) M-CSF, (b) M-CSF + RANKL, (c) M-CSF + RANKL + 1,25D; *Cyp27b1* KO splenocytes treated with (d) M-CSF, (e) M-CSF + RANKL, (f) M-CSF + RANKL + 1,25D. Images were taken using a 4× objective.

strikingly reduced when compared to matched littermate controls (Fig. 5A–D), consistent with reduced total osteoclast numbers in the *Cyp27b1* KO cultures. However, the expression of the markers *Ctr* and of the VoA3 subunit of the V-ATPase was not significantly different in *Cyp27b1* KO cultures compared with WT (Fig. 5E and F). Gene expression of *Mcp1* was increased in the *Cyp27b1* KO cultures (Fig. 5G).

We also examined the possible influence of loss of *Cyp27b1* expression on cell survival. The expression ratio of *Bax*:*Bcl2* mRNA in the *Cyp27b1* KO cultures was decreased, consistent with

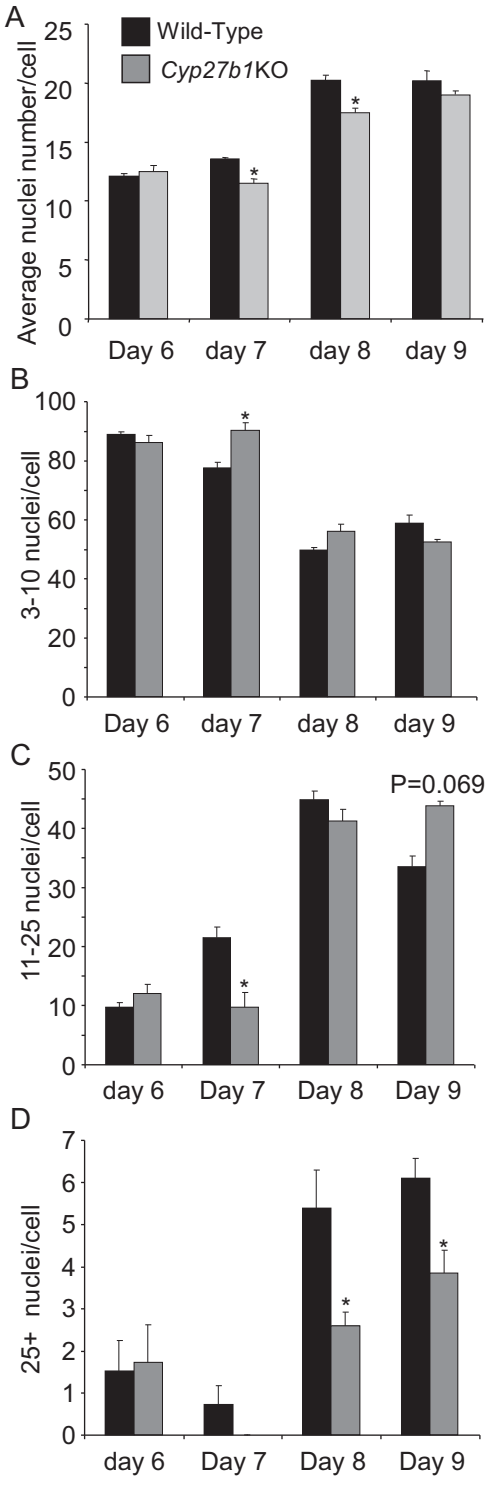

Fig. 3. The effects of *Cyp27b1* deletion on TRAP positive osteoclast nuclei number. Splenocytes were cultured under control or pro-osteoclastogenic conditions, as described in Section 2 and stained for TRAP. The number of nuclei per osteoclast was counted by light microscopy and categorised into groups: (a) combined average nuclei per cell, (b) osteoclasts containing 3–10 nuclei/cell, (c) osteoclasts containing 11–25 nuclei/cell and (d) osteoclasts containing >25 nuclei/cell. Data shown are combined counts from three independent experiments, each using splenocytes pooled from at least 4 animals/group, and shown as means ± SEM. Significant differences from WT are indicated by asterisks ($p < 0.05$).

increased survival of the osteoclasts that formed relative to WT cells (Fig. 5H). Using two-way ANOVA, all four experimental replicates demonstrated a reduced ratio of *Bax*:*Bcl2* mRNA on day 6, while in two of the experimental replicates, significant decreases were also observed on days 7 and 8.

4. Discussion

Splenocytes isolated from *Cyp27b1* KO mice displayed decreased potential to form osteoclasts *in vitro* under standard culture conditions, suggesting an intrinsic defect in osteoclastogenesis in the absence of CYP27B1 activity. This is consistent with our previous finding that *Cyp27b1* mRNA knockdown in RAW 264.7 cells inhibited osteoclast formation [6]. This finding is also consistent with the treatment of WT osteoclast precursors with 25D resulting in enhanced osteoclastogenesis [14].

Consistent with expectations [14,19,20], treatment of WT cultures with 1,25D inhibited osteoclast formation. Osteoclast formation in *Cyp27b1* KO cultures was similarly affected by 1,25D although the effect did not achieve statistical significance ($p = 0.07$). This may indicate that there is a maximum threshold of reduction that can be achieved in this model through modifications to either the vitamin D autocrine or endocrine pathways. The addition of 25D to WT cultures appeared to alter the kinetics of osteoclast formation, with fewer osteoclasts at day 8 but increased numbers at day 9. This is generally consistent with our previous findings that the addition of 25D enhanced TRAP positive osteoclast formation in RAW 264.7 cultures, although not in peripheral blood mononuclear cell (PBMC) or splenocyte-derived osteoclast cultures, however gene expression markers for osteoclastogenesis were increased by 25D in all models tested [6,14]. As expected, 25D had no discernible effect on *Cyp27b1* KO cultures. The observation that isolated osteoclasts are inhibited by 1,25D while osteoblasts are stimulated to express pro-osteoclastogenic cytokines, including RANKL and M-CSF [7–9], indicate two competing actions of 1,25D on osteoclastogenesis. This may be in order to exert tight control of the activity of osteoclasts that form *in vivo*.

Analysis of the osteoclast-like cells that formed in *Cyp27b1* KO cultures demonstrated reduced average nuclei number per osteoclast, with a clear reduction in the number of large (>25 nuclei) osteoclasts. Size is thought to play an important if not fully elucidated role in osteoclast activity. Large osteoclasts possess greater bone resorbing machinery and are therefore capable of forming larger resorption pits, however, they may be less motile than their smaller counterparts. This may in part explain our resorption data that indicated, despite the reduction in $TRAP^+$ cell number and size, *Cyp27b1* KO cells had increased resorptive activity per osteoclast formed. This is consistent with our previous findings that local 1,25D synthesis in osteoclasts, derived from human peripheral blood mononuclear cell precursors, inhibits the resorptive activity of WT osteoclasts [14]. That the effect on the resorbing activity of *Cyp27b1* KO derived osteoclasts was due to their inability to metabolise 25D into 1,25D is supported by our previous finding using splenocytes derived from *Vdr*-null mice, which also generated osteoclasts with enhanced resorption activity [14].

Consistent with our previous study showing that CYP27B1 activity was associated with increased expression of osteoclastogenesis-related genes in the resulting cultures [6], here we observed decreased mRNA expression of several key markers including *Trap*, *Nfatc1*, *Car2* and *Ctsk*. The reduction of the transcription factor NFATC1 may explain the decreased expression of the other markers and the reduction in osteoclast size and number. The reduction in expression of these genes would be expected to result in a reduction in resorptive activity, however the converse was found. Interestingly, gene expression of *V0a3* and *Ctr* were unchanged while the expression of *Mcp1* mRNA was

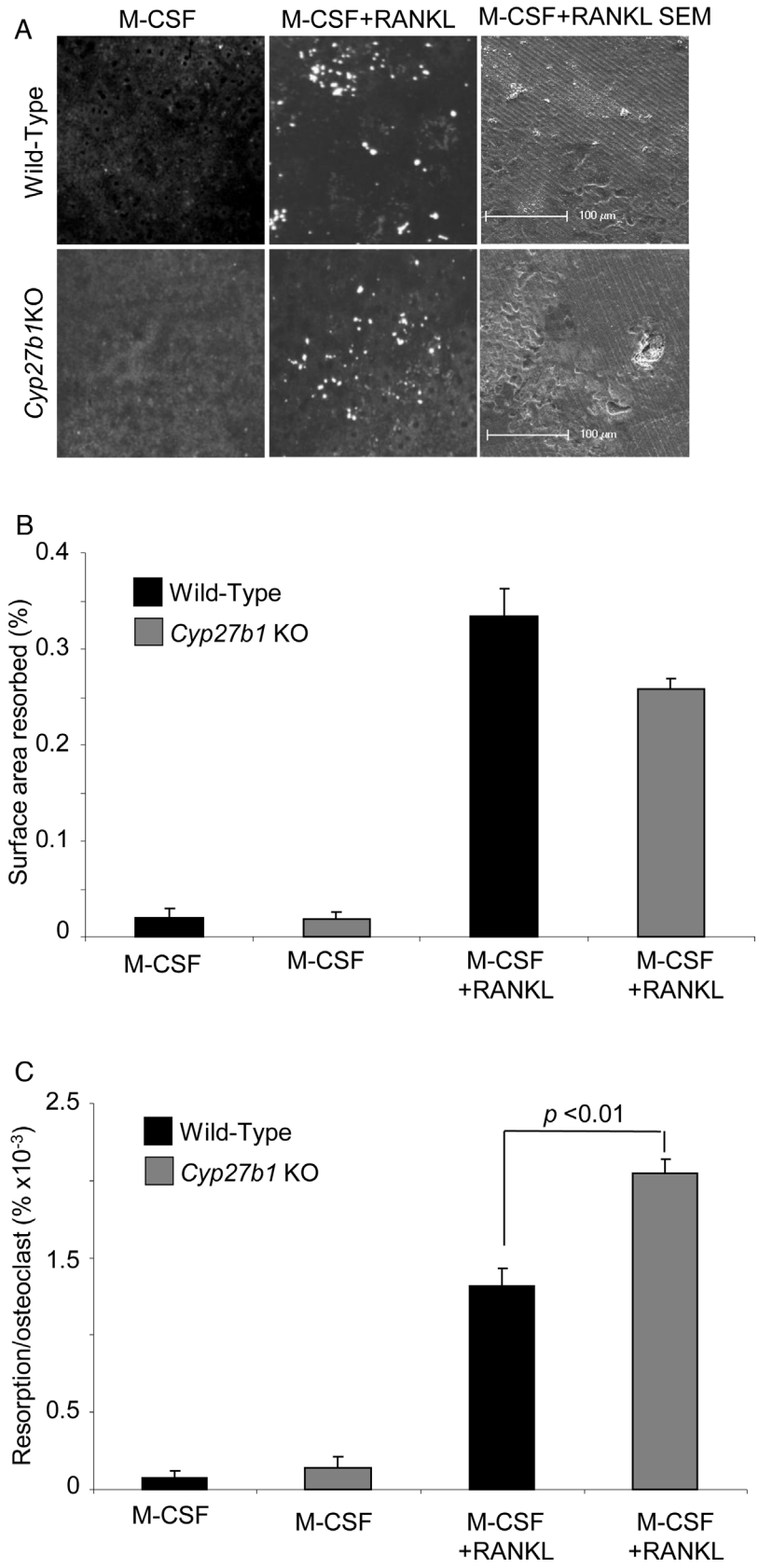

Fig. 4. The effect of *Cyp27b1* deletion osteoclast resorptive activity. Splenocytes were seeded at the same density into either dentine, Osteologic™ slides or 96-well assay plates and cultured under osteoclastogenic conditions or in the presence of M-CSF alone, as described in Section 2. After 14 days of culture, wells were stained for TRAP and slides were stained to reveal resorption areas: (A) Von Kossa stained Osteologic™ slides; dentine was cleaned and analysed by scanning electron microscopy; (B) quantified total area resorbed; (C) resorption per TRAP-positive osteoclast. Quantified data are means ± SEM of quadruplicate wells and are representative of 2 independent experiments. Significant differences between genotypes are indicated by asterisks ($p < 0.05$).

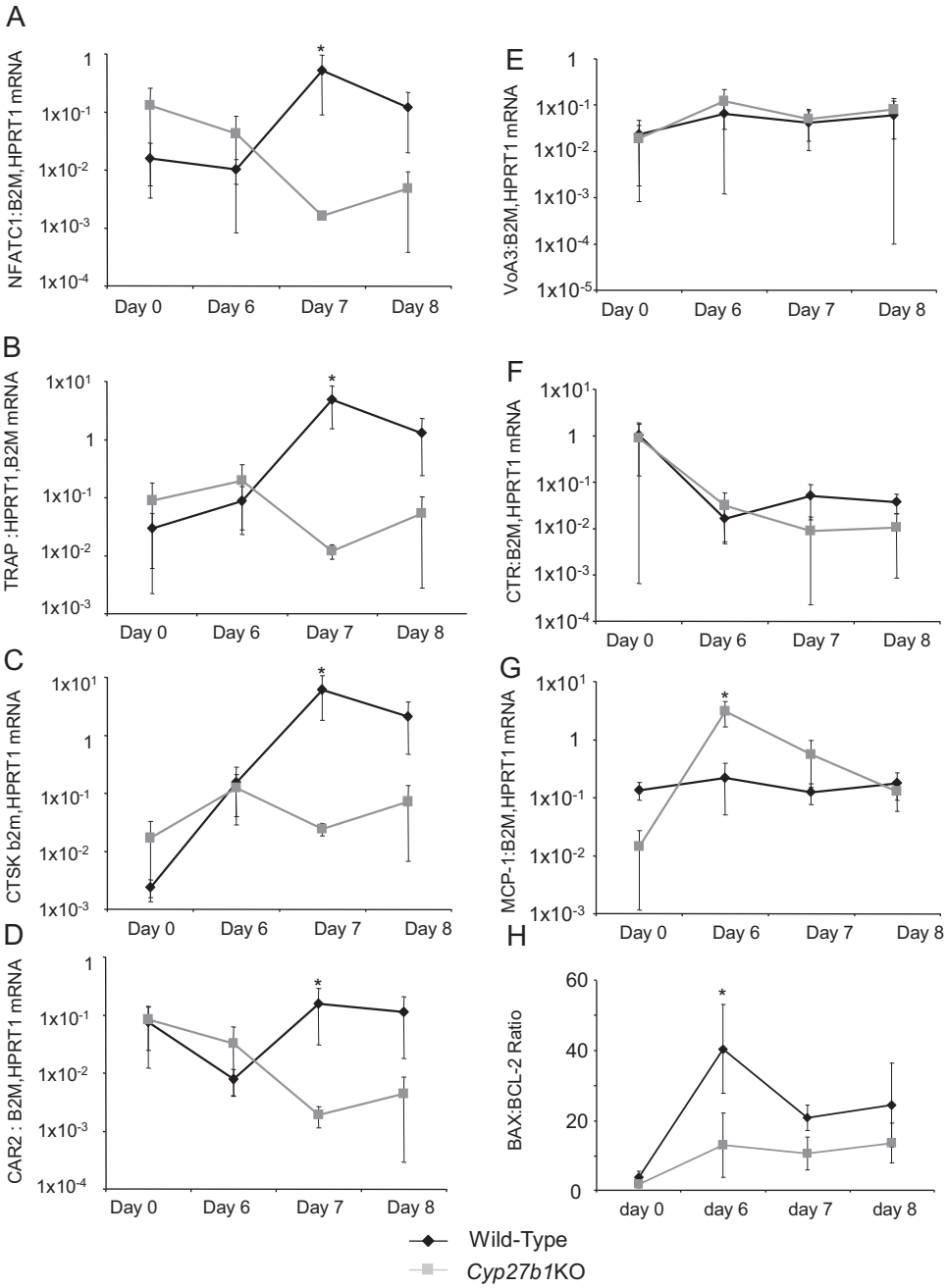

Fig. 5. The effect of *Cyp27b1* deletion on osteoclastogenic gene expression. Splenocytes pooled from four mice of each genotype were seeded into 24-well tissue culture plates at 1×10^6 cells/well and cultured under osteoclastogenic conditions, as described in Section 2. Gene expression by real-time RT-PCR was performed for the mRNA expression of (a) *Nfatc1*, (b) *Trap*, (c) *Ctsk*, (d) *Car2*, (e) *Voa3*, (f) *CTR*, (g) *MCP-1* and (h) *Bax/Bcl-2* data shown are means ± SEM of 3 independent experiments. Significant differences between genotypes are indicated by asterisks ($p < 0.05$).

increased in *Cyp27b1* KO cultures. MCP-1 acts to increase osteoclast fusion [21], however its increased expression was in direct contrast to the observed TRAP staining, suggesting that its expression may be elevated as a potential negative feedback mechanism to overcome the effect of *Cyp27b1* deletion.

The observed decrease in the number of large osteoclasts and increased number of smaller osteoclasts in the *Cyp27b1* KO cultures indicated that CYP27B1 may influence cell fate in terms of osteoclast apoptosis or survival. Apoptosis in many cell types, including osteoclasts [22,23], is regulated in part through the interplay between the pro-survival/anti-apoptotic factor B Cell lymphoma-2 (BCL-2) and the pro-apoptotic BCL-2 associated X protein, (BAX); BAX acts to increase the porosity of the outer mitochondrial membrane and promote the release of factors leading to caspase activation and apoptosis, an activity that is inhibited by BCL-2 [24,25]. We therefore examined the mRNA expression ratio of *Bax*:*Bcl2* as a surrogate measure for osteoclast survival. The reduction in this apoptotic index indicated that net *Cyp27b1* KO osteoclast survival is increased. Given that *Cyp27b1* KO cultures contained a greater number of small osteoclasts, this may indicate that in this model while large multinucleated osteoclasts do not form, the smaller cells that do form have increased survival potential. Increased osteoclast survival leading to increased resorptive activity has been demonstrated in several pathways, such as signalling through the osteoclastic protein-tyrosine phosphatase (PTP-oc) [26] and through the integrin/c-Cbl and Cbl-b pathways

[27]. However, the converse has also been demonstrated, where decreased osteoclast survival was associated with increased resorptive activity [28,29]. Alternatively, we cannot rule out that the decreased *Bax*:*Bcl2* ratio may indicate that cell types other than osteoclasts have increased survival in these cultures.

A limitation of this study is that experiments were undertaken with only haemopoietic cells present, in order to examine the effect of *Cyp27b1* deletion independently of effects in other cells that influence osteoclastogenesis, such as osteoblasts and osteocytes. This approach means that the observed osteoclast behaviour from these cultures may not be identical to those observed *in vivo*. However, a previous study [15] reported that the number of osteoclasts present in TRAP-stained bone taken from mice with global *Cyp27b1* deletion was unusually low for the very high levels of parathyroid hormone present. As well as the tendency for reduced osteoclast number it was observed that *Cyp27b1* KO mice lacking the rescue diet had smaller osteoclasts than their WT counterparts [15], consistent with the findings presented here.

Overall, these findings are further supportive of an important intrinsic role for autocrine vitamin D metabolism regulating the formation and activity of osteoclasts. At the same time, our findings imply that endocrine-derived 1,25D, independent of effects on mesenchymal-derived cells, has an inhibitory role on osteoclast formation.

Acknowledgements

This study was supported by funding from the National Health and Medical Research Council of Australia (NHMRC), Grant no. APP1029926. PHA was supported by an NHMRC RD Wright Fellowship and GJA is an NHMRC Senior Research Fellow.

References

[1] S.L. Teitelbaum, Osteoclasts: what do they do and how do they do it? Am. J. Pathol. 170 (2) (2007) 427–435.
[2] P.H. Anderson, G.J. Atkins, The skeleton as an intracrine organ for vitamin D metabolism, Mol. Aspects Med. 29 (6) (2008) 397–406 Invited Review.
[3] G.J. Atkins, P.H. Anderson, D.M. Findlay, K.J. Welldon, C. Vincent, A.C.W. Zannettino, P.D. O'Loughlin, H.A. Morris, Metabolism of vitamin D3 in human osteoblasts: evidence for autocrine and paracrine activities of 1α,25-dihydroxyvitamin D3, Bone 40 (2007) 1517–1528.
[4] M. van Driel, M. Koedam, C.J. Buurman, M. Hewison, H. Chiba, A.G. Uitterlinden, H.A. Pols, J.P. van Leeuwen, Evidence for auto/paracrine actions of vitamin D in bone: 1alpha-hydroxylase expression and activity in human bone cells, FASEB J. 20 (13) (2006) 2417–2419.
[5] A.G. Turner, M.A. Hanrath, H.A. Morris, G.J. Atkins, P.H. Anderson, The local production of 1,25(OH)D promotes osteoblast and osteocyte maturation, J. Steroid Biochem. Mol. Biol. 144 (Pt. A) (2014) 114–118.
[6] M. Kogawa, P.H. Anderson, D.M. Findlay, H.A. Morris, G.J. Atkins, The metabolism of 25-(OH) vitamin D3 by osteoclasts and their precursors regulates the differentiation of osteoclasts, J. Steroid Biochem. Mol. Biol. 121 (1–2) (2010) 277–280.
[7] N.J. Horwood, J. Elliott, T.J. Martin, M.T. Gillespie, Osteotropic agents regulate the expression of osteoclast differentiation factor and osteoprotegerin in osteoblastic stromal cells, Endocrinology 139 (11) (1998) 4743.
[8] T. Suda, Y. Ueno, K. Fujii, T. Shinki, Vitamin D and bone, J. Cell. Biochem. 88 (2) (2003) 259–266.
[9] P.A. Baldock, G.P. Thomas, J.M. Hodge, S.U. Baker, U. Dressel, P.D. O'Loughlin, G. C. Nicholson, K.H. Briffa, J.A. Eisman, E.M. Gardiner, Vitamin D action and regulation of bone remodeling: suppression of osteoclastogenesis by the mature osteoblast, J. Bone Miner. Res. 21 (10) (2006) 1618–1626.
[10] G.P. Thomas, S.U. Baker, J.A. Eisman, E.M. Gardiner, Changing RANKL/OPG mRNA expression in differentiating murine primary osteoblasts, J. Endocrinol. 170 (2) (2001) 451–460.
[11] Y. Yamamoto, T. Yoshizawa, T. Fukuda, Y. Shirode-Fukuda, T. Yu, K. Sekine, T. Sato, H. Kawano, K. Aihara, Y. Nakamichi, T. Watanabe, M. Shindo, K. Inoue, E. Inoue, N. Tsuji, M. Hoshino, G. Karsenty, D. Metzger, P. Chambon, S. Kato, Y. Imai, Vitamin D receptor in osteoblasts is a negative regulator of bone mass control, Endocrinology 154 (3) (2013) 1008–1020.
[12] G.J. Atkins, P. Kostakis, B. Pan, A. Farrugia, S. Gronthos, A. Evdokiou, K. Harrison, D.M. Findlay, A.C. Zannettino, RANKL expression is related to the differentiation state of human osteoblasts, J. Bone Miner. Res. 18 (6) (2003) 1088–1098.
[13] D. Goltzman, Inferences from genetically modified mouse models on the skeletal actions of vitamin D, J. Steroid Biochem. Mol. Biol. 148 (2015) 219–224.
[14] M. Kogawa, D.M. Findlay, P.H. Anderson, R. Ormsby, C. Vincent, H.A. Morris, G.J. Atkins, Osteoclastic metabolism of 25(OH)-vitamin D3: a potential mechanism for optimization of bone resorption, Endocrinology 151 (10) (2010) 4613–4625.
[15] D.K. Panda, D. Miao, I. Bolivar, J. Li, R. Huo, G.N. Hendy, D. Goltzman, Inactivation of the 25-hydroxyvitamin D 1alpha-hydroxylase and vitamin D receptor demonstrates independent and interdependent effects of calcium and vitamin D on skeletal and mineral homeostasis, J. Biol. Chem. 279 (16) (2004) 16754–16766.
[16] D.K. Panda, D. Miao, M.L. Tremblay, J. Sirois, R. Farookhi, G.N. Hendy, D. Goltzman, Targeted ablation of the 25-hydroxyvitamin D 1alpha -hydroxylase enzyme: evidence for skeletal, reproductive, and immune dysfunction, Proc. Natl. Acad. Sci. U. S. A. 98 (13) (2001) 7498–7503.
[17] A.S. Stephens, S.R. Stephens, N.A. Morrison, Internal control genes for quantitative RT-PCR expression analysis in mouse osteoblasts, osteoclasts and macrophages, BMC Res. Notes 4 (2011) 410.
[18] G.J. Atkins, S. Bouralexis, D.R. Haynes, S.E. Graves, S.M. Geary, A. Evdokiou, A.C. Zannettino, S. Hay, D.M. Findlay, Osteoprotegerin inhibits osteoclast formation and bone resorbing activity in giant cell tumors of bone, Bone 28 (4) (2001) 370–377.
[19] I. Itonaga, A. Sabokbar, S.D. Neale, N.A. Athanasou, 1,25-Dihydroxyvitamin D(3) and prostaglandin E(2) act directly on circulating human osteoclast precursors, Biochem. Biophys. Res. Commun. 264 (2) (1999) 590–595.
[20] H. Takasu, A. Sugita, Y. Uchiyama, N. Katagiri, M. Okazaki, E. Ogata, K. Ikeda, c-Fos protein as a target of anti-osteoclastogenic action of vitamin D, and synthesis of new analogs, J. Clin. Invest. 116 (2) (2006) 528–535.
[21] K. Miyamoto, K. Ninomiya, K.H. Sonoda, Y. Miyauchi, H. Hoshi, R. Iwasaki, H. Miyamoto, S. Yoshida, Y. Sato, H. Morioka, K. Chiba, K. Egashira, T. Suda, Y. Toyama, T. Miyamoto, MCP-1 expressed by osteoclasts stimulates osteoclastogenesis in an autocrine/paracrine manner, Biochem. Biophys. Res. Commun. 383 (3) (2009) 373–377.
[22] F.R. Amaral, V.F. Bernardes, A.P. Duarte, N.B. Pereira, A.C. Vasconcelos, R.S. Gomez, C.C. Gomes, Quantitative expression analysis of apoptotic/antiapoptotic genes and association with immunolocalization of BAX and BCL-2 in peripheral and central giant cell lesions of the jaws, Tumour Biol. 32 (5) (2011) 997–1003.
[23] L.M. Wright, W. Maloney, X. Yu, L. Kindle, P. Collin-Osdoby, P. Osdoby, Stromal cell-derived factor-1 binding to its chemokine receptor CXCR4 on precursor cells promotes the chemotactic recruitment, development and survival of human osteoclasts, Bone 36 (5) (2005) 840–853.
[24] M. Paul-Samojedny, D. Kokocinska, A. Samojedny, U. Mazurek, R. Partyka, Z. Lorenz, T. Wilczok, Expression of cell survival/death genes: Bcl-2 and Bax at the rate of colon cancer prognosis, Biochim. Biophys. Acta 1741 (1-2) (2005) 25–29.
[25] W.J. Placzek, J. Wei, S. Kitada, D. Zhai, J.C. Reed, M. Pellecchia, A survey of the anti-apoptotic Bcl-2 subfamily expression in cancer types provides a platform to predict the efficacy of Bcl-2 antagonists in cancer therapy, Cell Death Dis. 1 (2010) e40.
[26] M. Amoui, M.H. Sheng, S.T. Chen, D.J. Baylink, K.H. Lau, A transmembrane osteoclastic protein-tyrosine phosphatase regulates osteoclast activity in part by promoting osteoclast survival through c-Src-dependent activation of NFkappaB and JNK2, Arch. Biochem. Biophys. 463 (1) (2007) 47–59.
[27] E. Purev, L. Neff, W.C. Horne, R. Baron, c-Cbl and Cbl-b act redundantly to protect osteoclasts from apoptosis and to displace HDAC6 from beta-tubulin, stabilizing microtubules and podosomes, Mol. Biol. Cell 20 (18) (2009) 4021–4030.
[28] H. Masuda, J. Hirose, Y. Omata, N. Tokuyama, T. Yasui, Y. Kadono, T. Miyazaki, S. Tanaka, Anti-apoptotic Bcl-2 family member Mcl-1 regulates cell viability and bone-resorbing activity of osteoclasts, Bone 58 (2014) 1–10.
[29] H. Wakeyama, T. Akiyama, K. Takahashi, H. Amano, Y. Kadono, M. Nakamura, Y. Oshima, H. Itabe, K.I. Nakayama, K. Nakayama, K. Nakamura, S. Tanaka, Negative feedback loop in the Bim-caspase-3 axis regulating apoptosis and activity of osteoclasts, J. Bone Miner. Res. 22 (10) (2007) 1631–1639.

Chapter 5

Further examination of osteoclastogenesis in the *Cyp27b1*KO mouse model

This chapter covers additional work undertaken with the *Cyp27b1*KO mouse model that was not included in Reinke *et al.*, J. Steroid Biochemistry and Molecular Biology, 2016 as seen in Chapter 4, due to journal constraints on manuscript length, and as such represents an addendum to that chapter. The data consists predominantly of mRNA expression, examining genes not covered in the published paper, as well as the effects of vitamin D metabolites 25D and 1,25D and their subsequent effects on gene expression. Using the remaining mRNA from this work we examined vitamin D sensitivity of the V-ATPase and all 26 of its individual subunits in the osteoclast using techniques as described. Subunit gene expression is examined for alterations either due to global deletion of *Cyp27b1* or the addition of exogenous 1,25D.

5.1 Introduction

As discussed in Chapter 4, CYP27B1 is a critical component of vitamin D metabolism in both endocrine and autocrine vitamin D synthesis. We sought to gain insight into its autocrine role in osteoclasts through the use of *Cyp27b1* global osteoclast KO mice (*Cyp27b1*KO). This chapter presents the results that were not included in the published paper by Reinke *et al.* (122).

Here, we examined the mRNA expression of multiple genes from *Cyp27b1*KO osteoclasts with results also for both 25D and 1,25D treatments. Our published study reported mRNA expression for WT cells against *Cyp27b1*KO osteoclasts for a set of seven genes, as well as the ratio of *Bax* to *Bcl-2* expression as a molecular readout of propensity for cell death (122). However, results were also obtained for the mRNA expression of a number of other genes related to osteoclast formation, function and survival. As well as osteoclast related genes, all 26 individual subunits in the V-ATPase pump were examined and these are presented here (Figure 5.1 and Table 5.1).

Subunits	Gene Acronym	Function
V_1A	ATP6V1a	Catalytic ATP binding site
V_1B_1	ATP6V1b	Non-catalytic ATP binding site
V_1B_2	ATP6V1b2	Non-catalytic ATP binding site
V_1C_1	ATP6V1c	Peripheral stator
V_1C_2	ATP6V1c2	Peripheral stator
V1D	ATP6V1d	Central Rotor
V_1E_1	ATP6V1e	Peripheral stator
V_1E_2	ATP6V1e2	Peripheral stator
V_1F	ATP6V1f	Central Rotor/torque generation
V_1G_1	ATP6V1g	Peripheral stator
V_1G_2	ATP6V1g2	Peripheral stator
V_1G_3	ATP6V1g3	Peripheral stator
V_1H	ATP6V1h	Catalytic Subunit
V_0A_1	ATP6V0a	H^+ ion Translocation
V_0A_2	ATP6V0a2	H+ ion Translocation
V_0A_3/TCIRG	ATP6V0a3	H+ ion Translocation

V_0A_4	ATP6V0a4	H+ ion Translocation
V_0B	ATP6V0b	H+ ion Translocation
V_0C	ATP6V0c	H+ ion Translocation
V_0D_1	ATP6V0d	Coupling ATP hydrolysis and proton translocation
V_0D_2	ATP6V0d2	Pre osteoclast fusion
V_0E	ATP6V0e	Maturation and bone resorption
V_0E_2	ATP6V0e2	Unknown
Ac45	ATP6AP1	Regulation
M8-9	ATP6AP2	C-terminal truncation

Table 5.1: Shows the subunits and their reported functions within the V-ATPase hydrogen ion pump.

5.1.1 *C-fos*

C-fos is a member of the AP-1 family of transcription factors. It is part of the signalling cascade that results in osteoclast maturation from RANKL/RANK and M-CSF/c-FMS signalling, and acts directly on NFATC1 altering *Nfatc1* expression (123). *C-fos* null mice have been shown to be unable to form osteoclasts. The presence of *C-fos* directs precursor cells toward an osteoclastic maturation pathway (5).

5.1.2 *Clcn-7*

CLCN-7 is a chloride channel present on the osteoclast that ensures membrane potential is constant. The CLCN-7 chloride channel is used to exchange hydrogen carbonate ions for chloride ions to ensure that the membrane potential of the osteoclast remains constant during resorption (124, 125).

5.1.3 *Mcl-1*

Mcl-1 is a member of the BCL-2 family that was identified as an early expressed gene in myeloid cell lines. It has been demonstrated to enhance cell viability and bone resorption in osteoclasts. The mechanistic pathways behind this are as yet not fully elucidated (91).

5.1.4 *Bim*

Bim is a pro-apoptotic member of the BCL-2 family and induces apoptosis via cytochrome C release from mitochondria. It has been demonstrated that *Bim* is essential for osteoclast apoptosis (126, 127).

5.1.5 *Bcl-xl*

Bcl-xL is an anti-apoptotic family member of the BCL-2 family and acts to prevent apoptosis by inhibiting the function of the pro-apoptotic members of the BCL-2 family. The role of *Bcl-xL* is still being elucidated, as mice that are *Bcl-xL*-null die *in utero*. However it has been reported that osteoclast maturation and their resorptive activity are regulated by *Bcl-xL* (128, 129).

5.1.6 *V_1F*

The role of v_1f is as yet not fully elucidated. However v_1f cross-links with the v_1h subunit forming a tether, to inhibit rotary movement of the stators against the V-ATPase pump's rotary components (130). Additionally, the v_1f subunit has been established to be critical in ensuring maximum torque in rotational movement of the subunit. The loss of the v_1f subunits results in 120° backward rotation and the failure to produce ADP (65).

5.1.7 *V_1H*

The v_1h subunit-cross links with the v_1f subunit to lock down rotary action in free V_1 domains (131), resulting in v_1h being considered as a regulatory subunit within the V-ATPase pump. This

is reinforced by deletion of v_1h resulting in unregulated V-ATPase activity (131). However, the role of v_1h in osteoclasts is as yet not fully elucidated.

5.1.8 *V_0D_2*

The subunit, v_0d_2, is well investigated, including its role within the osteoclast. The deletion of v_0d_2 results in defective murine bone resorption and an osteopetrotic phenotype (64). V_0d_2 has two identified functions in the osteoclast; precursor fusion and the acidification of the resorptive zones (68). We have observed previously (3) that NFATC1 is down regulated by 1,25D in the osteoclast in the absence of stromal signaling. Furthermore, NFATC1 has been shown to up-regulate the expression of v_0d_2 transcript (63). It was therefore hypothesized that v_0d_2 would demonstrate vitamin D sensitivity.

5.2 Methods

Methods are as indicated in Chapters 2 and 3, unless otherwise stated.

5.2.1 Oligonucleotide primers

Oligonucleotide primers for all 26 subunits of the V-ATPase were kindly provided by Professor Ming-Hao Zheng (University of Western Australia). A representative time point was selected for analysis, corresponding to peak osteoclast TRAP-positive cell numbers in WT cultures. Messenger RNA expression was undertaken for both WT and *Cyp27b1*KO splenocyte cultures in the single time point assays. Messenger RNA-specific primers (Table 6.2) were designed as previously described (section 2.18), for further in-depth assays for v_1f, v_1h and v_0d_2.

5.2.2 Statistics

Gene expression was analysed using Student T-tests for the single time point experiments. Two way ANOVAs were used to analyse the gene expression for mRNA over time course with appropriate post-hoc tests (Tukey's). All statistical analyses were performed using GraphPad Prism software (v6.05 GraphPad Software, San Diego, CA, USA). Analysis for TRAP staining assays was undertaken using T-tests in GraphPad Prism.

Name	Forward Primer	Reverse Primer	Annealing	Size
Atp6V$_1$h	5' CGAGGCTATCCAGGTCTGTG 3'	5' TTTAGCACACTGGCTGCCTT 3'	60	134bp
Atp6V$_0$D$_2$	5' ATTCTTGAGTTTGAGGCCGACA 3'	5' CAGCTTGAGCTAACAACCGC 3'	60	145bp
Atp6V$_1$f	5' CGCCACCCTAATTTCCTGGT 3'	5' AGAAATTGCCTGAAAGTGTCTTCG 3'	60	74bp

Table 5.2: **Primers are mouse specific and designed for amplification of V-ATPase subunits.**

5.3 Results

5.3.1 Gene expression analysis

In our previous report (122) we excluded results obtained for *Clcn-7*, *Mcl-1*, *Trem-2*, *Cyp24*, *Bim*, *Bcl-xl* and *C-fos* due to space restrictions. *C-fos* and *Clcn-7* mRNA showed significant reduction in expression due to the deletion of *Cyp27b1* compared to WT. *Cyp24* and *Trem-2* both showed trends towards the reduction in mRNA expression due to the deletion of *Cyp27b1*. *Mcl-1* showed no significant modification in mRNA expression (Fig 5.1).

Figure 5.1: **The effects of *Cyp27b1*KO deletion on osteoclast gene expression.** Splenocytes were cultured under control of pro-osteoclastogenic conditions, as described in Chapter 2, for the times indicated. mRNA was combined from at least three experiments each using splenocytes pooled from at least 4 animals/group and shown as means ± SEM. Housekeeping genes are denoted along the Y axis in this case being *Hprt1* and *B2m*. (a) *Clcn-7* (b) *Mcl-1* (c) *Trem-2* (d) *Cyp24* (e) *C-fos*. Significant differences are indicated by asterisks ($p<0.05$) and trends by # ($p<0.10$).

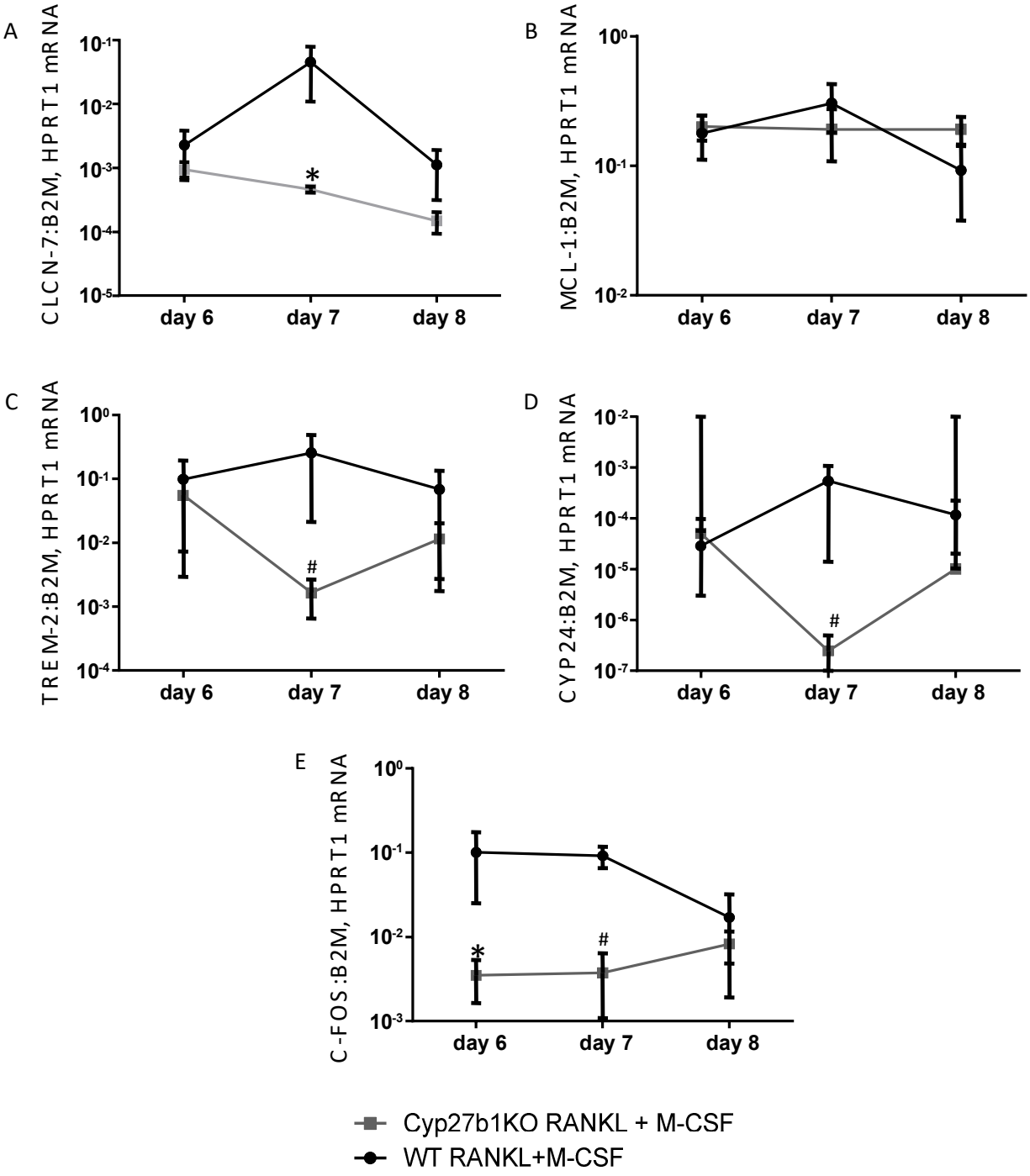
A
CLCN-7:B2M, HPRT1 mRNA
day 6
day 7
day 8
B
MCL-1:B2M, HPRT1 mRNA
C
TREM-2:B2M, HPRT1 mRNA
D
CYP24:B2M, HPRT1 mRNA
E
C-FOS:B2M, HPRT1 mRNA
Cyp27b1KO RANKL + M-CSF
WT RANKL+M-CSF

The expression of other genes were examined but showed no significant changes; this included *Hif1-α*, *Oscar*, *Sost* and *Dc-stamp* (data not shown), thus, they were not pursued further. Gene expression was also examined for the genes shown in Fig 5.1 for both 25D and 1,25D treatments. For all of the above genes, mRNA expression was unchanged in *Cyp27b1*KO mice when 25D was added to osteoclastogenic cell culture media. The addition of 25D to WT littermate-matched cultures similarly resulted in no significant changes (data not shown).

Gene expression was also examined after 1,25D (1 nM) was added to osteoclastogenic culture media. The addition of 1,25D to WT osteoclast cultures at days 0, 3 and 6 resulted in an increase in *Mcl-1* mRNA expression at early (d6) and late (d9) time points. It also resulted in a trend towards reduced *C-fos* expression on d7 (Fig 5.2).

Figure 5.2. The effects of 1,25D addition to WT osteoclast gene expression. Splenocytes were cultured under control of pro-osteoclastogenic conditions, as described in Chapter 2, for the times indicated. mRNA was combined from at least three experiments each using splenocytes pooled from at least 4 animals/group and shown as means ± SEM. Housekeeping genes are denoted along the Y axis in this case being *Hprt1* and *B2m*. Significant differences are indicated by asterisks ($P<0.05$) and trends by #($P<0.10$). (a) *Clcn-7* (b) *Trem-2* (c) *C-fos* (d) *Mcl-1* (e) *Cyp24*.

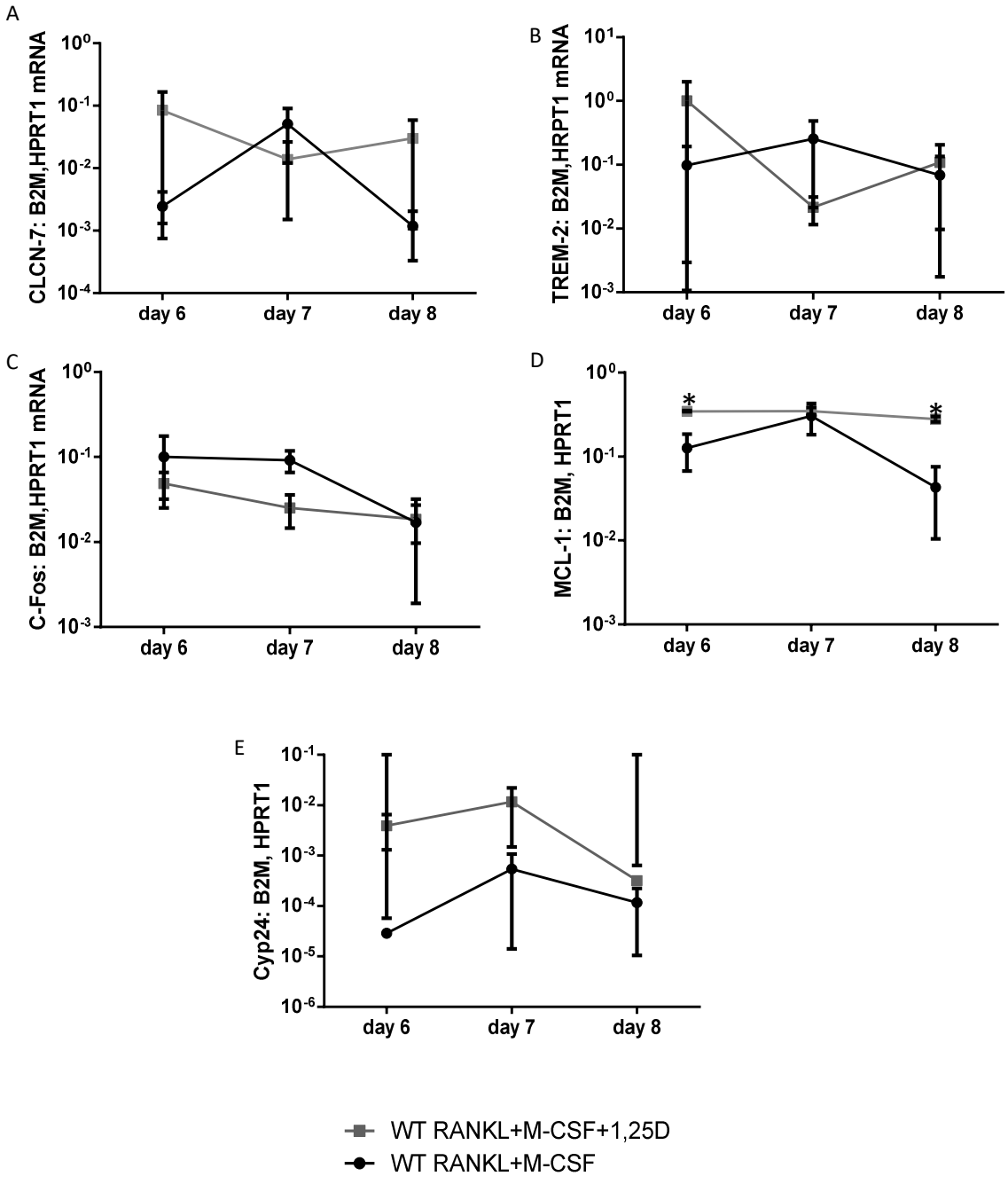
A
CLCN-7: B2M,HPRT1 mRNA
10^{0}
10^{-1}
10^{-2}
10^{-3}
10^{-4}
day 6
day 7
day 8
B
TREM-2: B2M,HRPT1 mRNA
10^{1}
10^{0}
10^{-1}
10^{-2}
10^{-3}
day 6
day 7
day 8
C
C-Fos: B2M,HPRT1 mRNA
10^{0}
10^{-1}
10^{-2}
10^{-3}
day 6
day 7
day 8
D
MCL-1: B2M, HPRT1
10^{0}
10^{-1}
10^{-2}
10^{-3}
*
*
day 6
day 7
day 8
E
Cyp24: B2M, HPRT1
10^{-1}
10^{-2}
10^{-3}
10^{-4}
10^{-5}
10^{-6}
day 6
day 7
day 8
WT RANKL+M-CSF+1,25D
WT RANKL+M-CSF

In *Cyp27b1*KO mice, the presence of 1,25D resulted in a reduction in *Trem-2* mRNA expression on day 7, increased *Mcl-1* mRNA expression on day 7, with strong increases in *Cyp24* mRNA expression persisting on days 6 and 7 (Fig 5.3).

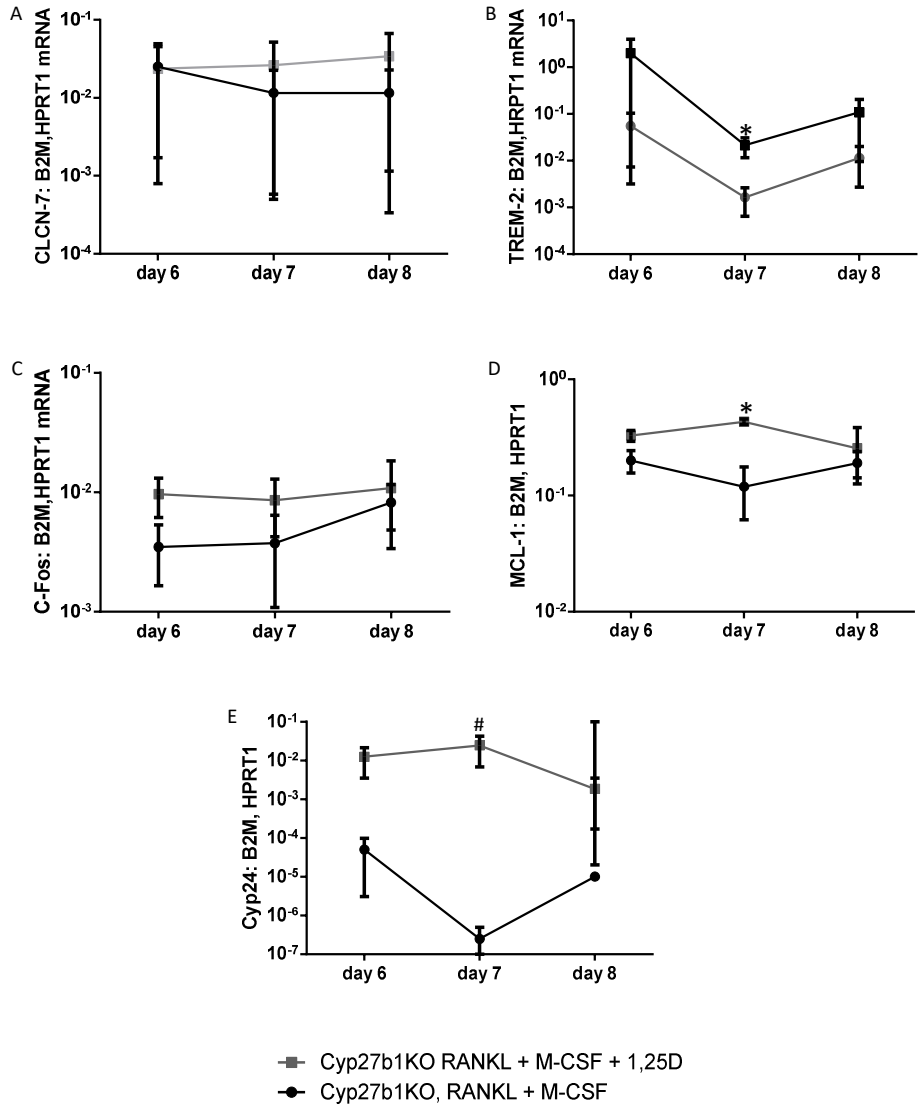

Figure 5.3. **The effects of 1,25D addition to *Cyp27b1*KO osteoclast gene expression.** Splenocytes were cultured under control of pro-osteoclastogenic conditions, as described in Chapter 2, for the times indicated. mRNA was combined from at least three experiments each using splenocytes pooled from at least 4 animals/group and shown as means ± SEM. Housekeeping genes are denoted along the Y axis in this case being *Hprt1* and *B2m*. Significant differences are indicated by asterisks ($P<0.05$) and trends by #($P<0.10$). (a) *Clcn-7* (b) *Trem-2* (c) *C-fos* (d) *Mcl-1* (e) *Cyp24 (Cyp24a1)*.

The deletion of *Cyp27b1* had no significant effect on *Bim* and *Bcl-xL* mRNA expression in these stromal-free osteoclast cultures. A trend was observed for increased *Bcl-xL* expression in the *Cyp27b1*KO cultures. The addition of 25D and 1,25D resulted in a significant decrease in *Bcl-xL* mRNA expression in WT cultures but had no effect in *Cyp27b1*KO cultures. The addition of 25D and 1,25D also resulted in a significant decrease in the expression of *Bim* mRNA in WT cultures but had no effect on *Cyp27b1*KO cultures (Fig 5.4 and 5.5).

Figure 5.4. **The effects of *Cyp27b1*KO deletion combined with the addition of Vitamin D metabolites on *Bcl-xl* gene expression in osteoclasts.**

Splenocytes were cultured under pro-osteoclastogenic conditions, as described in Chapter 2, for the times indicated. mRNA was combined from at least three experiments each using splenocytes pooled from at least 4 animals/group and shown as means ± SEM. Housekeeping genes are denoted along the Y axis in this case being *Hprt1* and *B2m*. (a) WT against *Cyp27b1*KO, (b) WT under 25D, (c) *Cyp27b1*KO under 25D, (d) WT under 1,25D, (e) *Cyp27b1*KO under 1,25D. Significant differences are indicated by asterisks ($P<0.05$) and trends by # ($P<0.10$).

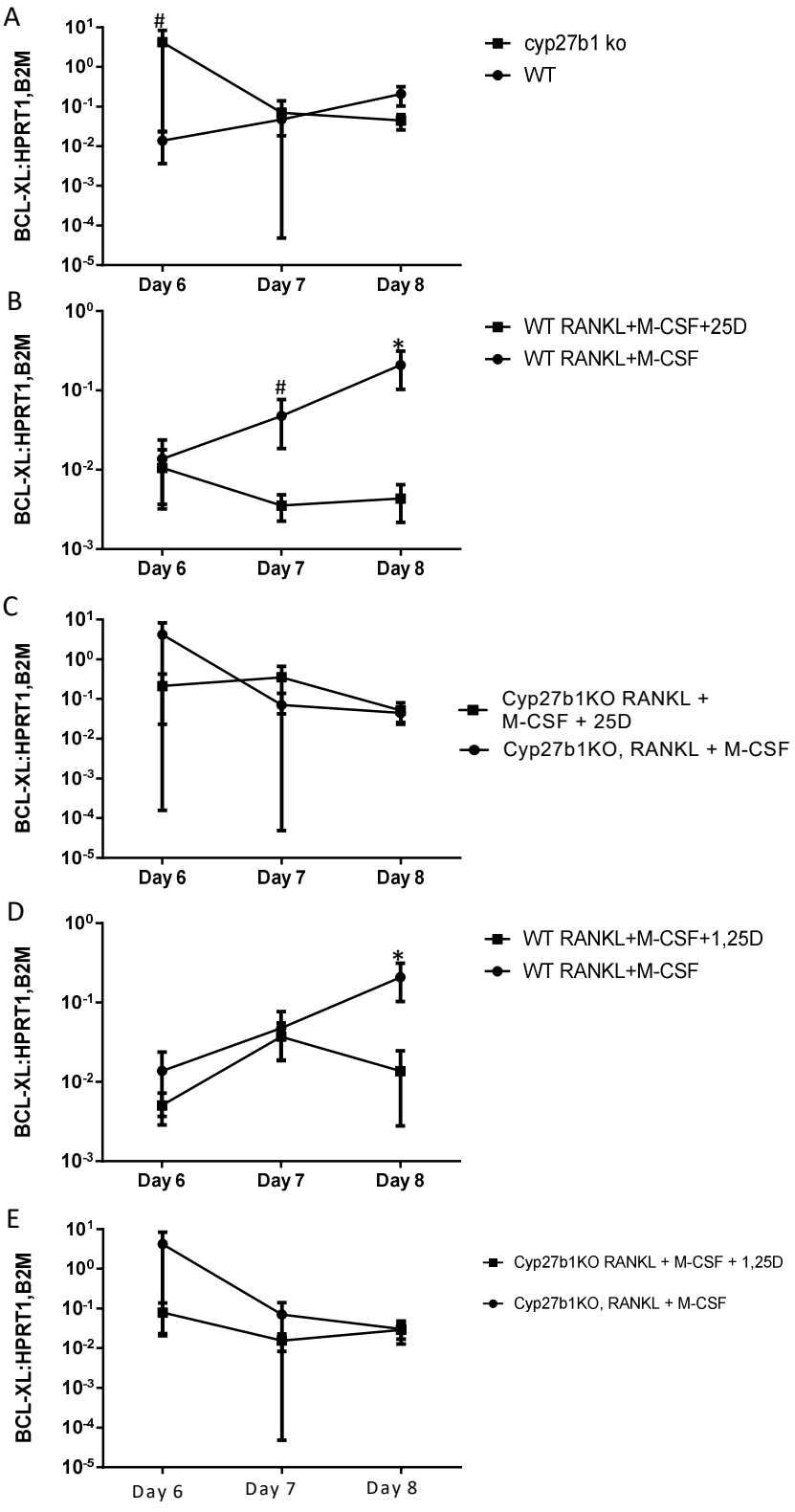
A
BCL-XL:HPRT1,B2M
Day 6
Day 7
Day 8
cyp27b1 ko
WT
B
WT RANKL+M-CSF+25D
WT RANKL+M-CSF
C
Cyp27b1KO RANKL + M-CSF + 25D
Cyp27b1KO, RANKL + M-CSF
D
WT RANKL+M-CSF+1,25D
WT RANKL+M-CSF
E
Cyp27b1KO RANKL + M-CSF + 1,25D
Cyp27b1KO, RANKL + M-CSF

Figure 5.5. **The effects of *Cyp27b1*KO deletion combined with the addition of Vitamin D metabolites on *Bim* gene expression in osteoclasts.**

Splenocytes were cultured under pro-osteoclastogenic conditions, as described in Chapter 2, for the times indicated. mRNA was combined from at least three experiments each using splenocytes pooled from at least 4 animals/group and shown as means ± SEM. Housekeeping genes are denoted along the Y axis in this case being *Hprt1* and *B2m*. Significant differences are indicated by asterisks ($P<0.05$) and trends by # ($P<0.10$). (a) WT against *Cyp27b1*KO, (b) WT under 25D, (c) *Cyp27b1*KO under 25D, (d) WT under 1,25D, (e) *Cyp27b1*KO under 1,25D.

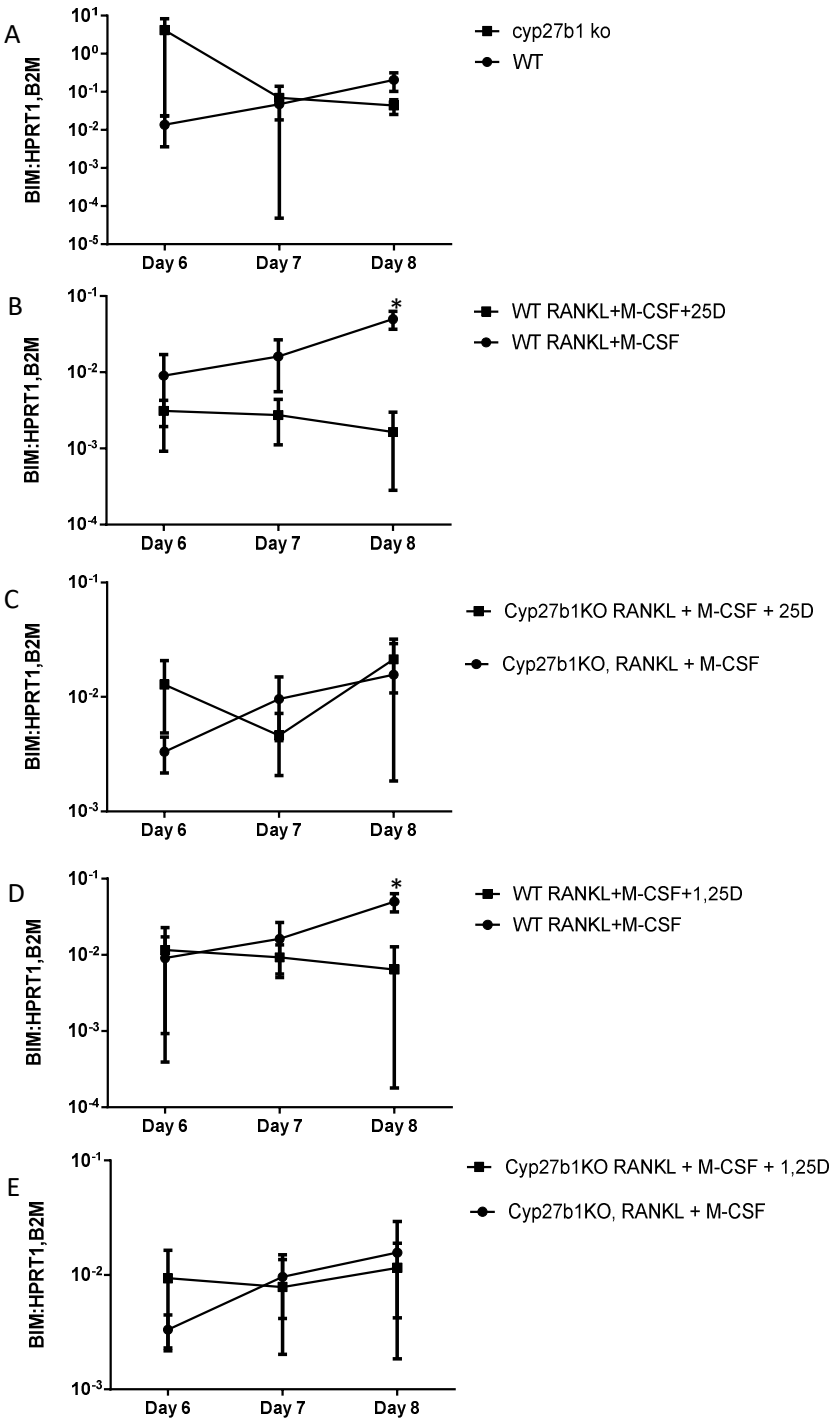
A
BIM:HPRT1,B2M
Day 6
Day 7
Day 8
cyp27b1 ko
WT
B
BIM:HPRT1,B2M
*
WT RANKL+M-CSF+25D
WT RANKL+M-CSF
C
BIM:HPRT1,B2M
Cyp27b1KO RANKL + M-CSF + 25D
Cyp27b1KO, RANKL + M-CSF
D
BIM:HPRT1,B2M
*
WT RANKL+M-CSF+1,25D
WT RANKL+M-CSF
E
BIM:HPRT1,B2M
Cyp27b1KO RANKL + M-CSF + 1,25D
Cyp27b1KO, RANKL + M-CSF

5.3.2 V-ATPase Subunit gene expression analysis

In this study, we examined mRNA expression of individual V-ATPase subunits from a single time point, day 8 corresponding with peak osteoclast formation. The deletion of *Cyp27b1* resulted in an increase in v_1a, v_1b_1, v_1b_2, v_1c_1, v_1c_2, v_1d, v_1g_2, v_0a_1, v_0a_2, v_0a_4, v_0d_1, v_0d_2 and v_0e_1 gene expression. Conversely, the v_1f, v_1h and v_0c subunits were shown to be decreased due to the deletion of *Cyp27b1*. The gene expression of the remaining subunits v_1e, v_1e_2, v_1g_1, v_1g_3, v_0a_3, v_0e_2, AC45, M8-9 showed no significant changes due to the deletion of *Cyp27b1* (Fig. 5.6). Subunits showing changes in gene expression were preferentially selected for further analysis. The deletion of *Cyp27b1* resulted in a genotype change in the subunits v_1a_2, v_1b_1, v_1g_2, v_1g_3, v_0a_1, v_0a_3, v_0a_4, v_0d_1, and v_0d_2. This change was consistent with an increase in expression in all these subunits, indicating that the loss of *Cyp27b1* at the germline level results in deregulation in eight of the subunits of the V-ATPase. 1,25D was added to cultures in order to by-pass the deletion of *Cyp72b1* and act directly on the VDR ideally resulting in the restoration of the autocrine vitamin D pathway. It was observed that in WT cultures exogenous 1,25D increased the expression of 50% of the subunits and decreased the expression of only two. Of particular note v_1h considered a regulatory subunit was one of the few subunits decreased. The actions of 1,25D in *Cyp27b1*KO cultures was remarkably similar to that of the WT cultures although there was often a greater level of change in the KO cultures. The major exceptions were v_1c and v_1h.

Figure 5.6: **Gene expression of V-ATPase subunits in WT and *Cyp27b1*KO osteoclast cultures.** Mouse splenocytes were seeded at a density of $1x10^6$ cells per well into 24 well culture plates with α-MEM and FBS 10% (v/v) with M-CSF (25ng/ml) and RANKL (100ng/ml), in the presence or absence of 1,25D (1nM). a)V_1a, b) V_1b, c) V_1b_2, d) V_1c_1, e) V_1c_2, f) V_1d, g) V_1e, h) V_1e_2, i) V_1f, j) V_1g, k) V_1g_2, l) V_1g_3, m) V_1h, n) V_0a_1, o) V_0a_2, p) V_0a_3, q) V_0a_4, r) V_0c_1, s) V_0c_2, t) V_0d_1, u) V_0d_2, v) V_0e_1, w) V_0e_2, x) AC45, y) M8-9 Significant differences between genotypes are indicated by (a). Differences between WT and exogenous 1,25D are indicated by (b). # indicates a trend instead of significance, defined as a non-significant change with a value for $p < 0.1$

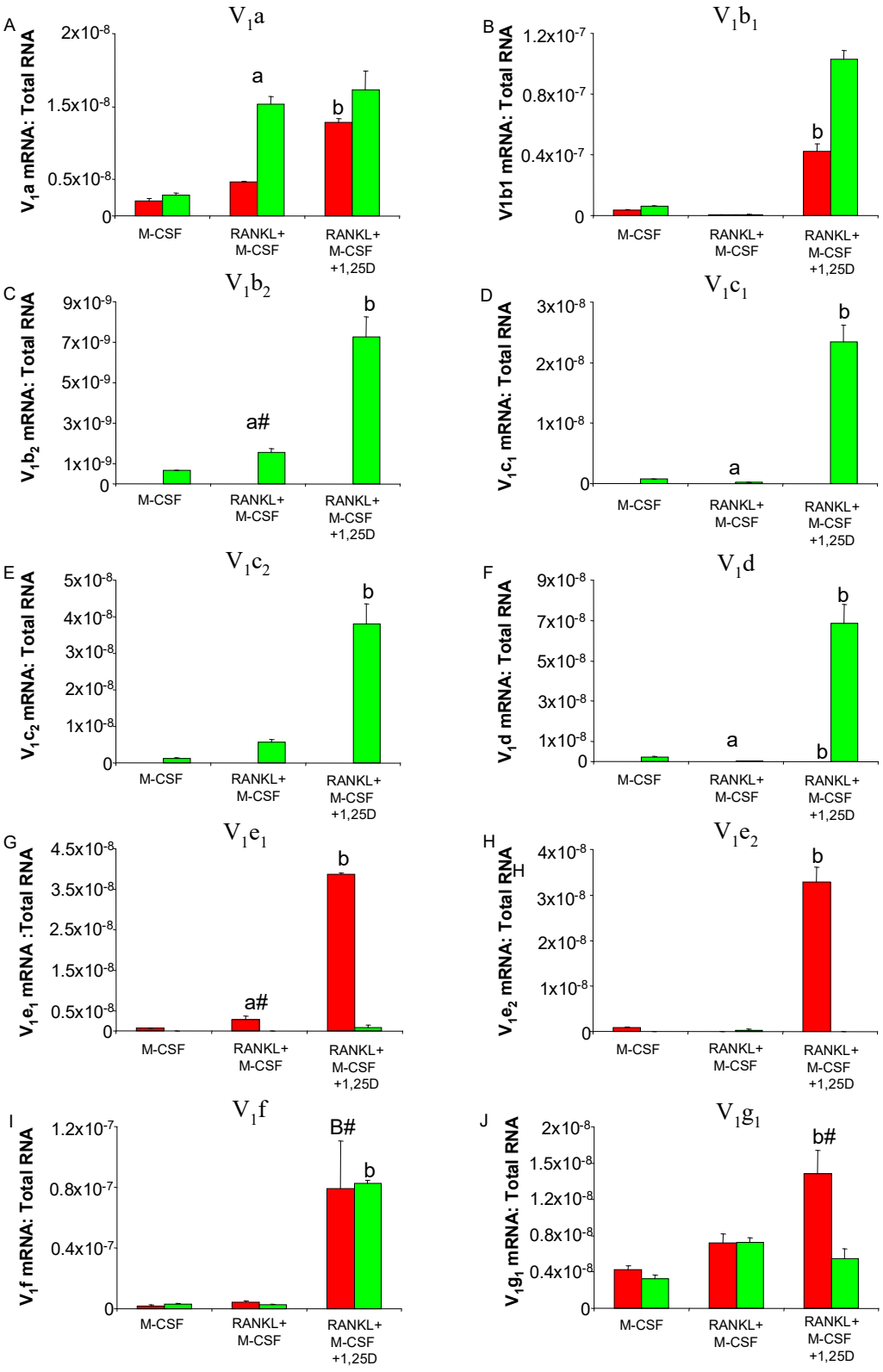
A
V_1a
V_1a mRNA: Total RNA
2x10-8
1.5x10-8
0.5x10-8
0
a
b
M-CSF
RANKL+ M-CSF
RANKL+ M-CSF +1,25D
B
V_1b_1
V1b1 mRNA: Total RNA
1.2x10-7
0.8x10-7
0.4x10-7
0
b
C
V_1b_2
V_1b_2 mRNA: Total RNA
9x10-9
7x10-9
5x10-9
3x10-9
1x10-9
a#
D
V_1c_1
V_1c_1 mRNA: Total RNA
3x10-8
2x10-8
1x10-8
a
E
V_1c_2
V_1c_2 mRNA: Total RNA
5x10-8
4x10-8
3x10-8
2x10-8
1x10-8
F
V_1d
V_1d mRNA: Total RNA
9x10-8
7x10-8
5x10-8
3x10-8
1x10-8
G
V_1e_1
V_1e_1 mRNA :Total RNA
4.5x10-8
3.5x10-8
2.5x10-8
1.5x10-8
0.5x10-8
H
V_1e_2
V_1e_2 mRNA: Total RNA
4x10-8
3x10-8
2x10-8
1x10-8
I
V_1f
V_1f mRNA: Total RNA
1.2x10-7
0.8x10-7
0.4x10-7
B#
J
V_1g_1
V_1g_1 mRNA: Total RNA
2x10-8
1.5x10-8
1.2x10-8
0.8x10-8
0.4x10-8
b#

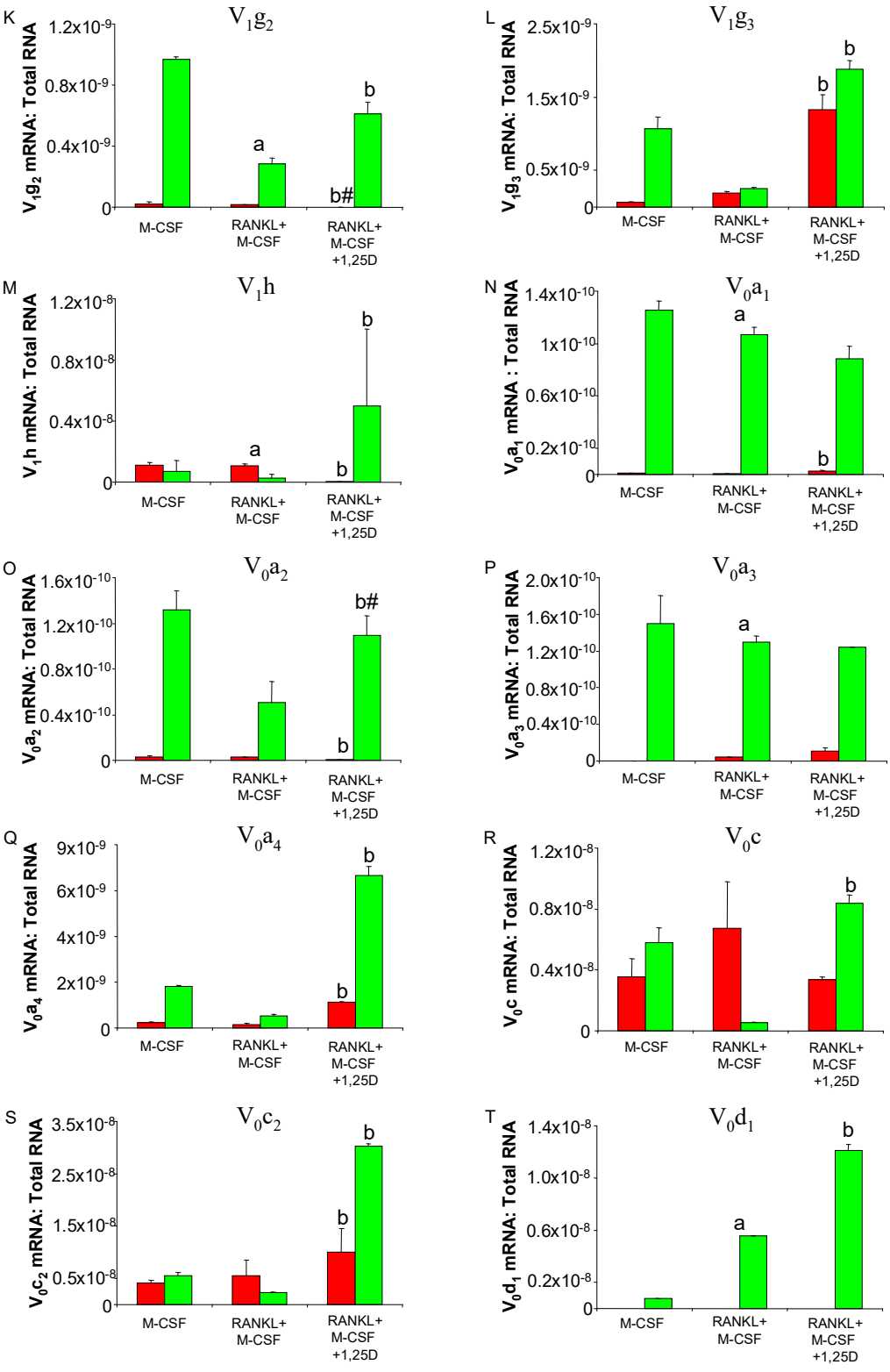
K
V_1g_2
V_1g_2 mRNA: Total RNA
1.2x10-9
0.8x10-9
0.4x10-9
0
a
b
b#
M-CSF
RANKL+ M-CSF
RANKL+ M-CSF +1,25D
L
V_1g_3
V_1g_3 mRNA: Total RNA
2.5x10-9
1.5x10-9
0.5x10-9
b
b
M
V_1h
V_1h mRNA: Total RNA
1.2x10-8
0.8x10-8
0.4x10-8
a
b
b
N
V_0a_1
V_0a_1 mRNA : Total RNA
1.4x10-10
1x10-10
0.6x10-10
0.2x10-10
a
b
O
V_0a_2
V_0a_2 mRNA: Total RNA
1.6x10-10
1.2x10-10
0.8x10-10
0.4x10-10
b#
b
P
V_0a_3
V_0a_3 mRNA: Total RNA
2.0x10-10
1.6x10-10
1.2x10-10
0.8x10-10
0.4x10-10
a
Q
V_0a_4
V_0a_4 mRNA: Total RNA
9x10-9
6x10-9
4x10-9
2x10-9
b
b
R
V_0c
V_0c mRNA: Total RNA
1.2x10-8
0.8x10-8
0.4x10-8
b
S
V_0c_2
V_0c_2 mRNA: Total RNA
3.5x10-8
2.5x10-8
1.5x10-8
0.5x10-8
b
b
T
V_0d_1
V_0d_1 mRNA: Total RNA
1.4x10-8
1.0x10-8
0.6x10-8
0.2x10-8
a
b

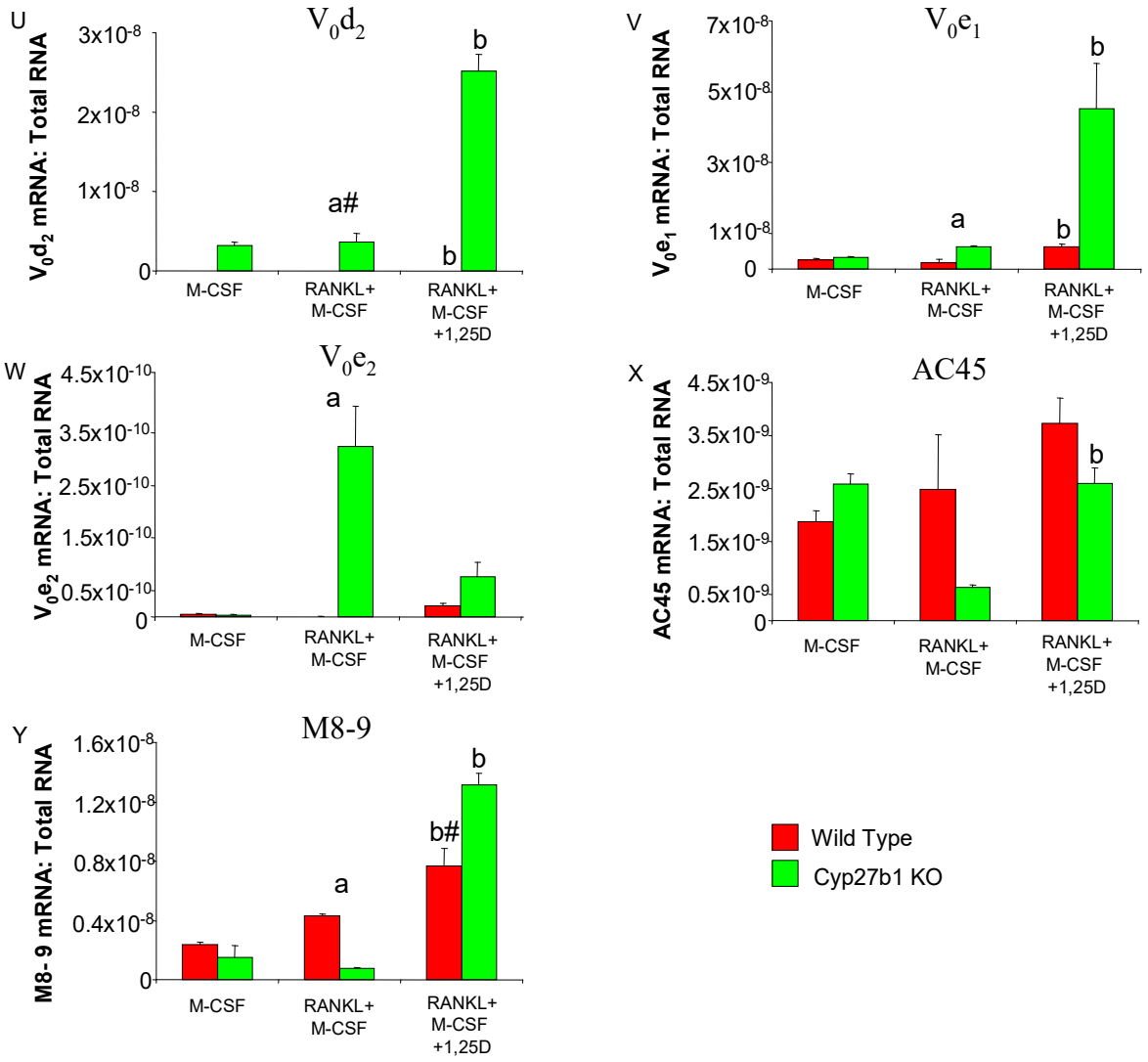
U
V_0d_2
V_0d_2 mRNA: Total RNA
3x10-8
2x10-8
1x10-8
0
a#
b
b
M-CSF
RANKL+ M-CSF
RANKL+ M-CSF +1,25D
V
V_0e_1
V_0e_1 mRNA: Total RNA
7x10-8
5x10-8
3x10-8
1x10-8
0
a
b
b
M-CSF
RANKL+ M-CSF
RANKL+ M-CSF +1,25D
W
V_0e_2
V_0e_2 mRNA: Total RNA
4.5x10-10
3.5x10-10
2.5x10-10
1.5x10-10
0.5x10-10
0
a
M-CSF
RANKL+ M-CSF
RANKL+ M-CSF +1,25D
X
AC45
AC45 mRNA: Total RNA
4.5x10-9
3.5x10-9
2.5x10-9
1.5x10-9
0.5x10-9
0
b
M-CSF
RANKL+ M-CSF
RANKL+ M-CSF +1,25D
Y
M8-9
M8- 9 mRNA: Total RNA
1.6x10-8
1.2x10-8
0.8x10-8
0.4x10-8
0
b
b#
a
M-CSF
RANKL+ M-CSF
RANKL+ M-CSF +1,25D
Wild Type
Cyp27b1 KO

5.3.3 V_1F subunit

Analysis of *v1f* gene expression revealed decreased expression in *Cyp27b1*KO osteoclast cultures compared to WT match littermates. A decrease in gene expression was observed under M-CSF/RANKL treated *Cyp27b1*KO cultures on day 7 and in *Vdr*KO cultures on day 6 when compared against WT littermate matched controls.

The addition of 1,25D to *Cyp27b1*KO osteoclast cultures resulted in increased expression of *v1f* on day 7 (Fig. 5.7).

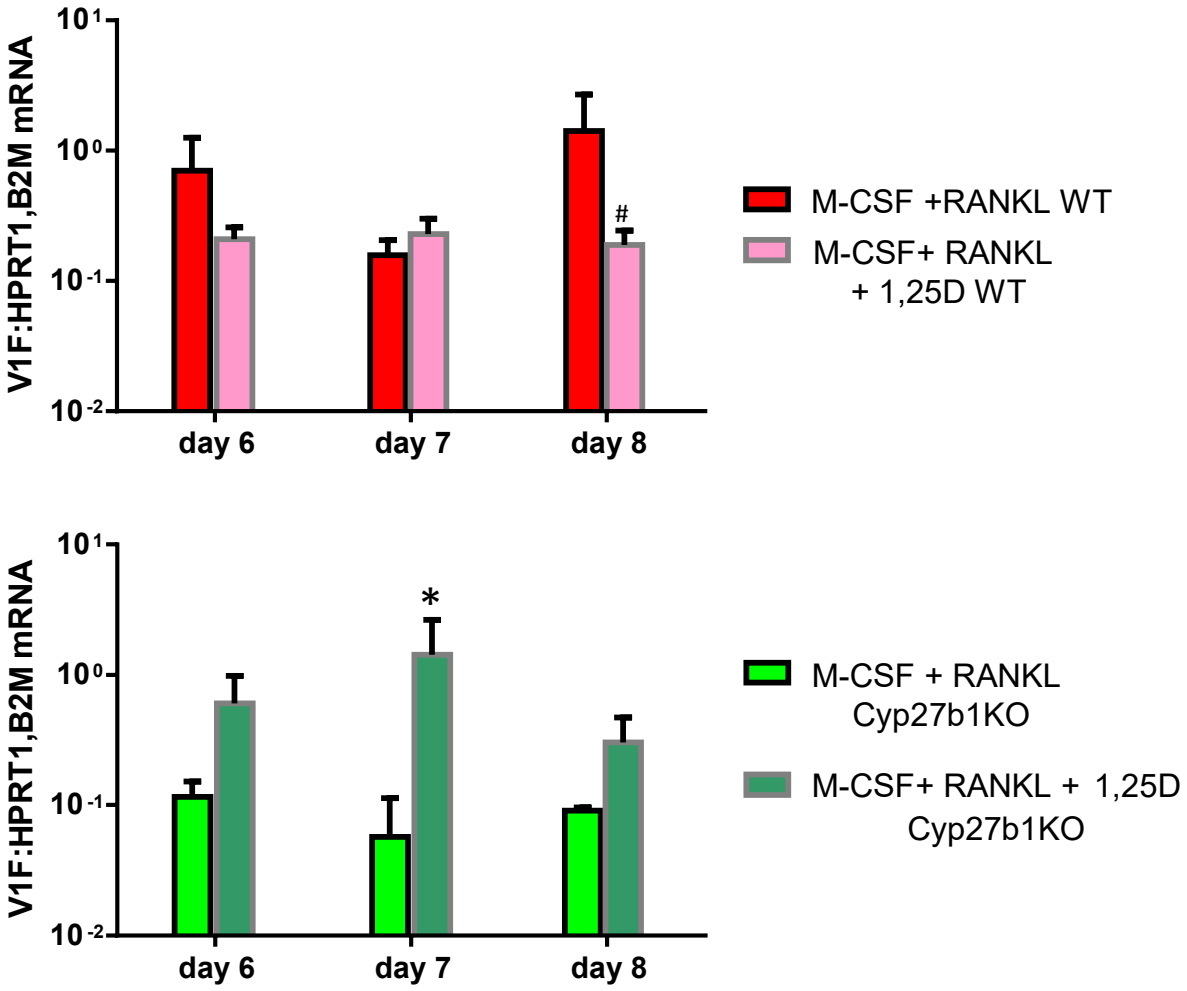

Figure 5.7. Gene expression over time for V-ATPase subunit v1f under the effect of Vitamin D metabolites and *Cyp27b1*KO. Mouse splenocytes were seeded at a density of 1x10^6 into 24 well culture plates with α-MEM and FBS 10% (v/v) with M-CSF (25ng/ml) and RANKL (100ng/ml). mRNA was combined from at least three experiments each using splenocytes pooled from at least 4 animals/group and shown as means ± SEM. a) WT splenocytes control and 1,25D treatment b) *Cyp27b1*KO splenocytes control and 1,25D treatment.

5.3.4 V_1H subunit

Analysis of *v1h* gene expression revealed decreased expression in *Cyp27b1* osteoclast cultures compared to WT-matched littermates on day 6 (Fig. 5.8). The addition of exogenous 1,25D resulted in a significant increase in *v1h* gene expression on day 8 in WT splenocytes. The addition of 1,25D to *Cyp27b1*KO osteoclast cultures however, had no significant effect on *v1h* expression. Significant increase in *Vdr*KO expression was observed (Fig. 5.8).

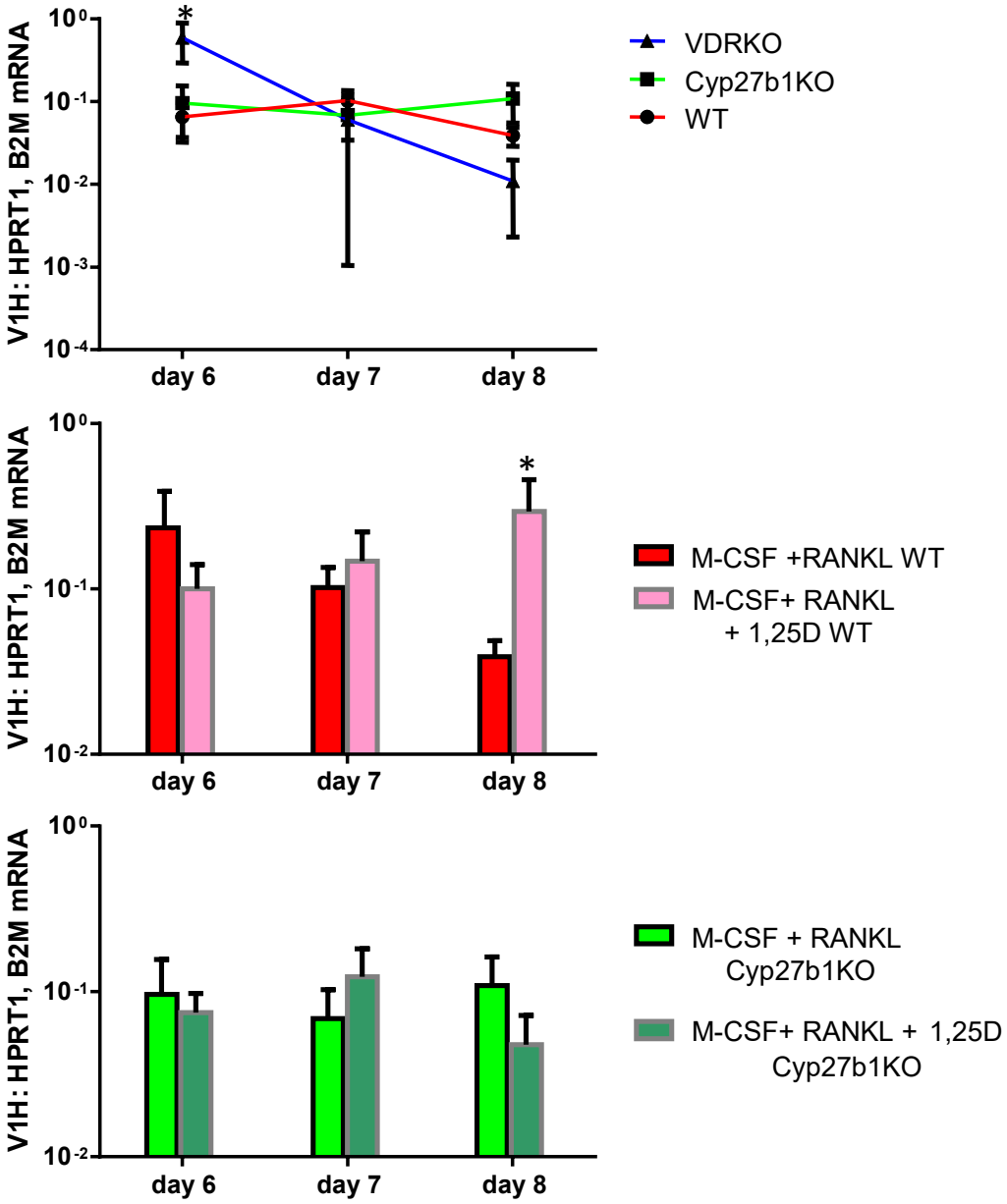

Figure 5.8: **Gene expression over time for V-ATPase subunit *v1h* under the effect of vitamin D metabolites *Vdr*KO and *Cyp27b1*KO.** Mouse splenocytes were seeded at a density of $1x10^6$ into 24 well culture plates with α-MEM and FBS 10% (v/v) with M-CSF (25ng/ml) and RANKL (100ng/ml). mRNA was combined from at least three experiments each using splenocytes pooled from at least 4 animals/group and shown as means ± SEM.

5.3.5 V_0D_2 subunit

Analysis of *v0d2* gene expression revealed no significant changes in expression in *Cyp27b1*KO osteoclast cultures compared to WT-matched littermates (Fig. 5.9). The response to 1,25D of both genotypes was also similar. In WT cultures, expression of *v0d2* was increased under the addition of 1,25D on day 6 (Fig. 5.9).

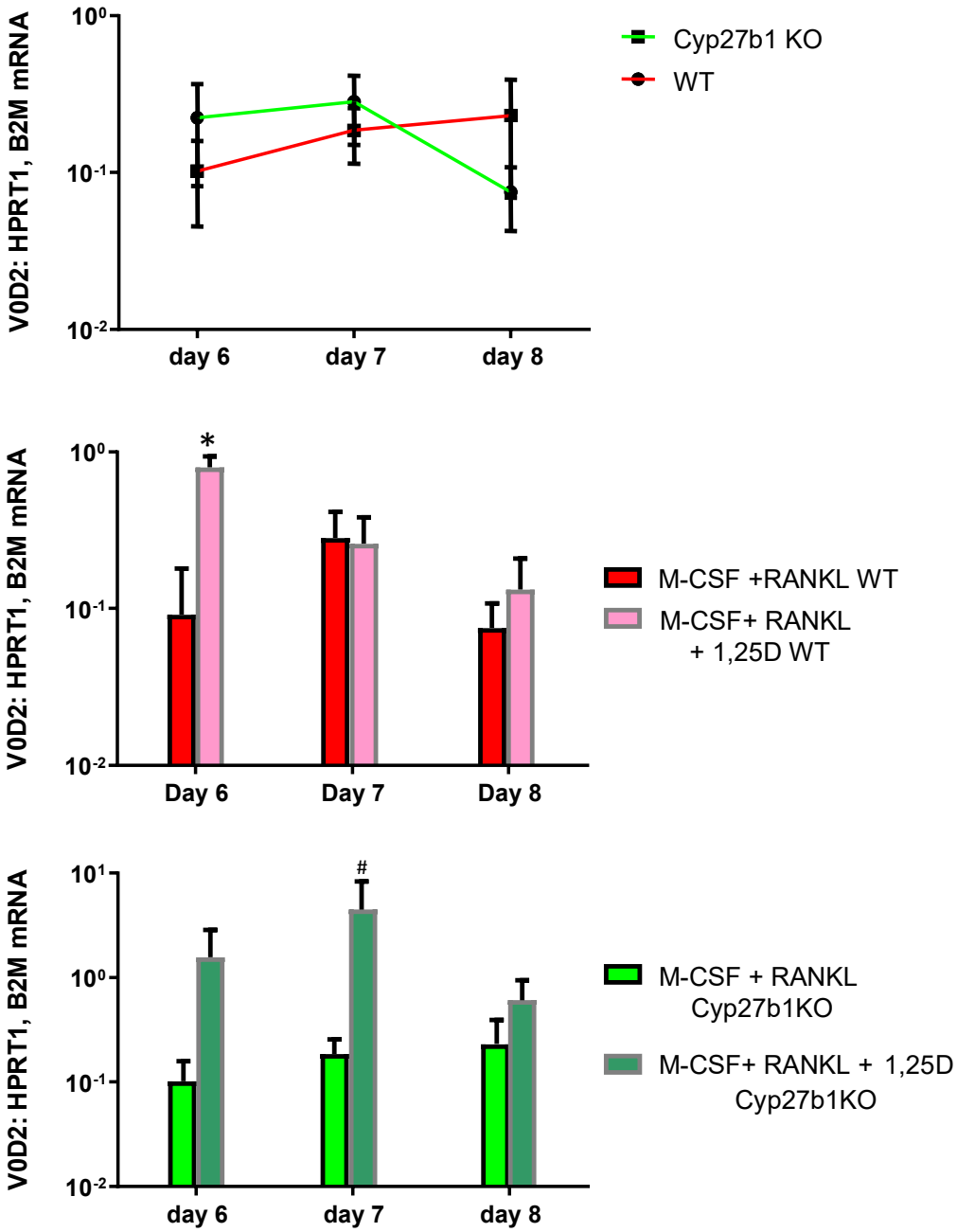

Figure 5.9: **Gene expression over time for V-ATPase subunit *v0d2* under the effect of vitamin D metabolites and *Cyp27b1*KO.** Mouse splenocytes were seeded at a density of 1x10^6 into 24 well culture plates with α-MEM and FBS 10% (v/v) with M-CSF (25ng/ml) and RANKL (100ng/ml).

5.4 Discussion

5.4.1 Osteoclast related genes

Our previous study (122) indicated that deletion of *Cyp27b1* increased osteoclast number, resorptive activity per osteoclast and resulted in a decrease in gene expression of *Nfatc1*, *Trap*, *Ctsk* and *Ca2*. The exception to this general decrease observed in most genes was *Mcp-1* expression, which was increased. *Cyp27b1*KO osteoclast potential for survival appeared to be increased based on the ratio of *Bax/Bcl-2* mRNA (122). *Cyp27b1*KO cultures displayed a trend towards reduced basal expression of *Cyp24a1* mRNA, which may be a result of the absent basal autocrine production of 1,25D in these cells (3, 7). However, *Cyp27b1*KO cultures responded robustly to exogenously added 1,25D with respect to *Cyp24a1* mRNA induction, consistent with no impairment of 1,25D signalling.

Gene expression was significantly reduced for *Clcn-7*. This was unexpected, particularly as we observed increased resorptive activity per osteoclast in *Cyp27b1*KO osteoclasts. As discussed, deletion of *Clcn-7* in mice results in abnormal bone dissolution and it was expected that the levels of *Clcn-7* would increase rather than decrease, as resorptive activity increased (124, 125). However, it is also possible that while *Clcn-7* is significantly reduced, other chloride channels such as Chloride Channel Three were unaffected or increased to compensate (132). It is also possible that the prolonged survival of *Cyp27b1*KO osteoclasts is solely responsible for the increased resorption observed independent of chloride channel activity.

C-fos mRNA expression was significantly decreased in early *Cyp27b1*KO osteoclastogenic cultures, as expected due to the decrease in *Nfatc1* expression,

encoding the primary regulator of osteoclastogenesis, which we reported was also decreased in these cultures (122). The reduced expression of *C-fos* and *Nfatc1* would have a follow-on effect, resulting in a subsequent decrease in mRNA expression for other genes regulated by these transcription factors. Surprisingly, the addition of 1,25D had no effect on *C-fos* gene expression. It was expected to be decreased under 1,25D signalling as the presence of 1,25D has been shown by our previous studies (122, 133) to reduce osteoclast number and gene expression. The lack of change in *C-fos* may indicate that exogenous 1,25D acts directly on NFATC1 or other upstream members of the cascade pathway.

Trem2 expression was examined since its gene product is part of an ITAM receptor that assists in the regulation of osteoclast maturation and formation, and TREM-2-null mice are demonstrated to have decreased osteoclast formation (58). A trend towards reduced expression of *Trem-2* was observed. While not statistically significant, this may have contributed to the reduced osteoclast formation and numbers observed. The addition of 1,25D however had no effect on *Trem2* gene expression, suggesting that its reduction could not be a direct result of *Cyp27b1*KO. There was no significant change in *Cyp24a1* mRNA levels in *Cyp27b1*KO, as expected (3, 7).

A trend towards increased *Mcl-1* expression under the treatment of 25D was consistent with previous observations that 25D increased osteoclast TRAP-positive numbers in RAW 264.7 cells (3, 134).The addition of 1,25D, unexpectedly, had direct effects on *Mcl-1* mRNA levels in WT and *Cyp27b1*KO splenocyte cultures. It has been established that MCL-1 acts to suppress apoptosis and increased levels in response to 1,25D would therefore be expected to result in reduced osteoclast apoptosis (135), an opposite effect to what we observed. The increased *Mcl-1* mRNA expression under

1,25D may act as a compensatory mechanism in an attempt to limit the increased cell apoptosis via down-regulating the *Bcl-2* and *Bax* mRNA expression ratio that also occurs under 1,25D treatment (136), and as seen in our previous study (122). It has been noted that 1,25D has an alternate action on mitochondria, acting to increase MCL-1 and decrease cytochrome C levels (135). The osteoclast has a unique mitochondrial structure, that includes an unusually dense electron transport chain and the ability to produce higher levels of ATP, and increases in MCL-1 may be a normal action to increase cell survival as the cell increases in size through fusion of mononuclear precursors. It would be interesting to observe *Mcl-1* expression in a co-culture of MLO-Y4 and splenocytes under 1,25D. The increase in *Mcl-1* in both WT and *Cyp27b1*KO osteoclasts under the treatment of 1,25D may be part of a mechanistic pathway that acts in conjunction with osteocyte produced factors to limit the 1,25D initiated RANKL presentation inhibiting osteoclast formation.

Bim (pro-apoptotic) and *Bcl-xl* (anti-apoptotic) expression were also examined, as additional members of the BCL-2 like family. BCL-XL, an alternate splicing of BCL-X, has been demonstrated to play a role in the regulation of osteoclast survival and resorption in both *in vivo* and *in vitro* (137). Furthermore, Iwasawa *et al.* (137) indicates that the ratio of BCL-XL and BIM protein critically regulates osteoclast survival. BIM and BCL-XL have directly opposite effects on osteoclast resorptive activity to that of apoptosis. The almost identical patterns of increased and decreased expression respectively observed in *Bim* and *Bcl-xl* indicates that mRNA expression levels are unaffected by the loss of vitamin D signalling pathways. The results also potentially indicate a 1:1 ratio for mRNA is required for equilibrium in the osteoclast. It was identified that both of these genes strongly respond to 1,25D and 25D treatments in WT

osteoclasts. The reason for the almost identical increase in mRNA expression in both genes is unknown but may indicate that *Bim* and *Bcl-xl* have functions beyond the regulation of apoptosis and resorption in response to 1,25D. Regardless, these findings indicate that the maintenance of this particular gene expression ratio is in some way important for the osteoclast.

The loss of *Cyp27b1* expression prevented the increase in mRNA expression of *Bim* and *Bcl-xL* under 1,25D and 25D treatments. The inability of 1,25D to stimulate the response seen in WT osteoclasts when *Cyp27b1* was knocked out was surprising. Our previous findings showed (3, 4) that exogenous 1,25D can act on *Cyp27b1*KO osteoclasts through the VDR. This indicates that the global deletion of *Cyp27b1* may affect the way *Bim* and *Bax* respond to vitamin D in mature osteoclasts.

5.4.2 V-ATPase subunits

The V-ATPase subunits gene expression from a single peak time point, corresponding to peak osteoclast formation, in WT and *Cyp27b1*KO mouse splenocyte cultures and 1,25D treatments indicated increased gene expression in 50% of the known V-ATPase subunits and decreased expression of the regulatory elements v_1h and v_1f in *Cyp27b1*KO cells. This was consistent with the increased resorptive activity observed in *Cyp27b1*KO mouse splenocyte cultures (122). V_1h gene expression was strongly increased in WT cultures by the addition of 1,25D as would be expected of a vitamin D responsive subunit. V_1f however was unchanged by the addition of 1,25D. This was unexpected, but as v_1f and v_1h function in tandem to form a tether between the two subunits, changes to v_1h would also likely have affected the pump activity regardless.

V_0c gene expression was not significantly altered or decreased under *Cyp27b1* deletion which was unexpected as it is the only repeated subunit in the V_0 domain that was not decreased. The lack of response of *v_0c* to 1,25D in the WT was surprising, especially as the V_0C protein is currently the only subunit recognised as able to instigate the assembly of the V_0 domain (130, 138) and that the *Cyp27b1*KO responded to 1,25D and may be worth further investigation.

The remaining subunits of the V-ATPase pump showed no changes in gene expression due to the deletion of *Cyp27b1*. This was unexpected as it is possible that the lack of changes in gene expression in these subunits is due to a lower number of subunit proteins in the V-ATPase superstructure, and this should be investigated further.

We examined the subunits of *v_1f*, *v_1h* and *v_0d_2* in further depth. The *v_0d_2* subunit was selected for its well established role in literature (63). The KO of *Vdr* and *Cyp27b1* had no significant effect on *v_1f* gene expression. This was not expected. While no significance was observed, there were indications that a higher number of experimental replicates may have enhanced the ability for the detection of changes in *v_1f* mRNA expression.

WT cultures under the treatment of 1,25D had increased expression of *v_1f*. This is highly supportive of vitamin D sensitivity being present within *v_1f*. It is clear that vitamin D in stromal free osteoclast cultures acts to ensure the regulation of the V-ATPase pump is present. The deletion of *Cyp27b1* resulted in the loss of vitamin D sensitivity. What is particularly unusual is that *v_1f* under 1,25D treatment in *Cyp27b1*KO cultures still loses it sensitivity. This may imply that the activation of the vitamin D metabolic pathway within the cells is more important than the levels of vitamin D present in regards to the V-ATPase pump.

The deletion of *Cyp27b1* had no significant effect on v_0d_2 expression. This was unexpected as v_0d_2 has been demonstrated to be critical to the V-ATPase pump and osteoclast formation (64, 68, 130, 138).

*Cyp27b1*KO and WT splenocytes in the absence of stromal signalling responded to 1,25D treatment with the up-regulation of v_0d_2 expression indicating that v_0d_2 is highly sensitive to the active form of vitamin D. This was unexpected as v_0d_2 plays an integral role in osteoclast fusion and 1,25D treated samples from previous chapters has continuously indicated reduced osteoclast numbers. An increase in v_0d_2 expression alters osteoclast fusion to less than optimal conditions.

The reduction in v_1h expression in *Cyp27b1*KO osteoclast cultures was not unexpected. The decrease in v_1h potentially indicates the loss of regulation in a percentage of V-ATPase pumps. Literature has demonstrated (138) that the deletion of v_1h does not prevent pump assembly and ATPase activity. There is however indications that the pump is no longer stable, resulting in uncontrolled hydrogen ion release. This would fit well with the increased resorptive activity observed in KO model osteoclast cultures (122, 133).

There are indications that the V-ATPase pumps may cease to function in cells due to ADP inhibition. Cells have a set capacity to generate energy. Cells that are unable to convert sufficient ADP to ATP to keep up with the demand of the pumps would result in a lower level of hydrogen ion release than expected. However the osteoclast unique mitochondrial structure has higher electron transport chain density than that of any other cell. This combined with multiple mitochondria from cell fusion means that the osteoclast is uniquely capable of converting large volumes of ADP to ATP. This

indicates that unlike in most other cells, hydrogen ion transport would either take much longer to be or not be inhibited through limitations on energy production.

vitamin D sensitivity was observed in v_1h with 1,25D increasing gene expression. In the majority of cases the addition of 1,25D results in decreased gene expression. However, in this case the increase in v_1h gene expression was expected. The addition of 1,25D reduced osteoclast numbers and gene expression responsible for resorption in the stromal free osteoclast cultures (122, 133). Increased regulation of hydrogen ion pumps would be expected in cells that have reduced resorptive activity.

5.5 Conclusion

The deletion of *Cyp27b1* resulted in reduced expression in the majority of osteoclast related genes examined. The addition of 1,25D was expected to restore gene expression in the *Cyp27b1*KO osteoclast, thus we expected to observe significant increases in gene expression under the treatment of 1,25D in *Cyp27b1*KO osteoclasts. We observed no changes in gene expression of *C-fos*, and *Clcn-7*. We observed a further decrease in *Trem-2* expression, indicating the potential for a further decrease in osteoclast number. The increase of *Mcl-1* expression under 1,25D was unexpected and potentially worth further investigation. Lastly *Bim* and *Bcl-xl* were demonstrated to both be vitamin D sensitive and to have a basal level of expression independent of vitamin D, and this may also be worthy of future investigation. Of particular interest would be the effect of *Bim* and *Bcl-xl* mRNA in osteoclasts that have *Cyp27b1* deleted only in mature osteoclasts, such as in a Cathepsin K - Cre conditional deletion model.

These experiments did not examine the effect of *Cyp27b1* deletion in congruence with mesenchymal-derived cells, and as such further experimental work to identify if the loss of *Cyp27b1* expression is as detrimental to osteoclastogenesis when stromal signalling is intact would be of future interest.

vitamin D regulation is clearly present within the V-ATPase pump with multiple subunits responding to vitamin D. The V-ATPase pump has indicated the potential for independent vitamin D regulation through alternate pathways on v_1h and v_0d_2. V_1f and v_0c with further research may also be vitamin D sensitive.

Chapter 6

Evidence for altered osteoclastogenesis in splenocyte cultures from *Vdr* knockout mice.

This chapter presents work undertaken with the *Vdr*KO mouse model and is represented by published manuscript. This chapter covers the effect of the deletion of VDR in a mouse model in *ex vivo* splenocyte culture. This is examined through TRAP positive assays, mRNA and bone resorptive cultures on an artificial bone resorptive substrate. This chapter is represented by a published manuscript and covers the effect of the deletion of VDR in a mouse model in *ex vivo* splenocyte culture

Journal of Steroid Biochemistry and Molecular Biology 177 (2018) 96–102

Contents lists available at ScienceDirect

Journal of Steroid Biochemistry and Molecular Biology

journal homepage: www.elsevier.com/locate/jsbmb

Evidence for altered osteoclastogenesis in splenocyte cultures from *VDR* knockout mice

Daniel C. Reinke[a], Yolandi Starczak[a,b], Masakazu Kogawa[a], Kate R. Barratt[b], Howard A. Morris[b], Paul H. Anderson[b,1], Gerald J. Atkins[a,1,*]

[a] Biomedical Orthopaedic Research Group, Centre for Orthopaedic & Trauma Research, University of Adelaide, Australia
[b] School of Pharmacy and Medical Sciences, University of South Australia, Adelaide, SA 5005, Australia

ARTICLE INFO

Keywords:
Osteoclast
Osteoclastogenesis
Vitamin D
Apoptosis
Vitamin D receptor

ABSTRACT

The indirect action of 1α,25(OH)$_2$-vitamin-D$_3$ (1,25D) on the osteoclast through stromal signalling is well established. The role of vitamin D in osteoclasts through direct 1,25D-VDR signalling is less well known. We showed previously that local 1,25D synthesis in osteoclasts modified osteoclastogenesis and osteoclastic resorptive activity. In this study, we hypothesised that osteoclasts lacking VDR expression would display an enhanced resorptive capacity due to the loss of 1,25D signalling. Splenocytes were cultured under osteoclast-differentiating conditions from mice with global deletion of the *Vdr* gene (VDRKO) and this was compared with age-matched wild-type littermate controls (WT). In VDRKO cultures, osteoclastogenesis was reduced, as indicated by fewer TRAP-positive multinucleated cells at all time points measured ($p < 0.05$) compared to WT levels. However, VDRKO osteoclasts demonstrated greater resorption on a per cell basis than their WT counterparts. VDRKO cultures expressed greatly increased *c-Fos* mRNA compared to WT. In addition, the ratio of expression of the pro-apoptotic gene *Bax* to the pro-survival gene *Bcl-2* was decreased in VDRKO cultures, implying that these osteoclasts may survive longer than WT osteoclasts. Our data indicate abnormal osteoclastogenesis due to the absence of *Vdr* expression, consistent with direct effects of vitamin D signalling being important for regulating the maturation and resorptive activities of osteoclasts.

1. Introduction

Primary regulation of calcium homeostasis occurs through the vitamin D receptor (VDR) in the kidney, the small intestine and the bone [1]. Kidney expressed CYP27B1 converts 25-hydroxyvitamin D$_3$ (25D) to 1α,25-dihydroxyvitamin D$_3$ (1,25D), the active circulating metabolite that binds to the VDR in target tissues, resulting in the regulation of gene expression [2]. The VDR has been demonstrated to be almost ubiquitously expressed in mammalian cells [3]. Despite this, the most clinically defined role for vitamin D is its role in calcium homeostasis and the related effects on bone regulation [4]. The focus of the current study is the effect of vitamin D on the osteoclast. Osteoclasts are specialised monocyte/macrophage-derived multinucleated cells that perform the critical function of bone resorption [5]. While the expression of VDR in osteoclasts is controversial [6], osteoclasts have been shown to respond to directly vitamin D and regulate osteoclast formation and resorption activity [7–9].

In the present study, the role of 1,25D activity in osteoclasts was addressed using the global VDR knockout mouse (VDRKO) [10]. VDRKO mice exhibit hypocalcaemia and an under-mineralised skeleton, phenotypically similar to rickets [11]. Normal bone mineralisation can be achieved in these mice when fed a high calcium, phosphate and lactose diet [12]. However, older VDRKO mice raised on the rescue diet demonstrate osteopenia despite achieving normal calcium levels, which involves dysregulated bone remodelling [13,14]. We hypothesised that the deletion of *Vdr* in osteoclast precursors present in splenocytes in VDRKO animals would result in aberrant osteoclastogenesis and osteoclastic resorption, similar to that we reported for mice with a global deletion of *Cyp27b1* [15]. We examined the importance of VDR mediated signalling in osteoclast and its effects on osteoclast maturation, proliferation, activity and gene expression.

* Corresponding author at: Centre for Orthopaedic and Trauma Research, University of Adelaide, Adelaide, South Australia, 5005, Australia.
E-mail address: gerald.atkins@adelaide.edu.au (G.J. Atkins).
[1] Co-senior author.

http://dx.doi.org/10.1016/j.jsbmb.2017.07.033
Received 4 May 2017; Received in revised form 24 July 2017; Accepted 26 July 2017
Available online 29 July 2017

2. Materials and methods

2.1. Animals

Global VDRKO mice [16] were housed at ambient temperature with unrestricted access to water and food, with established 12 h day-night cycles. VDRKO mice were fed the rescue diet containing 2% calcium, 1.25% phosphate and 20% lactose [12]. WT mice were fed a standard chow diet. All animal procedures were approved and performed in accordance to requirements of the animal research ethics committees of the University of Adelaide and the University of South Australia.

2.2. Osteoclastogenesis

Mice were humanely euthanized at 8 weeks of age using carbon dioxide and vertebral dislocation. Spleens were removed and placed in Minimal Essential Medium-Alpha (αMEM; Sigma Chemical Co., St Louis, MO, USA). Spleens were dissected and the pieces gently ground through a 20 μm cell strainer using a 1 cc syringe. Red cell lysis buffer was then added and cells washed three times in αMEM, containing 10% charcoal stripped FCS (HyClone, Logan, UT, USA), 1% penicillin, 2 mM L-glutamine and HEPES. Cells were extracted from four spleens per genotype and then pooled, counted using trypan blue exclusion, and plated into standard 96-well tissue culture plates for TRAP staining and into Osteologic™ slides (BD Biosciences, Bedford, USA) at 2×10^5 cells/well, or at 1×10^6cells/well into 24 well plates for TRIzol based RNA extraction [17]. Some cells were plated onto sperm whale dentine slices (16 mm^2) and cultured for 21 days to visualise the extent of bone resorption [18].

Cells were fed using differentiation media consisting of αMEM supplemented as above, with the addition of: recombinant human M-CSF (Millipore, Temecula, CA, USA) (25 ng/ml = *untreated/UT*) or M-CSF + RANKL (Millipore) (100 ng/ml = *positive control*). The effects of exogenous 1,25D (1 nM) were assessed in some experiments (Wako Pure Chemicals, Japan), a concentration we have shown to have equivalent effects to that of a physiological concentration of 25D (100 nM) in terms of inhibiting resorption in cultures of both RAW 264.7 cells and peripheral blood mononuclear cells (PBMC) [9].

2.3. TRAP staining

TRAP staining was performed on quadruplicate culture wells using a commercial kit (Sigma Chemical Co.), as described previously [15]. Osteoclasts were defined as cells containing three or more nuclei that stained magenta. Osteoclast number and multinuclearity were assessed using light microscopy at 3 time points between days 6 and 9, encompassing early and peak formation periods in WT cells [15].

2.4. Analysis of gene expression by real-time RT-PCR

RT-PCR was performed essentially as described previously [15]. Briefly, RNA extracted was isolated using the TRIzol method (Invitrogen, Carlsbad, USA). Real-time RT-PCR was performed undertaken using the SYBR Green incorporation technique for multiple genes in a real-time thermocycler (MyIQ, Bio-Rad, NSW, Australia). These included nuclear factor of activated T-cells, cytoplasmic, calcineurin-dependent 1 (*Nfatc1*), tartrate resistant acid phosphatase *(Trap),* calcitonin receptor (*Ctr*), carbonic anhydrase 2 (*Car2*), cathepsin K (*Ctsk*), monocyte chemotactic protein 1 (*Mcp1*), *Bax* and *Bcl2*. Expression was normalised to that of the housekeeping genes *B2m* and *Hprt1*, which have been shown to be stably expressed during osteoclast differentiation [19]. All primers (Table 1) were designed to be mRNA-specific and were purchased from Geneworks (Thebarton, SA, Australia).

2.5. Resorption activity

Resorptive activity was measured, as described previously [18]. Briefly, after 14 days of culture under osteoclastogenic conditions resorption on Osteologic™ slides was visualised using Von Kossa staining. Light microscopic images were converted to black and white then resorption was quantified using Image J (V 1.47, National Institutes of Health) software. Resorption was also assessed by seeding cells onto whale dentine slices cut to 16 mm^2, culturing for 21 days under osteoclastogenic conditions in 96-well plates, then processing dentine for scanning electron microscopy [18].

2.6. Statistical analysis

Data were analysed using either two-way ANOVA followed by Holm-Šídák multi-comparison post-hoc tests, or multiple or standard Student's T-tests, using GraphPad Prism software (v6.05 GraphPad Software, San Diego, CA, USA). In all cases a value for $p < 0.05$ was considered significant.

3. Results

3.1. Relative osteoclastogenic potential of VDRKO splenocytes

In this study, we examined the osteoclastogenic potential of splenocytes derived from VDRKO mice or WT littermate controls. As shown in Fig. 1, the deletion of VDR resulted in decreased $TRAP^+$ multinucleated osteoclast formation. The addition of exogenous 1,25D (1 nM) to WT osteoclasts resulted in the reduction of $TRAP^+$ osteoclast number by 77% on day 6 and 48% on day 9. A 34% reduction in total osteoclast number was observed on day 7 (Fig. 1). Exogenously treated 1,25D (1 nM) WT cultures retained a higher level of $TRAP^+$ osteoclasts than VDRKO cultures on days 8 and 9 (Fig. 1B). The addition of 1,25D to WT cultures resulted in a similar decrease in osteoclast number as that seen in untreated VDRKO cultures. Phenotypic analysis of splenocytes at day 0 using PCR amplification of the myeloid/osteoclast progenitor marker CD11b, indicated that there was no difference in expression, suggesting that the defect in osteoclastogenesis is likely at a late stage of progenitor development (data not shown). As expected, the addition of exogenous 1,25D to VDRKO osteoclast cultures had no effect on osteoclastogenesis (Fig. 1B).

3.2. Effects of VDR deletion on osteoclast size

Analysis of the number of nuclei/cell showed significantly more small osteoclasts (3–10 nuclei/cell) present in *VDRKO* cultures than in WT cultures at days 6 and 7 (Fig. 2). An increase in the percentage of larger $TRAP^+$ osteoclasts (11–25 nuclei/cells) were observed in WT cultures at days 6 and 7 (Fig. 2).

3.3. Effect of genotype on resorptive activity

The ability for resulting osteoclasts to resorb mineralised bone-like substrate was confirmed using whale dentine (Fig. 3A) and was quantified on a mineralised collagen substrate (Osteologic™). No difference in the total area resorbed per well was observed between genotypes (Fig. 3B). By correcting for the peak numbers of $TRAP^+$ osteoclasts formed in replicate wells observed at day 8, VDRKO-derived osteoclasts were calculated to have resorbed more surface per osteoclast when compared to WT (Fig. 3C).

3.4. Effect of genotype on osteoclast gene expression

Analysis of osteoclastogenesis associated gene expression revealed a complex change in VDRKO cultures. *C-fos* is a transcription factor expressed upstream of *Nfatc1* and is essential in the maturation and

Table 1
Oligonucleotide primers used in this study.

Gene	Forward Primer (5′–3′)	Reverse Primer (5′–3′)	Annealing Temp (°C)	Product Size (bp)
B2M	CTGCTACGTAACACAGTTCCACCC	CATGATGCTTGATCACATGTCTGG	60	214
Bax	TGCTACAGGGTTTCATCCAGG	TTGGATCCAGACAAGCAGCC	60	383
Bcl-2	GACTGAGTACCTGAACCGGC	ATAGTTCCACAAAGGCATCCCAG	60	74
Ca2	GAGCTTCACTTGGTTCACTGG	TGTGAGGCAGGTCCAATCTTC	60	133
Cd11b	TGATGCTTACCTGGGTTATGCT	GAAGAGCTTCACACTGCCAC	60	329
C-fos	GTGAAGACCGTGTCAGGAGG	CTGTCTCCGCTTGGAGTGTA	60	175
Clcn-7	TCCATGTCCTACCCACTCCAGC	CAGGCCGAGAGTCATGGGATTATAG	60	144
Ctr	GCCCTCTTATGAAGGAGAAGGT	GATAGGCTGTGGCTCCAGCG	60	92
Ctsk	TCTCTGTACCCTCTGCATTTAGC	GGCCAACTCAAGAAGAAAACTG	60	230
Hprt11	GGTTAAGCAGTACAGCCCCA	TGCAGATTCAACTTGCGCTC	60	234
Mcp-1	GGCTGGAGAGCTACAAGAGG	TTGAGCTTGGTGACAAAAACTACAG	60	73
Nfatc1	AGGACACCCCATTGTGCAGCT	CGTCAGCCGTCCCAATGAACA	60	80
Trap	CGACAAGAGGTTCCAGGAGAC	GGGAAGTTCCAGCGCTTGGAG	60	113

formation of osteoclasts; expression of this gene was strongly elevated in VDRKO cultures throughout the time course examined (Fig. 4A). Expression of the master osteoclast transcription factor, *Nfatc1*, was stable in WT cultures but trended downwards in VDRKO cultures, with significantly reduced expression at day 7 (Fig. 4B). The osteoclast marker *Trap* increased with time in cultures of both genotypes but however was mildly decreased at day 7 in VDRKO culture (Fig. 4C). No differences were observed for *Clcn7,* encoding the chloride channel critical for maintaining the membrane potential of osteoclasts during resorption (Fig. 4D). Levels of *Ctsk* mRNA, encoding the critical major protease expressed by osteoclasts, were significantly decreased in VDRKO cultures compared to WT on days 7 and day 8 (Fig. 4E). Levels of the osteoclast marker *Ctr* were elevated at days 0 and 8 in VDRKO cultures (Fig. 4F). *Mcp-1*, also known as *Ccl2*, is a chemokine known to accelerate osteoclast maturation and is thought to act during osteoclast fusion; expression of *Mcp-1* was increased in VDRKO osteoclasts compared to WT (Fig. 4G). The expression of triggering receptor expressed on myeloid cells two (*Trem-2*), another regulator of osteoclast formation and activity was not altered in VDRKO cultures (Fig. 4H).

We also examined the possible influence of loss of *Vdr* expression on cell survival. The expression ratio of *Bax*:*Bcl2* mRNA in the VDRKO cultures was found to be decreased at day 6 and day8, consistent with increased survival of the osteoclasts that formed, relative to WT cells (Fig. 4I).

4. Discussion

In this study, osteoclasts derived from VDRKO mouse splenocytes showed a decreased potential to form osteoclasts relative to cells from WT littermates, indicating an intrinsic defect in osteoclastogenesis in the absence of VDR activity. A similar defect was demonstrated previously in CYP27B1KO osteoclasts, indicating that impairment of the autocrine vitamin D signalling pathway in osteoclasts resulted in an intrinsic defect in osteoclast formation [15]. In our previous study [15], WT osteoclasts that formed in the presence of 1,25D were smaller, similar to both CYP27B1KO and VDRKO osteoclasts. In the case of WT,

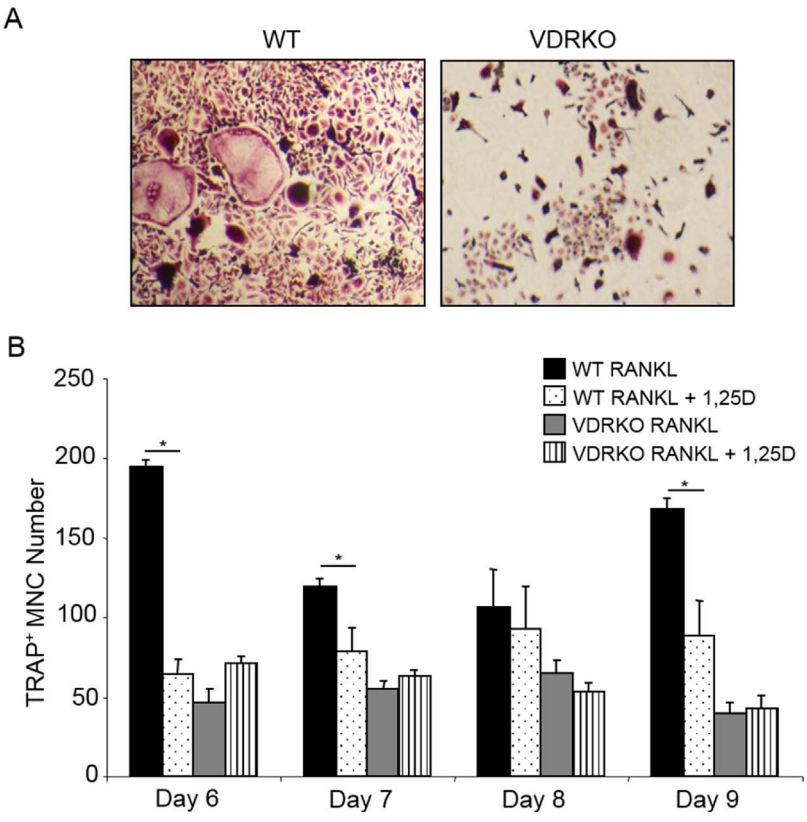

Fig. 1. The effects of *VDR* deletion and 1,25D addition on TRAP$^+$ osteoclast formation. Splenocytes were cultured under control or pro-osteoclastogenic conditions in the absence or presence of 1,25D (1 nM), as described in Materials and Methods for the times indicated, and assayed for TRAP$^+$ multinucleated cell formation: A) Representative images of WT littermate control and VDRKO osteoclast cultures (10x objective). B) Osteoclast formation from WT and VDRKO splenocytes. Total TRAP$^+$ cell numbers were combined from three independent experiments, each using splenocytes pooled from at least 4 animals/group, and shown as means ± SEM. Significant differences from WT are indicated by asterisks ($p < 0.05$).

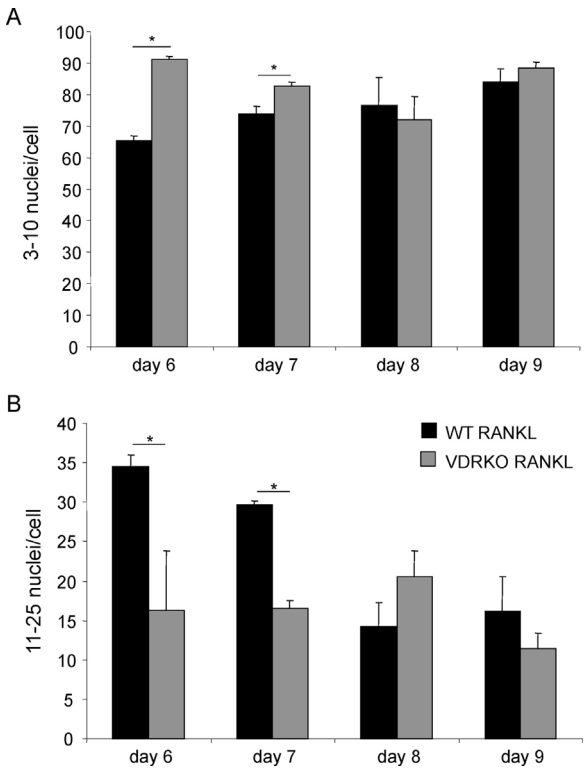

Fig. 2. The effects of *Vdr* deletion on osteoclast nuclei number. Splenocytes from either WT or VDRKO mice were cultured and stained for TRAP, as described in Materials and Methods. The number of nuclei per TRAP$^+$ cell were counted at days 6–9 by light microscopy and categorised into osteoclasts containing A) 3–10 nuclei/cell or B) 11–25 nuclei/cell. Data shown are combined counts from three independent experiments, each using splenocytes pooled from at least 4 animals/group, and shown as means ± SEM. Significant differences from WT are indicated by asterisks ($p < 0.05$).

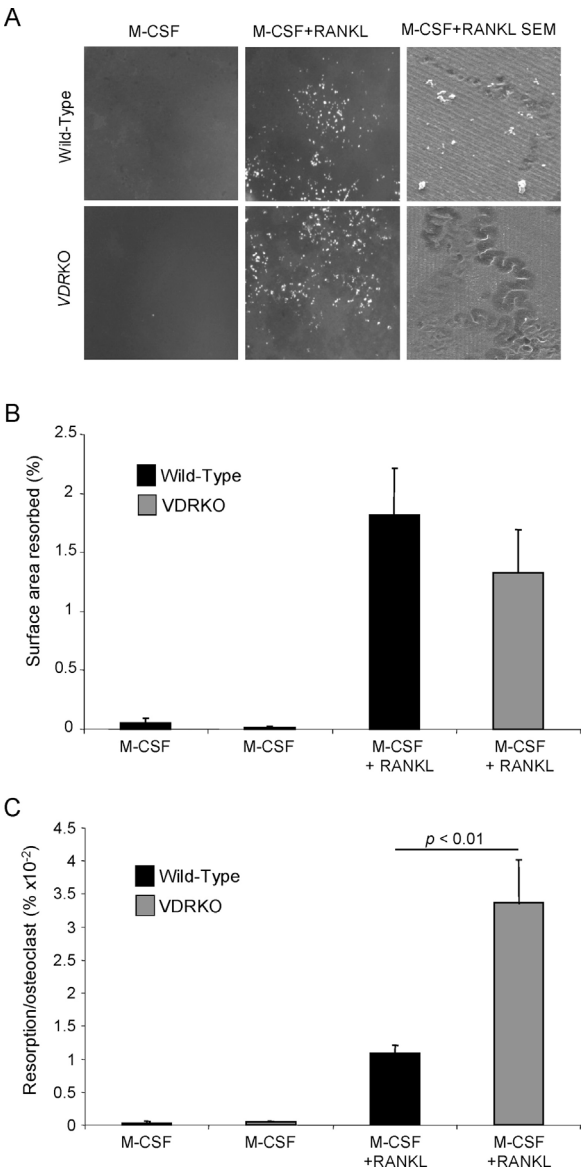

Fig. 3. The effect of *Vdr* deletion on osteoclast resorptive activity. Splenocytes were seeded at identical density onto either dentine, Osteologic™ slides or 96-well assay plates and cultured in the presence of M-CSF alone or under osteoclastogenic conditions, as described in Materials and Methods. After 14 days of culture, wells were stained for TRAP and slides were stained to reveal resorption areas: (A) appearance of either Von Kossa stained Osteologic™ slides visualised by light microscopy or dentine visualised by scanning electron microscopy; (B) quantified total area resorbed; (C) resorption corrected for the numbers of TRAP$^+$ osteoclasts formed in replicate wells. Quantified data are means ± SEM of quadruplicate wells and are representative of 2 independent experiments. Significant differences between genotypes are indicated by asterisks ($p < 0.05$).

this translated into inhibition of activity. However, when either of the *Cyp27b1* or *Vdr* genes are deleted, the resulting osteoclasts have increased resorptive activity. These observations are consistent with there being at least two distinct roles for VDR signalling in the osteoclast lineage: optimisation of osteoclastogenesis and inhibition or amelioration of mature osteoclastic resorbing activity, as we have previously suggested [9]. Previous histological analysis of both VDRKO and CYP27B1KO mouse bone revealed defective osteoclast formation relative to WT in response to hypocalcaemia and elevated PTH levels [13]. Studies targeting the specific actions of VDR in the osteoclast lineage are emerging. Nakamichi et al. [20] used a cathepsin K-Cre knock-in transgenic mouse model to delete *Vdr* selectively in osteoclasts; in this model one allele of the cathepsin K open reading frame is replaced with Cre. They reported an apparent increase in bone mineral density in these mice together with a decreased number of osteoclasts (N.Oc/BS), although neither finding was commented upon [20]. In an accompanying paper [21], our group used a more traditional cathepsin K-Cre mouse model, where Cre is expressed under a transgenic cathepsin K promoter, to similarly delete *Vdr* in osteoclast lineage cells. We found no difference in osteoclast number, however these mice had reduced trabecular number (Tb.N) suggestive of increased resorptive activity. In the current study, osteoclasts derived from VDRKO mice also had reduced overall size compared to that of their WT counterparts. Osteoclast fusion requires several physiological conditions to be met, including the availability of sufficient numbers of osteoclast precursors and then a number of complex interactions at the cell membrane and cytoskeletal levels [22,23]. Cell size is thought to play a role in osteoclast resorptive capabilities. Larger osteoclasts, in particular those with more than 20 nuclei, have more bone resorptive machinery but are considered to be less motile, and decreased motility reduces the number of resorption events that can be performed [24–27]. Consistent with this concept, our results indicate that the smaller VDRKO osteoclasts have increased resorptive capacity per osteoclast formed compared to WT.

Defects in the ability of osteoclasts to fuse have been demonstrated to involve genes such as *Mcp-1* [28,29] and *Trem-2* [30]. However, the expression of *Trem-2* was unchanged in VDRKO osteoclast cultures compared with WT, and VDRKO osteoclast cultures exhibited increased expression of *Mcp-1* mRNA at day 6, which together argue against these genes being causative of the observed effects. Intriguingly, we observed strongly increased *c-fos* mRNA expression in VDRKO cells, both at baseline and throughout osteoclastogenic culture. *C-fos* encodes a major transcription factor induced as a direct consequence of RANKL signalling through the RANK receptor, and is directly upstream of *Nfatc1* expression. The increased expression of *c-fos* in VDRKO mice indicates

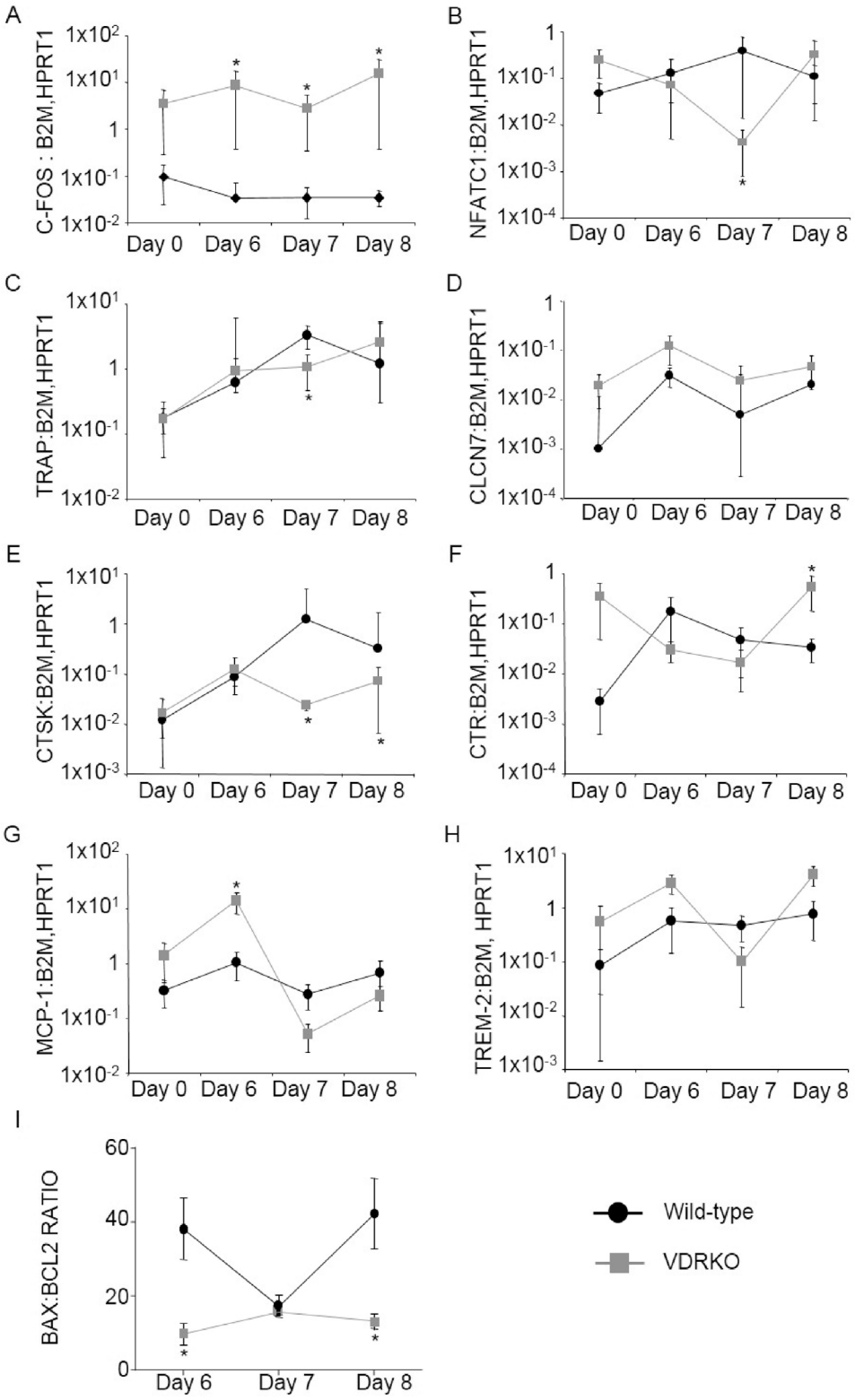

Fig. 4. The effect of *VDR* deletion on osteoclastogenic gene expression. Splenocytes pooled from four mice of each genotype were seeded into 24-well tissue culture plates at 1×10^6 cells/welland cultured under osteoclastogenic conditions, as described in Materials and Methods. Gene expression by real-time RT-PCR was performed for the mRNA expression of a) *C-fos,* b) *Nfatc1,* c) *Trap*, d) *Clcn7,* e) *Ctsk,* f) *Ctr,* g) *Mcp1*, h) *Trem-2* and i) the *Bax/Bcl-2* mRNA ratio. Data shown are means ± SEM of 3 independent experiments. Significant differences between genotypes at specific time points are indicated by asterisks ($p < 0.05$).

that the splenocytes in culture should have a stronger potential for osteoclastogenesis than WT cells. Increased *C-fos* expression would be expected to result in increased *Nfatc1* expression and there was a trend for increased *Nfatc1* mRNA expression in VDRKO cultures at day 0. *Nfatc1*is considered to be a master transcriptional regulator in osteoclasts [31,32]. The expression of genes such as *Oscar*, *Ctsk*, *Ca2*, *Trap*, *Clcn-7* and *Nfatc1* itself are all dependent on NFATC1 activity [33]. While the reduction in *Nfatc1* mRNA expression observed at day 7 is a robust indicator that osteoclast behaviour has been modified due to the loss of VDR signalling, and a similar reduction in *Nfatc1* mRNA levels at this time point was observed in mice lacking CYP27B1 expression [15], further investigation will be required to determine the mechanisms affected by this change. It is also possible that the loss of the VDR results in modifications to pathways in addition to the RANKL/*C-fos*/*Nfatc1* pathway [34].

Loss of VDR signalling was also associated with decreased *Trap* and

Ctsk mRNA expression at day 7, which may relate directly to the reduction in *Nfatc1* levels at this time point. TRAP is an essential protein in osteoclast function involved in both resorptive activity [35], and providing the stimulus for the detachment of osteopontin (OPN) from the bone surface with effects on osteoclast motility [36,37]. Cathepsin K is a protease that is highly efficient in the degradation of type 1 collagen [38] and *Ctsk*-null mice present with a phenotype of osteopetrosis [39]. The reduced expression of *Ctsk* mRNA observed here was expected to result in decreased bone resorption, however the converse was found. It may be that the observed decreased *Trap* and *Ctsk* mRNA expression were part of a homeostatic negative control response to ameliorate the increased osteoclast resorptive activity; we previously reported similar reductions in the expression of these genes in osteoclasts derived from the CYP27B1KO mouse [15].

The expression of other components of the resorption machinery in osteoclasts was unchanged, including that of carbonic anhydrase 2 (*Ca2*), the enzyme responsible for the generation of hydrogen ions essential for bone mineral dissolution; this was unexpected, as the *Ca2* gene contains a VDR binding site [40–42]. While *Ca2* is essential for H^+ production, it is the V-ATPase hydrogen pump, a complex bi-domain ion transporter that consists of 26 identified subunits [43], that is responsible for secreting acid. Here, only the expression of the largest subunit, *Voa3* [43], was examined, and this was found to be unchanged in VDRKO cultures. However, it remains possible that one or more other subunits were altered, contributing to a more active or dysregulated V-ATPase in VDRKO osteoclasts. Chloride channel *Clcn-7*, deletion of which results in failure of osteoclasts to secrete H^+ [44], was also unchanged in VDRKO cultures.

Calcitonin receptor (CTR) expression demonstrated increased expression at baseline and at day 8 of osteoclastogenesis. Calcitonin binding to CTR results in inhibition of osteoclast activity through the dissolution of the sealed zone and ruffled membrane [45]. The trend towards increased *Ctr* expression indicates that the VDRKO osteoclasts are potentially more sensitive to regulation by calcitonin, however it is difficult to see how this could result in a change in activity *ex vivo*.

Both increased and decreased cell survival have been demonstrated to increase osteoclastic resorptive activity [46–49]. We thus assessed the effect of *Vdr* deletion on osteoclast survival through the examination of the expression ratio of *Bax* to *Bcl-2* mRNA [50]. *Bax* is a pro-apoptotic protein that increases the porosity of the mitochondrial membrane and promotes caspase activation. *Bcl-2* promotes cell survival through its ability to bind pro-apoptotic proteins such as *Bax*. We observed a decrease in this apoptotic index for VDRKO osteoclast cultures, indicating that these cells may have increased survival propensity compared to WT. It is potentially this increased survival that contributes to the observed increased number of resorption events per osteoclast in VDRKO cultures. However, further work will need to be conducted, perhaps including tracking the lifespan of individual osteoclasts, to confirm this.

While further work will be required to elucidate the precise molecular mechanisms responsible for the effects of *Vdr* ablation, overall, our findings suggest that VDR signalling in osteoclast precursors is critical for normal osteoclastogenesis and for ameliorating mature osteoclast activity. The current findings are consistent with those we reported previously for osteoclastogenesis in the CYP27B1KO mouse [15], thus disruption of VDR signalling due to either endocrine or autocrine sources of 1,25D appear critical in this regard. Because of the additional established role for vitamin D in stromal osteoblast and osteocyte regulation of osteoclastogenesis [51], our findings support the concept that vitamin D has multiple roles in bone resorption, with vitamin D signals deriving from either, or all of, endocrine, autocrine and local paracrine sources.

Acknowledgements

This study was supported by funding from the National Health and Medical Research Council of Australia (NHMRC), Grant no. APP1029926. PHA was supported by a NHMRC Career Development Fellowship and GJA is an NHMRC Senior Research Fellow.

References

[1] S. Hurwitz, Homeostatic control of plasma calcium concentration, Crit. Rev. Biochem. Mol. Biol. 31 (1996) 41–100.
[2] J.L. Omdahl, H.A. Morris, B.K. May, Hydroxylase enzymes of the vitamin D pathway: expression, function, and regulation, Annu. Rev. Nutr. 22 (2002) 139–166.
[3] M.R. Haussler, Vitamin D receptors: nature and function, Annu. Rev. Nutr. 6 (1986) 527–562.
[4] K.Y. Renkema, R.T. Alexander, R.J. Bindels, J.G. Hoenderop, Calcium and phosphate homeostasis: concerted interplay of new regulators, Ann. Med. 40 (2008) 82–91.
[5] S.L. Teitelbaum, Bone resorption by osteoclasts, Science 289 (2000) 1504–1508.
[6] A.P. Mee, J.A. Hoyland, I.P. Braidman, A.J. Freemont, M. Davies, E.B. Mawer, Demonstration of vitamin D receptor transcripts in actively resorbing osteoclasts in bone sections, Bone 18 (1996) 295–299.
[7] M. Kogawa, P.H. Anderson, D.M. Findlay, H.A. Morris, G.J. Atkins, The metabolism of 25-(OH)vitamin D_3 by osteoclasts and their precursors regulates the differentiation of osteoclasts, J. Steroid Biochem. Mol. Biol. 121 (2010) 277–280.
[8] M. Kogawa, D.M. Findlay, P.H. Anderson, G.J. Atkins, Modulation of osteoclastic migration by metabolism of 25(OH)-vitamin D(3), J. Steroid Biochem. Mol. Biol. (2012).
[9] M. Kogawa, D.M. Findlay, P.H. Anderson, R. Ormsby, C. Vincent, H.A. Morris, G.J. Atkins, Osteoclastic metabolism of 25(OH)-vitamin D3: a potential mechanism for optimization of bone resorption, Endocrinology 151 (2010) 4613–4625.
[10] T. Yoshizawa, Y. Handa, Y. Uematsu, S. Takeda, K. Sekine, Y. Yoshihara, T. Kawakami, K. Arioka, H. Sato, Y. Uchiyama, S. Masushige, A. Fukamizu, T. Matsumoto, S. Kato, Mice lacking the vitamin D receptor exhibit impaired bone formation, uterine hypoplasia and growth retardation after weaning, Nat. Genet. 16 (1997) 391–396.
[11] O. Dardenne, J. Prudhomme, S.A. Hacking, F.H. Glorieux, R. St-Arnaud, Rescue of the pseudo-vitamin D deficiency rickets phenotype of CYP27B1-deficient mice by treatment with 1,25-dihydroxyvitamin D3: biochemical, histomorphometric, and biomechanical analyses, J. Bone Miner. Res. 18 (2003) 637–643.
[12] O. Dardenne, J. Prud'homme, S.A. Hacking, F.H. Glorieux, R. St-Arnaud, Correction of the abnormal mineral ion homeostasis with a high-calcium high-phosphorus, high-lactose diet rescues the PDDR phenotype of mice deficient for the 25-hydroxyvitamin D-1alpha-hydroxylase (CYP27B1), Bone 32 (2003) 332–340.
[13] D.K. Panda, D. Miao, I. Bolivar, J. Li, R. Huo, G.N. Hendy, D. Goltzman, Inactivation of the 25-hydroxyvitamin D 1alpha-hydroxylase and vitamin D receptor demonstrates independent and interdependent effects of calcium and vitamin D on skeletal and mineral homeostasis, J. Biol. Chem. 279 (2004) 16754–16766.
[14] J.W. Ryan, Y. Starczak, H. Tsangari, R.K. Sawyer, R.A. Davey, G.J. Atkins, H.A. Morris, P.H. Anderson, Sex-related differences in the skeletal phenotype of aged vitamin D receptor global knockout mice, J. Steroid Biochem. Mol. Biol. 164 (2016) 361–368.
[15] D.C. Reinke, M. Kogawa, K.R. Barratt, H.A. Morris, P.H. Anderson, G.J. Atkins, Evidence for altered osteoclastogenesis in splenocyte cultures from Cyp27b1 knockout mice, J. Steroid Biochem. Mol. Biol. 164 (2016) 353–360.
[16] O. Dardenne, J. Prud'homme, A. Arabian, F.H. Glorieux, R. St-Arnaud, Targeted inactivation of the 25-hydroxyvitamin D(3)-1(alpha)-hydroxylase gene (CYP27B1) creates an animal model of pseudovitamin D-deficiency rickets, Endocrinology 142 (2001) 3135–3141.
[17] M. Kogawa, P.H. Anderson, D.M. Findlay, H.A. Morris, G.J. Atkins, The metabolism of 25-(OH)vitamin D3 by osteoclasts and their precursors regulates the differentiation of osteoclasts, J. Steroid Biochem. Mol. Biol. 121 (2010) 277–280.
[18] C. Vincent, M. Kogawa, D.M. Findlay, G.J. Atkins, The generation of osteoclasts from RAW 264.7 precursors in defined, serum-free conditions, J. Bone Miner. Metab. 27 (2009) 114–119.
[19] A.S. Stephens, S.R. Stephens, N.A. Morrison, Internal control genes for quantitative RT-PCR expression analysis in mouse osteoblasts, osteoclasts and macrophages, BMC Res. Notes 4 (2011) 410.
[20] Y. Nakamichi, N. Udagawa, K. Horibe, T. Mizoguchi, Y. Yamamoto, T. Nakamura, A. Hosoya, S. Kato, T. Suda, N. Takahashi, VDR in osteoblast-lineage cells primarily mediates Vitamin D treatment-induced increase in bone mass by suppressing bone resorption, J. Bone Miner. Res. 32 (2017) 1297–1308.
[21] Y. Starczak, K.R. Barratt, D.C. Reinke, R. St-Arnaud, H.A. Morris, R.A. Davey, G.J. Atkins, P.H. Anderson, Absence of vitamin D receptor in mature osteoclasts results in altered osteoclastic activity and bone loss, J. Steroid Biochem. Mol. Biol. (2017) in press.
[22] N. Levaot, A. Ottolenghi, M. Mann, G. Guterman-Ram, Z. Kam, B. Geiger, Osteoclast fusion is initiated by a small subset of RANKL-stimulated monocyte progenitors, which can fuse to RANKL-unstimulated progenitors, Bone 79 (2015) 21–28.
[23] K. Soe, A.S. Hobolt-Pedersen, J.M. Delaisse, The elementary fusion modalities of osteoclasts, Bone 73 (2015) 181–189.
[24] H. Witwicka, S.Y. Hwang, P. Reyes-Gutierrez, H. Jia, P.E. Odgren, L.R. Donahue, M.J. Birnbaum, P.R. Odgren, Studies of OC-STAMP in osteoclast fusion: a new knockout mouse model, rescue of cell fusion, and transmembrane topology, PLoS One 10 (2015).
[25] R.L. Lees, J.N. Heersche, Macrophage colony stimulating factor increases bone

resorption in dispersed osteoclast cultures by increasing osteoclast size, J. Bone Miner. Res. 14 (1999) 937–945.
[26] T. Domon, Y. Yamazaki, A. Fukui, Y. Ohnishi, S. Takahashi, T. Yamamoto, M. Wakita, Three-dimensional distribution of the clear zone of migrating osteoclasts on dentin slices in vitro, Tissue Cell 34 (2002) 326–336.
[27] K. Piper, A. Boyde, S.J. Jones, The relationship between the number of nuclei of an osteoclast and its resorptive capability in vitro, Anat. Embryol. (Berl.) 186 (1992) 291–299.
[28] K. Miyamoto, K. Ninomiya, K.H. Sonoda, Y. Miyauchi, H. Hoshi, R. Iwasaki, H. Miyamoto, S. Yoshida, Y. Sato, H. Morioka, K. Chiba, K. Egashira, T. Suda, Y. Toyama, T. Miyamoto, MCP-1 expressed by osteoclasts stimulates osteoclastogenesis in an autocrine/paracrine manner, Biochem. Biophys. Res. Commun. 383 (2009) 373–377.
[29] O.J. Sul, K. Ke, W.K. Kim, S.H. Kim, S.C. Lee, H.J. Kim, S.Y. Kim, J.H. Suh, H.S. Choi, Absence of MCP-1 leads to elevated bone mass via impaired actin ring formation, J. Cell. Physiol. 227 (2012) 1619–1627.
[30] M. Colonna, I. Turnbull, J. Klesney-Tait, The enigmatic function of TREM-2 in osteoclastogenesis, Adv. Exp. Med. Biol. 602 (2007) 97–105.
[31] Q. Zhao, X. Wang, Y. Liu, A. He, R. Jia, NFATc1: functions in osteoclasts, Int. J. Biochem. Cell Biol. 42 (2010) 576–579.
[32] D. Sitara, A.O. Aliprantis, Transcriptional regulation of bone and joint remodeling by NFAT, Immunol. Rev. 233 (2010) 286–300.
[33] T. Nakashima, M. Hayashi, H. Takayanagi, New insights into osteoclastogenic signaling mechanisms, Trends Endocrinol. Metab. 23 (2012) 582–590.
[34] S.L. Teitelbaum, F.P. Ross, Genetic regulation of osteoclast development and function, Nat. Rev. Genet. 4 (2003) 638–649.
[35] A.R. Hayman, T.M. Cox, Tartrate-resistant acid phosphatase knockout mice, J. Bone Miner. Res. 18 (2003) 1905–1907.
[36] A.R. Hayman, Tartrate-resistant acid phosphatase (TRAP) and the osteoclast/immune cell dichotomy, Autoimmunity 41 (2008) 218–223.
[37] K. Harada, H. Itoh, Y. Kawazoe, S. Miyazaki, K. Doi, T. Kubo, Y. Akagawa, T. Shiba, Polyphosphate-mediated inhibition of tartrate-resistant acid phosphatase and suppression of bone resorption of osteoclasts, PLoS One 8 (2013) e78612.
[38] Y.T. Konttinen, M. Takagi, J. Mandelin, J. Lassus, J. Salo, M. Ainola, T.F. Li, I. Virtanen, M. Liljestrom, H. Sakai, Y. Kobayashi, T. Sorsa, R. Lappalainen, A. Demulder, S. Santavirta, Acid attack and cathepsin K in bone resorption around total hip replacement prosthesis, J. Bone Miner. Res. 16 (2001) 1780–1786.
[39] K. Soe, D.M.H. Merrild, J.M. Delaisse, Steering the osteoclast through the demineralization-collagenolysis balance, Bone 56 (2013) 191–198.
[40] D.S. Margolis, J.A. Szivek, L.W. Lai, Y.H. Lien, Phenotypic characteristics of bone in carbonic anhydrase II-deficient mice, Calcif. Tissue Int. 82 (2008) 66–76.
[41] P. Lehenkari, T.A. Hentunen, T. Laitala-Leinonen, J. Tuukkanen, H.K. Vaananen, Carbonic anhydrase II plays a major role in osteoclast differentiation and bone resorption by effecting the steady state intracellular pH and Ca2+, Exp. Cell Res. 242 (1998) 128–137.
[42] A.V. Rousselle, D. Heymann, Osteoclastic acidification pathways during bone resorption, Bone 30 (2002) 533–540.
[43] A. Qin, T.S. Cheng, N.J. Pavlos, Z. Lin, K.R. Dai, M.H. Zheng, V-ATPases in osteoclasts: structure, function and potential inhibitors of bone resorption, Int. J. Biochem. Cell Biol. 44 (2012) 1422–1435.
[44] K.A. Szewczyk, K. Fuller, T.J. Chambers, Distinctive subdomains in the resorbing surface of osteoclasts, PLoS One 8 (2013) e60285.
[45] J. Keller, P. Catala-Lehnen, A.K. Huebner, A. Jeschke, T. Heckt, A. Lueth, M. Krause, T. Koehne, J. Albers, J. Schulze, S. Schilling, M. Haberland, H. Denninger, M. Neven, I. Hermans-Borgmeyer, T. Streichert, S. Breer, F. Barvencik, B. Levkau, B. Rathkolb, E. Wolf, J. Calzada-Wack, F. Neff, V. Gailus-Durner, H. Fuchs, M.H. de Angelis, S. Klutmann, E. Tsourdi, L.C. Hofbauer, B. Kleuser, J. Chun, T. Schinke, M. Amling, Calcitonin controls bone formation by inhibiting the release of sphingosine 1-phosphate from osteoclasts, Nat. Commun. 5 (2014) 5215.
[46] M. Amoui, M.H. Sheng, S.T. Chen, D.J. Baylink, K.H. Lau, A transmembrane osteoclastic protein-tyrosine phosphatase regulates osteoclast activity in part by promoting osteoclast survival through c-Src-dependent activation of NFkappaB and JNK2, Arch. Biochem. Biophys. 463 (2007) 47–59.
[47] E. Purev, L. Neff, W.C. Horne, R. Baron, c-Cbl and Cbl-b act redundantly to protect osteoclasts from apoptosis and to displace HDAC6 from beta-tubulin, stabilizing microtubules and podosomes, Mol. Biol. Cell 20 (2009) 4021–4030.
[48] H. Masuda, J. Hirose, Y. Omata, N. Tokuyama, T. Yasui, Y. Kadono, T. Miyazaki, S. Tanaka, Anti-apoptotic Bcl-2 family member Mcl-1 regulates cell viability and bone-resorbing activity of osteoclasts, Bone 58 (2014) 1–10.
[49] H. Wakeyama, T. Akiyama, K. Takahashi, H. Amano, Y. Kadono, M. Nakamura, Y. Oshima, H. Itabe, K.I. Nakayama, K. Nakayama, K. Nakamura, S. Tanaka, Negative feedback loop in the Bim-caspase-3 axis regulating apoptosis and activity of osteoclasts, J. Bone Miner. Res. 22 (2007) 1631–1639.
[50] M. Paul-Samojedny, D. Kokocinska, A. Samojedny, U. Mazurek, R. Partyka, Z. Lorenz, T. Wilczok, Expression of cell survival/death genes: Bcl-2 and Bax at the rate of colon cancer prognosis, Biochim. Biophys. Acta 1741 (2005) 25–29.
[51] P.H. Anderson, G.J. Atkins, A.G. Turner, M. Kogawa, D.M. Findlay, H.A. Morris, Vitamin D metabolism within bone cells: effects on bone structure and strength, Mol. Cell. Endocrinol. 347 (2011) 42–47.

Chapter 7

Absence of Vitamin D in mature osteoclasts results in altered osteoclastic activity and bone loss.

This chapter looks at *in vivo* osteoclasts activity in mice that lack CYP27B1 and VDR in mature osteoclast and osteocytes. The $Ctsk^{Cre}/Vdr^{-/-}$ and $Ctsk^{Cre}/Cyp27b1^{-/-}$ mice were developed in order to study osteoclast cells with intact signalling in precursor cells but impaired signalling in maturity as a way to isolate the role of vitamin D in osteoclasts and it precursors.

This chapter utilises multiple techniques involving the analysis of the femoral bone, osteoclast numbers and mRNA expression. This chapter is represented by a published manuscript and covers the effect of VDR and CYP27B1 ablation through the use of conditional $Ctsk^{Cre}$ receptor KO mice in an *in vitro* mouse model.

Journal of Steroid Biochemistry and Molecular Biology 177 (2018) 77–82

Contents lists available at ScienceDirect

Journal of Steroid Biochemistry and Molecular Biology

journal homepage: www.elsevier.com/locate/jsbmb

Absence of vitamin D receptor in mature osteoclasts results in altered osteoclastic activity and bone loss

Yolandi Starczak[a], Daniel C. Reinke[b], Kate R. Barratt[a], Jackson W. Ryan[a], Patricia K. Russell[c], Michele V. Clarke[c], René St-Arnaud[d,e], Howard A. Morris[a], Rachel A. Davey[c], Gerald J. Atkins[b,1], Paul H. Anderson[a,*,1]

[a] School of Pharmacy and Medical Sciences, University of South Australia, Adelaide, SA 5005, Australia
[b] Biomedical Orthopaedic Research Group, Centre for Orthopaedic & Trauma Research, University of Adelaide, Australia
[c] Department of Medicine, Austin Health, University of Melbourne, Heidelberg, Victoria, Australia
[d] Department of Surgery and Human Genetics, McGill University, Montreal, Quebec, Canada
[e] Research Centre, Shriners Hospitals for Children, Montreal, Quebec, Canada

ARTICLE INFO

Keywords:
Osteoclast
Osteoclastogenesis
Vitamin D
Vitamin D receptor
CYP27B1

ABSTRACT

Mature osteoclasts express the vitamin D receptor (VDR) and are able to synthesise and respond to $1,25(OH)_2D_3$ via CYP27B1 enzyme activity. Whether vitamin D signalling within osteoclasts is necessary for the regulation of osteoclastic bone resorption in an *in vivo* setting is unclear. To determine the requirement for the VDR- and CYP27B1-mediated activity in mature osteoclasts, conditional deletion mouse models were created whereby either Vdr or Cyp27b1 gene was inactivated by breeding either $Vdr^{fl/fl}$ or $Cyp27b1^{fl/fl}$ mice with Cathepsin K-Cre transgenic mice ($Cstk^{Cre}$) to generate $Ctsk^{Cre}/Vdr^{-/-}$ and $Ctsk^{Cre}/Cyp27b1^{-/-}$ mice respectively. To account for potential $Ctsk^{Cre}$-meaited off-target deletion of Vdr, $Dmp1^{Cre}$ were also used determine the effect of Vdr deletion in osteocytes. Furthermore, $Ctsk^{Cre}/Vdr^{-/-}$ mice were ovariectomised (OVX) to assess the role of VDR in osteoclasts under bone-loss conditions and bone marrow precursor cells were cultured under osteoclastogenic conditions to assess osteoclast formation. Six-week-old $Ctsk^{Cre}/Vdr^{-/-}$ female mice demonstrated a 15% decrease in femoral BV/TV ($p < 0.05$). In contrast, BV/TV remained unchanged in $Ctsk^{Cre}/Cyp27b1^{-/-}$ mice as well as in $Dmp1^{Cre}/VDR^{-/-}$ mice. When $Ctsk^{Cre}/Vdr^{-/-}$ mice were subjected to OVX, the bone loss that occurred in $Ctsk^{Cre}/Vdr^{-/-}$ was predominantly due to a diminished volume of thinner trabeculae when compared to control levels. These changes in bone volume in $Ctsk^{Cre}/Vdr^{-/-}$ mice occurred without an observable histological change in osteoclast numbers or size. However, while cultured bone marrow-derived osteoclasts from $Ctsk^{Cre}/Vdr^{-/-}$ mice were marginally increased when compared to $VDR^{fl/fl}$ mice, elevated expression of genes such as Cathepsin K, Nfatc1 and VATPase was observed. Collectively, these data indicate that the absence of VDR in mature osteoclasts causes exacerbated bone loss in young mice and during OVX which is associated with enhanced osteoclastic activity and without increased osteoclastogenesis.

1. Introduction

1α,25-Dihydroxyvitamin D_3 ($1,25(OH)_2D_3$) is well known to regulate calcium homeostasis and skeletal health. In addition to the well-known activities of $1,25(OH)_2D_3$ in stimulating the intestinal absorption of calcium, we and others have identified roles for $1,25(OH)_2D_3$ in directly regulating serval bone cell types including osteoblasts, osteocytes and osteoclasts [1,2].

A current view is that $1,25(OH)_2D_3$ promotes both increasing the expression of the key osteoclast differentiation factor RANKL, and decreasing the expression of its antagonist, OPG [3]. While some controversy exists as to the presence of VDR in osteoclasts [4], overwhelming *in vitro* evidence supports the notion that vitamin D directly controls the resorptive activity of osteoclasts. $1,25(OH)_2D_3$ has been shown to facilitate adhesion of osteoclast precursors to stromal osteoblasts via induction of inter-cellular adhesion molecule, ICAM-1 [5] and osteoclast adhesion molecule, αVβ3 integrin [6]. As well, $1,25(OH)_2D_3$ directly supports RANKL-induced osteoclast formation from the mouse osteoclast precursor cell line, RAW 264.7 [7]. In addition, human osteoclast precursors can metabolise $25(OH)D_3$ into $1,25(OH)_2D_3$ by the

* Corresponding author.
E-mail address: paul.anderson@unisa.edu.au (P.H. Anderson).
[1] Co-senior authors.

https://doi.org/10.1016/j.jsbmb.2017.10.022
Received 8 May 2017; Received in revised form 24 October 2017; Accepted 26 October 2017
Available online 28 October 2017

enzyme CYP27B1 and this is required for the expression of a number of important osteoclast markers, and transcription factors, NFATc1 and c-FOS [2]. However, the resorptive activity of mature osteoclasts, was also shown to be inhibited by both 25(OH)D and $1,25(OH)_2D_3$ [2].

Consistent with these findings, splenocyte derived osteoclastic precursor cells derived from either VDR-*null* or CYP27B1-*null* mice demonstrate markedly reduced osteoclastogenesis [8,9]. While fewer osteoclasts form in these from VDR-*null* or CYP27B1-*null* mice, osteoclasts that do form exhibited greater resorptive activity per osteoclast and increased survival as indicated by lower BAX:BCL-2 ratio [8–10]. The findings from these studies suggest a role for the synthesis and activity of vitamin D being able to directly regulate both the formation and in turn the subsequent activity of osteoclasts.

Whether these *in vitro* and *ex vivo* observations translate in a role for vitamin D activity within osteoclasts in an *in vivo* setting is unclear. Thus, to assess the role for VDR- and CYP27B1-mediated activity in osteoclasts in *vivo*, osteoclast-specific VDR and CYP27B1 knockout mice, $Ctsk^{Cre}/Vdr^{-/-}$ and $Ctsk^{Cre}/Cyp27b1^{-/-}$, respectively, were generated. We demonstrate the relative impact of VDR and CYP27B1 deletion within mature osteoclasts on bone structure, osteoclast generation and subsequent bone resorption. These data expand the evidence that vitamin D activity contributes to the regulation of bone resorption via direct activities within osteoclasts.

2. Materials and methods

2.1. Animals

All animals used in the generation of both Osteoclast-specific mouse models ($Ctsk^{Cre}/Vdr^{-/-}$ $Ctsk^{Cre}/Cyp27b1^{-/-}$ and $Dmp1^{Cre}/Vdr^{-/-}$ were of *C57B6* background. Cathepsin-K-*Cre* ($Ctsk^{Cre}$) mice [11] were obtained from Assoc. Prof. R Davey (University of Melbourne, Australia). Dentin matrix protein-1-*Cre* $Dmp1^{Cre}$ mice were obtained from Prof L Bonewald (Indiana University) [12]. VDR-LoxP [13] (gift from Dr. S Kato, University of Tokyo) and CYP27B1-LoxP [14] (gift from Prof. R St-Arnaud, University of McGill) were mated with the Ctsk-*Cre* mice to generate $Ctsk^{Cre}/Vdr^{-/-}$ and $Ctsk^{Cre}/Cyp27b1^{-/-}$ mice respectively as well as VDR-LoxP or CYP27B1-LoxP litter-matched control mice. VDR-LoxP mice were mated with Dmp1-*Cre* mice to generate $Dmp1^{Cre}/Vdr^{-/-}$ in order to determine whether the $Ctsk^{Cre}/Vdr^{-/-}$ bone phenotype might be due to non-specific Vdr deletion in osteocytes. All animal procedures were approved by the University of South Australia, Animal Ethics Committee. Mice were housed in IVC caging, with a maximum 5 gender-matched animals/cage and a standard 12 hr light/dark cycle. Mice were provided *ad libitum* access to standard chow and tap water.

2.2. DNA and mRNA analyses

DNA and mRNA were extracted from whole tibia from littermate Vdrfl/fl and respective knockout mice by previously published procedures [15]. The presence of mutated Vdr DNA was amplified using specific primers (F: 5′-CCTTGGTGAGCTGAGTTTACTCTT-3′; R: 5′-CTTCCCACCACTTTGTACTACCA-3′). Messenger RNA was analysed using mRNA specific primers for Vdr, (F: 5′-TCGGATCTGTGGAGTGTGTGGAG-3′, R: 5′-TTGTCCTTGGTGATGCGGCAATCT-3′). These mRNA specific primers are design to specifically amplify mRNA in the region of exon 2. The floxed VDR mice have exon 2 of the vitamin D receptor gene flanked by short intronic loxP sites. Exon 2 encodes the 1 st zinc finger of the DNA binding domain of the in D receptor. Previously, the deletion of exon 2 was shown to result in a frame shift, resulting in complete deletion of the vitamin D receptor protein [16]. Other primers used include Cathepsin- K (5′-ggccaactcaagaagaaaactg-3′, R: 5′-tctctgtaccctctgcatttagc-3′); NFATc1 (5′-AGGACACCCCATTGTGCAGCT-3′, R: 5′- cgtcagccgtcccaatgaaca −3′), and VATPase (5′- GCTGCAGAGCGGCTCAAG-3′, R: 5′- AAGGGGAATGTGATGATGGTGTAG-3′).

2.3. Ovariectomy

Female $Vdr^{fl/fl}$ and $Ctsk^{Cre}/Vdr^{-/-}$ mice (n = 4-5/group) were ovariectomised at 10 weeks of age. Briefly, mice received a bilateral ovariectomy (OVX) under isofluorane induced anaesthesia. A small incision (0.5 cm) on the mid-dorsal aspect of the mouse was created to allow blunt-nosed scissors to separate the skin from the peritoneal layer to cut through the peritoneal layer to retrieve and excise the ovary on each flank.

2.4. Biochemistry

Serum calcium (Ca), phosphate (P) and alkaline phosphatase (ALP) levels were measured using the KoneLab 20XT Clinical Chemistry Analyser (ThermoScientific, MA, USA), using standard protocols and reagents (ThermoScientific, USA). Serum C-terminal telopeptide (cross-laps, CTX) was measured using a RatLaps EIA Kit (Immunodiagnostic Systems Limited, UK).

2.5. Micro-computed tomography (μCT)

Right femora were subjected to *ex vivo* micro-computed tomography (μCT) using the 1174 μCT system (Bruker). Micro-architecture was analysed using high-resolution micro-CT in order to obtain multiple x-ray transmission images. The scanning resolution had a voxel size of 6.5 μm/pixel, with an x-ray tube potential of 50 kVp and 800 μA. To measure trabecular micro-architecture within the femur (metaphysis) a rotation step of 0.4 ° and a frame averaging of 2 was used. Cross-sectional images were reconstructed using the nRecon software (Version 1.6.9.18) (Bruker, BEL). Realignment of datasets was performed using Dataviewer software (v.1.5.1, Bruker, BEL). All bone quantification from reconstructed and realigned datasets was performed using CTan software (v.1.7, Bruker, BEL). A 2 mm metaphyseal region of interest was isolated from the distal femur. Parameters assessed include, bone volume (BV/TV, %), trabecular thickness (Tb.Th, mm) and trabecular number (Tb.N, #/mm). Analyses of trabecular volume parameters for Ovariectomy intervention studies were undertaken using the Skyscan 1076 (Bruker, BEL) for live *in vivo* scanning of femurs of ovariectomised animals (0.5 mm filter, 52 kVp and 112 μA, 9 μm pixel size, 5890 ms exposure time, rotation step of 0.80 and a frame averaging of 1). All analyses were done using the same software/programs as mentioned above.

2.6. Histology

Femora were then subjected to ethanol dehydration steps prior to being placed into a Methyl Methacrylate (MMA): Polyethylene Glycol 400 (PEG) solution (100% MMA: 10% PEG). Femurs were left in the MMA: PEG solution for 14 days, at which time polymerisation was induced using a solution containing MMA: PEG: Perkadox (0.4%). Trimmed resin blocks were sectioned in the sagittal plane at 5 μm thickness. Sections were prepared for TRAP staining or left unstained for fluorochrome label analyses. TRAP stained slides were used to measure metaphyseal osteoclasts numbers (N.Oc, #/mm), osteoclast surface per bone surface (Oc.S/BS, %), number of osteoclasts per bone perimeter (N.Oc/B.Pm, #/mm), and osteoclast size (nm^2). Unstained slides were used measurement of the mineralising surface (MS/BS) mineral apposition rate (MAR, μm/day) and bone formation rate/bone surface (BFR/BS, $\mu m^3/\mu m^2$/day). The All analyses were performed using OsteoMeasure™ Version 3.3.0.2 (OsteoMetrics, Inc. Decatur, GA, USA)

Expression of osteoclastic genes was analysed using real-time, quantitative PCR using iScript Reverse Transcription Supermix for RT-qPCR (BioRad). Relative gene expression was normalized to that of the beta-2-microglobulin (β2 M) housekeeping gene using the comparative cycle threshold (Ct) method (deltaCT).

2.7. Bone marrow cultures

The role for the VDR in osteoclast formation and activity was assessed in bone marrow cultures. Flushed diaphyseal bone marrow from the femora and tibiae of $Vdr^{fl/fl}$ and $Ctsk^{Cre}/Vdr^{-/-}$ mice were suspended in αMEM (Sigma Chemical Co., St Louis, MO, USA) containing 10% foetal calf serum (FCS), 1% penicillin and streptomycin, 2 nM L-glutamine and 1% hydroxyethyl piperazineethanesulfonic acid (HEPES). Cells were then seeded overnight at 37 °C before treating with M-CSF (25 ng/mL, Millipore, Temecula, CA, USA), with or without RANKL (100 ng/mL, Millipore, Temecula, CA, USA) in 10% stripped FCS (HyClone, Logon, UT, USA). Cultures were fed fresh media and cytokines every 3 days and harvested on day 9 of culture.

2.8. Statistical analysis

Either unpaired T-test or Analysis of Variance were used to analyse datasets. The analysis was performed using GraphPad, Prism (Version 5.01) (GraphPad Software Inc., California, USA). A P value of less than or equal to $p < 0.05$ was considered to be statistically significant.

3. Results

$Ctsk^{Cre}/Vdr^{-/-}$ and $Ctsk^{Cre}/Cyp27b1^{-/-}$ mice demonstrated deletion of Vdr and Cyp27b1 within whole bone respectively as determined by DNA analysis (data not shown) and by an approximate 70% and 90% reduction in bone Vdr and Cyp27b1 mRNA expression in bone respectively when compared to floxed littermate control levels (Fig. 1).

In both $Ctsk^{Cre}/Vdr^{-/-}$ and $Ctsk^{Cre}/Cyp27b1^{-/-}$ mice, body weight and femur length were unchanged when compared to their respective controls (Table 1). Likewise, serum measures of calcium, phosphate were unchanged in both $Ctsk^{Cre}/Vdr^{-/-}$ and $Ctsk^{Cre}/Cyp27b1^{-/-}$ mice when compared to $Cyp27b1^{fl/fl}$ levels. Serum CTX, a biomarker for bone resorption, was not significantly different between either $Ctsk^{Cre}/Vdr^{-/-}$ or $Ctsk^{Cre}/Cyp27b1^{-/-}$ and their respective littermate controls (Table 1).

$Ctsk^{Cre}/Vdr^{-/-}$ mice demonstrated 15% reduction in BV/TV% when compared to control mice ($p < 0.05$) (Fig. 2). The reduction in $Ctsk^{Cre}/Vdr^{-/-}$ mice was due to reduced Tb.N ($p < 0.05$), rather than Tb.Th. Despite a reduction in BV/TV% in $Ctsk^{Cre}/Vdr^{-/-}$ mice, no significant differences were observed in osteoclastic parameters of Oc.S/BS, N.Oc/B.Pm and Mean Oc.Size. Similarly, trabecular bone loss in $Ctsk^{Cre}/Vdr^{-/-}$ mice was not associated with any change in the bone formation parameters of MS/BS, MAR or BFR/BS (Fig. 2). In support of these observations, no changes were observed in tibial RankL mRNA or RankL:Opg (data not shown).

In contrast, despite the marked abrogation of Cyp27b1 in $Ctsk^{Cre}/Cyp27b1^{-/-}$ mice, unchanged BV/TV%, Tb.N and Tb.Th when compared to controls and unchanged osteoclastic parameters when compared to control levels suggests that Cyp27b1 in mature osteoclasts plays a negligible role under normal growing conditions (Fig. 3).

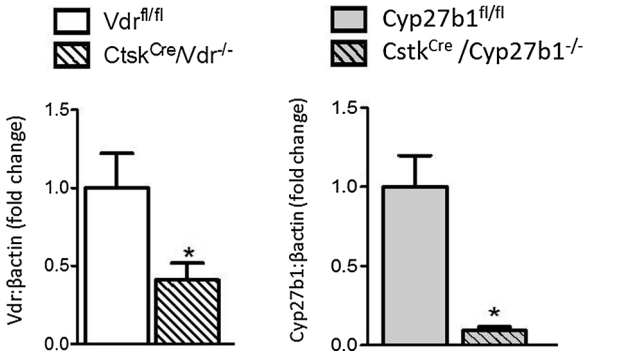

Fig. 1. (A) *Vdr* or *Cyp27b1* mRNA deletion in mouse tibia for floxed Vdr or Cyp27b1 control ($Vdr^{fl/fl}$ or $Cyp27b1^{fl/fl}$) and osteoclast-specific Vdr or Cyp27b1 knockout female mice ($Ctsk^{Cre}/Vdr^{-/-}$ or $Ctsk^{Cre}/Cyp27b1^{-/-}$). Values are presented as means ± SEM, n = 8. $^{*}p < 0.05$.

Since cathepsin K has been shown to be expressed in osteocytes [17], non-specific Cathepsin-K-*Cre* mediated deletion in osteocytes may contribute to the low bone volume phenotype in $Ctsk^{Cre}/Vdr^{-/-}$ mice. To account for the potential of non-specific deletion of VDR in osteocytes, $Dmp\text{-}1^{Cre}/VDR^{-/-}$ were also generated to evaluate the effect on bone mineral. However, despite a marked decline in mRNA levels for Vdr in $Dmp\text{-}1^{Cre}/VDR^{-/-}$ tibial cortical bone, no change in femoral metaphyseal trabecular bone volume was observed in age-matched female (Suppl Fig. 1) or male mice (data not shown). In addition, no changes to cortical bone were observed in $Dmp\text{-}1^{Cre}/VDR^{-/-}$ mice (data not shown).

To assess the effects of VDR deletion in osteoclasts under conditions of accelerated bone loss, $Ctsk^{Cre}/Vdr^{-/-}$ female were subjected to bilateral ovariectomy surgery to ablate oestrogen levels, as previously described [18]. $Ctsk^{Cre}/Vdr^{-/-}$ mice exhibited a 33% (± 0.05) reduction in BV/TV% over 28 days from surgery (Fig. 4A). The decline in bone volume was comparable to femoral bone loss in $Vdr^{fl/fl}$ mice over the same period of time and was predominantly due to a loss in Tb.N. However, when trabecular thickness in $Ctsk^{Cre}/Vdr^{-/-}$ mice was analysed according the distribution of bone volume within partitions of trabecular thicknesses ranging from 0.008 to 1.12 mm, significant differences in bone volume were observed. $Ctsk^{Cre}/Vdr^{-/-}$ mice demonstrated a marked decline in the proportion of thin trabeculae up to 0.06 mm in width when compared to $Vdr^{fl/fl}$ mice at 28 days post-surgery(Fig. 4B). For trabeculae greater than 0.06 mm, bone volume was comparable between $Ctsk^{Cre}/Vdr^{-/-}$ and $Vdr^{fl/fl}$ mice. Despite the OVX-induced loss of thin trabeculae in $Ctsk^{Cre}/Vdr^{-/-}$ mice, no significant changes in the osteoclast parameters of Oc.S/BS, N.Oc/B.Pm and Mean Oc.Size occurred when compared to $Vdr^{fl/fl}$ control mice.

To further examine the effects of VDR deletion specifically within osteoclasts, bone marrow-derived osteoclasts were generated under osteoclastogenic conditions from $Ctsk^{Cre}/Vdr^{-/-}$ mice and compared to $Vdr^{fl/fl}$ cultures (Fig. 5). At day 9 of culture, Vdr mRNA levels were absent in $Ctsk^{Cre}/Vdr^{-/-}$ cultures. While osteoclast numbers were marginally greater in $Ctsk^{Cre}/Vdr^{-/-}$ cultures, this did not reach statistical significance. Despite this, mRNA levels for *Ctsk*, *Nfatc1* and *vATPase* where markedly increased when compared to levels in $Vdr^{fl/fl}$ cultures, suggesting enhanced osteoclastic activity.

4. Discussion

In this study, the conditional deletion of *Vdr* in osteoclasts in the mouse model of $Ctsk^{Cre}/Vdr^{-/-}$ resulted in decreased femoral BV/TV in young mice, despite no measurable changes to osteoclast recruitment on the surface of bone or levels of circulating CTX. In addition, tibial mRNA for genes, such as Rankl, was unchanged $Ctsk^{Cre}/Vdr^{-/-}$ mice suggesting that osteoblastic and osteoclastic signalling did not contribute to the change bone phenotype in these mice. Furthermore, $Dmp1^{Cre}/Vdr^{-/-}$ mice exhibit unchanged bone volume when compared to control littermate mice, consistent with previous observations [19], indicating that the bone-loss phenotype in $Ctsk^{Cre}/Vdr^{-/-}$ mice is not due to non-specific VDR deletion in osteocytes.

To further examine the role of VDR in regulating osteoclastic activity in $Ctsk^{Cre}/Vdr^{-/-}$ mice, females were ovariectomised to induce accelerated bone loss via enhanced bone resorption [18,20–24]. While the overall bone loss in $Ctsk^{Cre}/Vdr^{-/-}$ mice was comparable to that in ovariectomised $Vdr^{fl/fl}$ mice, $Ctsk^{Cre}/Vdr^{-/-}$ mice exhibited markedly increased loss of the thinner trabeculae than control mice. This indicates that while osteoclastogenesis did not appear to be significantly altered in $Ctsk^{Cre}/Vdr^{-/-}$ mice, the increased focal resorption, resulting in loss of thinner trabeculae could be due to more active osteoclasts.

Consistent with this notion, $Ctsk^{Cre}/Vdr^{-/-}$ bone marrow cultured

Table 1
Body weight (g), femur length (mm), Ca, Calcium; P, Phosphate and CTX, Cross-laps for floxed Vdr or Cyp27b1 control ($Vdr^{fl/fl}$ and $Cyp27b1^{fl/fl}$) and osteoclast-specific Vdr or Cyp27b1 knockout ($Ctsk^{Cre}$/Vdr-/- and $Ctsk^{Cre}$/Cyp27b1-/-) female mice at 6 weeks of age. Values are presented as means ± SEM, n = 8–15.

	$Vdr^{fl/fl}$	$Cstk^{Cre}/Vdr^{-/-}$	$Cyp27b1^{fl/fl}$	$Ctsk^{Cre}/Cyp27b1^{-/-}$
Body weight (g)	20.41 ± 0.60	21.06 ± 0.39	21.10 ± 0.31	20.95 ± 0.52
Fem. length (mm)	13.70 ± 0.23	13.92 ± 0.11	13.83 ± 0.20	14.09 ± 0.19
Ca (mmol/L)	2.38 ± 0.06	2.55 ± 0.23	2.68 ± 0.13	2.62 ± 0.14
P (mmol/L)	2.16 ± 0.11	2.14 ± 0.12	2.91 ± 0.15	2.73 ± 0.18
CTX (ng/ml)	108.0 ± 26.5	88.8 ± 12.3	136.8 ± 41.6	143.6 ± 57.9

in osteoclast-forming conditions demonstrated an increased osteoclastogenic potential through elevated expression in genes generally associated with resorptive activity. This is consistent with our previous findings where by osteoclasts derived from mice with global deletion of VDR (VDRKO) have increased survival propensity and increased resorption events per osteoclast in culture [9].

In contrast to the role of VDR, the deletion of Cyp27b1 in the $Ctsk^{Cre}/Cyp27b1^{-/-}$ mouse model resulted in no change in bone volume, suggesting that at least in this model of young animals, the synthesis of $1,25(OH)_2D_3$ in osteoclasts does not play an important role in regulating bone resorption. This is in contrast to *in vitro* evidence which demonstrates that the conversion of $25(OH)D_3$ to $1,25(OH)_2D_3$, which occurs via the Cyp27b1 enzyme, is important for regulating osteoclastic activity [8]. Splenocytes derived from $Cyp27b1^{-/-}$ mice exhibit both reduced osteoclastogenesis, and yet increased resorptive activity per osteoclast formed, suggesting that autocrine activities of vitamin D in osteoclast precursor cells and mature osteoclasts has specific roles defined by the stage of osteoclast development [8]. Since the $Ctsk^{Cre}/Cyp27b1^{-/-}$ mouse model only examines the effect of Cyp27b1 absence in mature osteoclasts, it remains to be determined whether Cyp27b1 plays a significant role in the generation of osteoclasts, rather than activity in an *in vivo* setting. Furthermore, it remains possible that Cyp27B1 activity in osteoclasts may play a role under conditions other than during normal growth which would require further investigation.

While further studies are required to determine the mechanisms, by which vitamin D activity regulates osteoclastic bone resorption, our findings suggest that VDR-mediated activity in mature osteoclast is required moderate osteoclastic activity during growth and in OVX-induced bone loss.

Acknowledgements

We would like to acknowledge the contributions of Michele Clarke

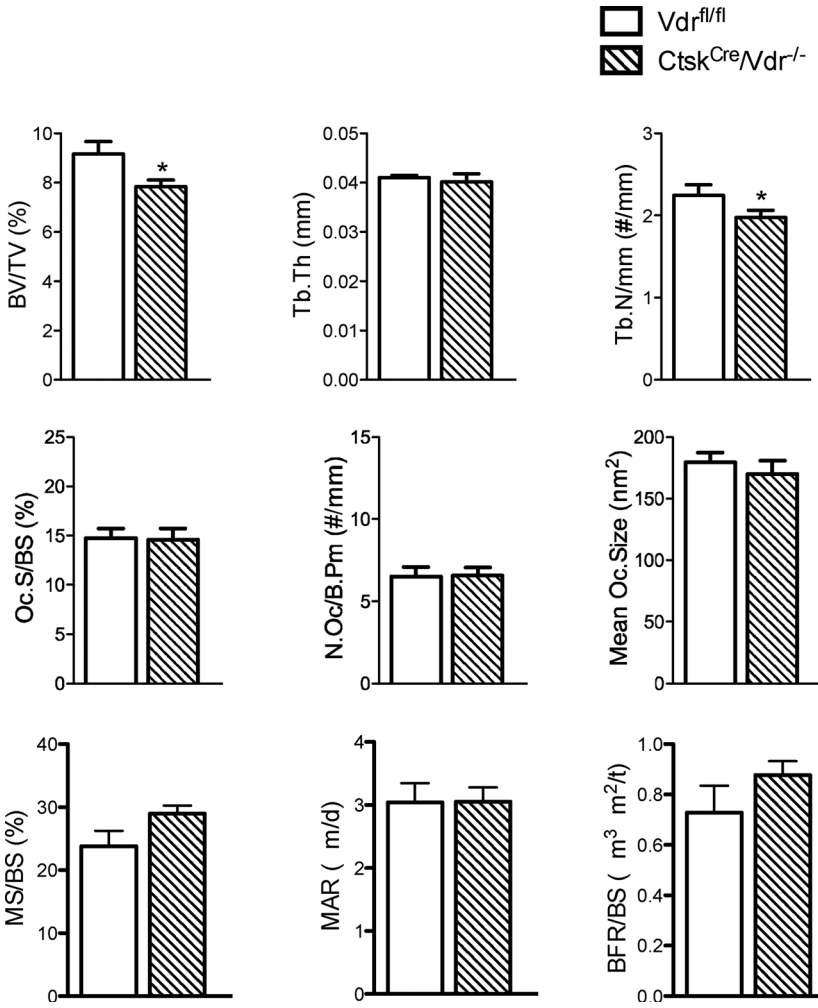

Fig. 2. Histomorphometric analyses of the distal femoral metaphysis in $Ctsk^{Cre}/Vdr^{-/-}$ and $Vdr^{fl/fl}$ mice. Bone volume/tissue volume (BV/TV, %); Trabecular thickness (Tb.Th, mm); Trabecular number (Tb.N, #/mm); Osteoclast surface per bone surface (Oc.S/BS, %); Osteoclast number per bone perimeter (N.Oc/B/Pm, #/mm); Mean osteoclast size (Mean Oc. Size, μm^2); Mineralised surface per bone surface (MS/BS, %), Mineral apposition rate, (MAR, μm/d); Bone formation ate per bone surface (BFR/BS, $\mu m^3\,\mu m^2$/day), Values presented as means ± SEM, n = 8–12. $^*p < 0.05$.

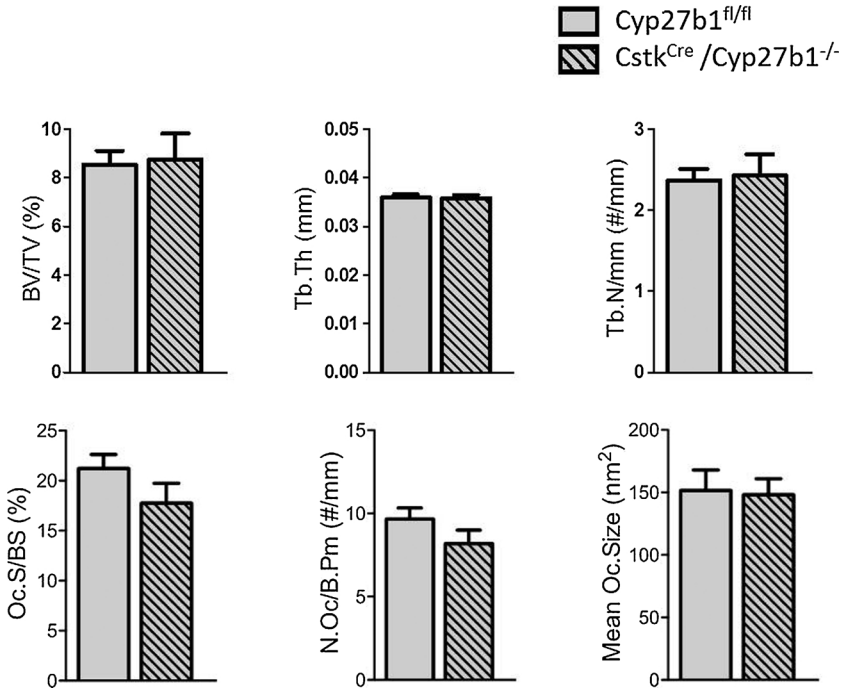

Fig. 3. Histomorphometric analyses of the distal femoral metaphysis in Ctsk^{Cre}/Cyp27b1$^{-/-}$ and Cyp27b1$^{fl/fl}$ mice. Bone volume/tissue volume (BV/TV, %); Trabecular thickness (Tb.Th, mm); Trabecular number (Tb.N, #/mm); Osteoclast surface per bone surface (Oc.S/BS, %); Osteoclast number per bone perimeter (N.Oc/B/Pm, #/mm); Mean osteoclast size (Mean Oc. Size, μm^2); Values presented as means ± SEM, n = 8–12. $^*p < 0.05$.

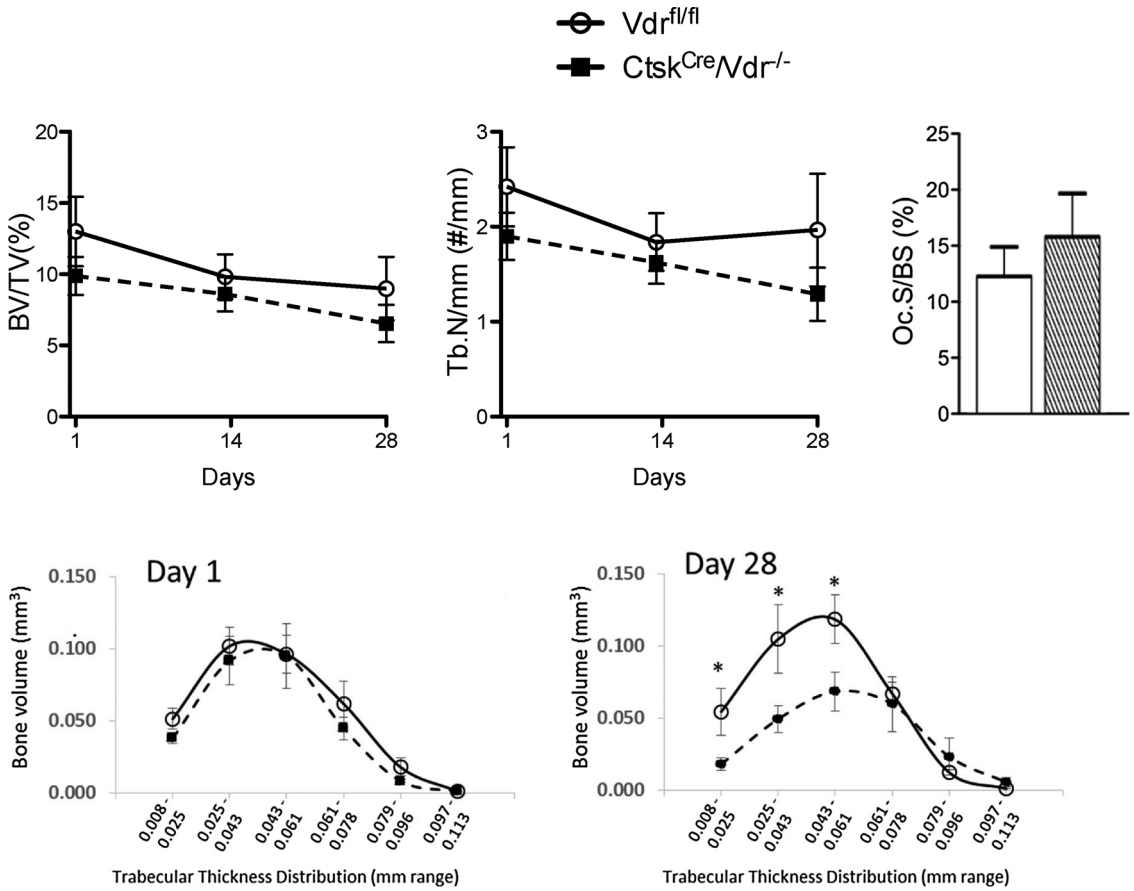

Fig. 4. (A) The effect of bilateral OVX on Ctsk^{Cre}/Vdr$^{-/-}$ and Vdr$^{fl/fl}$ mice with respect to (A) distal femoral metaphyseal bone of at 1, 14 and 28 days post-surgery and (B) distribution of trabecular bone volume by thickness at Day 1 and Day 28 post-surgery. Bone volume/Tissue volume (BV/TV, %); Trabecular thickness (Tb.Th, mm); Trabecular number (Tb.N, #/mm); Osteoclast surface per bone surface (Oc.S/BS, %); Osteoclast number per bone perimeter (N.Oc/B/Pm, #/mm). Values presented as means ± SEM, n = 4–5.

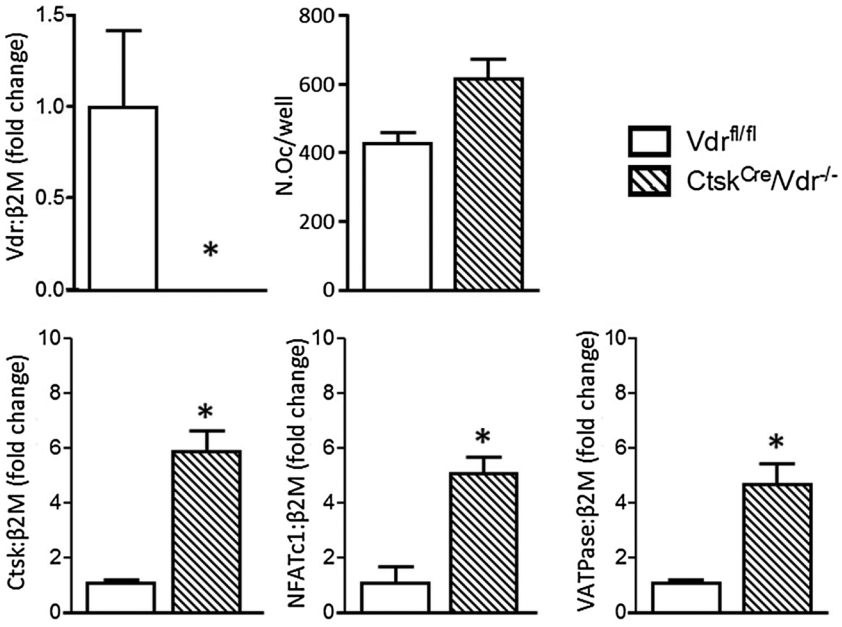

Fig. 5. Bone marrow–derived osteoclasts from $Ctsk^{Cre}/Vdr^{-/-}$ and $Vdr^{fl/fl}$ mice. Average number of osteoclasts per well, (N.Oc/well); Vitamin D receptor, Vdr; Cathepsin K, Ctsk; Nuclear factor of activated T-cells, NFATc1; Vacuolar-type H+ −ATPase, vATPase. Values presented as means ± SEM. *p < 0.05.

and Patricia Russel (University of Melbourne) for the assistance in the creation of mice and Rebecca Sawyer (University of South Australia) for assistance in the histological analyses. This study was supported by funding from the National Health and Medical Research Council of Australia (NHMRC), GNT1029926. PHA was supported by and NHMRC RD Wright Fellowship and GJA is an NHMRC Senior Research Fellow.

Appendix A. Supplementary data

Supplementary data associated with this article can be found, in the online version, at https://doi.org/10.1016/j.jsbmb.2017.10.022.

References

[1] M. Kogawa, P.H. Anderson, D.M. Findlay, H.A. Morris, G.J. Atkins, The metabolism of 25-(OH)vitamin D3 by osteoclasts and their precursors regulates the differentiation of osteoclasts, J. Steroid Biochem. Mol. Biol. 121 (2010) 277–280.
[2] M. Kogawa, D.M. Findlay, P.H. Anderson, R. Ormsby, C. Vincent, H.A. Morris, G.J. Atkins, Osteoclastic metabolism of 25(OH)-Vitamin D3: a potential mechanism for optimization of bone resorption, Endocrinology 151 (2010) 4613–4625.
[3] N.A. Athanasou, The osteoclast—what's new? Skeletal Radiol. 40 (2011) 3.
[4] Y. Wang, H.F. De Luca, J. Zhu, Indentification of vitamin D receptor in osteoblasts and chondrocytes but not osteoclasts in mouse bone, J. Bone Miner. Res. (2013).
[5] Y. Okada, I. Morimoto, K. Ura, K. Watanabe, S. Eto, M. Kumegawa, L. Raisz, C. Pilbeam, Y. Tanaka, Cell-to-cell adhesion via intercellular adhesion molecule-1 and leukocyte function-associated antigen-1 pathway is involved in 1alpha,25(OH) 2D3, PTH and IL-1alpha-induced osteoclast differentiation and bone resorption, Endocr. J. 49 (2002) 483–495.
[6] M.M. Medhora, S. Teitelbaum, J. Chappel, J. Alvarez, H. Mimura, F.P. Ross, K. Hruska, 1 alpha 25-dihydroxyvitamin D3 up-regulates expression of the osteoclast integrin alpha v beta 3, J. Biol. Chem. 268 (1993) 1456–1461.
[7] C. Vincent, M. Kogawa, D.M. Findlay, G.J. Atkins, The generation of osteoclasts from RAW 264.7 precursors in defined, serum-free conditions, J. Bone Miner. Metab. 27 (2009) 114–119.
[8] D.C. Reinke, M. Kogawa, K.R. Barratt, H.A. Morris, P.H. Anderson, G.J. Atkins, Evidence for altered osteoclastogenesis in splenocyte cultures from Cyp27b1 knockout mice, J. Steroid Biochem. Mol. Biol. 164 (2016) 353–360.
[9] D.C. Reinke, Y. Starczak, M. Kogawa, K.R. Barratt, H.A. Morris, P.H. Anderson, G.J. Atkins, Evidence for altered osteoclastogenesis in splenocyte cultures from VDR knockout mice, J. Steroid Biochem. Mol. Biol. (2017), http://dx.doi.org/10.1016/j.jsbmb.2017.07.033 (Epubaheadofprint).
[10] D.C. Reinke, M. Kogawa, K.R. Barrat, H.A. Morris, P.H. Anderson, G.J. Atkins, Evidence for altered osteoclastogenesis in splenocyte cultures from Cyp27b1 knockout mice, J. Steroid Biochem. Mol. Biol. (2015).
[11] W.S. Chiu, J.F. McManus, A.J. Notini, A.I. Cassady, J.D. Zajac, R.A. Davey, Transgenic mice that express Cre recombinase in osteoclasts, Genesis 39 (2004) 178–185.
[12] Y. Lu, Y. Xie, S. Zhang, V. Dusevich, L.F. Bonewald, J.Q. Feng, DMP1-targeted Cre expression in odontoblasts and osteocytes, J. Dent. Res. 86 (2007) 320–325.
[13] T. Yoshizawa, Y. Handa, Y. Uematsu, S. Takeda, K. Sekine, Y. Yoshihara, T. Kawakami, K. Arioka, H. Sato, Y. Uchiyama, S. Masushige, A. Fukamizu, T. Matsumoto, S. Kato, Mice lacking the vitamin D receptor exhibit impaired bone formation, uterine hypoplasia and growth retardation after weaning, Nat. Genet. 16 (1997) 391–396.
[14] O. Dardenne, J. Prud'homme, A. Arabian, F.H. Glorieux, R. St-Arnaud, Targeted inactivation of the 25-hydroxyvitamin D(3)-1(alpha)-hydroxylase gene (CYP27B1) creates an animal model of pseudovitamin D-deficiency rickets, Endocrinology 142 (2001) 3135–3141.
[15] P.H. Anderson, S. Iida, J.H.T. Tyson, A.G. Turner, H.A. Morris, Bone CYP27B1 gene expression is increased with high dietary calcium and in mineralising osteoblasts, J. Steroid Biochem. Mol. Biol. 121 (2010) 71–75.
[16] S.J. Van Cromphaut, M. Dewerchin, J.G. Hoenderop, I. Stockmans, E. Van Herck, S. Kato, R.J. Bindels, D. Collen, P. Carmeliet, R. Bouillon, G. Carmeliet, Duodenal calcium absorption in vitamin D receptor-knockout mice: functional and molecular aspects, Proc. Natl. Acad. Sci. U. S. A. 98 (2001) 13324–13329.
[17] M. Prideaux, C. Schutz, A.R. Wijenayaka, D.M. Findlay, D.G. Campbell, L.B. Solomon, G.J. Atkins, Isolation of osteocytes from human trabecular bone, Bone 88 (2016) 64–72.
[18] T. Kameda, H. Mano, T. Yuasa, Y. Mori, K. Miyazawa, M. Shiokawa, Y. Nakamaru, E. Hiroi, K. Hiura, A. Kameda, N.N. Yang, Y. Hakeda, M. Kumegawa, Estrogen inhibits bone resorption by directly inducing apoptosis of the bone-resorbing osteoclasts, J. Exp. Med. 186 (1997) 489–495.
[19] L. Lieben, R. Masuyama, S. Torrekens, R. Van Looveren, J. Schrooten, P. Baatsen, M.H. Lafage-Proust, T. Dresselaers, J.Q. Feng, L.F. Bonewald, M.B. Meyer, J.W. Pike, R. Bouillon, G. Carmeliet, Normocalcemia is maintained in mice under conditions of calcium malabsorption by vitamin D-induced inhibition of bone mineralization, J. Clin. Invest. 122 (2012) 1803–1815.
[20] S. Krum, G. Miranda-Carboni, P. Hauschka, J. Carroll, T. Lane, L. Freedman, M. Brown, Estrogen protects bone by inducing Fas ligand in osteoblasts to regulate osteoclast survival, Eur. Mol. Biol. Organ. 27 (2008) 535–545.
[21] P.a.C. Sambrook, Osteoporosis, Lancet 367 (2006) 2010–2018.
[22] P.A. Baldock, R.J. Moore, T.C. Durbridge, H.A. Morris, Comparison of three methods for estimation of bone resorption following ovariectomy in the distal femur and the proximal tibia of the rat, Bone 24 (1999) 597–602.
[23] P.A. Baldock, H.A. Morris, A.G. Need, R.J. Moore, T.C. Durbridge, Variation in the short-term changes in bone cell activity in three regions of the distal femur immediately following ovariectomy, J. Bone Miner. Res. 13 (1998) 1451–1457.
[24] B. Lawrence Riggs, The mechanisms of estrogen regulation of bone resorption, J. Clin. Invest. 106 (2000).

Chapter 7a

Further analysis of the role of Vitamin D in osteoclastogenesis in co-cultures with intact osteocyte-like signalling through the use of conditional *Vdr* knockout splenocytes

This sub-chapter consists of unpublished data relating to the study by Reinke *et al.* (Chapter 6) and Starczak *et al.* (Chapter 7). *Ex vivo* co-cultures were conducted using the mouse MLO-Y4 osteocyte-like cell line together with splenocytes derived from $Ctsk^{cre}$/ $Vdr^{-/-}$ mice, using assays including TRAP staining, dentine bone resorption and mRNA expression.

7a.1 Introduction

In our previous studies (122, 133), we examined the effect of *Vdr* gene KO at the global level (*Vdr*KO) and conditionally in mature osteoclasts (Ctsk-Cre.Vdr$^{fl/fl}$) (139). Global deletion was examined using *Vdr*KO *ex vivo* splenocyte cultures. The conditional KO was examined using *in vivo* Ctsk^{cre}/vdr$^{-/-}$ model. While both of these types of experimental techniques contribute to the elucidation of the role of VDR in the osteoclast, they examine different aspects of the vitamin D pathway in this lineage. The global *Vdr*KO model has a germ-line deletion that potentially alters the development of osteoclast precursors as well as the activity of mature osteoclasts. This means that all stages of the osteoclast from precursor to final stage, mature multinucleated cells, are affected. This results in an inability to differentiate between effects on osteoclastogenesis and activity. Furthermore, the use of splenocyte monocultures means there is no influence of external endocrine/paracrine signalling, except that modelled by the addition of recombinant RANKL and M-CSF, reducing the similarity to *in vivo* physiological conditions. The Ctsk^{cre}/vdr$^{-/-}$, on the other hand, enables the examination of the effects of *Vdr* ablation in mature multinucleated osteoclasts actively expressing cathepsin K, enabling the differentiation between activity and osteoclastogenesis. A potential limitation of the Ctsk^{cre}/vdr$^{-/-}$ model used in our previous study (139) is that VDR activity could only be studied in cathepsin K expressing cells, notably active osteoclasts but potentially also osteocytes (140). However, the use of an osteocyte-specific deletion mouse model, Dmp-1^{Cre}/VDR$^{-/-}$, demonstrated that there was no notable effect on bone density and formation in *in vivo* cultures (139), suggesting that osteoclast expression was mainly affected in the cathepsin K promoter-driven model.

In this study, we modified the experimental technique used in the previous chapters to develop a co-culture system that enables a more complete examination of the vitamin D pathways in osteoclasts. We utilised the MLO-Y4 cell line in co-culture with the $Ctsk^{cre}/vdr^{-/-}$ splenocytes. The MLO-Y4 cell line was chosen as it is a widely accepted osteocyte model and has been demonstrated to support osteoclastogenesis. However, MLO-Y4 and $Ctsk^{cre}/vdr^{-/-}$ cells are both murine, preventing the ability to distinguish between osteocyte and osteoclast-derived gene expression. In these experiments, mature osteoclasts derived from $Ctsk^{cre}/vdr^{-/-}$ precursors lack the ability to respond to 1,25D. However, VDR signalling in the stromal osteocyte compartment remains intact. This is important, since osteocytes have been demonstrated to be key controllers of osteoclastogenesis in adult mouse bone (51, 52, 141) (142).

Experimental results from these cultures will enable us to identify the effect of vitamin D deletion on osteoclast activity, separate from osteoclastogenesis while enabling us to examine the contribution of stromal VDR signalling.

7a.2 Methods

Methods were followed, as detailed in Chapter 2, unless otherwise stated. The use of human derived SAOS-2 cell lines were tested as well as the MLO-Y4 cell line, in order to permit cell compartment-specific analysis of gene expression, by designing species-specific oligonucleotide primers, as our group has done previously. Primers were identified from electronic comparison of gene sequences. In most cases this allowed the identification of gene sequences that were species-specific. The exception to this was *Ctsk*. The human and murine *Ctsk* sequences have 100% sequence identity and so were

not examined. Unfortunately pilot studies indicated that SAOS-2 cells were unable to sufficiently support osteoclastogenesis to be of use for this study. Monocultures of either MLO-Y4 or splenocytes without RANKL or M-CSF were used as negative controls.

7a.3 Results and Discussion

WT and $Ctsk^{cre}/vdr^{-/-}$ co-cultures in the absence of exogenously added 1,25D had decreased osteoclast formation than WT and $Ctsk^{cre}/vdr^{-/-}$ co-cultures under 1nM of exogenous 1,25D (Fig 7a.1). The decreased osteoclast formation was expected as this co-culture model specifically derives osteoclastogenesis instigating factors, such as RANKL, from the MLO-Y4 cell line. This cell line has been demonstrated to express RANKL and pro-osteoclastogenic factors under the presence of 1,25D (121).

The ablation of VDR in cultures treated with 1,25D resulted in an increase in MNC number on day 9. The timing of the decrease coincides with the peak number of mature osteoclasts. Mature osteoclasts have the highest levels of cathepsin K expression and this would result in the highest level of VDR suppression due to the design of the $Ctsk^{cre}/vdr^{-/-}$ model. The reduction of MNC at peak osteoclast formation due to the ablation of the VDR in mature osteoclasts was unexpected and indicates the potential for the VDR to act as an inhibitor. This is further supported by previous studies (133). These studies indicated that decreased osteoclast number was observed when the VDR signalling pathway was intact in the presence of 1,25D. Additionally it was observed by (139) that the loss of VDR in mature osteoclasts resulted in decreased bone density, further supporting the inhibitory role of vitamin D.

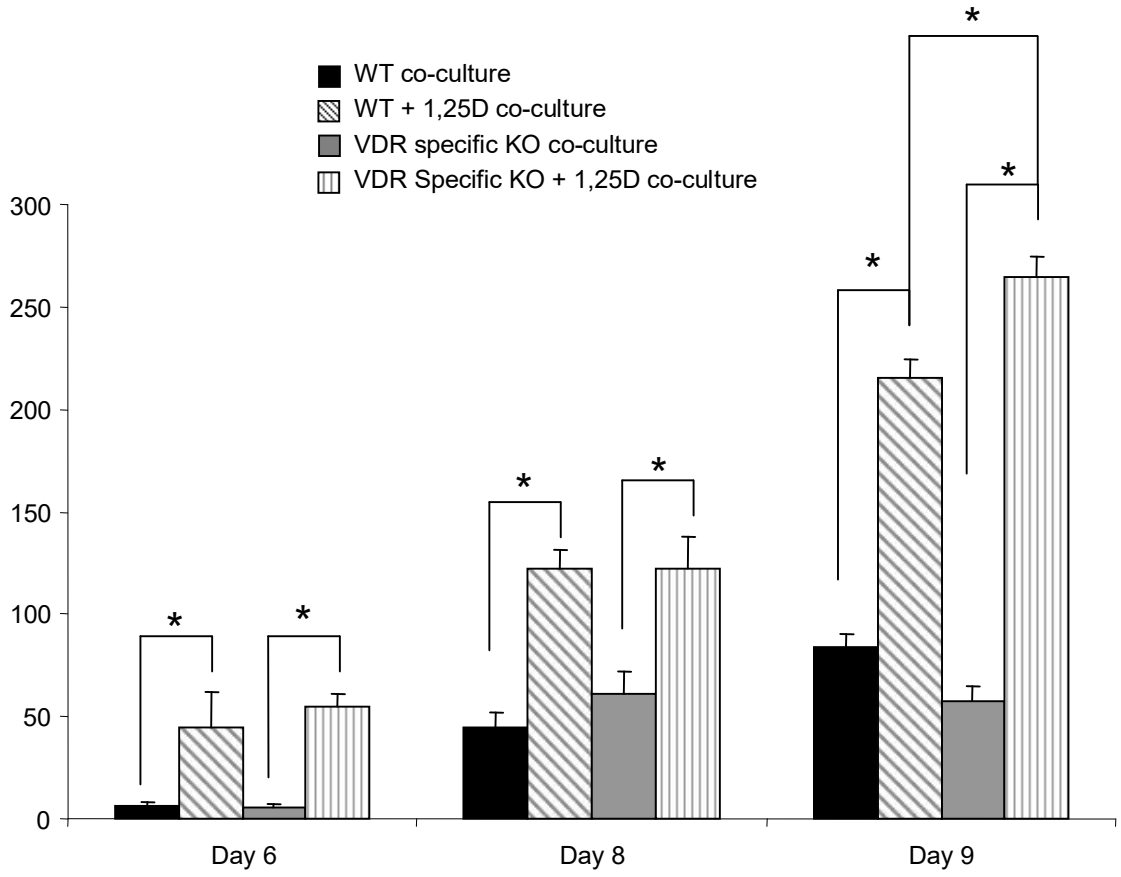

Fig 7a.1: The effect of VDR deletion and vitamin D metabolite addition in mature osteoclasts under co-culture with MLO-Y4 cell line. Splenocytes were cultured under four treatments; 1) WT co-culture of spleen and MLOY-4, 2) WT co-culture of spleen + MLO-Y4 + 1 nM 1,25D, 3) *Vdr*KO co-culture of spleen and MLOY-4, 4) *Vdr*KO co-culture of spleen + MLO-Y4 + 1 nM 1,25D and assayed for TRAP+ multinucleated cell formation. Total TRAP positive cell numbers were combined from two independent experiments, each using splenocytes pooled from at least 4 animals/group, and shown as means ± SEM. Significant differences from WT are indicated by asterisks ($p < 0.05$).

Co-culture experiments under osteoclast inducing conditions without the addition of exogenous 1,25D had lower levels of resorptive activity compared with cultures that had exogenous 1,25D as expected. These results in conjunction with MNC number as seen in Figure 7a.1 indicate that the presence of 1,25D is required for optimal osteoclast formation in a MLO-Y4 co-culture. WT and $Ctsk^{cre}/vdr^{-/-}$ splenocytes in MLO-Y4 co-culture were not significantly different from each other in the absence of exogenous 1,25D with equal levels of resorbed area on dentine (Fig 7a.2-7a.3).

Average area resorbed was significantly increased (3.3 fold) under 1,25D signalling under the ablation of VDR in mature osteoclasts (Fig 7a.3a). Osteoclast activity was alternatively measured as average resorption per osteoclast. Resorption per osteoclast was also increased in the presence of exogenous 1,25D under the ablation of the VDR in mature osteoclasts but had a lower fold increase of 1.4 (Fig 7a.3b).

The increase in osteoclast number and resorptive activity under exogenous 1,25D in mature osteoclasts with ablated VDR further reinforces the concept of exogenously added 1,25D acting as an inhibitor. Our previous papers have also demonstrated that the addition of exogenous 1,25D to WT spleen monocultures also resulted in a decrease in osteoclast formation and resorption (122, 133). The use of co-cultures in this case also allows us to observe the effect on VDR ablated mature osteoclasts, which was obscured in previous papers due to the germline deletion of VDR and CYP27B1. This indicates that there is a distinct but separate response to autocrine and exogenous 1,25D enhancing the importance of the role of the vitamin D receptor in the osteoclast.

The increased resorptive activity observed in osteoclasts, concurs well with the study done by (139) in ovariectomised mice in physiological conditions which have decreased bone volume. VDR ablation in *in vivo* cell cultures showed reduced thin trabecular bone

volume. This reinforces the role of VDR in osteoclasts as that of inhibitory when exposed to exogenous 1,25D. The lack of response from *Cyp27b1*KO cultures in mature osteoclasts as stated in Starczak *et al.* (139) is a clear indicator that the stage of maturation of hematopoietic stem cells plays a critical role in the determination of osteoclast response to both autocrine and endocrine vitamin D and its metabolites. The stage of maturation does not seem to change the inhibitory effect exogenous 1,25D has in both developing and mature osteoclasts.

To summarise, the deletion of the VDR specifically in the mature osteoclast resulted in increased; resorption, osteoclast number and resorption per osteoclast. The VDR in co-culture acted to suppress osteoclast number and resorption, acting as another regulatory element restricting osteoclast numbers. This strongly suggests that direct effects of 1,25D are more important physiologically than the indirect effects, at least in terms of osteoclast formation. Additionally, it also indicates that the changes in resorptive activity observed in global KO mice are likely caused by alterations to the osteoclast in maturation. This may indicate that the formation of the V-ATPase channels as seen in Chapter 5 occur during immature osteoclasts, as currently we hypothesise that increased hydrogen ion secretion is responsible for the increased resorption observed. Further work involving the use of $Ctsk^{cre}/vdr^{-/-}$ mice in a monoculture, using RANKL and M-CSF to stimulate osteoclastogenesis would be worth undertaking.

Fig 7a.2: The effect of VDR deletion on osteoclast resorptive activity in mature osteoclasts. MLO-Y4 cells were seeded onto dentine and left over night. Splenocytes were then seeded at optimal density into the dentine containing 96-well plates and culture under cell supportive conditions. After 21 days of culture, dentine was removed, cleaned and analysed by scanning electron microscopy. Quantified data are means ± SEM of quadruplicate wells and are representative of 2 independent experiments.

A Spleen Mono Culture WT

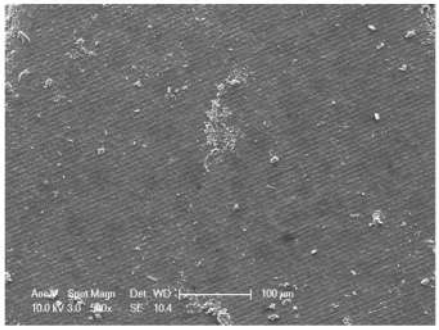

E Spleen Mono Culture KO

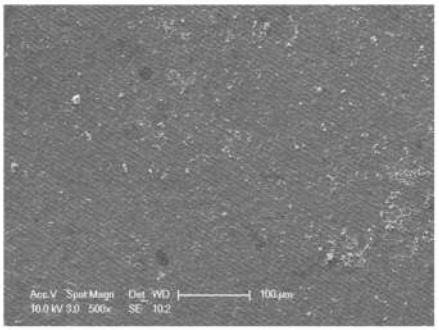

B MLO-Y4 Mono culture WT

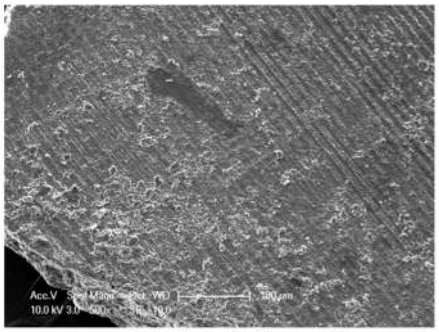

F MLO-Y4 Mono culture KO

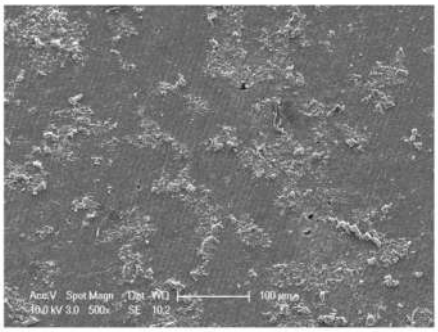

C Co Culture WT

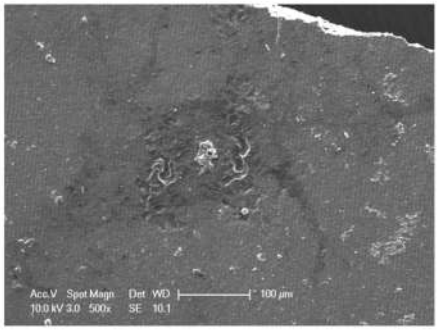

G Co-Culture KO

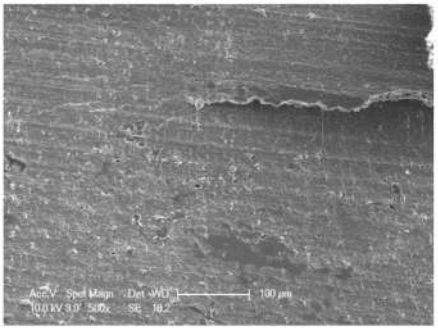

D Co-Culture WT + 1,25D

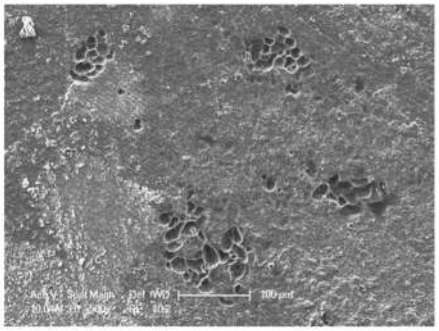

H Co-Culture KO +1,25D

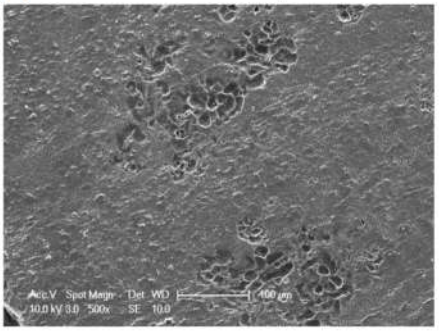

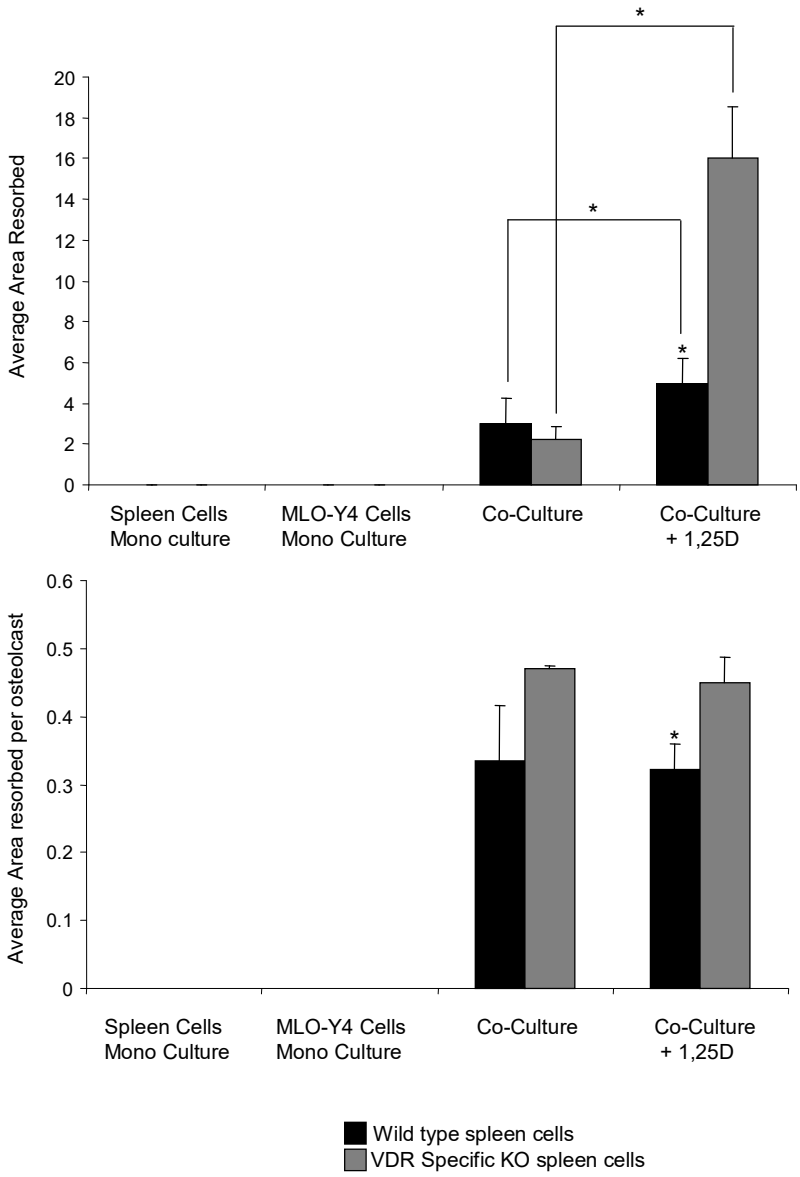

Fig 7a.3: The effect of VDR deletion on osteoclast resorptive activity in mature osteoclasts. Dentine was analysed using image J and Graphpad Prism. a) Average total area resorbed b) Average area resorbed per event. Quantified data are means ± SEM of quadruplicate wells and are representative of 2 independent experiments. Significant differences between genotypes are indicated by asterisks ($p < 0.05$).

Chapter 8

Concluding Remarks

8.0 Conclusions

The vitamin D endocrine system is an exceedingly complex system. The vitamin D receptor has been demonstrated to be almost ubiquitously expressed throughout the human body (1). The understanding of the endocrine system as an adjunct of the calcium and phosphate system is relatively well understood. However, the effect of vitamin D metabolism at the cellular level is poorly understood. Previous studies have established that the autocrine conversion of 25D to 1,25D occurs within the osteoblasts and osteoclasts and that as these cells mature the level of this conversion increases. This has been demonstrated in murine RAW264.7 and human PBMC cultures (Chapter 1). This indicates that the role of autocrine conversion of 25D and 1,25D plays a significant role in the regulation of bone remodelling. Initial examination was undertaken through the use of murine spleen cells extracted from *Cyp27b1*KO mice. Initial findings were inconsistent and indicated the need for further optimisation (Chapter 3). Optimisation of murine osteoclast cultures resulted in the key findings that cell density and FBS were the primary regulators of changes within osteoclast *ex vivo* cell cultures. It was also established that the use of a pooled population from multiple murine spleens resulted in more reproducible and consistent cultures in terms of resulting osteoclast numbers. The use of heterozygous murine model was untenable as either a positive or negative control as there was a lack of reproducibility in the cultures, with the results appearing to mimic those from either WT or KO cell cultures seemingly randomly.

8.1 Deletion of CYP27B1

Examination of *Cyp27b1*KO murine *ex vivo* cell model against WT littermate matched controls were undertaken through TRAP staining, Von Kossa staining, dentine

resorption assays and RT-PCR gene expression analysis. The deletion of CYP27B1 resulted in increased osteoclast numbers, increased resorption per cell on osteoid and dentine and in particular, the derangement of prominent osteoclast genes including *Nfatc1, Trap, C-fos* and *Ca2*. The deletion of *Cyp27b1* also resulted in the derangement of the ratio of *Bax* to *Bcl-2* suggesting that the osteoclasts formed had reduced rate of apoptosis.

The loss of CYP27B1 resulting in decreased gene expression and decreased $TRAP^{+}$ MNC was expected, as it had been observed previously that the presence of 25D resulted in increased gene expression and osteoclast proliferation (3, 4, 7). Increased resorptive activity per osteoclast was also observed, which is counterintuitive but highly consistent with our group's findings that the addition of 25D to osteoclast forming cultures with CYP27B1 intact reduced the resorptive activity of osteoclasts formed; thus, it was proposed that circulating 25D levels may serve to optimise osteoclastogenesis by promoting osteoclastic gene expression while ameliorating resorption activity (3). This signified the potential for research into alternate pathways that could result in altered resorptive activity, such as, effects of vitamin D on the many sub-units of the V-ATPase pump.

We investigated the effect of the conditional KO of *Vdr* and *Cyp27b1* in mature osteoclasts derived from murine splenocytes (Chapter 7). $Ctsk^{cre}/Vdr^{-/-}$ mice maintain functional vitamin D metabolic pathways in all other cell types and additionally in the immature precursors of the osteoclast, since the promoter driving Cre-recombinase expression and gene deletion is that of *Ctsk*, a gene product normally expressed by mature, actively resorbing osteoclasts. The Ctsk-Cre model has been well validated as osteoclast-specific (143). This potentially allows us to examine the effect of autocrine vitamin D pathways in mature osteoclast in both *in vivo* and *ex vivo* models. It was

demonstrated that the loss of CYP27B1 *in vivo* in mature osteoclasts, as is the case in $Ctsk^{Cre}$-$Cyp27b1^{-/-}$ mice, had no effect on bone volume. The lack of resorption change in these mice was disappointing. It does however indicate that the effects seen in the *ex vivo* models may be related to changes in osteoclast precursors and immature osteoclasts that are not yet producing sufficient CTSK to trigger CYP27B1. In contrast, the loss of VDR in mature osteoclasts resulted in significantly reduced bone volume without affecting osteoclast number (139), consistent with the notion that vitamin D signalling specifically in mature osteoclasts reduces or ameliorates their activity.

Ovariectomised mice were used as a model of pathologic bone loss and demonstrated bone loss was exacerbated in the absence of osteoclastic VDR. This increased loss of bone volume may be indicative of both altered survival and resorptive events by the osteoclast.

This model provides useful insight into the role of vitamin D signalling in mice. In particular, this study demonstrates how much there is still to be elucidated about the role of autocrine vitamin D signalling in the osteoclast.

8.2 Deletion of VDR

The clear changes in osteoclastic fusion and resorption seen with splenocyte cultures from *Cyp27b1*KO mice implied that a similar response should be seen when *Vdr* was deleted (Chapter 6).

The deletion of VDR from the osteoclasts resulted, as expected, in a similar reduction in osteoclast formation with decreased osteoclast numbers, decreased gene expression, and increased resorptive activity. Of particular note was that the gene expression

patterns were nearly identical between *Vdr*KO and *Cyp27b*1KO osteoclast cultures for multiple sets of genes, strongly suggesting that overlapping metabolic pathways were affected.

The ratio of *Bax* and *Bcl-2* was also increased in *Vdr*KO osteoclast cultures consistent with these osteoclasts having increased survival. This provided two potential and not mutually exclusive hypotheses for increased resorptive activity despite reduced gene expression. The first being increased survival resulting in osteoclasts that were active for longer. The second being changes to the osteoclasts' primary form of hydrogen ion secretion, the V-ATPase pump.

8.3 The Effect of 1,25D on *Cyp27b1*KO and *Vdr*KO Osteoclasts.

As hypothesised the addition of 1,25D to both KO mouse models was unable to restore functionality in the osteoclasts. The lack of response in *Vdr*KO osteoclasts was expected if the KO of the VDR receptor was successful. The inability of exogenous 1,25D to restore function in *Cyp27b1*KO osteoclasts indicated that the conversion of 25D to 1,25D and the presence of the autocrine system within the osteoclast has its own functions. The addition of 1,25D to WT cultures in this experimental set also resulted in decreased osteoclastic formation and activity. This indicated that osteoclastic cultures in the absence of stromal cell signalling responded to exogenous 1,25D as an inhibitor.

8.4 V-ATPase Modification Due to Loss of Autocrine Vitamin D Pathway.

We also examined the effect of CYP27B1 deletion on all 26 subunits of the V-ATPase proton pump. It became apparent that the majority of genes were modified to some extent by the loss of the autocrine vitamin D pathway. The resultant gene expression indicated that the V-ATPase pump may become unstable and dysregulated when autocrine vitamin D metabolism is lost. We were unable to directly establish a link between altered gene expression and proton secretion with loss of the vitamin D metabolic pathway. This will require additional experimentation, including assessment of the protein levels of each of the subunits.

8.5 Limitations and Future Direction

The analysis in the above cell culture studies, in addition to examining osteoclast formation and activity, relied to a large extent on RT-PCR analysis. RT-PCR has positive attributes of being highly specific and quantitative. However, it would be preferable in future studies to include unbiased RNA approaches, such as RNA sequencing, to identify the full transcriptome of the genetically modified or treated cells. Coupled with bioinformatics, this could identify all cellular processes affected. During the course of this dissertation, the associated costs of RNA-Seq have reduced considerably, making this approach more feasible. Furthermore, changes in mRNA levels do not always result in equivalent changes in protein levels. This can be due to effects on promoter activity, post-translational processing, as well as protein turnover. It would be desirable to perform proteomic analysis, and similar to RNA-Seq, in an unbiased fashion. Even if the proteome was determined, it would still likely be necessary to perform antibody-based techniques to determine the composition of

specific structures such as the V-ATPase, as well as high fidelity imaging, in order to determine subtle changes.

Work was planned for a caspase 3 apoptosis assay, however due to restrictions in the availability of the mice, the use of an RNA based system of *Bax* and *Bcl-2* was used instead. Any further work in this area would ideally include a more thorough examination of apoptosis as well as senescence as possible cell fates.

To improve *in vivo* examination of the role of vitamin D signalling in osteoclasts, an inducible approach, such as tetracycline-inducible conditional gene knockout, at various stages of osteoclastogenesis could be used to distinguish between developmental and functional effects.

The findings within this thesis have added to the literature that autocrine activity of vitamin D has an important role in the regulation of the osteoclast. Furthermore, it has established that autocrine vitamin D metabolism affects osteoclast fusion, bone resorption activity, motility and precursor proliferation, and that these effects are still observable under the regulation of osteoblast-like cell cultures. This indicates that the regulation of vitamin D within the osteoclast lineage is an essential part of bone homeostasis and provides additional avenues of investigation into treating bone disorders.

9.0 References

1. Bouillon R, Carmeliet G, Verlinden L, van Etten E, Verstuyf A, Luderer HF, et al. Vitamin D and human health: lessons from vitamin D receptor null mice. Endocr Rev. 2008;29(6):726-76.
2. Atkins GJ, Anderson PH, Findlay DM, Welldon KJ, Vincent C, Zannettino ACW, et al. Metabolism of Vitamin D_3 in Human osteoblasts: Evidence for autocrine and paracrine activities of 1α,25-dihydroxyvitamin D_3. BONE. 2007;40:1517-28.
3. Kogawa M, Anderson PH, Findlay DM, Morris HA, Atkins GJ. The metabolism of 25-(OH)vitamin D_3 by osteoclasts and their precursors regulates the differentiation of osteoclasts. Journal of Steroid Biochemistry and Molecular Biology. 2010;121:277-80.
4. Kogawa M, Findlay DM, Anderson PH, Ormsby R, Vincent C, Morris HA, et al. Osteoclastic metabolism of 25(OH)-vitamin D3: a potential mechanism for optimization of bone resorption. Endocrinology. 2010;151(10):4613-25.
5. Teitelbaum SL, Ross FP. Genetic regulation of osteoclast development and function. Nature reviews Genetics. 2003;4(8):638-49.
6. Teitelbaum SL. Osteoclasts: what do they do and how do they do it? The American journal of pathology. 2007;170(2):427-35.
7. Kogawa M, Findlay DM, Anderson PH, Atkins GJ. Modulation of osteoclastic migration by metabolism of 25(OH)-vitamin D(3). The Journal of steroid biochemistry and molecular biology. 2012.
8. Anderson PH, Atkins GJ. The skeleton as an interaction organ for vitamin D metabolism. Molecular Aspects of Medicine. 2008;29:397-406.
9. FELDMAN D, PIKE JW, ADAMS JS. Vitamin D 3rd edition: Elsevier Inc; 2005.
10. Lieben L, Carmeliet G. The Involvement of TRP Channels in Bone Homeostasis. Frontiers in endocrinology. 2012;3:99.
11. Holick MF. Sunlight and vitamin D for bone health and prevention of autoimmune diseases, cancers, and cardiovascular disease. Am J Clin Nutr. 2004;80(6 Suppl):1678S-88S.
12. Bischoff-Ferrari HA, Giovannucci E, Willett WC, Dietrich T, Dawson-Hughes B. Estimation of optimal serum concentrations of 25-hydroxyvitamin D for multiple health outcomes. Am J Clin Nutr. 2006;84(1):18-28.
13. Baron R, Hesse E. Update on bone anabolics in osteoporosis treatment: rationale, current status, and perspectives. The Journal of clinical endocrinology and metabolism. 2012;97(2):311-25.
14. Haussler MR. VITAMIN D RECEPTORS: NATURE AND FUNCTION. Annu Rev Nutr. 1986;6:527-62.
15. Fairfield KM, Fletcher RH. Vitamins for chronic disease prevention in adults: scientific review. JAMA. 2002;287(23):3116-26.
16. Lehmann B, Genehr T, Knuschke P, Pietzsch J, Meurer M. UVB-induced conversion of 7-dehydrocholesterol to 1alpha,25-dihydroxyvitamin D3 in an in vitro human skin equivalent model. J Invest Dermatol. 2001;117(5):1179-85.
17. Yasuda K, Ikushiro S, Kamakura M, Takano M, Saito N, Kittaka A, et al. Human cytochrome P450-dependent differential metabolism among three 2alpha-substituted-1alpha,25-dihydroxyvitamin D(3) analogs. The Journal of steroid biochemistry and molecular biology. 2013;133:84-92.

18. Japelt RB, Jakobsen J. Vitamin D in plants: a review of occurrence, analysis, and biosynthesis. Front Plant Sci. 2013;4:136.
19. Brown AJ, Dusso A, Slatopolsky E. Vitamin D. Am J Physiol. 1999;277(2 Pt 2):F157-75.
20. Jones G, Strugnell SA, DeLuca HF. Current understanding of the molecular actions of vitamin D. Physiological reviews. 1998;78(4):1193-231.
21. Raiten DJ, Picciano MF. Vitamin D and health in the 21st century: bone and beyond. Executive summary. Am J Clin Nutr. 2004;80(6 Suppl):1673S-7S.
22. Looker AC, Dawson-Hughes B, Calvo MS, Gunter EW, Sahyoun NR. Serum 25-hydroxyvitamin D status of adolescents and adults in two seasonal subpopulations from NHANES III. Bone. 2002;30(5):771-7.
23. Fraser DR, Kodicek E. Unique biosynthesis by kidney of a biological active vitamin D metabolite. Nature. 1970;228(5273):764-6.
24. Omdahl JL, Morris HA, May BK. Hydroxylase enzymes of the vitamin D pathway: expression, function, and regulation. Annual review of nutrition. 2002;22:139-66.
25. Chun RF. New perspectives on the vitamin D binding protein. Cell biochemistry and function. 2012.
26. White P, Cooke N. The multifunctional properties and characteristics of vitamin D-binding protein. Trends Endocrinol Metab. 2000;11(8):320-7.
27. Anderson PH, May BK, Morris HA. Vitamin D metabolism: new concepts and clinical implications. Clin Biochem Rev. 2003;24(1):13-26.
28. Bikle DD. What is new in Vitamin D. Current Opinion in Rheumtology. 2007;19:383-8.
29. Morris HA, Anderson PH. Autocrine and paracrine actions of vitamin d. Clin Biochem Rev. 2010;31(4):129-38.
30. Bergwitz C, Juppner H. Regulation of phosphate homeostasis by PTH, vitamin D, and FGF23. Annual review of medicine. 2010;61:91-104.
31. Panda DK, Miao D, Bolivar I, Li J, Huo R, Hendy GN, et al. Inactivation of the 25-hydroxyvitamin D 1alpha-hydroxylase and vitamin D receptor demonstrates independent and interdependent effects of calcium and vitamin D on skeletal and mineral homeostasis. The Journal of biological chemistry. 2004;279(16):16754-66.
32. Dardenne O, Prud'homme J, Arabian A, Glorieux FH, St-Arnaud R. Targeted inactivation of the 25-hydroxyvitamin D(3)-1(alpha)-hydroxylase gene (CYP27B1) creates an animal model of pseudovitamin D-deficiency rickets. Endocrinology. 2001;142(7):3135-41.
33. Bischoff-Ferrari HA, Willett WC, Orav EJ, Lips P, Meunier PJ, Lyons RA, et al. A pooled analysis of vitamin D dose requirements for fracture prevention. The New England journal of medicine. 2012;367(1):40-9.
34. Anderson PH, Sawyer RK, May BK, O'Loughlin PD, Morris HA. 25-Hydroxyvitamin D requirement for maintaining skeletal health utilising a Sprague-Dawley rat model. The Journal of steroid biochemistry and molecular biology. 2007;103(3-5):592-5.
35. Anderson PH, Atkins GJ, Turner AG, Kogawa M, Findlay DM, Morris HA. Vitamin D metabolism within bone cells: Effects on bone structure and strength. Mol Cell Endocrinol. 2011;347:42-7.
36. ATKINS GJ, KOSTAKIS P, PAN B, FARRUGIA A, GRONTHOS S, EVDOKIOU A, et al. RANKL Expression Is Related to the Differentiation State of

Human Osteoblasts. JOURNAL OF BONE AND MINERAL RESEARCH 2003;18:1088-98.
37. Fazzalari NL, Kuliwaba JS, Atkins GJ, Forwood MR, Findlay DM. The ratio of messenger RNA levels of receptor activator of nuclear factor kappaB ligand to osteoprotegerin correlates with bone remodeling indices in normal human cancellous bone but not in osteoarthritis. J Bone Miner Res. 2001;16(6):1015-27.
38. Vincent C, Kogawa M, Findlay DM, Atkins GJ. The generation of osteoclasts from RAW 264.7 precursors in defined, serum-free conditions. Journal of bone and mineral metabolism. 2009;27(1):114-9.
39. Boonrungsiman S, Gentleman E, Carzaniga R, Evans ND, McComb DW, Porter AE, et al. The role of intracellular calcium phosphate in osteoblast-mediated bone apatite formation. Proc Natl Acad Sci U S A. 2012;109(35):14170-5.
40. Orimo H. The mechanism of mineralization and the role of alkaline phosphatase in health and disease. Journal of Nippon Medical School = Nippon Ika Daigaku zasshi. 2010;77(1):4-12.
41. Polewski MD, Johnson KA, Foster M, Millan JL, Terkeltaub R. Inorganic pyrophosphatase induces type I collagen in osteoblasts. Bone. 2010;46(1):81-90.
42. Simonet WS, Lacey DL, Dunstan CR, Kelley M, Chang MS, Luthy R, et al. Osteoprotegerin: a novel secreted protein involved in the regulation of bone density. Cell. 1997;89(2):309-19.
43. Subramaniam M, Hawse JR, Bruinsma ES, Grygo SB, Cicek M, Oursler MJ, et al. TGFbeta inducible early gene-1 directly binds to, and represses, the OPG promoter in osteoblasts. Biochemical and biophysical research communications. 2010;392(1):72-6.
44. Bucay N, Sarosi I, Dunstan CR, Morony S, Tarpley J, Capparelli C, et al. osteoprotegerin-deficient mice develop early onset osteoporosis and arterial calcification. Genes & development. 1998;12(9):1260-8.
45. Hofbauer LC, Khosla S, Dunstan CR, Lacey DL, Boyle WJ, Riggs BL. The roles of osteoprotegerin and osteoprotegerin ligand in the paracrine regulation of bone resorption. J Bone Miner Res. 2000;15(1):2-12.
46. Matsuo K, Irie N. Osteoclast-osteoblast communication. Arch Biochem Biophys. 2008;473(2):201-9.
47. Gooi JH, Pompolo S, Karsdal MA, Kulkarni NH, Kalajzic I, McAhren SH, et al. Calcitonin impairs the anabolic effect of PTH in young rats and stimulates expression of sclerostin by osteocytes. Bone. 2010;46(6):1486-97.
48. Xiong J, Onal M, Jilka RL, Weinstein RS, Manolagas SC, O'Brien CA. Matrix-embedded cells control osteoclast formation. Nature medicine. 2011;17(10):1235-41.
49. Nakashima T, Takayanagi H. New regulation mechanisms of osteoclast differentiation. Annals of the New York Academy of Sciences. 2011;1240:E13-8.
50. Atkins GJ, Findlay DM. Osteocyte regulation of bone mineral: a little give and take. Osteoporosis international : a journal established as result of cooperation between the European Foundation for Osteoporosis and the National Osteoporosis Foundation of the USA. 2012.
51. Rochefort GY, Pallu S, Benhamou CL. Osteocyte: the unrecognized side of bone tissue. Osteoporosis international : a journal established as result of cooperation between the European Foundation for Osteoporosis and the National Osteoporosis Foundation of the USA. 2010;21(9):1457-69.

52. Aguirre JI, Plotkin LI, Stewart SA, Weinstein RS, Parfitt AM, Manolagas SC, et al. Osteocyte apoptosis is induced by weightlessness in mice and precedes osteoclast recruitment and bone loss. J Bone Miner Res. 2006;21(4):605-15.
53. Loiselle AE, Jiang JX, Donahue HJ. Gap junction and hemichannel functions in osteocytes. Bone. 2012.
54. Desmoulin GT, Reno CR, Hunter CJ. Free axial vibrations at 0 to 200 Hz positively affect extracellular matrix messenger ribonucleic acid expression in bovine nucleus pulposi. Spine. 2010;35(15):1437-44.
55. Atkins GJ, Kostakis P, Vincent C, Farrugia AN, Houchins JP, Findlay DM, et al. RANK Expression as a cell surface marker of human osteoclast precursors in peripheral blood, bone marrow, and giant cell tumors of bone. J Bone Miner Res. 2006;21(9):1339-49.
56. Armstrong AP, Tometsko ME, Glaccum M, Sutherland CL, Cosman D, Dougall WC. A RANK/TRAF6-dependent signal transduction pathway is essential for osteoclast cytoskeletal organization and resorptive function. The Journal of biological chemistry. 2002;277(46):44347-56.
57. Qin A, Cheng TS, Pavlos NJ, Lin Z, Dai KR, Zheng MH. V-ATPases in osteoclasts: Structure, function and potential inhibitors of bone resorption. The international journal of biochemistry & cell biology. 2012;44(9):1422-35.
58. Colonna M, Turnbull I, Klesney-Tait J. The enigmatic function of TREM-2 in osteoclastogenesis. Advances in experimental medicine and biology. 2007;602:97-105.
59. Paradowska-Gorycka A, Jurkowska M. Structure, expression pattern and biological activity of molecular complex TREM-2/DAP12. Human immunology. 2013;74(6):730-7.
60. Otero K, Shinohara M, Zhao H, Cella M, Gilfillan S, Colucci A, et al. TREM2 and beta-catenin regulate bone homeostasis by controlling the rate of osteoclastogenesis. Journal of immunology. 2012;188(6):2612-21.
61. Muench SP, Scheres SH, Huss M, Phillips C, Vitavska O, Wieczorek H, et al. Subunit positioning and stator filament stiffness in regulation and power transmission in the V1 motor of the Manduca sexta V-ATPase. Journal of molecular biology. 2014;426(2):286-300.
62. Gu J, Tong XS, Chen GH, Wang D, Chen Y, Yuan Y, et al. Effects of 1alpha,25-(OH)2D3 on the formation and activity of osteoclasts in RAW264.7 cells. The Journal of steroid biochemistry and molecular biology. 2015;152:25-33.
63. Kim K, Lee SH, Ha Kim J, Choi Y, Kim N. NFATc1 induces osteoclast fusion via up-regulation of Atp6v0d2 and the dendritic cell-specific transmembrane protein (DC-STAMP). Mol Endocrinol. 2008;22(1):176-85.
64. Kim T, Ha H, Kim N, Park ES, Rho J, Kim EC, et al. ATP6v0d2 deficiency increases bone mass, but does not influence ovariectomy-induced bone loss. Biochemical and biophysical research communications. 2010;403(1):73-8.
65. Kishikawa J, Seino A, Nakanishi A, Tirtom NE, Noji H, Yokoyama K, et al. F-subunit reinforces torque generation in V-ATPase. Eur Biophys J. 2014;43(8-9):415-22.
66. Lee BS, Holliday LS, Krits I, Gluck SL. Vacuolar H+-ATPase activity and expression in mouse bone marrow cultures. J Bone Miner Res. 1999;14(12):2127-36.
67. Molina MF, Qu HQ, Rentfro AR, Nair S, Lu Y, Hanis CL, et al. Decreased expression of ATP6V1H in type 2 diabetes: a pilot report on the diabetes risk study in

Mexican Americans. Biochemical and biophysical research communications. 2011;412(4):728-31.
68. Wu H, Xu G, Li YP. Atp6v0d2 is an essential component of the osteoclast-specific proton pump that mediates extracellular acidification in bone resorption. J Bone Miner Res. 2009;24(5):871-85.
69. Miyauchi A, Alvarez J, Greenfield EM, Teti A, Grano M, Colucci S, et al. Recognition of osteopontin and related peptides by an alpha v beta 3 integrin stimulates immediate cell signals in osteoclasts. The Journal of biological chemistry. 1991;266(30):20369-74.
70. Anderson PH, Hendrix I, Sawyer RK, Zarrinkalam R, Manavis J, Sarvestani GT, et al. Co-expression of CYP27B1 enzyme with the 1.5kb CYP27B1 promoter-luciferase transgene in the mouse. Mol Cell Endocrinol. 2008;285(1-2):1-9.
71. Nakamura I, Pilkington MF, Lakkakorpi PT, Lipfert L, Sims SM, Dixon SJ, et al. Role of alpha(v)beta(3) integrin in osteoclast migration and formation of the sealing zone. Journal of cell science. 1999;112 (Pt 22):3985-93.
72. Faccio R, Takeshita S, Zallone A, Ross FP, Teitelbaum SL. c-Fms and the alphavbeta3 integrin collaborate during osteoclast differentiation. The Journal of clinical investigation. 2003;111(5):749-58.
73. Feng X, Novack DV, Faccio R, Ory DS, Aya K, Boyer MI, et al. A Glanzmann's mutation in beta 3 integrin specifically impairs osteoclast function. The Journal of clinical investigation. 2001;107(9):1137-44.
74. Ek-Rylander B, Andersson G. Osteoclast migration on phosphorylated osteopontin is regulated by endogenous tartrate-resistant acid phosphatase. Experimental cell research. 2010;316(3):443-51.
75. Geblinger D, Addadi L, Geiger B. Nano-topography sensing by osteoclasts. Journal of cell science. 2010;123(Pt 9):1503-10.
76. Faccio R, Novack DV, Zallone A, Ross FP, Teitelbaum SL. Dynamic changes in the osteoclast cytoskeleton in response to growth factors and cell attachment are controlled by beta3 integrin. The Journal of cell biology. 2003;162(3):499-509.
77. Ohlsson A, Cumming WA, Paul A, Sly WS. Carbonic anhydrase II deficiency syndrome: recessive osteopetrosis with renal tubular acidosis and cerebral calcification. Pediatrics. 1986;77(3):371-81.
78. Sly WS, Hewett-Emmett D, Whyte MP, Yu YS, Tashian RE. Carbonic anhydrase II deficiency identified as the primary defect in the autosomal recessive syndrome of osteopetrosis with renal tubular acidosis and cerebral calcification. Proc Natl Acad Sci U S A. 1983;80(9):2752-6.
79. Teitelbaum SL. Bone resorption by osteoclasts. Science. 2000;289(5484):1504-8.
80. Schlesinger PH, Blair HC, Teitelbaum SL, Edwards JC. Characterization of the osteoclast ruffled border chloride channel and its role in bone resorption. The Journal of biological chemistry. 1997;272(30):18636-43.
81. Anderson PH, Sawyer RK, Moore AJ, May BK, O'Loughlin PD, Morris HA. Vitamin D depletion induces RANKL-mediated osteoclastogenesis and bone loss in a rodent model. J Bone Miner Res. 2008;23(11):1789-97.
82. Dodds RA, James IE, Rieman D, Ahern R, Hwang SM, Connor JR, et al. Human osteoclast cathepsin K is processed intracellularly prior to attachment and bone resorption. J Bone Miner Res. 2001;16(3):478-86.
83. Zaidi M, Troen B, Moonga BS, Abe E. Cathepsin K, osteoclastic resorption, and osteoporosis therapy. J Bone Miner Res. 2001;16(10):1747-9.

84. Saftig P, Hunziker E, Wehmeyer O, Jones S, Boyde A, Rommerskirch W, et al. Impaired osteoclastic bone resorption leads to osteopetrosis in cathepsin-K-deficient mice. Proc Natl Acad Sci U S A. 1998;95(23):13453-8.
85. Zenger S, Hollberg K, Ljusberg J, Norgard M, Ek-Rylander B, Kiviranta R, et al. Proteolytic processing and polarized secretion of tartrate-resistant acid phosphatase is altered in a subpopulation of metaphyseal osteoclasts in cathepsin K-deficient mice. Bone. 2007;41(5):820-32.
86. Hollberg K, Hultenby K, Hayman A, Cox T, Andersson G. Osteoclasts from mice deficient in tartrate-resistant acid phosphatase have altered ruffled borders and disturbed intracellular vesicular transport. Experimental cell research. 2002;279(2):227-38.
87. Nakayama T, Mizoguchi T, Uehara S, Yamashita T, Kawahara I, Kobayashi Y, et al. Polarized osteoclasts put marks of tartrate-resistant acid phosphatase on dentin slices--a simple method for identifying polarized osteoclasts. Bone. 2011;49(6):1331-9.
88. Nagase Y, Iwasawa M, Akiyama T, Kadono Y, Nakamura M, Oshima Y, et al. Anti-apoptotic molecule Bcl-2 regulates the differentiation, activation, and survival of both osteoblasts and osteoclasts. The Journal of biological chemistry. 2009;284(52):36659-69.
89. Chan SL, Yu VC. Proteins of the bcl-2 family in apoptosis signalling: from mechanistic insights to therapeutic opportunities. Clinical and experimental pharmacology & physiology. 2004;31(3):119-28.
90. Placzek WJ, Wei J, Kitada S, Zhai D, Reed JC, Pellecchia M. A survey of the anti-apoptotic Bcl-2 subfamily expression in cancer types provides a platform to predict the efficacy of Bcl-2 antagonists in cancer therapy. Cell death & disease. 2010;1:e40.
91. Masuda H, Hirose J, Omata Y, Tokuyama N, Yasui T, Kadono Y, et al. Anti-apoptotic Bcl-2 family member Mcl-1 regulates cell viability and bone-resorbing activity of osteoclasts. Bone. 2014;58:1-10.
92. Kizildag S, Ates H, Kizildag S. Treatment of K562 cells with 1,25-dihydroxyvitamin D3 induces distinct alterations in the expression of apoptosis-related genes BCL2, BAX, BCLXL, and p21. Annals of hematology. 2010;89(1):1-7.
93. Wang Y, Zhu J, DeLuca HF. Where is the vitamin D receptor? Arch Biochem Biophys. 2012;523(1):123-33.
94. Wang Y, Zhu J, DeLuca HF. Identification of the vitamin D receptor in osteoblasts and chondrocytes but not osteoclasts in mouse bone. J Bone Miner Res. 2014;29(3):685-92.
95. Mee AP, Hoyland JA, Braidman IP, Freemont AJ, Davies M, Mawer EB. Demonstration of vitamin D receptor transcripts in actively resorbing osteoclasts in bone sections. Bone. 1996;18(4):295-9.
96. van Driel M, Koedam M, Buurman CJ, Hewison M, Chiba H, Uitterlinden AG, et al. Evidence for auto/paracrine actions of vitamin D in bone: 1alpha-hydroxylase expression and activity in human bone cells. Faseb J. 2006;20(13):2417-9.
97. Nagai J, Sato K, Yumoto R, Takano M. Megalin/cubilin-mediated uptake of FITC-labeled IgG by OK kidney epithelial cells. Drug metabolism and pharmacokinetics. 2011;26(5):474-85.

98. Geng S, Zhou S, Glowacki J. Effects of 25-hydroxyvitamin D(3) on proliferation and osteoblast differentiation of human marrow stromal cells require CYP27B1/1alpha-hydroxylase. J Bone Miner Res. 2011;26(5):1145-53.
99. van Driel M, Koedam M, Buurman CJ, Roelse M, Weyts F, Chiba H, et al. Evidence that both 1alpha,25-dihydroxyvitamin D3 and 24-hydroxylated D3 enhance human osteoblast differentiation and mineralization. J Cell Biochem. 2006;99(3):922-35.
100. Mundy GR, Elefteriou F. Boning up on ephrin signaling. Cell. 2006;126(3):441-3.
101. Zhao C, Irie N, Takada Y, Shimoda K, Miyamoto T, Nishiwaki T, et al. Bidirectional ephrinB2-EphB4 signaling controls bone homeostasis. Cell metabolism. 2006;4(2):111-21.
102. Benford HL, McGowan NW, Helfrich MH, Nuttall ME, Rogers MJ. Visualization of bisphosphonate-induced caspase-3 activity in apoptotic osteoclasts in vitro. Bone. 2001;28(5):465-73.
103. Kim K, Kim JH, Lee J, Jin HM, Lee SH, Fisher DE, et al. Nuclear factor of activated T cells c1 induces osteoclast-associated receptor gene expression during tumor necrosis factor-related activation-induced cytokine-mediated osteoclastogenesis. The Journal of biological chemistry. 2005;280(42):35209-16.
104. Li YC, Pirro AE, Amling M, Delling G, Baron R, Bronson R, et al. Targeted ablation of the vitamin D receptor: an animal model of vitamin D-dependent rickets type II with alopecia. Proc Natl Acad Sci U S A. 1997;94(18):9831-5.
105. Amling M, Priemel M, Holzmann T, Chapin K, Rueger JM, Baron R, et al. Rescue of the skeletal phenotype of vitamin D receptor-ablated mice in the setting of normal mineral ion homeostasis: formal histomorphometric and biomechanical analyses. Endocrinology. 1999;140(11):4982-7.
106. Dardenne O, Prudhomme J, Hacking SA, Glorieux FH, St-Arnaud R. Rescue of the pseudo-vitamin D deficiency rickets phenotype of CYP27B1-deficient mice by treatment with 1,25-dihydroxyvitamin D3: biochemical, histomorphometric, and biomechanical analyses. J Bone Miner Res. 2003;18(4):637-43.
107. Dardenne O, Prud'homme J, Hacking SA, Glorieux FH, St-Arnaud R. Correction of the abnormal mineral ion homeostasis with a high-calcium, high-phosphorus, high-lactose diet rescues the PDDR phenotype of mice deficient for the 25-hydroxyvitamin D-1alpha-hydroxylase (CYP27B1). Bone. 2003;32(4):332-40.
108. Kogawa M, Anderson PH, Findlay DM, Morris HA, Atkins GJ. The metabolism of 25-(OH)vitamin D3 by osteoclasts and their precursors regulates the differentiation of osteoclasts. J Steroid Biochem Mol Biol. 2010;121(1-2):277-80.
109. Vincent C, Kogawa M, Findlay DM, Atkins GJ. The generation of osteoclasts from RAW 264.7 precursors in defined serum-free conditions. Journal of Bone Mineral Metabolism. 2009;27:114-9.
110. Atkins GJ, Welldon KJ, Halbout P, Findlay DM. Strontium ranelate treatment of human primary osteoblasts promotes an osteocyte-like phenotype while eliciting an osteoprotegerin response. Osteoporosis international : a journal established as result of cooperation between the European Foundation for Osteoporosis and the National Osteoporosis Foundation of the USA. 2009;20(4):653-64.
111. Wijenayaka AR, Kogawa M, Lim HP, Bonewald LF, Findlay DM, Atkins GJ. Sclerostin stimulates osteocyte support of osteoclast activity by a RANKL-dependent pathway. PloS one. 2011;6(10):e25900.

112. Prideaux M, Wijenayaka AR, Kumarasinghe DD, Ormsby RT, Evdokiou A, Findlay DM, et al. SaOS2 Osteosarcoma cells as an in vitro model for studying the transition of human osteoblasts to osteocytes. Calcif Tissue Int. 2014;95(2):183-93.
113. Hayashi S, Yamane T, Miyamoto A, Hemmi H, Tagaya H, Tanio Y, et al. Commitment and differentiation of stem cells to the osteoclast lineage. Biochemistry and cell biology = Biochimie et biologie cellulaire. 1998;76(6):911-22.
114. Indo Y, Takeshita S, Ishii KA, Hoshii T, Aburatani H, Hirao A, et al. Metabolic regulation of osteoclast differentiation and function. J Bone Miner Res. 2013;28(11):2392-9.
115. Al Hadi H, Smerdon GR, Fox SW. Hyperbaric oxygen therapy suppresses osteoclast formation and bone resorption. Journal of orthopaedic research : official publication of the Orthopaedic Research Society. 2013;31(11):1839-44.
116. Yasuda H, Shima N, Nakagawa N, Yamaguchi K, Kinosaki M, Mochizuki S, et al. Osteoclast differentiation factor is a ligand for osteoprotegerin/osteoclastogenesis-inhibitory factor and is identical to TRANCE/RANKL. Proc Natl Acad Sci U S A. 1998;95(7):3597-602.
117. Fuller K, Wong B, Fox S, Choi Y, Chambers TJ. TRANCE is necessary and sufficient for osteoblast-mediated activation of bone resorption in osteoclasts. J Exp Med. 1998;188(5):997-1001.
118. Herrmann M, Schmidt J, Umanskaya N, Colaianni G, Al Marrawi F, Widmann T, et al. Stimulation of osteoclast activity by low B-vitamin concentrations. Bone. 2007;41(4):584-91.
119. Haynes DR, Atkins GJ, Loric M, Crotti TN, Geary SM, Findlay DM. Bidirectional signaling between stromal and hemopoietic cells regulates interleukin-1 expression during human osteoclast formation. Bone. 1999;25(3):269-78.
120. Atkins GJ, Haynes DR, Graves SE, Evdokiou A, Hay S, Bouralexis S, et al. Expression of osteoclast differentiation signals by stromal elements of giant cell tumors. Journal of bone and mineral research : the official journal of the American Society for Bone and Mineral Research. 2000;15(4):640-9.
121. Zhao S, Zhang YK, Harris S, Ahuja SS, Bonewald LF. MLO-Y4 osteocyte-like cells support osteoclast formation and activation. J Bone Miner Res. 2002;17(11):2068-79.
122. Reinke DC, Kogawa M, Barratt KR, Morris HA, Anderson PH, Atkins GJ. Evidence for Altered Osteoclastogenesis in Splenocyte Cultures from Cyp27b1 Knockout Mice. The Journal of steroid biochemistry and molecular biology. 2015.
123. Wagner EF, Matsuo K. Signalling in osteoclasts and the role of Fos/AP1 proteins. Ann Rheum Dis. 2003;62 Suppl 2:ii83-5.
124. Wang H, Pan M, Ni J, Zhang Y, Zhang Y, Gao S, et al. ClC-7 Deficiency Impairs Tooth Development and Eruption. Sci Rep. 2016;6:19971.
125. Szewczyk KA, Fuller K, Chambers TJ. Distinctive subdomains in the resorbing surface of osteoclasts. PloS one. 2013;8(3):e60285.
126. Wakeyama H, Akiyama T, Kadono Y, Nakamura M, Oshima Y, Nakamura K, et al. Posttranslational regulation of Bim by caspase-3. Annals of the New York Academy of Sciences. 2007;1116:271-80.
127. Tanaka S, Wakeyama H, Akiyama T, Takahashi K, Amano H, Nakayama KI, et al. Regulation of osteoclast apoptosis by Bcl-2 family protein Bim and Caspase-3. Advances in experimental medicine and biology. 2010;658:111-6.

128. Tai TW, Su FC, Chen CY, Jou IM, Lin CF. Activation of p38 MAPK-regulated Bcl-xL signaling increases survival against zoledronic acid-induced apoptosis in osteoclast precursors. Bone. 2014;67:166-74.
129. Xing L, Boyce BF. Regulation of apoptosis in osteoclasts and osteoblastic cells. Biochemical and biophysical research communications. 2005;328(3):709-20.
130. Cotter K, Stransky L, McGuire C, Forgac M. Recent Insights into the Structure, Regulation, and Function of the V-ATPases. Trends Biochem Sci. 2015;40(10):611-22.
131. Geyer M, Yu H, Mandic R, Linnemann T, Zheng YH, Fackler OT, et al. Subunit H of the V-ATPase binds to the medium chain of adaptor protein complex 2 and connects Nef to the endocytic machinery. The Journal of biological chemistry. 2002;277(32):28521-9.
132. Okamoto F, Kajiya H, Toh K, Uchida S, Yoshikawa M, Sasaki S, et al. Intracellular ClC-3 chloride channels promote bone resorption in vitro through organelle acidification in mouse osteoclasts. American journal of physiology Cell physiology. 2008;294(3):C693-701.
133. Reinke DC, Starczak Y, Kogawa M, Barratt KR, Morris HA, Anderson PH, et al. Evidence for altered osteoclastogenesis in splenocyte cultures from VDR knockout mice. The Journal of steroid biochemistry and molecular biology. 2017.
134. Thomas GP, Baker SU, Eisman JA, Gardiner EM. Changing RANKL/OPG mRNA expression in differentiating murine primary osteoblasts. J Endocrinol. 2001;170(2):451-60.
135. Wang X, Studzinski GP. Antiapoptotic action of 1,25-dihydroxyvitamin D3 is associated with increased mitochondrial MCL-1 and RAF-1 proteins and reduced release of cytochrome c. Experimental cell research. 1997;235(1):210-7.
136. Fingas CD, Altinbas A, Schlattjan M, Beilfuss A, Sowa JP, Sydor S, et al. Expression of apoptosis- and vitamin D pathway-related genes in hepatocellular carcinoma. Digestion. 2013;87(3):176-81.
137. Iwasawa M, Miyazaki T, Nagase Y, Akiyama T, Kadono Y, Nakamura M, et al. The antiapoptotic protein Bcl-xL negatively regulates the bone-resorbing activity of osteoclasts in mice. The Journal of clinical investigation. 2009;119(10):3149-59.
138. Diab H, Ohira M, Liu M, Cobb E, Kane PM. Subunit interactions and requirements for inhibition of the yeast V1-ATPase. The Journal of biological chemistry. 2009;284(20):13316-25.
139. Starczak Y, Reinke DC, Barratt KR, Ryan JW, Russell PK, Clarke MV, et al. Absence of vitamin D receptor in mature osteoclasts results in altered osteoclastic activity and bone loss. The Journal of steroid biochemistry and molecular biology. 2018;177:77-82.
140. Lotinun S, Ishihara Y, Nagano K, Kiviranta R, Carpentier VT, Neff L, et al. Cathepsin K-deficient osteocytes prevent lactation-induced bone loss and parathyroid hormone suppression. The Journal of clinical investigation. 2019;129:3058-71.
141. Nakashima T, Hayashi M, Fukunaga T, Kurata K, Oh-Hora M, Feng JQ, et al. Evidence for osteocyte regulation of bone homeostasis through RANKL expression. Nature medicine. 2011;17(10):1231-4.
142. Bellido T. Osteocyte-driven bone remodeling. Calcif Tissue Int. 2014;94(1):25-34.
143. Chiu WS, McManus JF, Notini AJ, Cassady AI, Zajac JD, Davey RA. Transgenic mice that express Cre recombinase in osteoclasts. Genesis. 2004;39(3):178-85.